

**Characterisation of  
Biofilm Structure:  
Investigation and Methods  
for Developing Strategies for  
Control and Prevention  
of Infections**

**Ruth M. Scully**

**DECLARATION**

This work has not been submitted in substance for any other degree or award at this or any other university or place of learning, nor is being submitted concurrently in candidature for any degree or other award.

Signed .....(candidate) Date .....

**STATEMENT 1**

This thesis is being submitted in partial fulfillment of the requirements for the degree of PhD

Signed .....(candidate) Date .....

**STATEMENT 2**

This thesis is the result of my own independent work/investigation, except where otherwise stated, and the thesis has not been edited by a third party beyond what is permitted by Cardiff University’s Policy on the Use of Third Party Editors by Research Degree Students. Other sources are acknowledged by explicit references. The views expressed are my own.

Signed .....(candidate) Date .....

**STATEMENT 3**

I hereby give consent for my thesis, if accepted, to be available online in the University’s Open Access repository and for inter-library loan, and for the title and summary to be made available to outside organisations.

Signed .....(candidate) Date .....

**STATEMENT 4: PREVIOUSLY APPROVED BAR ON ACCESS**

I hereby give consent for my thesis, if accepted, to be available online in the University’s Open Access repository and for inter-library loans **after expiry of a bar on access previously approved by the Academic Standards & Quality Committee.**

Signed .....(candidate) Date .....

# Acknowledgements

Acknowledgement is the recognition of the importance or quality of something, and in this vein I would like to recognise several important people without whom the quality of this work would never have been achieved

The late Dr Geoff Newman first gave me the confidence to believe that I could achieve this, and his wonderful personality will always be missed. It was Dr Mike Walker who kindly gave me the opportunity to start this work. I am extremely fortunate and indebted to him, and also to ConvaTec Ltd., for sponsoring me.

During this journey, I have had the privilege to work with ConvaTec staff such as Kate Meredith, who helped me with the Confocal preparation, and in getting to grips with imaging on my visits. Thanks to Wendy Rowe of the Cardiff Dental School, who kindly allowed me to use the Scanning Electron Microscope when ours was out of action. I am honoured to have met Prof Keith Harding and the Wound Healing Clinic team and to see first-hand how work such as mine might help future patients.

I am grateful to my colleagues in the Electron Microscopy Unit UHW for their patience during the stressful times and I would like to thank Xin Scudder for giving me support and encouragement, and especially as a successful PhD student, for her suggestions and understanding.

I would like to express my heartfelt thanks to all my friends who gave me endless sympathy and helped me survive all the stress, in what were sometimes difficult times, and not letting me give up. Thanks to those who helped me find the time by dog sitting, and to family who listened to my endless wittering on the subject with patience.

And finally, I would like the opportunity to express my sincere respect and gratitude for the support, kindness and inspiration of Dr Mike Walker and Daniel Metcalf, PhD, who gave me their assistance, guidance and wisdom, and had a patience and enthusiasm that never seemed to wane. Thank you both.

I would like to dedicate this to my late father and eldest sister, who always believed affectionately in 'clever clogs'.

## Abstract

The addition of antimicrobial agents to wound dressings is used to reduce the risk of wound infection, and help manage local wound infections, thereby facilitating wound progression, but their activity is impeded by biofilm tolerance. The aim of this work was to investigate the structure and development of wound pathogen biofilm, and to design a novel, challenging *in vitro* simulated chronic wound biofilm model to evaluate the antimicrobial and anti-biofilm effectiveness of several current wound dressings. This study demonstrates how rapidly biofilm can form on a model wound that has been contaminated by contact with planktonic bacteria, producing structured bacterial biofilm communities with nutrient and waste channels and the dispersal of bacterial cells at the surface. Light Microscopy (LM), Transmission Electron Microscopy (TEM), Scanning Electron Microscopy (SEM) and Confocal Laser Scanning Microscopy (CLSM) provided structural images of both biofilm formation and the presence of individual bacteria within the biofilm structure. After 24-48 hours, biofilm had become established, and dispersal of biofilm bacteria was visualised as early as 48 hours. By applying various dressings to the model and analysing representative fields of vision, biofilm was observable to varying extents beneath most of the dressings tested after 24 hours, and by 72 hours this had increased. Two dressings appeared to help prevent the growth of biofilm: a hydrated microbial cellulose dressing containing polyhexamethyl biguanidine dressing, and a next-generation antimicrobial dressing containing ionic silver in an anti-biofilm formulation. The results highlight the importance of dressing selection to manage biofilm in chronic and acute wounds, and these observations should help in the development of novel and effective control of wound infection.



# CONTENTS

LIST OF FIGURES .....	ix
ORGANISMS USED IN STUDY .....	xviii
LIST OF CONSUMABLES, OTHER MATERIALS AND EQUIPMENT .....	xviii
LIST OF PUBLICATIONS AND PRESENTATIONS .....	xxii
Chapter 1 .....	xxiv
General Introduction .....	xxiv
1.1 Bacteria and the natural order of things .....	1
1.2 The development of microscopy and the elucidation of bacteria .....	4
1.3 Preparation of samples for light microscopy .....	9
1.4 The development of electron microscopy .....	11
1.5 Fixation and processing for electron microscopy .....	13
1.6 Fluorescence microscopy and confocal laser scanning microscopy .....	17
1.7 From planktonic bacteria to biofilm .....	18
1.8 From planktonic bacteria to biofilm .....	24
1.9 Quorum Sensing in biofilm .....	28
1.10 The use of biofilm in Industry .....	30
1.11 Biofilm in the Body .....	32
1.12 The Effect of biofilm on the National Health Service .....	34
1.13 Biofilm and Wounds .....	37
1.14 The management of wounds .....	40
1.15 Skin Treatments and Wound Dressings .....	46
1.16 Investigating the Efficacy of Novel Dressings .....	49
1.17 Aims and Hypothesis .....	50

Chapter 2 .....	52
Microscopy protocols, evaluation of surfaces and development of a biofilm wound model .....	52
2.1 Introduction .....	53
2.1.1 The choice of organisms for <i>in vitro</i> studies .....	53
2.1.2 Preliminary techniques and preparation of bacteria for microscopy ...	57
2.1.3 Establishing and characterising a biofilm .....	59
2.2 Aims and objectives .....	65
2.3 Materials and Methods.....	66
2.3.1 Media preparation and maintenance of cultures .....	66
2.3.2 Overnight cultures and exponential growth of planktonic bacteria .....	67
2.3.3 Planktonic growth cultures and effect of silver .....	67
2.3.4 Fixation and harvesting of planktonic bacteria for TEM.....	68
2.3.5 TEM Processing and Observation.....	70
2.3.6 LM processing and observation .....	71
2.3.7 SEM Processing and Observation.....	72
2.3.8 Glass as a surface for growing biofilm.....	73
2.3.9 Plastic coverslips as a surface for growing biofilm .....	73
2.3.10 Determination of inoculum concentration for optimum biofilm growth	74
2.3.11 Timed growth of biofilm from 1-6 hours.....	76
2.3.12 Analysis of “slough-like” surface associated material.....	77
2.3.13 Agar as a surface for growing biofilm .....	78
2.3.14 Gauze as a surface for growing biofilm.....	79
2.3.15 PTTE cell culture inserts .....	80

2.3.16	PTTE/Agar “sandwich” model .....	82
2.3.17	A novel wound model.....	84
2.3.18	Statistical analysis.....	87
2.4	Results.....	88
2.4.1	Physiology, Growth and the Effect of Silver .....	88
2.4.2	TEM of Planktonic Bacteria and the Effect of Silver Nitrate on Bacterial Ultrastructure.....	90
2.4.3	SEM of Planktonic Bacteria.....	93
2.4.4	Biofilm growth on glass coverslips.....	94
2.4.5	Biofilm growth on plastic coverslips.....	95
2.4.6	The effect of inoculum concentration.....	97
2.4.7	Timed growth of biofilm from 1-6 hours .....	99
	Figure 2.13: Statistical Analysis of bacterial growth over a 1-6 hour period ..	100
2.4.8	Surface associated material: biofilm or slough? .....	101
2.4.9	Biofilm growth on surfaces for LM, TEM and SEM.....	102
2.4.10	Development of an agar model to protect the delicate nature of biofilm and process it intact .....	106
2.4.11	The meat model .....	111
2.5	Discussion .....	119
2.5.1	Growth and the Effect of Silver.....	119
2.5.2	TEM of Planktonic Bacteria and the Effect of Silver on Bacterial Ultrastructure.....	120
2.5.3	SEM of Planktonic Bacteria.....	123
2.5.4	Establishing and characterizing biofilm growth.....	124
2.5.5	A novel model .....	131

2.6	Conclusion .....	134
Chapter 3 .....		137
Testing the Efficacy of a Selection of Antimicrobial Dressings using the .....		137
<i>In Vitro</i> Model.....		137
3.1	Introduction .....	138
3.2	Control dressings chosen for the wound model study .....	139
3.2.1	Gauze.....	139
3.2.2	A non-silver Hydrofiber <sup>®</sup> dressing (NSHD) .....	139
3.3	Silver antimicrobial dressings chosen for the wound model study .....	140
3.3.1	Silver Dressings .....	140
3.3.2	A silver containing Hydrofiber dressing – SCHED .....	141
3.3.3	A next-generation antimicrobial dressing - NGAD .....	142
3.3.4	A cellulose ethyl sulphonate fibre silver dressing - CES-SD .....	142
3.3.5	An alginate carboxymethylcellulose nylon silver dressing – ACN-SD 143	
3.3.6	A nanocrystalline silver dressing NC-SD.....	144
3.4	Other non-silver antimicrobial dressings chosen for the wound model study 144	
3.4.1	A Polyhexamethyl biguanidine dressing - PHMBD.....	144
3.4.2	A Cadexomer iodine dressing - CID .....	145
3.5	Aims and Objectives .....	145
3.6	Materials and Methods.....	146
3.7	Results.....	153
3.7.1	3-6 hour dressing treated models.....	153
3.7.2	12 hour dressing treated models .....	156

3.7.1	24 hour dressing treated models .....	162
3.7.2	48 Hour dressing treated models .....	184
3.7.3	72 hour dressing treated models .....	208
3.8	Discussion .....	235
3.8.1	6 hour models .....	235
3.8.2	12 hour models.....	236
3.8.3	24 hour models.....	238
3.8.4	48 hour models.....	241
3.8.5	72 hour models.....	244
3.9	Conclusion .....	254
Chapter 4	.....	259
General Discussion	.....	259
4.1	Discussion .....	260
4.2	Conclusion .....	274
4.3	Limitations to the study and future recommendations.....	277
Appendix 1: Tryptone Soy Broth and Agar plates	.....	280
Appendix 2: Autoclaving .....	.....	281
Appendix 3: RK buffer.....	.....	281
Appendix 3: Preparation of agar pellets from cultures .....	.....	282
Appendix 4: TEM processing schedule using LR White (Newman and Hobot 1987; 2001) .....	.....	283
Appendix 5: Histological processing schedule.....	.....	284
Appendix 6: Staining Procedure for Light Microscopy .....	.....	285
Appendix 7: Processing Schedule for Scanning Electron Microscopy using Hexamethyldisilazane.....	.....	286

Appendix 8: Sputter coating samples with gold .....	287
Appendix 9: Helber Chamber counter.....	288
Appendix 10: Table of some wound dressings in use.....	289
REFERENCES .....	292
AMMONS, M.C., WARD, L.S., JAMES, G.A. (2011) Anti-biofilm efficacy of a lactoferrin/xylitol wound hydrogel used in combination with silver wound dressings. <i>International Wound Journal</i> , 8 (3):268-73.....	293
CAMPLIN, A.L., MADDOCKS, S.E. (2014). Manuka honey treatment of biofilms of <i>Pseudomonas aeruginosa</i> results in the emergence of isolates with increased honey resistance. <i>Annals of Clinical Microbiology Antimicrobials</i> , 12;13:19. doi: 10.1186/1476-0711-13-19. ....	298
EBERLEIN. T., HAEMMERLE, G., SIGNER, M., GRUBER MOESENBACHER, U., TRABER, J., MITTLBOECK, M., ABEL, M., STROHAL, R.J., (2012). Comparison of PHMB-containing dressing and silver dressings in patients with critically colonised or locally infected wounds. <i>Journal of Wound Care</i> , 21(1):12, 14-6, 18-20.....	301
MILLER, C.N., CARVILLE, K., NEWALL, N., KAPP, S., LEWIN, G., KARIMI, L., SANTAMARIA, N., (2011) Assessing bacterial burden in wounds: comparing clinical observation and wound swabs. <i>International Wound Journal</i> , 8(1):45-55. ....	316
TSANG, K.K., KWONG, E.W., TO, T.S., CHUNG, J.W., WONG, T.K. (2017). A Pilot Randomized, Controlled Study of Nanocrystalline Silver, Manuka Honey, and Conventional Dressing in Healing Diabetic Foot Ulcer. <i>Evid Based Complement Alternat Med</i> . 2017;2017:5294890. doi: 10.1155/2017/5294890. Epub 2017 Jan 25 .....	328

**LIST OF FIGURES**

Figure 1.1: Stromatolites, Sharks Bay Australia, showing a biofilm-type structure	2
Figure 1.2: Galileo's telescope	6
Figure 1.3: Robert Hooke's compound microscope	7
Figure 1.4: Ernst Ruska and Max Knoll with the electron microscope in 1936	12
Figure 1.5: The Mushroom and Tower biofilm structure	26
Figure 1.6: The Heterogeneous Mosaic biofilm structure	26
Figure 1.7: Schematic stages of biofilm formation within a wound	39
Figure 1.8: A stage IV pressure ulcer with a heavily colonised wound bed	46
Figure 2.1: 0.4 µm PET track-etched membrane cell culture insert in culture well	81
Figure 2.2: a, b and c: The stages of creating the Agar Model	83
Figure 2.3: The Meat Model	87
Figure 2.4: Absorbance v time showing growth curve for <i>P. aeruginosa</i>	88
Figure 2.5: Absorbance v time growth curve for <i>S. aureus</i>	89
Figure 2.6: TEM of <i>P. aeruginosa</i> and <i>S. aureus</i> with varying protocols of fixation	91
Figure 2.7: TEM of <i>P. aeruginosa</i> and <i>S. aureus</i> untreated and with addition of silver nitrate	92
Figure 2.8: SEM of planktonic bacteria <i>P. aeruginosa</i> and <i>S. aureus</i>	93
Figure 2.9: 72 hour biofilm growth on glass coverslips	94
Figure 2.10: 72 hour biofilm growth on plastic coverslips	95
Figure 2.11: SEM of wells with inoculum concentrations from $3.4 \times 10^7$ to $3.4 \times 10^2$	96
Figure 2.12: Comparison of bacterial growth over a 1-6 hour period	99
Figure 2.13: Biofilm growth by SEM from 1-6 hours	100
Figure 2.14: 6 hour growth with varying methods of biofilm collection	101
Figure 2.15: TEM of surface-associated material after 6 hours of growth	113
Figure 2.16: Biofilm grown on the surface of a TSB/agar plate	103
Figure 2.17: Biofilm growth on gauze, viewed by LM, CLSM, SEM and TEM	

	106
Figure 2.18: Biofilm growth on PTTE inserts viewed by SEM	106
Figure 2.19: 24 hour agar model of <i>P. aeruginosa</i> by LM	107
Figure 2.20: 24 hour agar model of <i>S.aureus</i> by LM	107
Figure 2.21: 24 hour biofilm growth in the agar model by TEM	108
Figure 2.22: 48 hour biofilm growth in the agar model by LM	109
Figure 2.23: TEM of 48 hour biofilm in the agar model with channels	110
Figure 2.24: Intact 72 hour biofilm on the meat model by LM	111
Figure 2.25: Waste/nutrient channels in 72 hour biofilm on meat model by LM	112
Figure 2.26: Bacterial dispersal on 72 hour biofilm on meat model by LM	112
Figure 2.27: Differing biofilm layers on the 72 hour meat model by LM	113
Figure 2.28: Layers of 72 hour biofilm on meat model by LM	113
Figure 2.29: Biofilm micro-colonies and channels in 72 hour biofilm by LM	114
Figure 2.30: TEM of lower dense biofilm layers at 72 hours	115
Figure 2.31: 72 hour biofilm upper layers on meat model by TEM	115
Figure 2.32: Channel detail of the 72 hour biofilm by TEM	116
Figure 2.33: TEM of thickened areas of biofilm in the 72 hour model	116
Figure 2.34: Equal variance tests of biofilm growth at 24 48 and 72 hours	117
Figure 2.35: Interval plot and Tukey plot of biofilm growth at 24 48 and 72 hours	118
Figure 3.1: Preparing a meat model with dressing	147
Figure 3.2: A meat model with gauze dressing after 12 hours of growth	149
Figure 3.3: A meat model with NSHD after 24 hours of growth	149
Figure 3.4: Gauze on meat model viewed under a stereo microscope	150
Figure 3.5: NSHD on meat model viewed under a stereo microscope	150
Figure 3.6: Meat and dressings processed <i>in-situ</i> for SEM	151
Figure 3.7: Agar models – meat set in an agar surround	152
Figure 3.8: 6 hour ACN-SD model by LM with fibres	153
Figure 3.9: The tissue beneath the 6 hour NC-SD stained with silver	154
Figure 3.10: 3 hour CID treated model by SEM	154



Figure 3.11: 3 hour CID treated model examined with SEM with iodine crystals	155
Figure 3.12: 6 hour CID treated model examined by SEM	155
Figure 3.13: 6 hour CID treated model by SEM showing a lack of iodine	156
Figure 3.14: Biofilm growth beneath gauze at 12 hours	157
Figure 3.15: 12 hour NGAD showing no visible growth by LM	157
Figure 3.16: SEM of 12 hour gauze dressing surface	158
Figure 3.17: SEM of 12 hour NSHD with slight gelling of fibres	158
Figure 3.18: The surface of the meat below the 12 hour SCHED	159
Figure 3.19: The 12 hour CES-SD by LM	159
Figure 3.20: The 12 hour NC-SD model with more silver deposition	160
Figure 3.21: Tissue surface and cadexomer beads of CID at 12 hours by SEM	161
Figure 3.22: 12 hour CID with cadexomer beads and growth	162
Figure 3.23: The 24 hour gauze with a continuous layer of biofilm by LM	163
Figure 3.24: 24 hour gauze model by SEM with areas of biofilm	163
Figure 3.25: The 24 hour NSHD model by LM	164
Figure 3.26: The 24 hour NSHD tissue surface by SEM	164
Figure 3.27: The 24 hour NSHD dressing by SEM	165
Figure 3.28: The 24 hour SCHED viewed by LM	165
Figure 3.29: The 24 hour SCHED by SEM showing occasional bacterial clusters	166
Figure 3.30: The 24 hour SCHED by TEM with bacterial clusters	166
Figure 3.31: Bacteria being disrupted in the 24 hour SCHED by TEM	167
Figure 3.32: CLSM of the 24 hour SCHED tissue surface	167
Figure 3.33: The 24 hour NGAD with virtually clean surfaces by TEM	168
Figure 3.34: CLSM 24 hour NGAD tissue surface with no biofilm	168
Figure 3.35: The sequestering effect of 24 hour Hydrofiber dressings	169
Figure 3.36: The 24 hour CES-SD model by LM	169
Figure 3.37: The 24 hour CES-SD dressing with bacteria	170
Figure 3.38: The 24 hour CES-SD tissue surface by SEM	170

Figure 3.39: CLSM imaging of 24 hour CES-SD dressing and tissue surface	171
Figure 3.40: 24 hour ACN-SD model by LM	172
Figure 3.41: SEM 24 hour ACN-SD tissue surface by SEM	172
Figure 3.42: TEM 24 hour ACN-SD tissue surface	173
Figure 3.43: 24 hour ACN-SD dressing surface on SEM	173
Figure 3.44: CLSM images of the tissue beneath the 24 hour ACN-SD	174
Figure 3.45: LM of NC-SD at 24 hours with darkening of the tissue surface	174
Figure 3.46: TEM of 24 hour NC-SD with silver deposition	175
Figure 3.47: Biofilm under the NC-SD at 24 hours by TEM	175
Figure 3.48: 24 hour NC-SD tissue surface by SEM	176
Figure 3.49: 24 hour NC-SD SEM biofilm on tissue surface	177
Figure 3.50: The surface and lower fibre layers of the NC-SD 24 hour	177
Figure 3.51: CLSM at 24 hours of the NC-SD and meat	178
Figure 3.52: PHMBD at 24 hours with few bacteria apparent in LM	178
Figure 3.53: Tissue surface below the PHMBD at 24 hour by SEM	179
Figure 3.54: PHMBD dressing surface at 24 hour SEM	179
Figure 3.55: Tissue surface below the PHMBD at 24 hour by TEM	180
Figure 3.56: PHMBD tissue surface and dressing at 24 hours by CLSM	180
Figure 3.57: The CID tissue surface at 24 hour by LM	181
Figure 3.58: The CID 24 hour model by SEM with cadexomer beads	182
Figure 3.59: An individual cadexomer bead from the 24 hour CID model by SEM	182
Figure 3.60: Biofilm growth in the CID 24 hour model by TEM	183
Figure 3.61: Imaging of cadexomer beads by CLSM of 24 hours	183
Figure 3.62: 48 hour gauze models with thick continuous growth by LM	184
Figure 3.63: 48 hour growth beneath gauze viewed by TEM	185
Figure 3.64: The 48 hour gauze dressing by SEM	185
Figure 3.65: 48 hour gauze tissue surface by SEM	186
Figure 3.66: LM of 48 hour NSHD	187
Figure 3.67: 48 hour NSHD by TEM	187
Figure 3.68: The 48 hour NSHD by SEM including model edge	188

Figure 3.69: The 48 hour NSHD dressing with swelling of fibres	189
Figure 3.70: SCHED at 48 hours by LM	189
Figure 3.71: A few fibres on the 48 hour SCHED tissue surface	190
Figure 3.72: TEM 48 hour SCHED model surface	190
Figure 3.73: The 48 hour NGAD model with clean surfaces below the agar	191
Figure 3.74: The 48 hour NGAD model by TEM	191
Figure 3.75: 48 hour NGAD tissue surface by SEM	192
Figure 3.76: 48 hour SCHED tissue surface and dressing by CLSM	193
Figure 3.77: 48 hour CLSM of NGAD tissue surface and dressing by CLS	193
Figure 3.78: CES-SD 48 hour model by LM	194
Figure 3.79: 48 hour CES-SD hour model by TEM	194
Figure 3.80: The CES-SD tissue surface at 48 hours by SEM	195
Figure 3.81: CES-SD 48 hour dressing and tissue surface by CLSM	196
Figure 3.82: 48 hour ACN-SD model by LM	196
Figure 3.83: 48 hour ACN-SD fibres by LM	197
Figure 3.84: SEM 48 hour ACN-SD model	197
Figure 3.85: TEM 48 hour ACN-SD model	198
Figure 3.86: SEM 48 hour ACN-SD model	198
Figure 3.87: CLSM 48 hour ACN-SD model	199
Figure 3.88: LM of NC-SD at 48 hours	199
Figure 3.89: TEM of NC-SD at 48 hours	200
Figure 3.90: NC-SD dressing surface by SEM	201
Figure 3.91: SEM of NC-SD by SEM at 48 hours	201
Figure 3.92: CLSM demonstrated NC-SD dressing and meat at 48 hours	202
Figure 3.93: PHMBD at 48 hours by LM	203
Figure 3.94: SEM of 48 hour PHMBD tissue surface	203
Figure 3.95: SEM of 48 hour PHMBD dressing surface	204
Figure 3.96 TEM of 48 hour PHMBD model surface	204
Figure 3.97: Tissue surface under 48 hour PHMBD with CLSM	205
Figure 3.98: 48 hour PHMBD dressing surface with CLSM	205
Figure 3.99: The CID sample at 48 hours by LM	206

Figure 3.100: The 48 hour CID sample with beads by SEM	207
Figure 3.101: TEM and CLSM of 48 hour CID showing biofilm around the beads	207
Figure 3.102: 72 hour gauze control models	208
Figure 3.103: SEM of 72 hour gauze and dressing	209
Figure 3.104: Interval plot and Tukey plot of 24 - 72 hour Gauze models	210
Figure 3.105: Increased growth on models of 72 hour NSHD controls	211
Figure 3.106: SEM of 72 hour NSHD tissue surface by SEM	211
Figure 3.107: Interval plot and Tukey plot of 24 - 72 hour NSHD models	212
Figure 3.108: The SCHED at 72 hours by LM with fibres and beginnings of growth	213
Figure 3.109: The SCHED tissue surface at 72 hours by SEM	214
Figure 3.110: Interval plot and Tukey plot of 24- 72 hour growth of SCHED models	215
Figure 3.111: The NGAD 72 hour model by LM	216
Figure 3.112: 72 hour SEM of central area of NGAD model after dressing removal	216
Figure 3.113: Interval plot and Tukey plot of 24- 72 hour growth of NGAD models	217
Figure 3.114: 72 hour CES-SD model by LM	218
Figure 3.115: 72 hour CES-SD surface and dressing by SEM	218
Figure 3.116: Interval plot and Tukey plot of 24- 72 hour growth of CES-SD models	219
Figure 3.117: 72 hour ACN-SD model by LM	220
Figure 3.118: 72 hour ACN-SD tissue surface by SEM	221
Figure 3.119: Interval plot and Tukey plot of 24- 72 hour growth of ACN-SD models	222
Figure 3.120: 72 hour growth and silver deposition under NC-SD by LM	223
Figure 3.121: 72 hour growth under NC-SD and on NC-SD dressing by SEM	224

Figure 3.122: Interval plot and Tukey plot of 24 - 72 hour growth of NC-SD models	225
Figure 3.123: PHMBD at 72 hours by LM	226
Figure 3.124: PHMBD tissue surface and dressing surface at 72 hours by SEM	226
Figure 3.125: Interval plot and Tukey plot of 24- 72 hour growth on PHMBD models	227
Figure 3.126: LM of 72 hour CID showing thick growth	228
Figure 3.127: 72 hour CID by SEM	228
Figure 3.128: Interval plot and Tukey plot of 24- 72 hour growth of CID models	229
Figure 3.129: At 24 hours, comparing tests for equal variances	230
Figure 3.130: At 48 hours, comparing tests for equal variances	231
Figure 3.131: At 72 hours, comparing tests for equal variances	231
Figure 3.132: At 72 hours; the control, the best and the worst performing dressings' tests for equal variances	232
Figure 3.133: Comparative interval plots of all dressings at 24, 48 and 72 hours	233
Figure 3.134: Bar chart of tukey pairwise comparison means of biofilm growth areas beneath dressings	234

## LIST OF REAGENTS

Reagent	Suppliers
Acetic acid	Sigma-Aldrich, Gillingham, UK

<b>Reagent</b>	<b>Suppliers</b>
Agar, biological no 1	Oxoid Ltd, Basingstoke, UK
Agarose	Sigma-Aldrich, Gillingham, UK
Calcium chloride	Sigma-Aldrich, Gillingham, UK
Eosin Y	Thermo Fisher Scientific, Loughborough, UK
Ethanol Analar	Thermo Fisher Scientific, Loughborough, UK
Glutaraldehyde (EM grade - 25% solution)	TAAB Laboratories Equipment Ltd., Reading, UK
Harris haematoxylin	Thermo Fisher Scientific, Loughborough, UK
Hexamethyldisilazane	Sigma-Aldrich, Gillingham, UK
Hydrochloric acid	Sigma-Aldrich, Gillingham, UK
Industrial D A (IDA)	Genta Medical, York, UK
Lead nitrate	Sigma-Aldrich, Gillingham, UK
LR White and Accelerator	TAAB Laboratories Equipment Ltd., Reading, UK
Scotts Tap Water Solution	Sigma-Aldrich, Gillingham, UK
Silver nitrate	Sigma-Aldrich, Gillingham, UK
Sodium acetate	Sigma-Aldrich, Gillingham, UK
Sodium barbitone	Sigma-Aldrich, Gillingham, UK
Sodium chloride	Sigma-Aldrich, Gillingham, UK
Sodium citrate	Sigma-Aldrich, Gillingham, UK
Sodium hydroxide	Sigma-Aldrich, Gillingham, UK
Sodium tetraborate (borax)	Sigma-Aldrich, Gillingham, UK
Tissue marking dye	Cancer Diagnostics, CellPath Ltd., Newton, UK

Reagent	Suppliers
Toluidine blue	Sigma-Aldrich, Gillingham, UK
Tryptone soy broth	Lab M, Bury, UK
Uranyl acetate (EM grade)	Agar Scientific Ltd., Stanstead, UK
Xylene	Genta Medical, York, UK

All reagents were analar grade unless otherwise stated  
All suppliers are UK based

## ORGANISMS USED IN STUDY

Organisms supplied courtesy of ConvaTec Ltd

<i>Pseudomonas aeruginosa</i>	(NCIMB 8626)
<i>Staphylococcus aureus</i>	(NCIMB 9518)

## LIST OF CONSUMABLES, OTHER MATERIALS AND EQUIPMENT

Name/Model	Company
Absorbent tissues	Tork, SCA Hygeine Products, Dunstable, UK
Acticoat 7™	Smith & Nephew, Hull, UK
Aluminium foil	Sainsbury Ltd
AQUACEL®	ConvaTec, Deeside, UK
AQUACEL® Ag	ConvaTec, Deeside, UK
AQUACEL® Ag Extra™	ConvaTec, Deeside, UK
Autoclave	Dixons Express Autoclave – Dixons Surgical Ltd, Wickford, UK
AxioCam HRC and Axiovision software	Carl Zeiss Microscopy, Cambridge, UK
Back bacon	Sainsbury's Cardiff, UK
Blockmaster embedding station	Raymond A. Lamb Ltd., Eastbourne, UK

<b>Name/Model</b>	<b>Company</b>
Whatman Cellulose nitrate filters, diameter 47mm, pore size 0.2µm	Thermo Fisher Scientific, Loughborough, UK
Cellwax	CellPath Ltd., Newton, UK
Chopping Board, plastic	Basics range, Sainsbury's Cardiff, UK
Cork borers	Sigma-Aldrich, Gillingham, UK
Cotton wool	Sainsbury's Cardiff, UK
Coverslips	Thermo Fisher Scientific, Loughborough, UK
Culture plates	Corning Life Sciences, Tewksbury, UK
Diamond marker	TAAB Laboratories Equipment Ltd., Reading, UK
DURAFIBER <sup>®</sup> Ag	Smith & Nephew, Hull, UK
1.5 ml microcentrifuge tubes	Thermo Fisher Scientific, Loughborough, UK
Filtration unit	Thermo Fisher Scientific, Loughborough, UK
Fine forceps	TAAB Laboratories Equipment Ltd., Reading, UK
Flasks	Thermo Fisher Scientific, Loughborough, UK
Fridge	Cool Zone, MicroMark, London, UK
Gauze	Systagenix, Gatwick, UK
Gelatine capsules (size '0'/vol 0.68ml)	TAAB Laboratories Equipment Ltd., Reading, UK
Glass coverslips	Thermo Fisher Scientific, Loughborough, UK
Glass knife maker	LKB Instruments, TAAB Laboratories Equipment Ltd., Reading, UK
Glass strips for knives	Leica Microsystems, Milton Keynes, UK
Glass slides	Thermo Fisher Scientific, Loughborough, UK
Gold grids, thin bar 200 hexagonal mesh, 3.05mm	Agar Scientific Ltd., Stanstead, UK
Heating block	Thermo Luckman, Thermo Fisher



<b>Name/Model</b>	<b>Company</b>
	Scientific, Loughborough, UK
Helber counting chamber	Scientific Laboratory Supplies, Nottingham, UK
Helios Epsilon Spectrophotometer	Thermo Fisher Scientific, Loughborough, UK
Hexagonal 300 mesh copper grids	Agar Scientific Ltd., Stanstead, UK
Iodoflex™	Smith & Nephew, Hull, UK
JEOL 1200 EXII TEM	JEOL UK Ltd, Welwyn Garden City, UK
JEOL 840A SEM	JEOL UK Ltd, Welwyn Garden City, UK
JEOL TEM and SEM Megaview camera system and SYS Analysis software	Olympus, KeyMed Ltd, Essex, UK
Leica RM2155 rotary microtome	Leica Microsystems, Milton Keynes, UK
Leica ST5010 XL autostainer	Leica Microsystems, Milton Keynes, UK
Leica TCS SP2, CLSM	Leica Microsystems, Milton Keynes, UK
Live/Dead® BacLight™ Viability Kit	Thermo Fisher Scientific, Loughborough, UK
Mini Flatbed orbital shaker	Stuart Scientific, Stone, Staffordshire, UK
Olympus BX51 microscope	Olympus, KeyMed Ltd, Essex, UK
Cocktail sticks	Sainsbury's Cardiff, UK
Petri dishes	Thermo Fisher Scientific, Loughborough, UK
Ph tester	Hanna Instruments, Thermo Fisher Scientific, Loughborough, UK
Pipettes	Thermo Fisher Scientific, Loughborough, UK
Processing cassettes and lids	Thermo Fisher Scientific, Loughborough, UK
PTTE membrane cell culture inserts	Falcon®, Corning Life Sciences, Tewksbury, UK
Pump, Dymax 5	Charles Austen Pumps Ltd, West Byfleet, UK
Rotamix	TAAB Laboratories Equipment Ltd.,

<b>Name/Model</b>	<b>Company</b>
	Reading, UK
Scalpels	TAAB Laboratories Equipment Ltd., Reading, UK
Self-adhesive carbon tabs	Agar Scientific Ltd., Stanstead, UK
SEM 25mm aluminium stubs	Agar Scientific Ltd., Stanstead, UK
Silvercel <sup>®</sup> Non-Adherent	Johnson & Johnson, Wokingham, UK
Sputter coater	EMScope, Leica Microsystems, Milton Keynes, UK
Stainless steel molds	Thermo Fisher Scientific, Loughborough, UK
Stereo microscope	Leica Microsystems, Milton Keynes, UK
Sterile loops	Thermo Fisher Scientific, Loughborough, UK
Stiefel biopsy punch	eSupplies Medical, Newport, Wales, UK
Stirrer/Hotplate	Corning Life Sciences, Tewksbury, UK
Suprasorb <sup>®</sup> X+PHMB	Activa Health Ltd, Lohmann-Rauscher, Burton on Trent, UK
TESCAN Scanning Electron Microscope	TESCAN, Cambridge, UK
Test tubes Pyrex <sup>®</sup>	Corning Life Sciences, Tewksbury, UK
Thermanox coverslips	Thermo Fisher Scientific, Loughborough, UK
Thermo-Excelsior Tissue processor	Thermo Fisher Scientific, Loughborough, UK
Tissue processing paper, Biowraps	Leica Microsystems, Milton Keynes, UK
Ultracut 2 Ultramicrotome	Leica Microsystems, Milton Keynes, UK
Universal containers	Thermo Fisher Scientific, Loughborough, UK
Watch glasses and miscellaneous labware	Thermo Fisher Scientific, Loughborough, UK
Waterbath	Grant Instruments, Royston, UK

## LIST OF ABBREVIATIONS

Abbreviation	Full name
<i>P. aeruginosa</i>	<i>Pseudomonas aeruginosa</i>
<i>S. aureus</i>	<i>Staphylococcus aureus</i>
LM	Light Microscopy
CLSM	Confocal Laser Scanning Microscopy
TEM	Transmission Electron Microscopy
SEM	Scanning Electron Microscopy
NSHD	Non-Silver Hydrofiber Dressing
SCHD	Silver Containing Hydrofiber Dressing
NGAD	Next Generation Antimicrobial Dressing
CES-SD	Cellulose Ethyl Sulphonate fibre Silver Dressing
ACN-SD	Alginate Carboxymethylcellulose Nylon Silver Dressing
NC-SD	Nano-Crystalline Dressing
PHMBD	Polyhexamethyl biguanidine Dressing
CID	Cadexomer Iodine Dressing
H&E	Haematoxylin and Eosin staining
LR White	London Resin White

## LIST OF PUBLICATIONS AND PRESENTATIONS

This work has been the subject of the following publications and presentations

### Publication in preparation

Scully, R., Walker, M., Hurlow, J., Metcalf, D.G., Parsons, P., Bowler, P. The *in vitro* performance and clinical considerations of cadexomer iodine and anti-biofilm hydrofiber wound dressings. *Journal of Wound Care*, 2017

### Oral and poster presentations

Scully, R., Hobot, J., Walker, M., Metcalf, D., (2014). Poster presentation of 'Stages of biofilm formation by a combination of microscopic methods' at 26th European Congress of Pathology, London, September 2014

Scully, R.M., Hobot, J., Walker, M., Metcalf, D., (2014). Poster presentation of 'at Wound Healing Conference, Harrogate, UK. November 2014:

1. 'Stages of biofilm formation by a combination of microscopic methods'
2. 'In vitro observations of biofilm formation beneath a range of antimicrobial wound dressings'

Scully, R.M., Hobot, J., Walker, M., Metcalf, D., (2014). Poster presentation of 'Stages of biofilm formation by a combination of microscopic methods' Postgraduate Research day, Cardiff, December 2014

Scully R.M., (2014). Oral presentation of 'Stages of biofilm formation by a combination of microscopic methods' at the Society of Electron Microscopy Technology, London, December 2014. (Image from abstract chosen by SEMT for front cover of meeting programme)

Scully, R.M., Hobot, J., Walker, M., Metcalf, D., (2014). Poster presentation of 'In vitro observations of biofilm formation beneath a range of antimicrobial wound dressings' at European Wound Management Association, Dublin, 5-9 May 2015

Scully R.M., (2015). Oral presentation of 'Stages of biofilm formation by a combination of microscopic methods' at the Association of Clinical Electron Microscopists, Pathological Society of Great Britain and Ireland, Dublin, June 2015

Scully, R.M., Hobot, J., Walker, M., Metcalf, D., (2016) Poster presentations at the Wound Healing Conference, Harrogate, UK. November 2016

3. An *in vitro* simulated chronic wound biofilm model used to assess the performance of silver-containing dressings against biofilm formation
4. Assessment of a cadexomer iodine-containing dressing against biofilm using an *in vitro* simulated chronic wound biofilm model

### **Additional dissemination of the work by others**

#### Publication

Microbial Biofilms – Importance and Applications: Chapter 4, Wound Biofilm and Therapeutic Strategies, D. Metcalf, P. Bowler and D. Parsons  
[www.intechopen.com/books/microbial-biofilms-importanceand-applications](http://www.intechopen.com/books/microbial-biofilms-importanceand-applications)

#### Presentations

Hurlow, J., GNP, CWOCN, presentation including images from 'Stages of biofilm formation by a combination of microscopic methods' at the European Wound Management Association meeting on 11-13 May 2016, Bremen, Germany

Bowler, P., MPhil, Vice President, Science & Technology, ConvaTec Ltd., presentations of Assessment of images from 'a cadexomer iodine-containing dressing against biofilm using an *in vitro* simulated chronic wound biofilm model' at 16 meetings to approximately 1200 clinicians (65% surgeons, 35% nurses) across China, Japan, Singapore & Malaysia including the 60<sup>th</sup> Japan Plastic Surgery Society meeting in Osaka, Japan 2017

# **Chapter 1**

## **General Introduction**

## 1.1 Bacteria and the natural order of things

Many only know bacteria as invisible 'creatures' that can make us ill, or are present in some food products or supplements which have been commercially advertised as making one 'more healthy'. But these creatures, although individually consisting of only a single cell, can be amazingly complex and can group together into structures which have both fascinated and perturbed the scientific world.

Bacteria are known to be one of the earliest life forms and to have existed for at least 3,500 million years (McNamara and Awramik, 1992). Fossils of dome-shaped structures, consisting of layers which formed in shallow water, have been found dating back 2,800 million years (Olsen and Pierson, 1986). These fossils, or Stromatolites, are thought to be due to communities of Cyanobacteria trapping, binding and cementing sedimentary grains (Figure 1.1 ). Cyanobacteria are the largest and most diverse group of photosynthetic bacteria, and were probably responsible for raising the levels of oxygen in the Earth's atmosphere from less than 1% to the 21% of today, allowing for the evolution of new aerobic species of bacteria which eventually led to the development of more complex life forms (Knoll, 2008).



**Figure 1.1: Stromatolites, Sharks Bay Australia, showing a biofilm-type structure**  
With kind permission of the Western Australia Department of Parks and Wildlife  
The shape of the structures show a resemblance to the proposed mushroom and tower  
biofilm structures suggested by Donlan and Costerton (2003).  
([http://www.sharkbay.org.au/visiting-shark-bay/parks-and-other-sites/hamelin\\_pool\\_stromatolites](http://www.sharkbay.org.au/visiting-shark-bay/parks-and-other-sites/hamelin_pool_stromatolites))

Bacteria are a part of a group of microorganisms (often abbreviated to microbes) which also include archaea, fungi, algae, protozoa and viruses, and play an important role in maintaining aspects of life on Earth. They are found in a wide range of habitats in the natural world, from boiling hot to icy cold, in extremes of pH or sulphurous conditions (the so-called extremophiles), and are able to co-exist inside the bodies of plants and animals. Those existing within humans and animals



do so by achieving a balance, ensuring the growth and survival of the host and bacteria.

Relatively few bacteria are pathogenic in animals. The majority of them are harmless, and many of them are beneficial or probiotic. The term probiotic is used to define bacteria that appear to have certain health benefits. Some of these bacteria are used in food products and include claims of boosting the immune system, as well as being helpful in treatment for conditions such as eczema, lactose intolerance, irritable bowel system, inflammatory bowel disease and persistent diarrhoea. Those affecting the digestive tract are more recognisable as being helpful, as until more research is done, it is not convincing enough that bacteria when swallowed could have any effect outside of the digestive system (Sanders et al., 2013). In cases of antibiotic-associated diarrhoea, these probiotics may have their place. Without probiotics, antibiotics tend to wipe out the protective bacteria of the gut, which results in diarrhoea. Typical dietary probiotics which may restore the natural balance include *Lactobacilli* and *Bifidobacterium* spp, as they are found amongst the indigenous bacteria of the human gut (Gomes and Malcata, 1999).

Microorganisms colonise the surface of human skin. The skin is the largest organ in the human body and at the moment of birth the epithelial surface is exposed to maternal and environmental organisms (Gregory, 2011). Studies estimate skin bacterial levels to be from 10 to 800,000 bacteria per square centimetre by adulthood (Evans et al., 1950). The estimated density of bacteria upon the skin at any one time depends upon the region sampled, with the variety of the multitude of

microorganisms being dependent upon the host characteristics, such as age, gender, ethnicity, anatomic location (Grice and Segre, 2011), and to a certain extent on the culture techniques used. This dynamic community can contain a variety of bacteria but those commonly isolated include *Staphylococcus*, *Corynebacterium*, *Propionibacterium*, *Micrococcus*, *Brevibacterium* and *Acinetobacter* spp. Alterations in the community type on the skin can be due to environmental characteristics or host demographics and the pathogenicity of bacteria often depends on the interaction between the bacteria and the host. If the host is compromised in any way, such as in immuno-suppression, it can have consequences regarding the health of an individual and can result in bacterial-related disease. Conditions including psoriasis, atopic dermatitis and acne can affect this microbial system but it remains unclear as to how the microorganisms and their precise pathogenic mechanisms can influence biological processes (Rosenthal et al., 2011). When they do cause disease bacteria can produce debilitating symptoms and can often be difficult to eradicate, such as those in chronic wounds where they are thought to prevent healing and cause persistent inflammation (Grice and Segre, 2011).

## **1.2 The development of microscopy and the elucidation of bacteria**

Although bacteria have existed for millions of years their discovery was only made in the 17<sup>th</sup> century, when work on glass lenses had gradually paved the way to the

invention of the light microscope. As early as the 1<sup>st</sup> century AD the Romans were using pieces of glass with varying thicknesses as magnifiers, or burning glasses, but it took until the 13<sup>th</sup> century for lenses to be adapted to be worn as spectacles. These magnifying lenses were one lens and one power (6 times to 10 times), but by the end of the 17<sup>th</sup> century much had been improved upon and numerous people have been credited in the development of the lens system integral to the compound light microscopes of today (Uluç et al., 2009).

Some of the most noteworthy people in early microscopy are:

*Zacharias Janssen:* Working with his father in 1590 as spectacle makers, they put several lenses in a tube and discovered that objects near the end of the tube appeared to be larger.

*Galileo Galilei:* Perhaps more renowned for his work on telescopes, he started experimenting with lenses after hearing of such lens work and by 1609 had developed a two lens system using a bi-concave eyepiece and a bi-convex objective lens. By 1624 this had been improved to a three lens system, but he turned his attention to the stars (Figure 1.2).

*Antonie van Leeuwenhoek:* A tradesman and scientist in Holland, he worked with magnifying glasses. By grinding and polishing he created small, rounder lenses with a greater magnification. He also observed animalcules in the plaque of teeth which were the first observations of living bacteria (Porter, 1976).

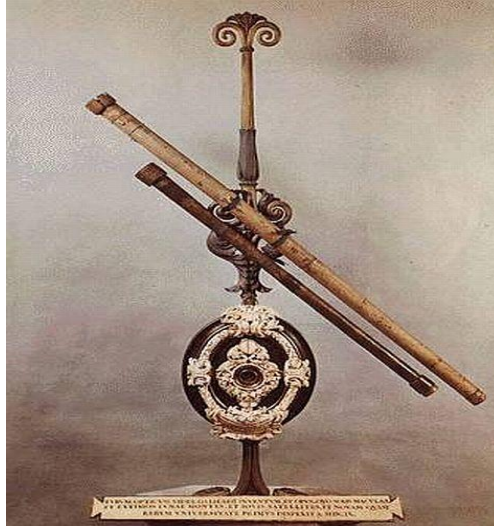


**Figure 1.2: Galileo's telescope**

The early work of those such as Galileo Galilei in the creation of lenses led to the gradual evolution of the microscope. This telescope only magnified up to x20 but was revolutionary. Courtesy of [galileotelescope.org](http://galileotelescope.org)

*Robert Hooke:* In England, he spent much of his life designing and improving lenses and hence the capabilities with microscopes. These microscopes were able to show things that no one had seen before and one can only imagine the excitement at the discovery of micro-organisms in droplets of water (Figure 1.3). The beautifully illustrated works 'Micrographia', published in 1665 by Hooke, demonstrated this to society for the first time and resulted in it becoming a best seller.

The gradual development of the parts that today we take for granted in the compound microscope occurred over the next three centuries. These include a sturdy stand, binocular systems, a concave mirror to light the specimen from below (Culpeper, 1727), apertures for better resolution (Goring, 1824), the effects of cover glasses (Lister, 1827) and apochromatic correction systems (Abbe, 1879).



**Figure 1.3: Robert Hooke's compound microscope**

Manufactured by London Instrument maker Christopher Cock in 1665, this microscope led to the compilation of drawings for the *Micrographia*, a book describing his observations. Courtesy of thescientist.com

Throughout the 19<sup>th</sup> century great strides were made by companies to create further improvements, the most famous being Carl Zeiss Jena, founded in 1847 by Carl Zeiss (1816–1888). Over the years the basic design of the compound microscope had undergone amazing changes to provide the high quality instruments of today's light microscopes.

An important discovery worthy of note was the work published by George Airy of the Cambridge Observatory who noted that light produced a series of concentric rings rather than a single point image (the Airy disc). If the airy discs overlap, due to two point sources being brought close together, there will come a point where they are so close that it will not be possible to distinguish or resolve the two objects

as separate entities. The minimum distance to achieve resolution of two objects is when the first minimum of one Airy disc coincides with the central maximum of the other (Strutt, 1879).

In 1873, Ernst Abbe published the formal mathematical basis for optical microscopy and showed this distance,  $d$ , to be:

$$d = \frac{0.61\lambda}{n \sin \alpha}$$

where  $d$  is resolution,  $\lambda$  is the wavelength of light,  $\alpha$  is the half angle of acceptance of the lens and  $n$  is the refractive index of the medium between the object and the lens. He recognised that the limit to resolution was due to the wavelength of light and not by the design of the lenses. The importance of this finding was that the resolution limit of the light microscope was established, so now attention could be turned to improving other factors.

Over the years various staining techniques were introduced and improved upon to help identify cellular structures and to improve their visibility with better contrast. In the 1930s techniques such as Giemsa and Feulgen staining showed the presence of chromatin bodies and DNA in bacteria (van Iterson, 1984). The problem with many of the staining techniques was that the chemicals in the methods used killed bacteria, but in 1953 Fritz Zernike won the Nobel Prize for his invention of the phase contrast microscope (in 1935), then being produced by Zeiss. Its system of annular rings scatters some of the light and creates a phase shift of half a wavelength of light, resulting in the ability to view specimens which are unstained. This allows them to stand out in contrast to the background, and hence the ability

to view live specimens such as bacteria. The importance of this was that here at last, the bacteria could be visualized live and processes such as proliferation could be studied. The later development of differential interference contrast exploited differences in the specimen's thickness and refractive index to produce differences in amplitude and colour (Normarski and Weill, 1954). It was due to these developments in light microscopy that the structure of bacteria and their growth gradually became elucidated.

### **1.3 Preparation of samples for light microscopy**

Colonies of bacteria may easily be sampled and smeared on to a slide for fixation and consequent staining to view under a microscope, but to examine the presence and effect of such microorganisms in tissue samples requires lengthier processing. Fixation has been recorded as far back as Hippocrates but it was during the late 19<sup>th</sup> century that there was a flurry of investigation into fixatives (Mitchell et al., 2011). Fixation prevents putrefaction and autolysis. There have been many different fixatives invented for different tissue types using various chemicals from water to alcohol-based mixtures to gaseous, and containing many chemicals such as aldehydes, mercury, picric acid and chloroform. Today most pathology laboratories advocate the use of a buffered formaldehyde fixation method, many of which are now supplied commercially. Once tissue samples are fixed, they are processed by dehydration and subsequent infiltration by a medium that can turn from a liquid state into a solid state, for the creation of sections for staining and

examination. Processing machines have been developed to do this on a mass scale, some processing 300 samples in 40 minutes. Routine light microscopy uses paraffin wax as its medium. Samples processed this way can be easily stained by a multitude of techniques.

In order to differentiate different cellular structures, histological staining methods were developed. The Gram staining method was devised in 1884 (Musumeci, 2014), and is still today almost always the first test performed for the identification of bacteria. The primary staining solution of the Gram's method is crystal violet and the method is based on the ability of certain bacteria to retain the crystal violet dye in the cell wall during solvent treatment due to a higher peptidoglycan and lower lipid content. These microorganisms are classified as Gram-positive, while those not stained by crystal violet are referred to as Gram negative.

As the structure of tissue samples and of bacteria was studied in more detail, the lack of morphological differentiation between the cytoplasm and the nuclear material in bacteria initially caused people to believe that they were different from other organisms. However, ground breaking light microscopy techniques by Mason and Powelson (1956) and Robinow (1956) demonstrated the presence of chromatin bodies in bacteria. A more detailed examination would await the electron microscope, which allowed for high-resolution imaging at much higher magnifications than that obtainable with the light microscope.



## 1.4 The development of electron microscopy

It was in 1924 that Louis De Broglie theorised that electrons were similar to light and travelled in waves. If the wavelength of electron beams was smaller than of light waves and could be utilised in the same way, then the resolution of a structure would be much higher and hence the magnification would be increased. In 1931 Ernst Ruska and Max Knoll produced the first electron lens using this theory and recognised the potential of an electron microscope (Figure 1.4). They built their transmission electron microscope (TEM) in 1936 and were able to image structures such as cotton as small as 50 nm. In the TEM, a high voltage is passed through a filament, such as tungsten, which causes it to emit electrons. The electrons travel through a high vacuum, where controlled electromagnetic lenses focus the electrons into a very thin beam. The electron beam passes through the specimen to be studied which, depending on the specimen density, scatters some of the electrons which diverge from the beam. These scattered electrons hit a fluorescent screen giving a shadow image of the specimen studied and its differing densities. Increases in the accelerating voltages improved the resolution further (FEI Electron Optics). Many companies subsequently started to produce the TEM, from RCA in North America, Metropolitan Vickers in Manchester England, Siemens and Carl Ziess in Germany, and Japan Electron Optics Laboratories (JEOL), Hitachi and Toshiba in Japan (Palucka, 2002).



**Figure 1.4: Ernst Ruska and Max Knoll with the electron microscope in 1936**

The original transmission electron microscope was designed to magnify objects approximately 400 times. (<http://poster.sciencemag.org/sem>)

The scanning electron microscope (SEM) was proposed by Max Knoll, and Manfred von Ardenne expressed the theoretical principles of it eliminating chromatic aberration inherent in its system (Bell and Erdman, 2012). The SEM was described and developed in 1945 by Zworykin, but the design of the first prototype was delayed until after the end of the Second World War when Oatley began to build an SEM based on Zworykin's microscope. This was followed by Smith (1956) who introduced non-linear amplification and a stigmator to correct lens imperfections. In 1960 Everhart and Thornley created a new detector, a scintillator to convert the electrons to light and a light pipe to send this to a photomultiplier

tube, which finally led to Pease and Nixon in 1963 combining all these methods and the marketing of the first commercial instrument by Cambridge Scientific Instrument Company as the "Stereoscan" (Oatley, 2004).

As with TEM, in SEM a tungsten filament produces a high energy electron beam. Where the TEM has electromagnetic lenses to control a stream of electrons, the SEM uses magnetic coils to adjust the focus of the beam on to the specimen. An area of the surface is scanned. The energy lost from the electrons is randomly scattered and absorbed. The secondary electrons produced are 'read' by the SEM detectors and an image produced.

Hence, in summary, in the TEM the electron beam passes through a specimen, producing an image of the inner structures of cells, whereas in the SEM the secondary electrons produce images of surfaces, resulting from an electron beam scanning the surface of an object.

## **1.5 Fixation and processing for electron microscopy**

In order to examine the ultrastructure of bacteria under the TEM it was also necessary to preserve them by some form of fixation. Light microscopy and its histological techniques were not adequate. In tissue samples osmium tetroxide, glutaraldehyde and uranyl acetate solutions are used alone or in combinations for fixation. Much progress was achieved by Ryter and Kellenberger (1958) to overcome bacterial fixation problems (Glauert and Thornley, August 1966). They examined the fine structure of the nucleus under different conditions and this

resulted in the development of a buffering solution, the RK conditions of fixation, which provided optimal preservation of the fine fibrillar nuclear material of *Escherichia coli* (Ryter et al., 1958). The method was subsequently found to give excellent results with many other bacteria. An improvement was found by Sechaud and Kellenberger (1972) who tried fixation with a combination of glutaraldehyde and uranyl acetate rather than osmium tetroxide alone, and found it to give good reproducible results and visualisation of viral structures hitherto unseen by just osmium tetroxide fixation. It also fixed rapidly. Schreil (1964) studied the effect of uranyl acetate and found that dehydration caused damage to the bacterial ultrastructure by forming coarse aggregates of DNA. Schreil (1964) determined that uranyl acetate had a stabilising effect on bacterial DNA and reduced damage in the dehydrations steps. For this reason, Kellenberger and Ryter (1964) advocated initially fixing in osmium tetroxide with calcium ions followed by uranyl acetate as part of the RK buffering system. Further, Silva et al (1971), by chemical assays, determined that the amount of lipid loss - mainly lipid phosphorous from membranes- was greater without uranyl acetate post fixation. With uranyl acetate the ultrastructure of membranes appeared well preserved and it also produced optimum contrast, leading to the conclusion that that it stabilised materials that would otherwise be lost. The stabilisation of bacterial DNA is not something that is experienced by the nuclear material of eukaryotes, where proteins are associated with the DNA structure and where fixation with aldehydes at concentrations of 2-10% causes gelation in these proteins by crosslinking and so inherently stabilises the DNA (Kellenberger et al., 1958; Kellenberger et al., 1981). In prokaryotic

bacteria there are no proteins associated with the DNA structure and hence no stabilisation of the bacterial DNA is possible. Any possible stabilisation of the DNA comes from the source of proteins provided by the growth media, e.g. tryptone, and prefixing the bacterial cells with a low concentration of osmium directly in the medium prior to following the RK conditions of processing (Kellenberger and Ryter, 1964).

Various other fixation methods were used to elucidate the structure of the bacterial cell but every protocol has been found to have its advantages and disadvantages. Fixation by aldehydes and osmium tetroxide promote permeabilisation across cell membranes with subsequent leakage of potassium then magnesium (Moncany and Kellenberger, 1981; Woldringh, 1973), which together with varying the salt concentrations of growth media were found to induce changes in nucleoid shape and organisation of the DNA plasm (Hobot et al., 1985). The problem of maintaining the true shape and organisation of the bacterial nucleoid and DNA plasm was solved by using cryosubstitution techniques, where rapid freezing, immobilisation in ice and replacement of ice by resin avoided the dangers posed to bacterial structure by chemical fixation and dehydration (Hobot et al., 1985).

Whether the cryosubstitution techniques used an osmium tetroxide /acetone mix followed by processing into epoxy resins, or a glutaraldehyde/acetone mix followed by infiltration with acrylic (methacrylate) resin at  $-35^{\circ}\text{C}$ , these studies showed how the DNA fibrils were organized in the nucleoid (Bjornsti et al., 1986), with the DNA containing plasma of the nucleoid being a highly hydrated gel (Hobot et al., 1985, 1987; Hobot, 1990). The nucleoid appeared as ribosome-free areas filled with

grainy structures intermingled with fibrous elements, containing the double-stranded DNA fibre with unwound, single stranded DNA at the edges of these areas.

Another area in the processing of bacteria besides fixation which was found to be important was the embedding medium or resin. In the 1950s, the introduction of methacrylate-based resins was met with several problems, notably uneven polymerisation, shrinkage and producing cellular swelling of bacteria (Birch-Andersen, 1960). The introduction by 1960 of epoxy resins overcame the drawbacks presented by the methacrylates, which were largely forgotten, and much of our understanding of cellular ultrastructure was elucidated by the increasing use of these highly stable epoxy resins (Glauert and Glauert, 1958; Maaløe and Birch-Andersen, 1956). In the early 1980s the methacrylates made a comeback by being reformulated so overcoming all previous drawbacks, (Causton, 1984; Kellenberger et al., 1980). These allowed new processing possibilities for preparing bacteria, especially by reducing the dangers posed to bacterial structures by dehydration in organic solvents required with epoxy resin processing, resulting in new aspects of bacterial ultrastructure being demonstrated (Hobot et al., 1984; Newman and Hobot, 1987; Hobot, 1990).

As SEM requires an intact surface that is completely dry and electrically conductive on the surface, preservation and processing are just as essential in SEM as in TEM. Non-conductive specimens will cause charging faults if not dried and coated correctly. Also, air drying of specimens will lead its structure to collapse on itself when introduced to a high vacuum. As for TEM, SEM fixation is followed by

dehydration with organic solvents, in order to prevent structural alterations to the surface. These solvents can then be replaced by a transitional phase of liquid carbon dioxide which is then turned into a gas phase using a critical point drier. The instantaneous drying preserves the three dimensional organisation of surface structures. More recently a final organic solvent, hexamethyldisilazane (HMDS), has been introduced which successfully allows specimens to be air dried (Araujo, 2003). The results indicate that the HMDS solvent is suitable for drying samples of bacterial cells for examination by SEM successfully without any damage occurring to surface structures.

## **1.6 Fluorescence microscopy and confocal laser scanning microscopy**

Fluorescence microscopy was developed by Heimstaedt (1911) and Lehman (1913) and used in the studying of auto fluorescence. It until the 1930s that suitable staining techniques were developed and these were followed by protein labelling with a fluorescent dye. Dyes such as ethidium bromide and acridine dyes have been used since the 1950s to visualize nucleic acids with ultraviolet light (Bradley and Wolf, 1959).

The fluorescent microscope relies on a light source (such as a high pressure mercury lamp) exciting an electron in an atom or molecule and boosting it to a higher energy level. When it returns to its natural state it emits a quantum of light. The microscope system includes excitation and contrast filters, and beam splitters.

One of the problems with fluorescence microscopy is that the excitation light not only illuminates the point of interest, it also illuminates the background (secondary fluorescence). By adding a pinhole this problem is solved. This pinhole is conjugate to the lens focal point (confocal pinhole) (Claxton et al., 2005). This basic concept of confocal microscopy was patented in 1957 by Marvin Minsky (Minsky, 1988). In the late 1960s specimens were scanned mechanically by a spinning Nipkow disc (Egger and Petran, 1967) and the first confocal laser scanning microscope (CLSM) was built by 1973. Mechanical scanning was used until computer technology advanced, and by the 1980s the images were manipulated digitally. The confocal microscope uses a laser as the excitation light and the image is measured from the pinhole to a detector linked to a computer. Modern CLSM are equipped with high power lasers and integrated electronics enabling video imaging. By scanning the specimen an image can be compiled which is of a higher resolution than the light microscope (theoretically 0.2 to 0.5  $\mu\text{m}$ ). The advantages are that with its depth of field, thicker specimens can be examined, and optical slices can be collated into three dimensional images, for example of the bacterial nucleoid (Valkenburg et al., 1985), making it ideal for looking at thick bacterial films – termed biofilm.

## **1.7 From planktonic bacteria to biofilm**

The deleterious effects of microbes in wounds have been recognized for decades (James et al, 2008) and at first it was presumed that these bacteria were planktonic



in structure. Planktonic microorganisms are free-floating and individual, maintained in some form of liquid medium. However, the planktonic state is not usually the true natural state that enables bacteria to survive so adeptly. It has become increasingly recognised that bacteria do not normally exist as solitary cells, but are colonial organisms working together as a community in a three dimensional structure, a composition termed biofilm. This term was coined by Costerton in 1978 as – *“a microbially derived sessile community characterized by cells that are irreversibly attached to a substratum or interface or to each other, embedded in a matrix of extracellular polymeric substance that they have produced, and exhibit an altered phenotype with respect to growth rate and gene transcription”*.

Consequently, it is now estimated that in non-healing chronic wounds approximately 75 - 80% of them contain biofilm (Römling and Balsalobre, 2012; Hurlow et al., 2016).

Biofilm can form on any natural or man-made surface. It is the slime forming in stagnant water, it grows in the lining of catheters, it is often a precursor to wound infections, on kidney (or struvite) stones in urinary tract infections, and can be found on contact lens surfaces (Proal, 2008). Antonie van Leeuwenhoek's early work on dental plaque resulted in the identification of what was later realised to be microbial biofilm (Percival et al., 2011).

The sticky or slimy nature of biofilm is due to the production of extracellular polymeric substance (EPS), which are found to be a common bacterial phenomenon. EPS is beneficial in that it protects biofilm from external threats and

is also important for its structural integrity (Nadell et al., 2009). EPS is not unique to bacteria; it can be found associated with other microbes, namely the archaea, algae and fungi (moulds and yeasts). Neither is all biofilm hazardous as some of the bacteria beneficial to humans, such as those of the gut, can form biofilm. Surprisingly little is still known about how the biofilm matrix of EPS is actually formed, but extensive research has been performed and some of the findings on the content and suggested formations of biofilm are highlighted below.

Selection favours those that can protect themselves in nature, so microorganisms forming into such a protected community is naturally beneficial. Persistence of microbial infections is therefore due, in part, to the ability of microorganisms to form these communities and to be ensconced and protected. Microbes at the surface of biofilm may be more susceptible to damage than those within the biofilm itself (Blaschek et al., 2007). Little is still known about the exact method of EPS production, but it is thought to be created by microbes using substances available in their environment and converting them into a slimy polymeric matrix (Tokuda, 1969). Carbohydrate strands were demonstrated to surround bacteria, and when the presence of polysaccharides were identified it proved that a glycocalyx is an essential component of biofilm structure (the earlier name of EPS was extracellular polysaccharide substance). The EPS forms a sticky tangled mat that enables microbes to stick together or to other surfaces (Tokuda, 1969). EPS varies greatly depending upon the microbe, the environment and nutrients, which can therefore lead to biofilm matrices of varying chemical composition. Other parameters such as

pH, temperature and levels of oxygen or nitrogen will also affect the composition and quality of biofilm structure (Zhang et al., 1998).

Like their planktonic counterparts, biofilm microorganisms must have a supply of nutrients to grow. Reduction in nutrient concentration will slow, halt or reverse the development of biofilm, but once nutrient content increases the biofilm will revert (Von Rege and Sand, 1998). The variable nature of biofilm is such that it can be highly complex, comprising multispecies containing many types of EPS, or it can comprise of a single species with its own specific EPS (Donlan, 2002). Biofilm can contain up to 97% water (Sutherland, 2001a). The presence of such a high level of water provides a highly hydrated environment protecting the cells against desiccation. Up to 90% of the dry weight in biofilm is the EPS matrix, so as little as 10% has been suggested to be microorganisms (Flemming and Wingender, 2010). A few biofilm matrices are cationic in nature, however most are anionic with D-glucuronic acid being the most common anionic molecule found within most biofilm, although d-galacturonic and d-mannuronic acids can also be present (Sutherland, 2001b). Primary conformation of EPS is often polysaccharides that have been visualized as fine strands attached to the microbial cell surface and forming a complex network surrounding the cell (Sutherland, 2001b). Proteins, lipids, extracellular DNA (eDNA) and other molecules also add to the heterogeneous nature and may interact with the polysaccharides, with protein often being the largest fraction (Jahn et al., 1998; Jahn et al., 1999; Bjarnsholt, 2013). This network of polysaccharide and macromolecules traps cells and cell products within it giving a final tertiary structure (Sutherland, 2001b). In biofilm extracted

from river waters humic acids (organic matter) and hexoses are present (Aguilera, 2008). Lectins are thought to be involved in the formation and stabilization of the polysaccharide matrix network and constitute a link between the microbial cell surface and EPS (Flemming and Wingender, 2010).

Microorganisms can secrete enzymes and surfactants which may help in the building and protection of the biofilm structure (Izano et al., 2007). *Staphylococcus aureus* (*S. aureus*) synthesizes poly-N-acetylglucosamine (a homopolysaccharide composed of unbranched long polymeric chains of D-glucosamine uniformly linked together by  $\alpha$ -1,6 glucosidic bonds), which is believed to be its most important biofilm matrix component and research links its presence to the binding of the biofilm to surfaces (Pamp et al., 2007).

Flemming and Wingender (2010) stated that the biofilm acts almost like an external digestive system because it has the ability to keep these extracellular enzymes close to the cells, and by keeping the contents of lysed cells available in the matrix, it can also act as a recycling centre. In dental plaque, the close proximity of bacteria can lead to the degradation of host complex molecules, such as salivary mucins (Marsh and Bradshaw, 1995). Type IV pili have also been found which are used by a number of bacteria. By using phase-contrast microscopy to analyse a collection of *Pseudomonas aeruginosa* (*P. aeruginosa*) mutants defective for surface attachment, flagella and type-IV pili, O'Toole et al., (2000) showed that these structures played an important role in the early events in biofilm development. *P. aeruginosa* pili were shown to have an affinity for binding with DNA and, as eDNA has been found in abundance in the extracellular matrix

material of *P. aeruginosa* biofilm, it is thought that the type IV pili might act as cross-linkers between the cells and eDNA (Pamp et al., 2007). The generation of eDNA is evidently in many cases regulated by means of quorum-sensing, which is a mechanism that enables bacteria to monitor their cell population density through the extracellular accumulation of signalling molecules. Treatment of bacterial growth with *P. aeruginosa* DNase has been shown to prevent the formation of biofilm (Vilain et al., 2009). Vesicles, which have been found in biofilm, are thought to be from the outer membranes of bacteria. They contain enzymes and DNA that can alter the biofilm matrix properties, perhaps even competing with other organisms within it (Flemming and Wingender, 2010; Schooling and Beveridge, 2006). Analysis of any of the content suggested within biofilm EPS will however be dependent upon the extraction methods used, be it centrifugation, sonication, filtration, or treatment with agents and ion exchange resins. If the cells within the EPS are damaged then the cellular contents will cause contamination (Aguilera, 2008).

There has been much thought into how the EPS helps adhesion of the biofilm. Tsuneda et al., (2003) examined the influence of EPS on bacterial cell adhesion onto solid surfaces and concluded that if the EPS amount is small, cell adhesion onto solid surfaces is inhibited by electrostatic interaction, and if it is large, cell adhesion is enhanced by polymeric interaction. Depending strongly on the forces acting on the EPS matrix, biofilm displays viscoelastic properties (Tsuneda et al., 2003).

In humans there are many surfaces on which biofilm can grow. For example, the respiratory tract (*Pseudomonas* spp or *aeruginosa*), intestinal mucosa (*Escherichia coli*), teeth (streptococci) and sutured skin wounds (*Staphylococcus aureus*) can all provide the ideal surface on which bacteria can anchor and develop into colonies and biofilm. These bacterial examples rarely develop on their own in these situations. Biofilm can be single species, such as those often found in clinical equipment infection e.g. those lining catheters, but biofilm is usually polymicrobial, containing multiple, diverse species often forming an almost symbiotic form of life (Donlan and Costerton, 2002). Wound infections like diabetic foot ulcer (DFU) infections are usually polymicrobial in nature. A study in India by Malik et al., (2013) showed that 68.5% of DFUs were polymicrobial whilst 31.4% were monomicrobial. There is an increasing effort to try to understand why bacteria are more commonly found associated with other bacterial species rather than as isolated organisms. The advantages of this behaviour is probably, as with any community, that the biofilm bacteria can cooperate in the distribution of nutrients, removal of wastes, and defence against exogenous threats (Serralta et al., 2001). The National Institutes of Health (US Department of Health and Social services) have stated that biofilm is involved in 80% of all known infections (Percival et al., 2008).

## **1.8 From planktonic bacteria to biofilm**

Planktonic bacteria, free floating and swimming, will attach to a surface given the opportunity. The flagellar/fimbriae-dependent bacteria will revert to twitching

motility, instead of swimming, once in contact with a surface, and relinquish their planktonic state. This twitching relies on pili and will continue whilst in contact with other cells while forming a monolayer of growth. This contact induces gene expression which encourages the cells to start to secrete EPS, proteins, polysaccharides and eDNA, to participate in quorum sensing and gradually to develop biofilm (Bjarnsholt et al., 2013).

The *P. aeruginosa* polysaccharide synthesis locus (expressing Psl exopolysaccharide, an initial component of its biofilm) is anchored, at attachment, on the cell surface in a helical pattern. This promotes cell-to-cell interactions and production of a matrix. Chemical dissociation of Psl from the bacterial surface disrupts the matrix as well as the biofilm structure (Ma et al., 2009). Other interactions such as van der Waal forces, hydrophobicity and charge, help the bacteria to firmly adhere to the surface (Wuertz et al., 2003).

Biofilm morphology has been observed *in vitro* to be at first flat and undifferentiated, then differentiating into towers and mushrooms shapes that can fuse together, producing channels and voids to deliver nutrients and remove waste products (Nadell et al., 2009). This structure, suggested by Donlan and Costerton (2002), is one formed from considerable work and consensus and has been drawn from mainly CLSM images (Figure 1.5).

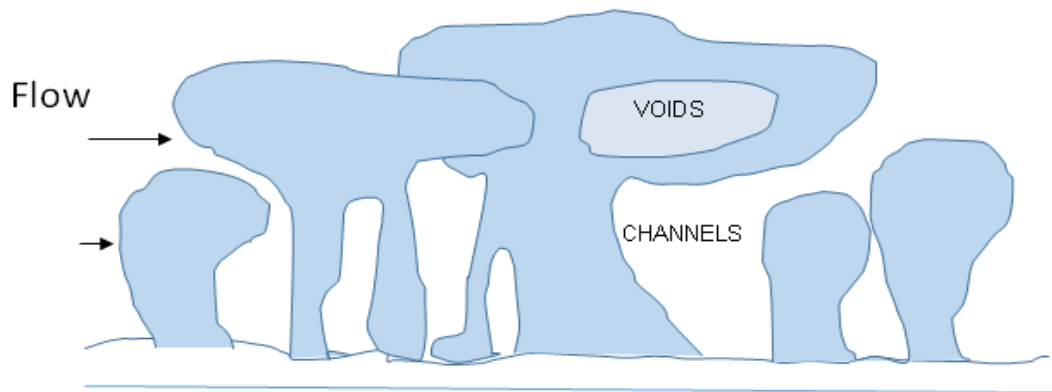


**Figure 1.5: The Mushroom and Tower biofilm structure**

In high shear the micro-colonies are visco-elastic and deformable. Water channels conduct convective flow and deliver nutrients to most parts of the biofilm community. Adapted from Donlan and Costerton (2003)

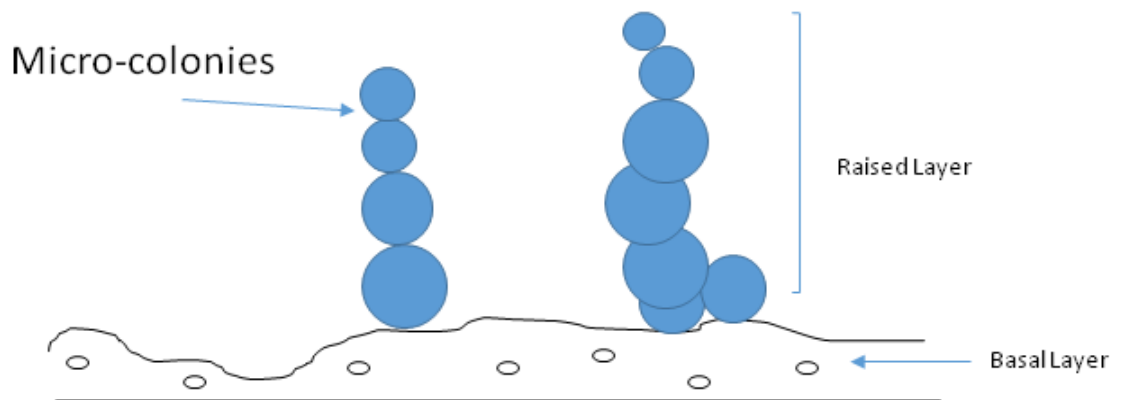


**Figure 1.6: The Heterogeneous Mosaic biofilm structure**

Microcolony stacks on a substratum base that are well separated from each other. Often, in addition to the stacks, is a background of individual cells attached to the surface forming a thin film. Adapted from Walker et al. (1995).



A second structure suggested by Walker (1995) is of stacks of microcolonies that grow into towers but do not fuse together – the “Heterogeneous Mosaic” biofilm model (Figure 1.6). Much of this work has been performed upon catheter biofilms (Wilks et al., 2008). A third structure, described by Wimpenny and Colasanti (1997), is one observed in dental studies of plaque. Here a dense amorphous biofilm structure is suggested with little evidence of water channels and plaque, although some CLSM studies have found small voids and channels within them (Lewandowski, 2005).

Whatever conceptual model the biofilm is thought to follow, they all have the main effect of immobilising constituent cells and encouraging interactions (cell-to-cell communication) and prolonged existence (Rice et al., 2005). Klausen et al., (2003) showed that *P. aeruginosa* had a highly differentiated biofilm that formed the stalks of mushrooms when grown *in vitro* in the presence of glucose, whereas the same strain formed a flat and undifferentiated biofilm in the presence of citrate. These adaptive strategies help bacteria overcome the stresses of their environment with resulting stabilisation and ecological success. Biofilm-associated cells can be differentiated from their planktonic, suspended counterparts by generation of an EPS matrix, reduced growth rates, and the up and down regulation of specific genes. During *P. aeruginosa* biofilm maturation, Psl exopolysaccharide accumulates on the periphery of 3-D-structured microcolonies, resulting in a Psl matrix-free cavity in the microcolony centre containing swimming and dead cells together with eDNA (Ma et al., 2009).

Once well established, biofilm can shed cells. This dispersal is an important stage in biofilm development, as it allows new biofilm to be formed. This dispersion may occur in response to environmental changes; it can be induced by nutrient starvation or sudden nutrient availability (Flemming and Wingender, 2010). Dispersion can be of single planktonic cells or clumps of biofilm, which spread and recolonise elsewhere. It has been suggested that the biofilm cells may secrete enzymes which break down parts of the matrix and cause changes to the structure (Sutherland, 2001a, 2001b). This could also cause the release of clumps of biofilm from the main structure, as could shearing effects from flow systems, erosion or abrasion. In wounds, there is some argument that slough is also biofilm released by a passive mechanical force (Parsek and Singh, 2003), although many regard slough as purely dead host (largely proteinaceous) material (Hurlow and Bowler, 2009).

Sometimes biofilm aggregates can be identified as opaque macroscopic flecks because they are so large, e.g., in the urine of patients with urinary tract infections due to *P. aeruginosa* (Costerton, 1984). In endocarditis, pace-makers can be susceptible to biofilm colonisation and have been found to be covered with thick *S. aureus* biofilm, which had possibly protected the organism against aggressive antibiotic therapy (Costerton, 1984).

## **1.9 Quorum Sensing in biofilm**

Bacteria are thought to communicate within biofilm matrices by the use of chemical signalling molecules, excreted from the cells, which can elicit profound

physiological changes. This cell-to-cell communication continues and, once a critical threshold concentration has been reached (a quorum), it can initiate a response and express genes in a cell-density-dependent manner (Winzer et al., 2002). The term 'quorum-sensing' has been coined to describe this ability of bacteria to monitor cell density before expressing a phenotype (Whitehead et al., 2001). This allows bacteria to coordinate, change and adapt to their environment. Wound adherent and wound non-adherent bacteria have been quantified in similar wounds and, although the non-adherent (planktonic) bacteria will vary more widely in number from wound-to-wound, the adherent (biofilm) bacteria have a narrower range suggesting a critical mass (Serralta et al., 2001).

A large number of different bacterial products can be found in spent culture supernatants and, theoretically, each of these molecules has the potential to serve in a quorum sensing system as a signalling molecule. However, what defines cell-to-cell signalling, as a phenomenon that deals with more than simply the presence of a toxic or nutritional molecule, is a cellular response that extends beyond the physiological changes that would be required to metabolise or detoxify (Winzer et al., 2002).

Two quorum-sensing processes have been described for bacteria, termed auto inducers (AI). AI type 1 is mainly involved in intra-species communication and the type 2 is associated with inter-species interaction. Gram-negative bacteria are thought to produce and release AI molecules, which are generally *N*-acetyl homoserine lactone molecules, whereas Gram-positive bacteria are thought to communicate with modified oligopeptides (Vu et al., 2009).

The microorganism on which most quorum-sensing-related studies have been initiated is *P. aeruginosa*, reflecting its significance as an opportunistic human pathogen. It has been found to have two quorum-sensing systems, LasI-LasR and RhII-RhIR, which are thought to regulate virulence factors such as exoenzyme S (ExoS) and exotoxin A (ToxA). Virulence factors in *S. aureus* include Panton-Valentine leukocidin (pvl), staphylococcal protein A (spa) and  $\alpha$ -hemolysin (hla) (Pastar et al., 2013).

## **1.10 The use of biofilm in Industry**

A material surface exposed in an aqueous medium will inevitably and almost immediately become conditioned or coated by polymers from that medium, resulting in a chemical modification of that surface. Upon this surface biofilm can then grow. On an intermediate timescale, biofilm can improve the strength of its structural matrix in response to mechanical stresses, such as water flow, by increasing its EPS production (Flemming and Wingender, 2010). The undesired effects of biofilm include corrosion of constructional material, heat loss in heat exchangers, or the decrease of product quality, as in the paper industry. Reducing microbially-induced corrosion is estimated to cost 3% of the world's domestic product (Ikuma et al., 2013). Biofilm also have the ability to harbour enteric pathogens in potable water systems due to its reduced susceptibility to antimicrobial agents (Blokker et al., 2013). Strategies to limit the growth of undesired microorganisms are often the addition of chemical biocides such as

chlorine, mechanical cleaning, or nutrient depletion. Using these approaches can be costly and time consuming and there are environmental restrictions for the use of these often harsh chemicals (Von Rege and Sand, 1998). Biofilm cells are also thought to exist in different metabolic states, which could make them less susceptible to antimicrobials (Ferriera et al., 2010).

A more positive finding of biofilm in industry is its biotechnological potential, such as the removal of toxic heavy metals ions from contaminated waters and sediments in chemical industries, which present an increasing hazard for all living organisms (Aguilera, 2008). Biofilm is used in bio-filtration to remove organic matter in drinking water and as a use for removing disinfection products (formed by reactions between disinfectants and natural organic matter) (Reinke and Sorg, 2012).

EPS anionic ligands have an affinity for multivalent cations such as  $\text{Ca}^{2+}$ ,  $\text{Cu}^{2+}$ ,  $\text{Mg}^{2+}$ , and  $\text{Fe}^{3+}$  and favour mineral precipitation. Biotechnological techniques, such as bioleaching, rely on microbes oxidizing solid compounds, recovering heavy metals and resulting in soluble and extractable elements decreasing the dangers for ecosystems and human health (Vu et al., 2009). In such situations biofilm is often exposed to turbulent flows. Because of the flexibility of the matrix it has the ability to change shape in response to the applied force. The shear stresses can affect biofilm physical morphology and dynamic behaviour, with elastic-like recovery and this shear force style of biofilm can be seen in dental plaque (Sutherland, 2001a).

## 1.11 Biofilm in the Body

Biofilm is known to grow on many surfaces of the human body including the lungs, intestinal tract and skin. Some play a protective role, such as those in the gut or vagina, but if its composition or its surroundings and nutrients alter (such as host immunosuppression), then biofilm can become pathogenic. As acknowledged by the National Institutes of Health, most chronic human infections, such as osteomyelitis, endocarditis, prostatitis, otitis media, sinusitis, and dental disease, are biofilm-based (Lasa et al., 2005).

*P. aeruginosa* is adept at forming biofilm in the lungs of patients suffering from cystic fibrosis or in the wounds of burns patients, and it is a potent producer of alginate (polysaccharide) slime. A green slime and a sweet odour in a wound are clinical indicators of its presence, where the green colour is caused by production of pigments such as pyocyanin (Hurlow and Bowler, 2009).

*S. aureus*, as part of the normal microflora of the skin and mucosal nasal passages, is harmless, but, as an opportunistic pathogen, it can be found to be a cause of invasive and chronic infections in medical device-related infections, and as biofilm in intra-operative appliances such as catheters. *S. aureus* biofilm can be indicated by a golden colour which is caused by the production of staphyloxanthin (Pamp et al., 2007).

Some clinical biofilms are able to incorporate particles from the host such as fibrin, which has been found in infective endocarditis, and is thought to protect the biofilm from the leukocytes of the host. Valve dysfunction injury promotes thrombus

formation to which the bacteria attach. Eliminating platelets from a fibrin-rich matrix can reduce bacterial formation, especially of *S. aureus*, as can inhibiting platelet aggregation by aspirin treatment (Parsek and Singh, 2003). Urinary catheters colonised by biofilm are known to become blocked by mineral encrustations due to biofilm organisms hydrolysing urea and the resulting high level of ammonia resulting in this precipitation (Donlan, 2002).

From the above it can be seen that biofilm can form and give rise to infections in many areas of the human body. It has been estimated that biofilm is associated with 65% of all hospital-related infections and, as such, is a great drain on the National Health Service (NHS) budget (Bowler and Percival, 2004). Treatments must be targeted at suppressing biofilm but not damaging host tissue or the host immune response cells.

Biofilm has been known for some time to be able to detach from surfaces as large aggregates (Costerton, 1984), each of which could grow up as individual colonies. Routine cultures grown from swabs of colonised catheters and intrauterine contraceptive devices are usually negative. This is mostly likely because the traditional culture techniques, which have been employed for years, will usually only detect planktonic bacteria. Even if the culture technique reports a predominant bacterium, there is no guarantee that this is the pathogenic bacteria that is causing the problem (Costerton, 1984). Ideally the colonised surfaces of such infections, including those of wounds, should be scraped to detach not only planktonic bacteria, but any biofilm-associated cells. These scrapings should be examined by laboratory techniques such as Fluorescence *In-Situ* Hybridisation (FISH) or

Polymerase Chain Reaction (PCR). However, using these forms of technical investigations on a regular basis would be costly for the NHS compared to the usual culture techniques, and also presumes the clinic is aware that they should be looking for biofilm (Oates et al., 2014). Looking at this problem of costs, thought has been given to looking at EPS as a marker, but due to its biochemical diversity it is unlikely that one staining approach could be used, as each group of compounds would need to be targeted separately (Neu and Lawrence, 2014).

### **1.12 The Effect of biofilm on the National Health Service**

Biofilm has great importance for public health because of its suspected role in infectious diseases and the connection with a variety of device-related infections. Antimicrobials employed must manage the bacterial infection but be gentle to the host, unlike in the industrial environment where harsher chemicals can be employed, but these gentler antimicrobials may not penetrate biofilm efficiently (Lima et al., 2001).

Antibiotic resistance is becoming increasingly higher on the agenda in healthcare and the media. Most of the public have heard of the term “MRSA” even if they are not aware of exactly what it is. Patients are given preoperative swabs from the nasal passage and groin to look for Methicillin-Resistant *S. aureus* (MRSA) and, if positive, are given preoperative antibiotics. Antibiotics might suppress planktonic bacteria but they usually fail to eradicate those embedded within a biofilm. It has



been estimated that biofilm bacteria are up to 1,000 times more resistant than planktonic bacteria (Martineau and Dosch, 2007).

Are bacteria transferring antibiotic resistance genes via biofilm to other bacteria, or are enzymes being produced by one antibiotic-resistant cell type and simply protecting neighbouring non-resistant cells purely by their mutual vicinity? Are they also causing previous relatively harmless bacteria to be converted into highly virulent forms? This is probable, due to the presence of vesicles from the outer membranes of bacteria which have been found in biofilm (Schooling and Beveridge, 2006), but it could also be due to the nature of the structure of the biofilm matrix itself preventing the antibiotics from attacking the safely protected bacteria. It may simply act as a barrier. If biofilm is disrupted then the bacteria become more susceptible to antibiotics and antimicrobials (Miller and Miller, 2011).

Deeper within biofilm, where there is less access to nutrients, bacteria may be entering a spore-like state in which they can survive for years (Costerton and Wilson, 2004; Ferreira et al., 2010), protected from the effects of antibiotics or antimicrobials. Those bacteria deep within biofilm are thought to accumulate in anaerobic niches, where concentrations of molecules and changing pH will be different for internal bacteria than those accumulated in more external or surface layers. This could effect the diffusion, thus penetration, of antibiotics deeper in to biofilm (Stewart and Costerton, 2001). These metabolically differing areas of biofilm therefore present many challenges to effective clinical treatment. One reason for biofilm resistance may simply be that some antibiotics, like penicillin, target cell wall synthesis and kill bacteria that are actively growing, those near to or

on the surface, but cannot kill those in a sessile state deeper within the biofilm (Costerton et al., 1999). These persister cells may survive and hence are tolerant to antibiotics without undergoing genetic change, and can result in relapse of persistent infections.

Another aspect that affects the NHS is the cost to the patient; not just in monetary value but also in physical and mental health. Estimates suggest that up to one third of patients who develop a foot ulcer experience depression (Malik et al., 2013).

With an increase in the number of obese people worldwide, there has been an increase in the number of people developing conditions such as diabetes and cardiovascular disease. These groups of people are at more risk of having poor circulation and developing chronic wounds, i.e. wounds that have not healed after 6 weeks, such as venous leg ulcers. Venous insufficiency, ischaemia and hypoxia have a major impact on wound chronicity (Hunt et al., 2000). Diabetic foot ulcers are a burden on the patient and the health care system (Malik et al., 2013).

It has been estimated that up to 1-2% of the worldwide population are suffering from a non-healing wound (Bjarnsholt, 2008). Chronic wound management is complex and prolonged. Ulcers that become colonised by biofilm are often difficult to eradicate and patients can suffer with them for years. Amputation sometimes results and this impacts on the physical and mental health of the individual.

Patients who undergo amputation can suffer with depression, post-traumatic stress disorder and phantom limb pain (Bhuvaneshwar et al., 2007).

The cost to the NHS is therefore substantial due to the length of time these wounds can exist and the differing treatment the patients have to undergo, including visits to or from community care settings to change dressings, and with ever more limited resources on health services it creates a considerable financial burden. Posnett and Franks (2007) estimated that the cost to the NHS of caring for patients with a chronic wound was circa 2.3–3.1 bn per year (at 2005–2006 costs); around 3% of the total estimated expenditure on health for the same period. Posnett and Franks (2008) estimated the cost of venous leg ulceration to the NHS of £168–198 million per year, while Kerr (2012) estimated that nearly £700 million is spent each year on foot ulcers and amputations. In the Government’s Quality, Innovation, Productivity and Prevention agenda 2012, it identified that the NHS had to make significant savings. It focused on reducing harm and expenditure in wound care, especially around pressure ulcer formation, which in 2010 was estimated to cost over £140,000 per case. In Wales £330 million is spent on wound care annually – 6% of the NHS budget (Cardiff University Wound Healing Research Unit September 2014). These costs begin to explain the amount of time and effort being used in research into biofilm in order to produce an evidence-based approach to clinical interventions.

### **1.13 Biofilm and Wounds**

Biofilm is known to persist in wounds, and once it is has been disrupted or removed by methods such as debridement and cleansing, it can and often does re-

form quickly (Wolcott et al., 2008) (Figure 1.7). A greater understanding of biofilm processes should lead to novel, effective strategies for biofilm control and a resulting improvement in patient management (Donlan, 2002).

Wounds often have a wide range of pathophysiological origins and, when colonising chronic wounds, bacteria are most likely to exist as biofilm communities (James et al., 2008) and hence treatment should target these specifically. These chronic wound biofilm communities will inevitably form immature, microscopic biofilm that the host defences may be able to deal with, but once the balance is tipped in favour of the bacteria, wound healing will be compromised, i.e. the wound becomes critically colonised. James et al., (2008) light (LM) and electron microscopy (EM) studies showed 60% of chronic wound samples examined contained biofilm whereas they were present in only 1 of 16 acute wounds sampled. Scientific research often examines biofilm formed by one type of bacteria *in vitro* but clinical research such as this has noted that wound biofilm is usually polymicrobial. Recently, research groups in the US and Europe (Bjarnsholt et al., 2008) also observed biofilm microscopically in approximately 60% of all chronic wounds and suggested that it is implicated in at least 80% of all human bacterial infections (Nusbaum et al., 2012).

There is still controversy amongst some as to whether biofilm can actually be seen in wounds. In the *Journal of Wound Care* in 2010 three of the world's leading researchers on biofilms told an audience that, in their view, biofilms are the main cause of wound chronicity (Cowan, 2011). And yet in 2012 Professors Keith Cutting and Richard White submitted differing articles on how "*there is, as yet, no*

*conclusive clinical or in vivo proof that wound biofilms exist*" (Cutting and White, 2012; Cowan, 2012). Some clinical cues which may be indicative of biofilm presence are (Metcalf et al., 2014; Percival et al., 2012):

- Excessive moisture
- Poor quality granulation tissue
- Signs of local infection
- A history of antibiotic failure, or recurring infection as therapy ceases
- Culture-negative swabs despite clinical suspicions
- Wound remaining recalcitrant despite antimicrobial interventions
- Malodour
- Polymicrobial microbiology

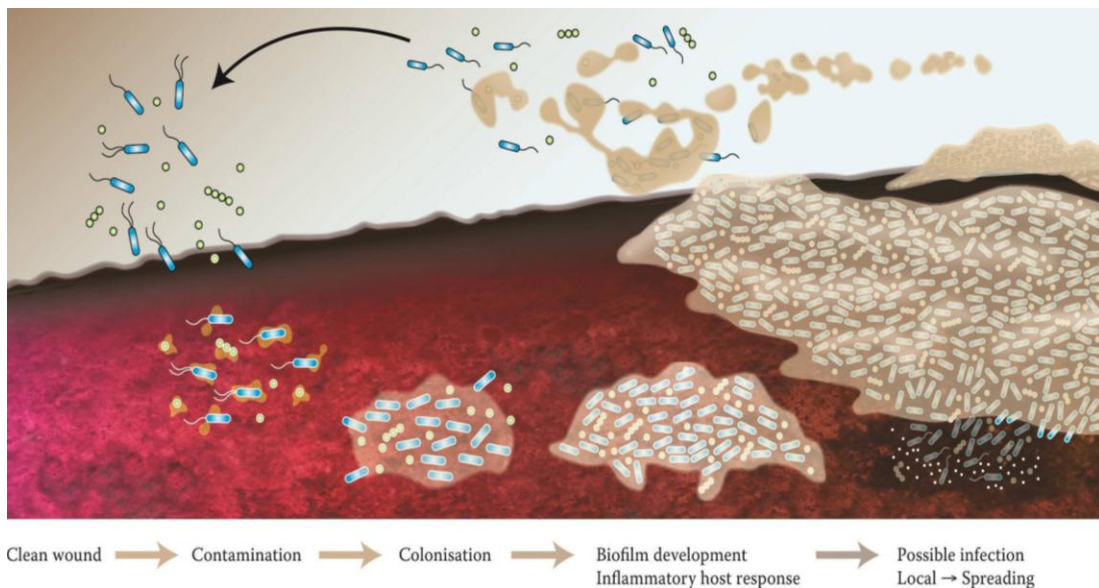


**Figure 1.7: Schematic stages of biofilm formation within a wound**

If a host is compromised biofilm may form and this progresses in steps. Planktonic bacteria become irreversibly attached to the surface and begin to excrete EPS, forming a protective matrix in which microcolonies can grow, to eventually produce a mature biofilm with further dispersal of bacteria (by kind permission, Dr. Daniel Metcalf, ConvaTec Ltd, 2014)

## 1.14 The management of wounds

Health care has increasingly become patient-centred, involving a balance of medical treatment with the rights and needs of a patient, as well as the responsibilities of all the stake holders and constituents in the health care system (Omi, 2007). Clinicians, healthcare organisations and industry all have important roles in ensuring that care is delivered effectively and takes account of the complex needs of individuals living with wounds (Wounds International, 2012 International Consensus). The risk of a wound becoming infected will be increased in any condition that will cause debilitation, immune suppression or decreased vascular supply, such as renal impairment, circulatory disease, respiratory disease, obesity, malnutrition, rheumatoid arthritis, steroid treatment, malignancy, or poor personal hygiene (Guo and Dipietro, 2010). A challenge with examining wounds in a clinical setting is that some patients may present to a clinic with infected wounds that may have been present for varying times and may have had previous antimicrobial treatment as well as antibiotics. There is no doubt that there is growing microbial resistance to antibiotics when used over long periods (Malik et al., 2013). Inefficient eradication of the the infecting pathogens may also contribute to a lack of wound healing (Bjarnsholt et al., (2008).

Four factors are important in patient wound care:

### I. Inflammation

By forming a biofilm matrix, microbial cells can also escape engulfment by host defences. Mammalian host phagocytic cells have difficulty ingesting them because

they are within this complex structure and often firmly attached to a surface (Ma et al., 2009). The polysaccharide component also blocks complement activation (Percival and Bowler, 2004; Malik et al., 2013). The structure of biofilm is such that only the exposed surface bacteria can be efficiently attacked by the host response. Biofilm releases antigens which stimulate the production of antibodies from the host, but these antibodies will only respond to the surface antigens and will often fail to penetrate into the matrix of the biofilm and will cause host tissue damage (Davis et al., 2006). The host's polymorphonucleocytes, in response to not being able to ingest biofilm, will release pro-inflammatory enzymes, proteases (e.g. matrix metalloproteinases and cytokines). This chronic inflammatory response unfortunately does not destroy the biofilm, but causes more damage to the surrounding host tissue (Hurlow and Bowler, 2009). This in turn becomes inflamed and susceptible to bacterial attack and hence more biofilm growth and, whereas the biofilm is thought to re-grow quickly, the host tissue is much slower to reform (Percival and Bowler, 2004). With host tissue damage present, it is difficult to treat the patient without causing more trauma and pain (Figure 1.8).

Research into fibroblasts by Pastar et al., (2013) has shown that they produce keratinocyte growth factor 1 which can act via a receptor, found on keratinocytes, to produce increased proliferation in wound healing and epithelial growth.

Suppression of keratinocyte growth factor 1 and other factors, by the presence of a mixed species biofilm in a porcine *in vivo* model, reduced the keratinocyte migration and proliferation, delaying wound healing. Suppression was found to be

higher in polymicrobial wounds compared to that produced by single species biofilm (Pastar et al., 2013).

## II. Exudate

By inducing an inflammatory response, the bacterial biofilm encourages the wound to produce more exudate (Parsons and Metcalf, 2014). Exudate effectively acts as a culture medium, supplying the bacteria with moisture and nutrients. Hence, if there is excessive, uncontrolled moisture in a wound it is likely to be supporting biofilm. Effective exudate management can promote healing (Keast et al., 2014).

Exudate is an aqueous fluid usually with a composition of protein-degrading enzymes, electrolytes and nutrients, growth factors and cells which can support cell proliferation and assist healing in an acute wound (Miller-Keane Encyclopedia and Dictionary of Medicine, 2003). Some moisture is conducive to healing but when exudate becomes excessive in a chronic wound it can be corrosive and prevent a wound from healing (Bianchi, 2012). New devices and techniques (pumps and dressings) in negative wound pressure therapy have been developed, to help control exudate in wounds, with the intention of preparing the wound bed for closure, and promoting granulation tissue formation (Gupta et al., 2007). This technique utilises a sealed dressing with a vacuum pump, which applies controlled, sub-atmospheric pressure to the surface of a wound, which draws out the exudate.

## III. Debridement

Dental plaque biofilm on teeth, gums and the tongue can be removed by regularly brushing and flossing to help prevent tooth decay and gum disease. Logic would



therefore dictate that the removal of wound biofilm would help an infected wound to heal. Clinical procedures recommend the removal of devitalised tissue, slough, fibrin, or infected tissue by trained, qualified nurses, as part of a regime of biofilm based wound care, although there appears to have been few randomized controlled trials that show that debridement speeds healing or reduces infection in chronic wounds (Edwards and Stapley, 2010) as they are challenging to conduct. Wolcott et al., (2008) performed a retrospective study on diabetic limb ulcer patients which included the use of debridement and antibiofilm agents of xylitol and lactoferrin and concluded that biofilm based wound care significantly increased healing rates in patients. Debridement of a wound to remove unwanted tissues (including biofilm, when present) can be done in different ways and several techniques are employed in the clinical environment.

Mechanical debridement with saline wet-to-dry dressings is not considered an effective debridement, but irrigation with safe irrigating fluids can be used (Keast and Lindholm, 2012). Sharp debridement employs the use of a clinical implement such as a curette or sharp blade by qualified nurses. Other methods include enzymatic debridement (Ramundo and Gray, 2011), high-pressure irrigation, ultrasonication, or applying a dressing that pertains to helping break up biofilm, creating a balanced level of moisture, and promoting autolytic debridement. Debriding cloths or pads, based on newer monofilament fibre technology (Haemmerle et al., 2011), have been recommended for use in clinics (Meads et al., 2015). Methods including hydro-surgery and ultrasound are expensive to use and require specific skills (Sainsbury, 2009). The method used will depend upon the patient's pain

tolerance levels (and possible suitability for anaesthesia) and the anatomical location, as well as the particular clinic's preference and nurse qualifications.

In 2009 Lead Researcher, Professor Keith Harding, from the Welsh Wound Innovation Centre, teamed up with a commercial producer of medicinal-quality larvae for a 12-month trial with 200 patients across 8 hospitals, to examine the efficiency of maggots at debriding wounds (Mudge et al., 2014). The larval treatment in this study was shown to be more effective at debriding the wound than hydrogel alone. Although maggot therapy is an ancient method (Sherman et al., 2000) it is the research into larval secretions that has had resurgence in research (Smith et al., 2006); a topic even discussed in a House of Commons debate in 2007, such is the need to find replacements for failing antibiotic therapy.

There is still some debate as to whether slough, found on the surface of an exposed wound, is linked to, comprised of, a component of, or a consequence of biofilm. Research is still on-going into its precise nature, but if slough is seen in a wound there is a possibility that it is due to the presence of biofilm, and thus the wound is usually treated as such (White, 2011). Slough is relatively easy to remove in most patients with dry gauze (Hurlow and Bowler, 2009), but if it is adjoining the underlying wound tissue it can be more difficult to remove. The material observed in a wound may be a combination of slough, biofilm, host devitalised tissue and fibrin (Metcalf et al., 2014). No method as yet debrides a wound completely of bacteria, so biofilm will still be likely to exist (Young, 2011). Debridement must therefore be done regularly for some wounds (Wolcott et al., 2009) and as such should be performed by qualified experienced healthcare workers. Skilful film

removal can inflict minimal harm to the wound bed, and in some wounds thick film can be removed almost completely in one piece (Hurlow and Bowler, 2009). Even the most experienced of clinical staff will find it difficult to distinguish biofilm in a necrotic wound from slough.

#### IV. Pain

Pain, associated with other inflammatory factors such as redness, odour, swelling or heat in a wound, can be indicative of the presence of a biofilm (Metcalf et al., 2014). Biofilm can be a precursor to infection and, if associated with a history of recurrence and antibiotic failure, a wound should be treated as biofilm-compromised (WUWHS, 2008). Operational pain (the pain caused when a dressing is changed or during debridement) can cause trauma to the wound and the patient. This acute wound pain has been the focus of dressing related procedures as in the European Wound Management Association Position documents (EWMA 2002-2008). These documents, and other similar documents, aim at giving strategies to assist in dressing application, removal and change. Some patients have been found to suffer with pain for 2 hours after the application of dressings (Tredget et al., 2002). The introduction of hydrocolloid based dressings has been noted to alleviate the pain and discomfort suffered by patients (Percival and Bowler, 2004).



**Figure 1.8: A stage IV pressure ulcer with a heavily colonised wound bed**  
Stage IV pressure ulcers are described as full thickness tissue loss with exposed bone, tendon or muscle. Slough or eschar may be present on some parts of the wound bed. In this image there may be a thin layer of suspected biofilm over some of the wound bed, particularly on the right side of the wound where this substance appears to be slightly thicker and opaque (by kind permission, Dr. Daniel Metcalf, ConvaTec Ltd, 2014)

### **1.15 Skin Treatments and Wound Dressings**

In clinical practice there are recommendations in the use of various wound care accessory products to treat wounds. Topical formulations such as sugar paste have long been used in some countries for pressure ulcers (Biswas et al., 2010),

as it creates low water activity and inhibits microbial growth. In an *in-vitro* study, plasma coagulation was said to be inhibited at 70% sucrose, while attachment of *S. aureus* was suppressed in the presence of 10% NaCl or 10% sea salt, and atopic dermatitis lesions were suppressed by 5% zinc oxide (Akiyama et al., 1998).

Skin cleansers may be considered for use around the wound to clear the peri-wound region of contaminants but must not be used on the actual wound. Ideally the act of wound cleansing should be performed prior to debridement to aid inspection of the wound, and then post-debridement (Wolcott and Fletcher, 2014). A cleanser should help prevent infection while doing no harm. Water is as effective as saline but tap water purity is an issue (Fernandez and Griffiths, 2012). Sodium hypochlorite solutions, chlorhexidine, potassium permanganate and dilute acetic acid use remains controversial, but in resource-poor settings they may be the only available means of managing bioburden in chronic wounds (Keast and Lindholm, 2012). Hypochlorous acid cleansing solution is available commercially based on the fact that immune cells produce hypochlorous acid in their defence mechanisms (Bullough and White, 2014).

Skin moisturisers can be used to hydrate, soften and protect the skin, whilst moisture barrier ointment can add protection from infection by other bodily fluids. They typically contain zinc to help dry the denuded skin, dimethicone to provide a protective layer and petrolatum providing a resistant layer (Wound Source Overview, 2016).

Gauze type dressings were used for many years, but in recent decades there has been much research into the use of other types of wound dressings. Many new dressings are available on the market and these provide functions such as protection from further injury or infection, together with providing an environment with conditions necessary to promote healing. According to the Wirral Community NHS Trust 2013 Wound Management Formulary and Guidelines the dressing choice is determined by a number of factors. These guidelines are similar to many in the U.K.:

- level of exudate
- tissue type
- depth of wound
- anatomical location
- malodour
- condition of peri-lesion skin
- pain
- quality of life
- activities of daily living
- fragility of skin
- temperature

The requirements of a wound dressing will often depend upon

- bacteria colonising the wound
- the amount of exudate and if negative wound pressure therapy is required
- its ability to help debride the wound and

- the patient health status

There are a plethora of different wound dressings available to clinics which can vary in materials, structure, absorbency, antimicrobial formulation, and the nature of attachment to the tissue surrounding the wound, an area which can be vulnerable. Typical antimicrobials in dressings include silver, iodine, honey and polyhexamethylene biguanide. The choice is sometimes ultimately what is available in a clinic. Ideally the clinic should be patient centred/empowered and achieving the highest quality of care. Often the reality is that the necessity to change dressings on a regular basis drives up the perceived cost of dressing usage, particularly if the dressings do not effectively support wound progression, and points to choice based upon financial restraints (Oates et al., 2014).

### **1.16 Investigating the Efficacy of Novel Dressings**

So where could future research lead us and how could it help to prevent and reduce the presence of biofilms, therefore reducing infected and chronic wounds in a clinical situation? How quickly does the biofilm form in a situation where there is constant exudate and a risk of infection even after debridement in a wound? One main thrust of some of the novel dressings that have been introduced in recent years, is their ability to form a gel matrix on contact with wound exudate and absorb it or, if containing antimicrobial agents, to kill any bacteria present. How effective are they against not only planktonic bacteria, but against biofilm

microorganisms, and in the prevention of biofilm formation or re-formation? Various dressings claim to be the best at tackling biofilm, but at what stage should these often more expensive dressings be considered to best suit both the patient and the clinic's budget, and for how long can these dressings remain in place on the wound before they become ineffective?

These are some of the questions that this research aims to address.

### **1.17 Aims and Hypothesis**

The presence of biofilm is now acknowledged to be one of the leading causes of delayed wound healing and wound infection, so effective anti-biofilm products are urgently required to improve standards of care (Bjarnsholt et al., 2008). The aim of this work was firstly to investigate the structure and development of wound pathogen biofilm *in vitro*, and to structurally differentiate between biofilm-associated organisms and their planktonic counterparts. Secondly, a novel, challenging *in vitro* simulated chronic wound model was developed that could be processed intact, and examined by a combination of Light Microscopy (LM), Transmission Electron Microscopy (TEM), Scanning Electron Microscopy (SEM) and Confocal Laser Scanning Microscopy (CLSM). Finally, the model was used to evaluate the antimicrobial and anti-biofilm effectiveness of several current wound dressings by these microscopical methods. By quantifying the amount of microbial growth, the dressings were evaluated to compare the respective dressings, as well as demonstrating which dressings were the most effective against biofilm



formation, the null hypothesis being that there is no difference in biofilm growth between the different dressings and all antimicrobial dressings are as effective as each other. Such research might provide further evidence to help clinicians have a greater understanding of which is the most appropriate antimicrobial dressing to apply to a chronic non-healing wound, in which a biofilm presence is suspected. This could help create appropriate wound care treatments to kill biofilm bacteria and/or prevent biofilm re-formation as part of protocols of care in more effective wound management. Overall these studies aimed to show how specific biofilm-forming wound pathogens can be controlled by the application of specifically targeted topical medical devices.

The main aims of this study were:

- To obtain the best methods of preservation and processing, for the visualisation of bacteria by various microscopy techniques;
- to trial surfaces for suitability for use with all the microscopy methods and to use one to develop a novel, challenging *in vitro* model for growing biofilm;
- to use the model to test the efficacy of different dressings against biofilm formation.

# **Chapter 2**

**Microscopy protocols, evaluation of surfaces  
and development of a biofilm wound model**

## 2.1 Introduction

### 2.1.1 The choice of organisms for *in vitro* studies

The bacterial species chosen for these studies *Pseudomonas aeruginosa* (*P. aeruginosa*) and *Staphylococcus aureus* (*S. aureus*).

*P. aeruginosa* is a ubiquitous opportunistic human pathogen and has been used in many laboratory studies (Gómez and Prince, 2007; Brockhurst et al., 2005). It is a Gram-negative rod shaped bacterium, which, although usually found growing in an aerobic environment, is capable of adapting to proliferate in situations where oxygen is partially or totally depleted (O'Neil et al., 2003). *P. aeruginosa* has a large number of genes involved in catabolism, transport and the efflux of organic compounds, and its genome complexity and virulence factors allow it to adapt and thrive in a diverse range of environments, and to resist antimicrobial substances (Stover et al, 2000).

*P. aeruginosa* is the most common gram-negative bacterium found in nosocomial infections (Delden and Iglewski, 1998), it has accounted for over 1 in 10 of all hospital-acquired infections (NNIS, 2004), and an additional 10-60% of infections may present after discharge (IFIC, 2011). *P. aeruginosa* outbreaks in burn units have been associated with high (60%) death rates (Chamoux et al., 1994). The International Federation of Infection control (IFIC) states that it has survival rates on dry surfaces of between 6 hours to 16 months, and that a European Centre for Disease Prevention and Control (ECDC) survey involving 12 countries in 2008 found 18.2% of ICU-acquired pneumonia was associated with *P. aeruginosa*, as well as catheter associated urinary tract infections. It is often associated with

infections of immunocompromised patients, particularly those suffering from AIDS, or severe burn wounds (Whitehead et al., 2001), and undergoes genetic change during chronic airway infection of cystic fibrosis patients (D'argenio et al., 2007). Although an uncommon cause of community-acquired pneumonia, *P. aeruginosa* is a common cause of hospital-acquired pneumonia. This is associated with the mechanical ventilation that is a necessity for patients with respiratory difficulties. Oxygen exposure vastly increases the occurrence of *P. aeruginosa* infections (Fujitani et al., 2011). *P. aeruginosa* produces a diverse array of virulence factors but usually requires a substantial break in the host defences, such as damage to a normal barrier (e.g. mucosal or epithelial), disruption of the normal host flora, or a lowering in the normal host immune defence (Delden and Iglewski, 1998). Once compromised, disease may establish, especially in the biofilm mode of growth, which impairs antibiotic activity (Fux et al., 2005). Virulence factors include exotoxins such as pyocyanin, alkaline phosphatase, elastase, exotoxin A, exoenzyme S and phospholipases, lipopolysaccharide, alginate, adhesions (Seth et al., 2012, Bomberger et al., 2009).

Following severe thermal injury, the damage to the skin compromises the patient's immune defences to sub-protective levels due to the burn causing extensive breaches in the skin barrier, and hence the compromise of host defence (Felts et al., 1999). One of the main survival strategies of *P. aeruginosa* in hostile environments (Bjarnsholt et al., 2008) is to form its mucoid, alginate biofilm creating a three-dimensional structure, (Nivens et al., 2001). It acts as a scavenger of free oxygen radicals, which may favour survival (Simpson et al., 1989). It also

prevents phagocytosis, and reduced diffusion and activity of antimicrobials (Allison et al., 1992).

*S. aureus* is a similarly ubiquitous bacterium and is a Gram-positive coccus found on skin and in wounds. It is renowned for being associated with hospital acquired infections, especially in the form of methicillin-resistant *S. aureus* (MRSA), a so called 'superbug' (Foster, 2004). It has been demonstrated to produce a variety of virulence factors, which help with adhesion, secretion and the organism's pathogenic ability to inactivate and evade the hosts defence systems (Dunman et al., 2001). It can produce numerous toxins that can cause unique presentations such as toxic shock syndrome (Kuroda et al., 2001). It's many virulence factors include membranes damaging toxins (leukotoxins, leukocidins, hemolysin, lipase), exotoxins (TSST, EFT, SEA-G, toxin 1, cytolytins, serine proteases, cysteine proteases, aureolysin), phagocytic inhibitors (protein A, coagulase) and invasins (hyaluronidase, staphylokinase) (Jarraud et al., 2002).

It is the second most frequent cause of nosocomial blood infections, accounting for 13% of blood infections. Wertheim et al., (2004) studied 14,000 patients carrying nosocomial *S. aureus*, and found they were three times more likely to develop bacteraemia, although bacteraemia-related death was higher in non carriers than carriers. *S. aureus* is usually controlled by the host immune response (Archer et al., 2011), but the immunocompromised host will be more susceptible to nosocomial infection than the normal host. If an internal epithelial breach occurs, it can spread via the circulatory system, and catheter-related infections can pose a serious threat of sepsis, with a mortality rate of up to 25% (Hann and Raad, 2005).

Immunosuppressed patients, such as cancer patients, are at high risk of sepsis (Danai et al., 2006). In humans, *S. aureus* is often present in the anterior nares, such that approximately 25% of populations are persistently colonized (Boost et al., 2008). The nasal carriage provides an opportunity for these bacteria to disseminate to other areas of the body (Brown et al., 2013). Preoperative nasal carriage of *S. aureus* has been identified as a significant risk factor in patients developing wound infections. A study of almost 2000 patients found that *S. aureus* was present in swabs from sternal wounds of 40 patients after cardiac surgery (Kluytmans et al., 1995). It has been reported as a predominant organism in many clinical investigations, with its presence being indicated in 43-88% of leg ulcers (Fazli et al., 2009), and is most commonly found in chronic wounds (Halcón and Milkus, 2004). The *S. aureus* bacterial biofilm is a matrix composed primarily of exopolysaccharides such as polysaccharide intercellular adhesion, which can significantly reduce the penetration and activity of glycopeptides such as Vancomycin (Chang et al., 2003).

*P. aeruginosa* and *S. aureus* are common wound pathogens and are often associated with delayed healing and infection (Oates et al., 2014). These specific strains are known to produce potent virulence factors and proteases that destroy tissue and impair healing (Koziel et al., 2013). What is important to a clinic, is that these bacteria are more tolerant or resistant to antimicrobial treatment in the biofilm form than in the planktonic form. Most antibiotics target a specific cellular or metabolic function and bacteria can adapt genetically to become resistant.

Antiseptics target more areas on a microbes surface and hence it is less likely to

become resistant to antiseptics as it would have to adapt by changing multicellular areas. As mentioned in Chapter 1, biofilm is protected physically by EPS. Due to microbes being embedded deep within this biofilm structure, and where there is more likely to be concentrations of molecules and changing pH, bacterial biofilm can become tolerant. These areas of biofilm therefore present many challenges to effective clinical treatment.

One reason for biofilm resistance may simply be that some antibiotics, like penicillin, target cell wall synthesis and kill bacteria that are actively growing, those near to or on the surface, but cannot kill those in a sessile state deeper within the biofilm (Costerton et al., 1999). These persister cells may survive and hence are tolerant to antibiotics without undergoing genetic change, and can result in relapse of persistent infections.

Consequently, along with their escalating involvement in infections, their exhibition of multiple-antibiotic resistance, and their ability to transform an acute infection to one that is persistent, chronic and recurrent, especially in wounds, this warrants these particular bacteria a considerable amount of attention (Wong et al., 2013).

This indicates the reason for choosing these two bacteria for the *in vitro* studies of this thesis.

### **2.1.2 Preliminary techniques and preparation of bacteria for microscopy**

Understanding and visualising the differences between planktonic and biofilm bacteria are important considerations when discussing bacterial tolerance.

As part of this thesis, basic microbiology techniques were used to ensure good quality results, and this was an essential first step. The preliminary experiments of the project therefore concentrated on microbiological techniques that included learning aseptic methods, autoclaving, and the plating of cultures to maintain a constant supply of available and viable bacteria. Once achieved, the growth and physiology of chosen bacteria for these studies were examined, including the monitoring of growth of a bacterial culture to determine harvesting points accurately.

A variety of fixation and processing protocols were employed in order to prepare samples for the microscopy techniques to be used in the study, and to optimise high quality images of planktonic cells. These included preparation for Transmission Electron Microscopy (TEM) and Scanning Electron Microscopy (SEM). Bacteria were prepared for TEM and SEM, in order to observe the external structural appearance of planktonic cells. This was in preparation for later sections of this Chapter, when the structure and development of biofilm was investigated, so that suitable protocols would be available to determine differences in appearance between planktonic and biofilm bacteria.

Several explanations have been put forward as to why microbial biofilms are more tolerant to antimicrobials than planktonic bacteria, and some studies have attempted to compare the susceptibilities of both types (Cerca et al., 2005). An antimicrobial is defined as an agent that kills microorganisms or inhibits their growth, and antimicrobial agents have been used for many years in the preservation of food (Delaquis, and Mazza, 1995). Natural remedies include acetic



and lactic acid as well as sulphites, and many herbs are known to have some antimicrobial properties, especially in the form of their essential oil. Other natural remedies include sugar paste and honey. A well-known antimicrobial is silver. As silver is used in many modern wound dressings claiming antimicrobial properties (Newman et al., 2006), silver nitrate was chosen as a suitable antimicrobial for the demonstration of the effects on bacterial growth in planktonic cultures of this study. The effect of the addition of silver nitrate was studied on planktonic bacteria and with TEM, to demonstrate the changes induced in bacteria treated with an antimicrobial agent.

### **2.1.3 Establishing and characterising a biofilm**

A biofilm is defined as being a community attached to a surface and enclosed in a matrix of EPS, and its formation is a multi-step process from attachment, to micro-colony, to maturation, and detachment (Snyder et al., 2009). The bacterial concentration for the initiation of growth of a biofilm appears to differ in the literature and ultimately appears to be the choice of the researcher. Loh et al., (2009) and Walker et al., (2011) started with a concentration of  $10^5$  cells/ml, whilst Percival et al., (2008) used  $10^6$ . However, many do not state the concentration. Preliminary work in this study required the investigation of growing varied initial concentrations of bacteria, to ascertain if an optimal concentration was needed to form a biofilm.

Another consideration is how quickly a biofilm is likely to form under the right conditions. Planktonic bacteria attach to a surface and develop an initial EPS.

Some suggest that this growth can occur within hours (Phillips et al., 2010; Koseki, 2014). Others state that biofilm only forms after 24 hours (Proal, 2008). This raised the question, should biofilm growth only be studied and observed after 24, 48 or even 72 hours, as most studies are performed, or should it be from as early as 1-3 hours? If bacterial growth could be visualized in the earliest hours, then it would be possible to ascertain how quickly bacteria start to group together in the first stages of biofilm formation. This would possibly present the best start time for future growth experiments.

It is suggested that a biofilm may be able to grow on just about any surface given the opportunity: rocks in streams, ship hulls, pipelines, catheters, implants, and on internal and external living tissue (Dunne, 2002). Any surface placed into a fluid environment acquires a conditioning film, comprised of primarily proteinaceous material that is present from that fluid (Donlan, 2001). A surface coated with a protein or mucin is classed as conditioned, and on this surface, a biofilm may develop (O'Toole, 2000). However, in order to visualise a series of grown biofilms with the respective microscopy techniques, any surface for this study needed to be suitable to grow a biofilm, yet still be able to survive the preparatory techniques in Light Microscopy (LM), Transmission Electron Microscopy (TEM), Scanning Electron Microscopy (SEM) and Confocal Laser Scanning Microscopy (CLSM). The processing methods for these techniques are different from each other and most include the use of agitation and harsh chemicals. For this reason, various surfaces, some more tried and tested than

others in research studies, would be investigated for their suitability to promote biofilm growth.

Glass is one of the most common surfaces on which to grow a biofilm, and studies have included glass tubing (Davies et al., 1993, Stoodley et al., 1999, Wilson, 1999), glass slides (Lawrence et al., 1991; Lewis, 2001, Prakash et al., 2003) and glass coverslips (Lembke et al., 2006; Khan et al., 2012), the latter used probably because they are easy to obtain and relatively inexpensive. Glass surfaces such as these lend themselves well to CLSM and SEM methods that are often used in biofilm studies. Glass was an adequate surface to use for the preliminary biofilm growth experiments, but due to initial difficulties with the glass coverslips this required changing methods to a more suitable surface.

According to some, the quality of a surface used to grow biofilms can decide the time course of attachment (Hänsch, 2012; Zeraik and Nitschke, 2012). Although bacteria attach readily to surfaces such as glass, many investigations have reported that bacteria can attach more rapidly to nonpolar surfaces, such as plastics (Donlan, 2002), and that *S. aureus* and *P. aeruginosa*, in particular, attach to strongly hydrophobic surfaces (Sinde and Carballo 2000).

Thermanox™ plastic coverslips have been used extensively in studies into biofilm growth (Sladek et al., 2007; Braga et al., 2008; Espinal et al., 2012), and are more pliable than glass which may make them more preferable for use. Therefore in this series of experiments as well as evaluating biofilm growth, an inoculum concentration for future studies was also performed using plastic coverslips, as

well as some studies to evaluate initial biofilm growth over an initial six hour period. However, other surfaces were required to be tested that would be more adaptable in the differing methods of microscopy (LM, TEM, SEM and CLSM) used in the study.

During these studies “slough-like” material was observed in some of the early studies and therefore it is important to differentiate this term from biofilm. Some clinicians use the terms “biofilm” and “slough” interchangeably, and incorrectly. However, biofilm is defined as a **living** community attached to a surface and enclosed in a matrix of EPS, and its formation is a multi-step process from attachment to microcolony, to maturation and detachment (Snyder et al., 2009). Slough on the other hand is defined as ‘a mass of **dead** tissue in, or cast out from, living tissue’ (Medical Dictionary, thefreedictionary.com). The World Union of Wound Healing Societies and the European Wound Management Association positioning papers always associate slough with necrotic tissue (World Union of Wound Healing Societies’ Expert Working Group, 2004, 2007, 2008) . However, some researchers have stated that, by using quorum sensing, the biofilm is detached and dispersed, and that this is “slough” (Rice et al., 2005). Some propose that programmed host cell death and autolysis are critical for the proper timing of biofilm development and dispersion, suggesting that a lot of the slough will contain dead cells as well as biofilm (Ma et al., 2009).

When biofilm is grown, using even small quantities of nutrient broth, a layer of “slough-like material” (possibly flocculated biofilm waste) may appear on the surface. Distinguishing between actual biofilm and this slough-like material, by

comparing methods of collection of biofilm growth on coverslips, was necessary to confirm what would constitute true biofilm growth on various model systems.

Processing techniques for microscopy often include agitation, which can cause the removal of biofilm and from the surface of a sample. Wrapping small histological samples in specialist tissue paper, or containing them in fine mesh containers, improves retention of friable tissues. However, these techniques do not prevent the moving of surfaces that are friable, but merely aim to contain the fragments with the main specimen. In order to prevent moving and detachment of biofilm from a surface, the surface of biofilm needs a protective cover.

In order to process very small and cytological samples into paraffin wax or resin, routine histological laboratories (in light and electron microscopy methods) commonly use agar or low melting point agarose. Agarose, in the warm liquid phase (melting point of 37°C, as opposed to agar's 45°C), can be poured on to, and mixed with, samples and allowed to set before processing. Pouring the liquid phase agar over biofilm might allow for the processing of biofilm whilst it is intact. If biofilm could survive the technique on a suitable surface, it may be possible to compare the structure of biofilm as it grows by LM and TEM methods with those of SEM.

In a natural environment, bacteria frequently form biofilm. Many different models have been used to try to mimic this environment, some *in vivo*, some *in vitro*. *In vivo* work has favoured the porcine, murine and lupine wound models (Sullivan et al., 2001), of which there are many examples (Roche et al., 2012; Phillips et al.,

2013; Gurjala et al., 2011; Thompson et al., 2014; Walton et al., 2014), but practical, ethical and moral concerns have made *in vitro* models an indispensable tool. There is a need for effective models, in the studying of biofilm and their infections, for testing novel dressings and other therapeutics methods. The use of data collection by non-invasive techniques is of substantial interest in order to decrease the number of animal numbers required for testing (Walton et al., 2014). Examples of *in vitro* models have been varied. Some models have involved glass and/or plastic such as the Lubbock model (Sun et al., 2008). This model was simple in surface but the media was complex, containing various broths and a chopped meat-based media formulation. Others have used various growth chambers, such as Thorn and Greenman (2009), which included cellulose support matrices and used a system relying on eluates to ascertain the growth rate. Some have used gels, such as that examined by Gilbert et al (1998), who grew *P. aeruginosa* on poloxamer hydrogel and found it mimicked many of the properties of other biofilm types grown *in vitro*. Poloxamer is a thermo-reversible matrix that is inert and non-ionic and can be dissolved in medium at temperature below 15°C. Once the temperature is increased to 37°C the matrix becomes semi-solid. This can then be reversed, which allows recovery and analysis of the biofilm (Benjamin et al., 2016). Clutterbuck et al., (2007) suggested that this model could be an alternative medium on which to conduct antibiotic susceptibility testing and Percival et al. (2007) used it to test silver dressings.

Although many of these models have had SEM or TEM performed upon them, the structure of biofilm in relation to testing a wound dressing is not always the primary result required. Once the examination of the growth and structure of biofilm in this study was complete and understood, the intention of the final series of studies in this section was to evaluate a new, and novel, *in vitro* model that could be addressed by the various modes of microscopy, and specifically to examine the effect of dressings upon biofilm development (the subject matter of Chapter 3).

## **2.2 Aims and objectives**

In order to observe biofilm in later studies planktonic bacteria were examined, and the best methods for their growth and visualisation by the various microscopy techniques were determined. A range of surfaces were evaluated for their suitability to be used in subsequent *in vitro* studies to develop a model to be used to evaluate antibacterial wound care dressings.

Specifically the following objectives were proposed:

- To demonstrate the physiology of growth cultures to find the exponential point, and the effect of the addition of an antimicrobial agent
- To find a suitable processing protocols and observe planktonic bacteria by LM, TEM, SEM
- To observe the effect of silver nitrate on bacterial ultrastructure by TEM
- To establish an appropriate concentration of bacteria to provide a confluent biofilm

- To investigate the stages of initial biofilm growth
- To examine surface-associated material from the surface of nutrient
- To evaluate physical surfaces that would allow adequate biofilm growth
- To process biofilm intact for all microscopy methods microscopy (i.e. LM, TEM, SEM, and for viewing with CLSM)
- To evaluate a novel *in vitro* 'biological' wound model ( the subject of a more in depth appraisal in Chapter 3)

## **2.3 Materials and Methods**

### **2.3.1 Media preparation and maintenance of cultures**

Cultures of *P. aeruginosa* (NCIMB 8626) and *S. aureus* (NCIMB 9518), used for this study, were maintained on plates of tryptone soy broth (TSB, 30g/L, Lab M, Bury, UK) in 2% w/v agar (Oxoid Ltd., Basingstoke, UK) (Appendix 1). Initial growth was at 37°C overnight, with storage afterwards at 4°C. The appropriate quantity of media (TSB for culture studies or TSB and agar for culture plates) was weighed, and dissolved, in deionised water in flasks (Thermo Fisher Scientific, Loughborough, UK). The mouth of flasks were plugged with cotton wool, and covered with aluminium foil, then placed in an autoclave (Dixons Express Autoclave, Dixons Surgical Ltd, Wickford, UK) for sterilisation of the media at 121°C for 15 minutes (Appendix 2). Flasks of TSB media were removed and stored at 4°C, 20ml of the TSB/agar media was poured into sterile Petri dishes (ThermoFisher, Loughborough, UK), and allowed to solidify, then stored at 4°C.



### **2.3.2 Overnight cultures and exponential growth of planktonic bacteria**

For growing an overnight culture, a flask containing a 50 ml volume of TSB was prepared. The flask was inoculated with either *P. aeruginosa* or *S. aureus* by a plastic disposable, sterile loop (ThermoFisher, Loughborough, UK), from a previously grown, plated culture. Incubation was in a water bath (Grant Instruments, Royston, UK) at 37°C with aeration supplied via a pipette and tubing attached to an air pump (Dymax 5, Charles Austen Pumps Ltd, West Byfleet, UK). For exponential growth, fresh medium (100 ml) was inoculated with a 1/200 dilution from an overnight culture and growth monitored with a spectrophotometer (Helios Epsilon wavelength 610nm, Thermo Fisher Scientific, Loughborough, UK). Use of spectrophotometry is a common procedure to measure bacterial density. The spectrophotometer gives a measure of light absorbance, which is directly proportional to the bacterial density. The data consisted of measurements of bacterial population density at 20 minute time points and continued until the measurements decreased in steps which indicated a slowing down in bacteria growth. The growth curves served as a guide to the estimated number of organisms in a culture, in order to estimate more accurately the exponential growth point for each experiment. The growth rate was monitored by estimation of optical density.

### **2.3.3 Planktonic growth cultures and effect of silver**

1/200 dilution of overnight cultures of *P. aeruginosa* and *S. aureus* were introduced into fresh TSB flasks (4 x 100 ml, for each bacterial culture). After 2 hours 20

minutes (*P. aeruginosa*) and 2 hours (*S. aureus*) (see Results Section 2.4.1), the exponentially growing cultures were treated as follows:

- (1) Control cultures – No change. Continued growth for a further 4 hours at 37°C.
- (2) Cultures treated with silver –1 ml of silver nitrate (Sigma-Aldrich, Gillingham, UK) added (stock sol. 1 mg/ml, final concentration in TSB culture 10 µg/ml) for 4 hours at 37°C.

2 ml aliquots of culture were taken from the cultures at 20 minute intervals over 6 hours, and the optical density as absorbance measured in a spectrophotometer.

#### **2.3.4 Fixation and harvesting of planktonic bacteria for TEM**

For TEM *P. aeruginosa* and *S. aureus* were cultured in separate flasks of TSB (2 x 100 ml for each bacterial culture), and treated as a control or treated with silver as in 2.3.3 above. Growth was continued in both flasks for 1 hour. The flask treated with silver nitrate was fixed in a final dilution of 2.5% v/v glutaraldehyde (25% v/v stock solution, TAAB Laboratories Equipment Ltd., Reading, UK).

The contents of the control flask was divided into six Universal containers (Thermo Fisher Scientific, Loughborough, UK). Each container was allocated one fixative protocol from the list below, to give a total of six different types of fixation, in order to choose the best protocol for future use. The fixatives were prepared in Ryter-Kellenberger (RK) buffer (Ryter et al., 1958; Appendix 3). Bacteria were harvested from the cultures by a filtration system attached to a vacuum mechanism (Hobot et

al., 1985). A cellulose nitrate filter, 47 mm diameter, pore size 0.2  $\mu\text{m}$ , (Whatman, Thermo Fisher Scientific, Loughborough, UK) which is smaller than the organism to be captured was used. Some of the culture was poured in – enough to fill up to 5 ml approximately, and the vacuum turned on. When the culture had filtered the vacuum was switched off, and using a spatula, gently scraped off the filter and re-suspended in universals containing fixative.

The choice of fixation protocols were:

- 2.5% v/v glutaraldehyde (25% v/v stock solution) added directly into the culture, for 24 hours, then harvested by filtration
- 2.5% v/v glutaraldehyde added directly into the culture, for 24 hours, harvested by filtration, and followed by fixation in 0.5% w/v uranyl acetate prepared in RK buffer, for 2 hours
- 2.5% v/v glutaraldehyde added directly into the culture, for 24 hours, harvested by filtration, and followed by fixation in 0.1% w/v uranyl acetate prepared in RK buffer, for 2 hours
- 1% v/v glutaraldehyde added directly into the culture, for 24 hours, harvested by filtration, and followed by fixation by 0.5% w/v uranyl acetate prepared in RK buffer, for 2 hours
- 1% v/v glutaraldehyde added directly into the culture, for 24 hours, harvested by filtration, and followed by fixation by 0.1% w/v uranyl acetate prepared in RK buffer, for 2 hours

- harvested by filtration then fixed with 0.5% w/v uranyl acetate prepared in RK buffer, for 2 hours, followed by 2.5% v/v glutaraldehyde, for 24 hours

For each sample, molten aqueous 3% w/v agarose (low melting point 37°C, Sigma-Aldrich, Gillingham, UK) was prepared and small drops placed in 1.5 ml microcentrifuge tubes. The agarose was kept molten by placing the tubes in a heating block at 45°C (Thermo Luckman, Thermo Fisher Scientific, Loughborough, UK). In all cases after the final fixation step the bacterial sample was filtered as before, washed with double distilled water, re-filtered, and gently scrapped off the filter paper. This was placed into the molten agarose in the microcentrifuge tubes (Thermo Fisher Scientific, Loughborough, UK) and gently stirred. When the agarose had set, it was cut into small pieces (approximately 1 mm<sup>3</sup>) for processing into resin for TEM or paraffin wax for LM.

### **2.3.5 TEM Processing and Observation**

TEM processing was by partial dehydration into the acrylic resin London Resin White (LR White, hard grade, TAAB Laboratories Equipment Ltd., Reading, UK) following the protocol of Newman and Hobot (1987; 2001) as in Appendix 4. All steps were at room temperature with agitation. After overnight infiltration with resin the agar blocks were placed into gelatine capsules (size '0'/vol 0.68 ml, TAAB Laboratories Equipment Ltd., Reading, UK) to which had been added cold (0°C) LR White resin with accelerator (15 µl per 10 ml of resin), to allow for Cold Catalytic

Polymerisation at 0°C for 24 hours, followed by 2 hours at 50°C. The gelatine capsules were then removed and the blocks were ready for sectioning.

Semithin sections (400nm) were cut on a Reichert Jung Ultramicrotome (Leica Microsystems, Milton Keynes, UK), with glass knives (Leica Microsystems, Milton Keynes, UK), placed on water droplets on slides and dried on a hot plate (Corning Life Sciences, Tewkesbury, UK). Sections were stained with 0.5% Toluidine Blue in 1% borax (Sigma-Aldrich, Gillingham, UK) for 5-10 seconds, before rinsing in tap water and drying. Once the semithin sections had been examined, and a suitable area of interest chosen, ultrathin sections were cut (100nm), and picked up on hexagonal 300 mesh copper grids (TAAB Laboratories Equipment Ltd., Reading, UK). Once dry, these were stained with 4% w/v aqueous uranyl acetate (TAAB Laboratories Equipment Ltd., Reading, UK) for 5 minutes, washed in three drops of deionised water, stained with a lead citrate solution (Sigma-Aldrich, Gillingham, UK) for 30 seconds, water washed again, and air dried. Sections were viewed in a JEOL 1200 EXII TEM operating at 80 kV with a tungsten filament, using a SIS MegaView III digital camera, (JEOL UK Ltd, Welwyn Garden City, UK).

### **2.3.6 LM processing and observation**

For LM, samples were processed with a routine histological laboratory processing protocol (Appendix 5) on a Thermo Scientific Excelsior Tissue Processor (Thermo Fisher Scientific, Loughborough, UK) (all steps were under vacuum with agitation), and blocks were embedded into Cell Wax (CellPath Ltd., Newton, UK), using a

tissue embedding station (Blockmaster II, Raymond A. Lamb Ltd., Eastbourne, UK) and stainless steel moulds (Thermo Fisher Scientific, Loughborough, UK). From these blocks 5  $\mu\text{m}$  sections were cut on a Leica rotary microtome (Leica RM2155, Leica Microsystems, Milton Keynes, UK), and picked up on to glass slides. Histological sections were stained with a Harris's Haematoxylin (Shandon™, Thermo Scientific) and Eosin Y cytoplasmic counterstain (Shandon™, Thermo Scientific) (H&E) which was performed on a Leica ST5010 XL autostainer (Appendix 6). Slides were mounted with coverslips by hand and viewed by LM using an Olympus BX51 microscope (Olympus, KeyMed Ltd, Essex, UK), with attached AxioCam HRC and Axiovision software (Carl Zeiss Microscopy, Cambridge, UK).

### **2.3.7 SEM Processing and Observation**

For SEM *P. aeruginosa* and *S. aureus* were cultured in TSB as in 2.3.2. After exponential growth, an aliquot of 25% v/v glutaraldehyde was added to give a final concentration in the medium of 2.5% v/v glutaraldehyde. Fixation continued for 24 hours at 37°C after which the cells were harvested as for TEM, washed on the filter with double distilled water and processed for SEM with a protocol using Hexamethyldisilazane, (Sigma-Aldrich, Gillingham, UK) (Appendix 7). All steps were performed at room temperature in a glass petri dish. Filters were then placed onto self-adhesive carbon tabs (25 mm diameter, Self-adhesive carbon conductive tabs, Agar Scientific Ltd., Stanstead, UK), which had been adhered to the surface of an aluminium stub (32 mm x 10 mm, Agar Scientific Ltd., Stanstead, UK).

Specimens were sputter coated with gold for 2.5 minutes (EMscope sputter coater, Leica Microsystems, Milton Keynes, UK) (Appendix 8), and examined in a JEOL 840A SEM operating with a tungsten filament at 5 kV, using SIS analysis software (JEOL UK Ltd, Welwyn Garden City, UK).

In order to examine some of the techniques throughout the following studies described in this Chapter, *P. aeruginosa* only was used in the following studies, unless otherwise stated

### **2.3.8 Glass as a surface for growing biofilm**

Square glass coverslips (32 x 32mm, Thermo Fisher Scientific, Loughborough, UK) were etched with a diamond marker in the top left hand corner before autoclaving, to demonstrate the top surface, then placed in 5 cm diameter sterile Petri dishes, one coverslip per dish. A 9 ml volume of the exponential phase culture was pipetted over the glass coverslips and the Petri dishes were allowed to incubate at 37°C for 72 hours. The culture medium was removed and a 5 ml volume of 2.5% v/v glutaraldehyde in RK buffer (pH 6) was added to each dish and fixed for 2 hours. The samples were then processed for SEM.

### **2.3.9 Plastic coverslips as a surface for growing biofilm**

Round plastic coverslips (13 mm diameter, Thermo Fisher Scientific, Loughborough, UK) were placed inside the wells of plastic, sterile culture plates (12 well, diameter 22.1 mm, Corning Life Sciences, Tewksbury, UK) and a 2.25 ml volume of the exponential phase bacterial culture was added to the wells. These

were then incubated for 72 hours at 37°C, after which time, a 0.25 ml volume of 25% v/v glutaraldehyde was added to each well to give a final concentration of 2.5% v/v glutaraldehyde per well. Fixation was overnight at room temperature, before the samples were processed for examination with SEM.

In a second series of studies larger plastic, sterile culture plates (34.8 mm well diameter, Corning Life Sciences, Tewksbury, UK) were used, with the same sized coverslips as above, the prepared culture of *P. aeruginosa* added to each well, and incubated at 37°C, with gentle agitation of 50 rpm, on a flat-bed mini orbital shaker. After 72 hours the contents were fixed with the addition of 0.5 ml of 25% v/v glutaraldehyde in 2 ml of TSB. Each culture was processed for SEM, LM or TEM techniques.

#### **2.3.10 Determination of inoculum concentration for optimum biofilm growth**

To determine the optimum seeding for the biofilm development, bacterial counts were performed and a set of serial dilutions prepared. Biofilm was grown then each dilution was examined by SEM, to see the differing growth rates and to decide at which dilution future biofilm should be grown.

*P. aeruginosa* cells were taken from the exponential phase bacteria. After 2.5 hours, the population density of bacteria in the culture was determined using a Helber counting chamber (Scientific Laboratory Supplies, Nottingham, UK) (Appendix 9) as follows:



- 1) It was estimated that the growing culture would have a concentration of around,  $2-4 \times 10^8$  bacteria/ml;
- 2) By counting the number of particles in a grid of known volume on a Helber chamber the number of microorganisms per  $\text{cm}^3$  can be calculated. The factor for the Helber chamber is  $2 \times 10^7$ ;
- 3) Therefore, to obtain a sufficient number of bacterial cells to count per square (approx. 10-20), the culture was diluted 1:10 by adding a 1ml volume of culture to a 9 ml volume of sterile TSB.
- 4) The dilution was added to the Helber chamber, and the number of bacterial cells per square was calculated by counting 32 squares and calculating the average number of cells per square (n).
- 5) At a dilution of 1:10, 54 cells were counted per 32 squares,  
i.e. average no. per square = 1.6875  
Therefore, taking the dilution factor into consideration,  $n = 16.875$
- 6) The actual concentration of bacteria in the growth culture was then calculated by using the following formula, taking the dilution factor into consideration:  $n \times 2 \times 10^7$ .
- 7) Number of bacterial cells per ml =  $16.875 \times 2 \times 10^7 = 33.75 \times 10^7 = 3.38 \times 10^8$
- 8) Number of bacteria per ml in the growth culture at 2.75 hours =  $3.38 \times 10^8$

Appropriate dilutions of the growth culture were prepared to give final concentrations of  $1 \times 10^7$ ,  $1 \times 10^6$ ,  $1 \times 10^5$ ,  $1 \times 10^4$ ,  $1 \times 10^3$ , and  $1 \times 10^2$ . This was

achieved by adding 9 ml volumes of sterile TSB to each of six autoclaved Pyrex<sup>®</sup> test tubes (Corning Life Sciences, Tewksbury, UK). Next, 1 ml volumes of the exponential phase growth culture were added to the first tube and mixed. A 1 ml volume was taken from this tube, added to the second tube, and mixed. Then, a 1 ml volume was taken from this tube, added to the third tube, and mixed, and so on to the last tube. Each dilution was 1:10.

2.5 ml volumes of each of the six dilutions was added to six wells of culture plates (well diameter of 34.8 mm) containing the coverslips, and incubated for 72 hours at 37°C. After 72 hours, the culture medium was removed and 5ml of 2.5% v/v glutaraldehyde in RK buffer (pH 6) was added to each dish. Fixation was for 2 hours at room temperature and the samples were processed for SEM.

### **2.3.11 Timed growth of biofilm from 1-6 hours**

The previous experiment (2.3.10) had investigated the preparation and growth of inoculua. A bacterial population density of  $1 \times 10^7$  cells/ml was chosen as the standard. A 1:10 dilution was prepared from exponential phase bacterial cultures of *P. aeruginosa*, in sterile TSB by adding a 2 ml volume of the exponential growth culture,  $1 \times 10^8$ /ml, to an 18 ml volume of sterile TSB in an autoclaved test tube. Plastic coverslips were placed inside the wells of plastic, sterile culture plates (34.8 mm well diameter) and a 2.5 ml volume of the prepared culture added to each well, which was then incubated at 37°C for 1, 2, 3, 4, 5 and 6 hours. Three similar plates were prepared. At each time point, a 0.5 ml volume of 25% v/v glutaraldehyde was

added to a 2 ml volume of TSB. This 2.5 ml fixative solution was added to the appropriate well to give a 2.5% final dilution of fixative. After fixing overnight at room temperature, the fixative was gently replaced by RK buffer and the coverslips processed for SEM using. Images were recorded and measurements were taken from 10 samples using the SEM Analysis software. Any clumps of bacteria were encircled and the total number of areas added for comparison with other time points. Growth of bacteria that had developed into three-dimensional groups were measured but not those that were only dividing in a flat two-dimensional group.

#### **2.3.12 Analysis of “slough-like” surface associated material**

A 1:10 dilution was prepared from exponential phase bacterial cultures of *P. aeruginosa*, in sterile TSB. Plastic coverslips were placed inside the wells of one of three sterile, plastic 6-well culture plates (34.8 mm well diameter). Prepared culture (2.5ml) was added to each well of all three plates which were then incubated at 37°C for 1, 2, 3, 4, 5 and 6 hours. After each time was ended 0.5 ml of 25% v/v glutaraldehyde in 2 ml of TSB was added to the appropriate well to give a 2.5% final dilution of fixative.

After growth and fixation, the coverslips were placed into the base of the wells of the second plate. In the third plate, the coverslips were used to collect “debris”/“slough-like” material from the surface of the wells and these were placed in a new, clean 6 well plate. The samples were then processed for SEM. Some of the surface debris was also processed for TEM for further examination.

It was observed that these coverslips were hard, could not easily be cut and were not infiltrated by resin. To overcome these problems in TEM, the coverslips were placed in a Petri dish and LR White resin poured in until the coverslip was just covered. The edge of a gelatine capsule was placed quickly into a layer of LR White resin accelerator then placed immediately onto the coverslip. This enabled it to stick and seal immediately. To enable filling with premixed LR White resin and accelerator using a pipette, a small hole was made at the top of the capsule. The block was set at 5°C. The next day the coverslip was carefully removed, with the intention of leaving a biofilm on the capsule surface, such that when this end was sawn off, and cut in half, the two film edges could be placed face to face, before putting onto a fresh capsule of LR White resin and allowed to set.

As suggested in the introduction, a biofilm can grow on just about any surface. Other surfaces were tested for their suitability in growing biofilm and adaptability in the respective microscopy techniques of LM, TEM, SEM and CLSM.

### **2.3.13 Agar as a surface for growing biofilm**

A prepared plate of 3% TSB in 2% w/v agar (as in 2.3.1) was covered in a thin layer of the *P. aeruginosa* culture by a metal lawn plate spreader, previously sterilised by autoclaving, and colonies allowed to grow at 37°C. After 24 hours, plates were flooded with 2.5% v/v glutaraldehyde in TSB medium and fixed overnight. Next day, thin slices of agar plus colonies were gently placed in RK buffer. These were then processed for SEM.

After viewing, smaller culture growths were attempted by growing for only 6 hours on thinner layers of 3% TSB in 2% w/v agar. When a few small groups of bacteria were visible, the plates were flooded with fixative as before and thin slices were processed and examined by SEM.

#### **2.3.14 Gauze as a surface for growing biofilm**

A 1:10 dilution was prepared from exponential phase bacterial cultures of *P. aeruginosa* and *S. aureus*, in sterile TSB. Two 2.5 cm diameter discs of pre-cut sterile gauze dressing (NA Gauze; Systagenix, Gatwick, UK) were placed into a 100 ml aseptic Universal container and 20 ml of TSB added. The broth was inoculated with 50 µl of each culture and placed on a shaker (Stuart Scientific, Stone, UK) in an incubator (Grant Instruments, Royston, UK) at 37°C for 48 hours (50 oscillations per minute). Broth was changed aseptically after 24 hours to refresh nutrient availability. After 48 hours, the biofilm-attached gauze was removed and washed briefly by immersion for 15 seconds into a Universal container containing 20 ml of sterile saline, then placed into a CLSM specimen-viewing chamber. BacLight™ Viability Kit (BVK, Thermo Fisher Scientific, Loughborough, UK) for live/dead bacterial staining (live bacteria stain green, dead bacteria red) was prepared in 5 ml sterile saline, then poured gently over the gauze and left for 10 minutes at room temperature in the dark. The BVK is comprised of two dyes; a green (SYTO 9™) which will pass through bacterial cell walls regardless as to whether they are alive or dead. The red dye (Propidium Iodide [PI]), will only enter the bacterial cell if the cell wall has been damaged. These are

both stains for nucleic acids and the red PI dye actively competes for the same sites as the green dye and replaces it. Consequently, it is possible to determine which bacteria have died.

The prepared chamber, with stained gauze biofilm and excess stain, was placed onto the stage of a CLSM for imaging. Images were taken using a Leica TSC SP2 DM IRE2 Confocal Laser Scanning Microscope (Leica Microsystems, Milton Keynes, UK), lasers included the argon laser (488nm) and the helium/neon laser (543 nm). A Plan-Apochromat 40x/1.25 oil objective was used. Images were prepared using Leica AF Lite software.

Once viewed by CLSM, the sample was removed from the chamber and placed in a Universal container containing 20ml of 2.5% v/v glutaraldehyde in RK buffer to fix. A few pieces of the sample were cut and processed for all other types of microscopy. Prior to processing for LM and TEM, samples were wrapped gently in tissue processing paper (Biowraps, Leica Microsystems, Milton Keynes, UK ) to protect them from loss of content during the processing cycles. For LM, samples were processed with the previously described protocol on the Thermo-Excelsior Tissue Processor (all steps were under vacuum with agitation). 5 µm sections were cut, stained and viewed as per the agar blocks in the previous studies.

### **2.3.15 PTTE cell culture inserts**

0.4µ PTTE membrane cell culture inserts (Falcon<sup>®</sup>, Corning Life Sciences, Tewksbury, UK) were placed inside the wells of 6-well culture plates. A 1:10 dilution was prepared from an exponential phase bacterial culture of *P. aeruginosa*

in sterile TSB. A 100  $\mu$ l volume of the bacterial dilution was added to the inside of each insert. The outer area of the well was gently filled with 2.5 ml of TSB (Figure 2.1).

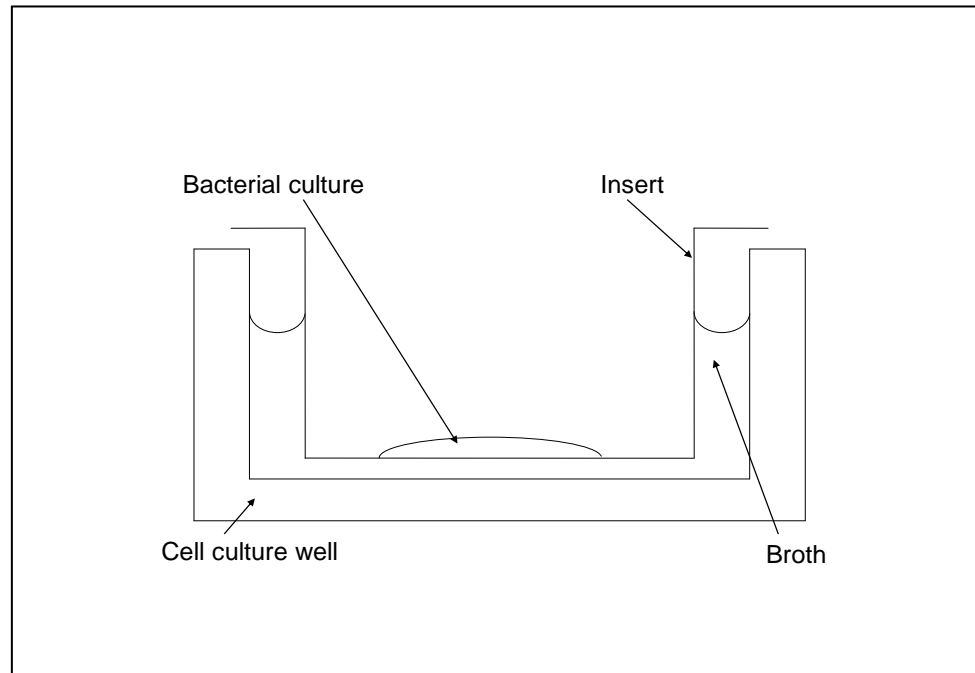


**Figure 2.1: 0.4  $\mu$ m PET track-etched membrane cell culture insert in culture well**  
The insert was placed inside a culture well containing nutrient and the bacterial culture pipetted on to the surface of the insert

The plates were incubated with agitation of 50 rpm on a flatbed mini orbital shaker (Stuart Scientific, Stone, Staffordshire, UK), at 37°C for 24 hours. The outer culture media was then removed and 2.5 ml of 2.5% v/v glutaraldehyde in TSB was added, drop by drop, into the well and gently inside the surface of the well. This was left for 3 hours then gently removed and replaced by enough RK buffer to almost fill the well, approximately 10ml.

Two of the membrane inserts from each plate were processed for SEM within the wells. When dry the membrane was stuck on to a stub using a self-adhesive carbon tab. A scalpel was used to cut around the edge of the membrane in order to remove the hard plastic surround, leaving the thin membrane ready to sputter coat. The other inserts were taken for processing for LM and TEM (Appendix 3 and 5.7). Both LM and TEM samples were wrapped in hard tissue paper to help prevent biofilm loss during processing.

#### **2.3.16 PTTE/Agar “sandwich” model**

A 1:10 dilution was prepared from exponential phase bacterial cultures of *P. aeruginosa* and *S. aureus*, in sterile TSB. 0.4 µm PTTE inserts were placed inside the wells of two 6-well culture plates. One plate was designated for *P. aeruginosa*, one for *S. aureus*. A 100 µl volume of the bacterial dilution was added to the inside of each insert in the appropriate plate. The plates were incubated with agitation of 50 rpm on a flatbed mini orbital shaker, at 37°C for 24 hours. The outer culture media was then removed and 2.5 ml of 2.5% v/v glutaraldehyde in TSB was added, drop by drop, into the well and gently inside the surface of the well. This was left for 3 hours then gently removed and replaced by enough RK buffer to almost fill the well, approximately 10ml. Two of the membrane inserts from each plate were processed for SEM within the wells, and when dry the membrane was stuck on to a stub, then the plastic surround removed to leave the thin membrane ready to sputter coat. The other inserts were treated as follows:



A 3% w/v solution of agarose in distilled water was prepared, heated until the agarose dissolved and allowed to cool but not set. The RK buffer was carefully removed from the well area outside each insert, and then from the inside of the insert, by pipette. Whilst still fluid, the agar solution was gently dropped inside the insert until the whole surface was covered by a layer of agar (Figure 2.2a). This was allowed to set. The insert was removed from the well and inverted.

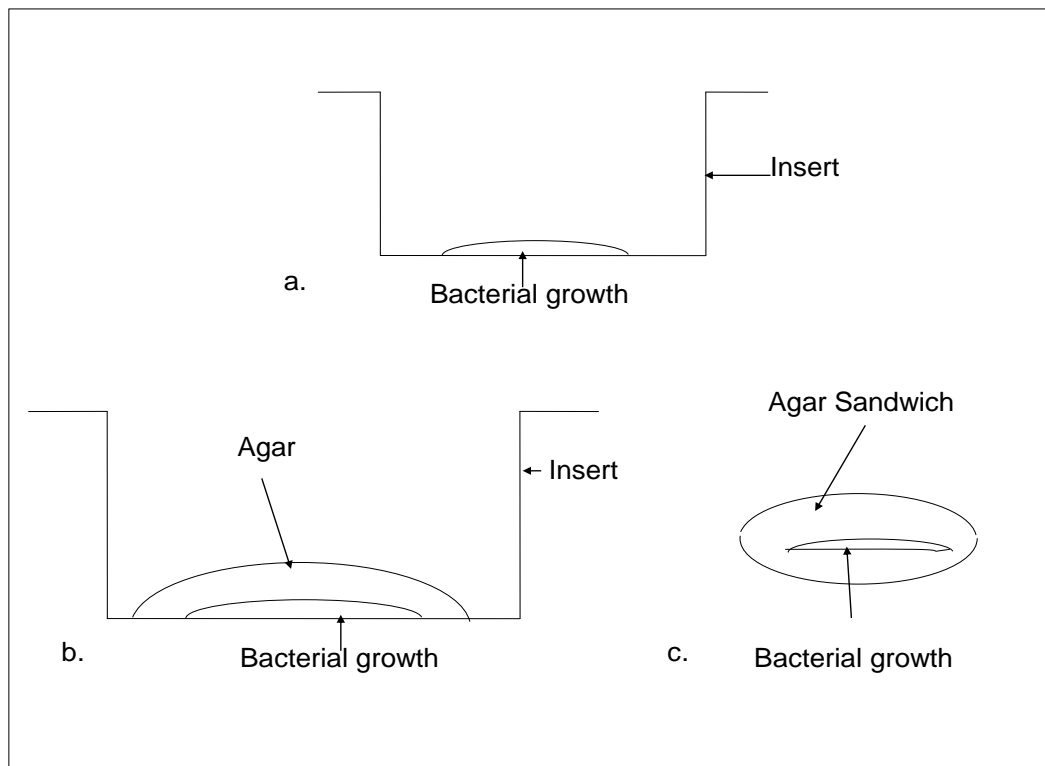


**Figure 2.2: a, b and c: The stages of creating the Agar Model**

Biofilm growth on an insert was removed from the well (a), agar was placed over the growth (b), then the insert and film was removed and the other side coated in agar to encapsulate the growth (c)

A scalpel was run around the edge of the thin film to cut through it and the underlying agar. Using a stereomicroscope, the film was gently peeled away to leave the biofilm embedded in the agar. Another layer of molten agar was added to

this surface to sandwich the biofilm in the agar (Figure 2.2b) Once set this structure was bisected carefully to see if the layer of biofilm could be seen within it (Figure 2.2c). Two agar 'sandwiches' were then taken from each plate to be processed by TEM, and the remainder were processed for paraffin wax embedding, section cutting and staining with H&E, and viewed by LM.

This was repeated for a 48 hour growth using three 6-well culture plates. One plate was designated for *P. aeruginosa*, one for *S. aureus*, and the third for an equally mixed culture of both organisms. A 100 µl volume of the bacterial suspension was added to the inside of each insert in the appropriate plate, and 50 µl of each culture was added to the insert in the plate designated for a mixed culture. The plates were then treated as above, but as a 48 hour growth.

### **2.3.17 A novel wound model**

The model chosen was more representative of a wound environment and was used to allow biofilm to grow more naturally in a simulated wound setting. Ethanol sterilised pork belly slices were pre-trialled alongside back bacon for bacterial growth (Sainsbury's Cardiff, UK), which occurred in both methods. Back bacon was therefore chosen due to its consistency in thickness and being obtained from the same batch, and the model subsequently called the meat model. PTTE inserts (0.4 µm ) were placed inside the wells of three 6-well culture plates. One plate was designated for *P. aeruginosa*, one for *S. aureus*, and the third for an equally mixed culture of both organisms. A piece of back bacon, was sterilised by submerging briefly in ethanol (confirmed by analysis of controls), and placed on a previously

ethanol sterilised plastic chopping board (Sainsbury's Cardiff, UK) . A thin slice (3 mm) was cut from the meat, using a number 8 (13 mm diameter) cork borer (Sigma-Aldrich, Gillingham, UK ) and placed on the inside film surface of each insert. 1:10 dilution was prepared from exponential phase bacterial cultures of *P. aeruginosa* and *S. aureus*, in sterile TSB. 100 µl of the bacterial dilution was added to the centre of the meat in the appropriate plate, and 50 µl of each culture was added to the centre of the meat in the plate designated for a mixed culture (Figure 2.3). Some meat models were designated controls and not inoculated.

The outside well area of the insert was filled with 2-3 ml of TSB broth until the insert was about to float. Incubation of the plates was at 37°C for 72 hours with gentle agitation (50 rpm on a flatbed mini orbital shaker). At 24 and 48 hours the TSB culture was aseptically topped up in the well outside the insert. After 72 hours the remaining TSB was pipetted from the outer area and drops of 2.5% v/v glutaraldehyde in TSB were added into the insert, to gently flood the inside but not disturb the biofilm, and in the outer area of the well. This was left for 24 hours, to ensure fixation of the meat, and fixative was then gently replaced by RK buffer.

In one culture plate the RK buffer was carefully pipetted from outside and inside the insert, removing as much excess fluid as possible from the inside of the insert. The meat was lifted out of the insert, the insert was removed, and the meat placed in the well to process *in situ* for SEM. For the other culture plates, a 2% w/v agarose solution was prepared and allowed to cool but not set. The RK buffer was carefully pipetted from the outside area within the well and from the area inside the

inserts. Once this fluid had been removed, the insert was taken out and placed on absorbent paper hand towels (Tork, SCA Hygeine Products, Dunstable, UK). This removed any further fluid that could drain through the base of the insert. The slice of meat was carefully removed and the base of the meat placed on the absorbent paper towels to remove excess fluid. Using fine-forceps the meat was carefully tilted and the base finely coated with a thin layer of tissue marking dye (Cancer Diagnostics, CellPath Ltd., Newton, UK) using a cocktail stick, then placed back on to the absorbent tissues for a few minutes. This was to help distinguish the base of the biofilm from the surface after processing.

Whilst still fluid, the agar solution was gently poured inside a watch-glass (Thermo Fisher Scientific, Loughborough, UK ) and the meat was placed into the agar, biofilm-side down, but not touching the base of the glass, taking care not to include bubbles. The agar was allowed to start to set, and then more agar was poured over to completely cover the meat. This whole model was left until set, then removed from the watch-glass and placed in 2.5% v/v glutaraldehyde in RK buffer and fixed for 24 hours at room temperature. The whole meat/agar model was processed and cut for LM as in 2.3.16. A punch biopsy was taken from the centre of one core using a 6 mm Stiefel biopsy punch (eSupplies Medical, Newport, Wales, UK) and pieces processed for TEM.

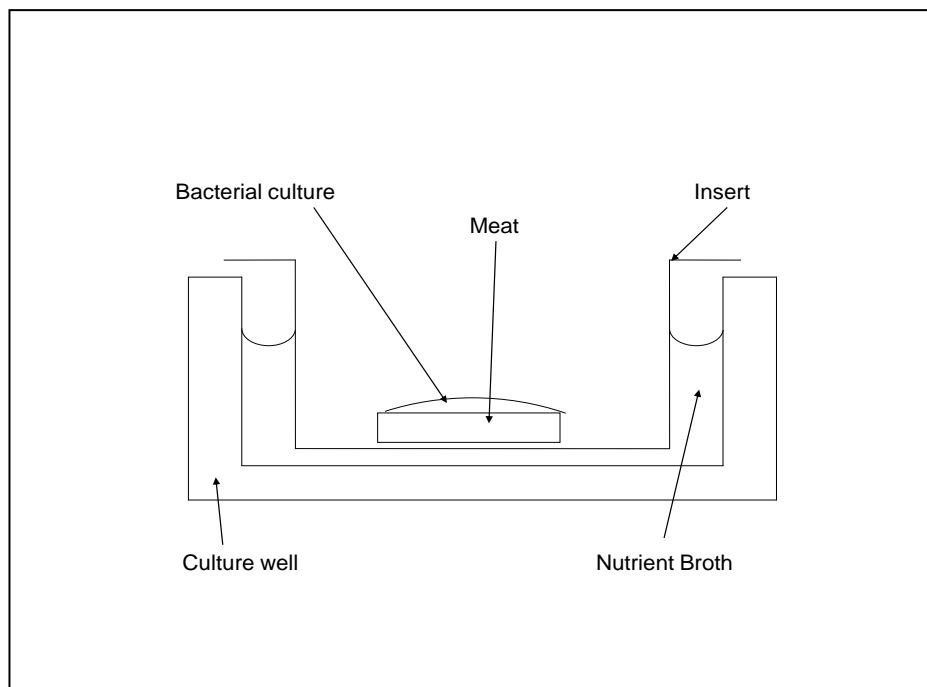


**Figure 2.3: The Meat Model**

Biofilm was grown on a meat surface, constantly supplied with nutrient through the pores of an insert. The whole meat model was placed in agar.

### **2.3.18 Statistical analysis**

The increase in growth of the biofilm from 24 to 72 hours was confirmed quantitatively by taking LM images at x4 magnification and measuring the area of biofilm using Image J software. Two-sample t-tests and Analysis of Variance (ANOVA) statistical tests were conducted using Minitab 17 software to compare the means of biofilm areas.

## 2.4 Results

### 2.4.1 Physiology, Growth and the Effect of Silver

Although the plating of cultures and the growth of exponential bacteria in a medium are basic microbiology techniques, they are also an essential step in the beginnings of any research studies utilising bacteria. Separate cultures of *P. aeruginosa* and *S. aureus* were incubated in TSB culture medium at 37°C with aeration to observe their growth and find their exponential point.

The results of bacterial growth for both organisms as recorded by the spectrophotometer, are shown graphically in Figure 2.4 and Figure 2.5.

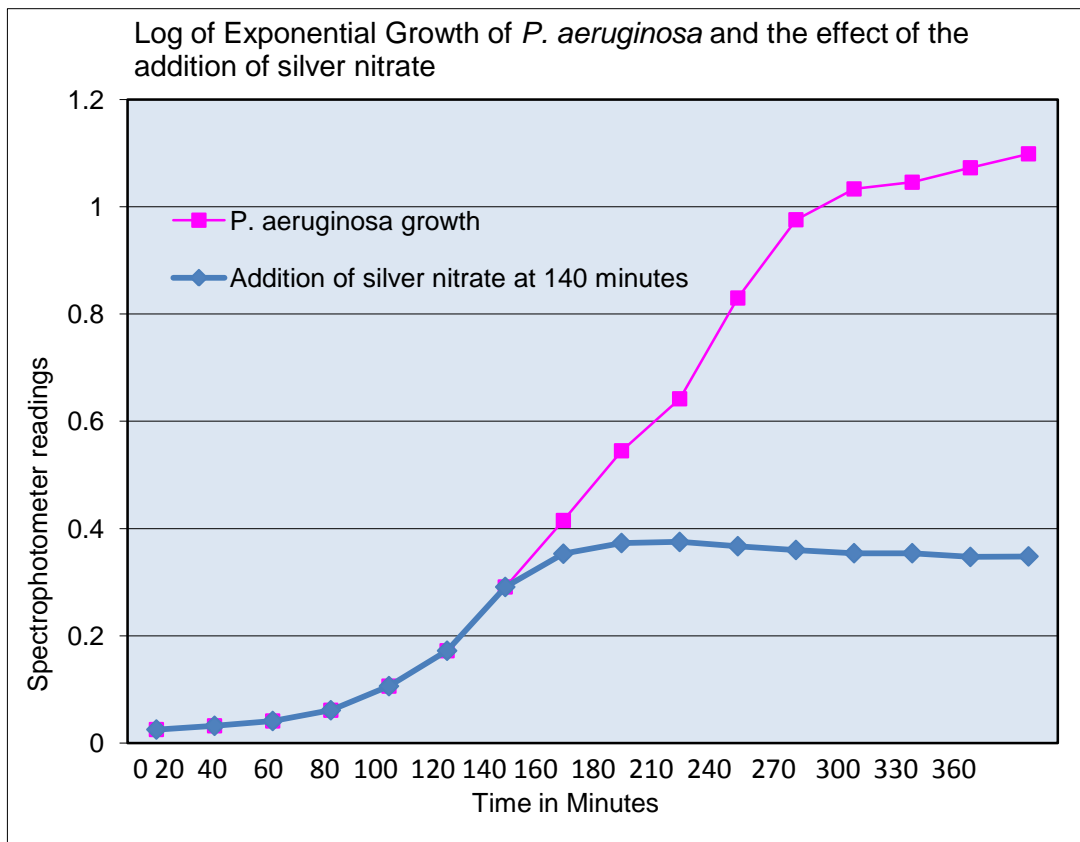


**Figure 2.4: Absorbance v time showing growth curve for *P. aeruginosa***

Absorbance vs time showing growth curve for *P. aeruginosa*: with silver nitrate addition to culture at 2 hours, 20 minutes. Note the sharp cessation of growth upon addition of the silver solution.

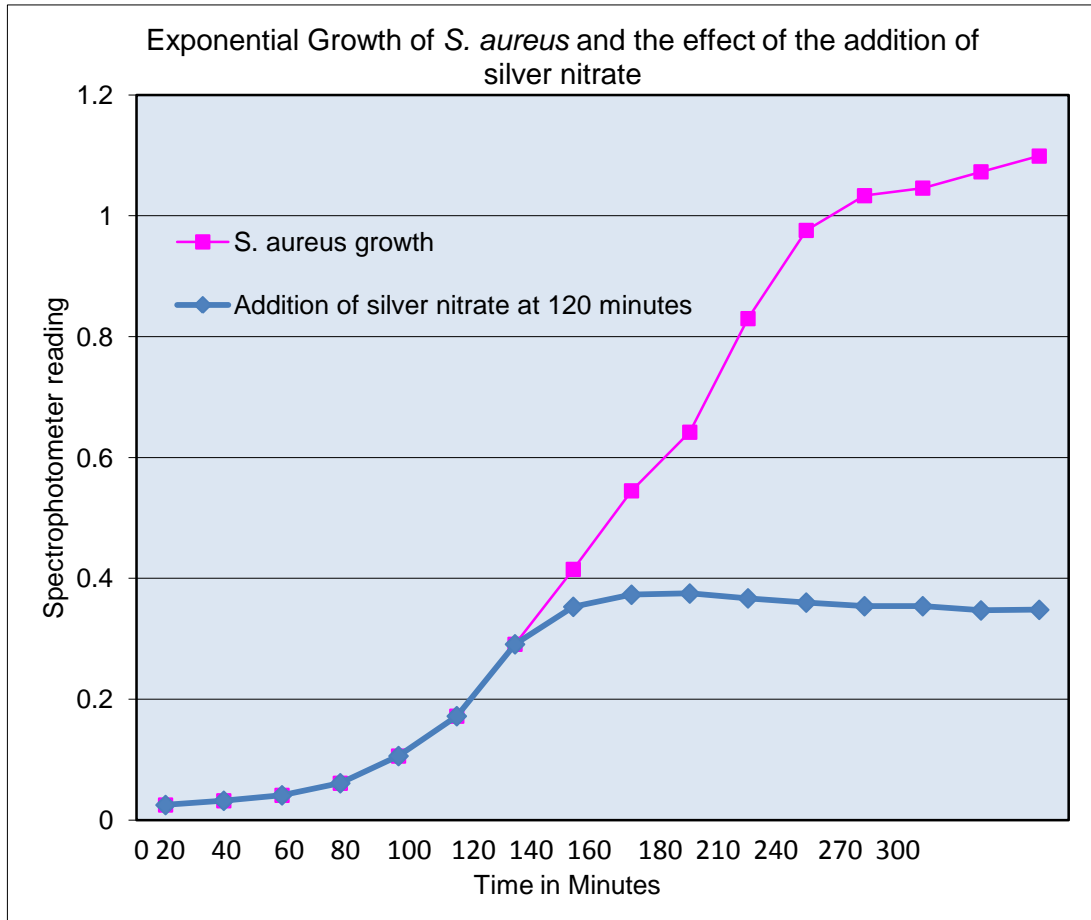


**Figure 2.5: Absorbance v time growth curve for *S. aureus***

Absorbance vs time growth curve for *S. aureus*: silver nitrate addition to culture at 2 hours. Note the sharp cessation of growth upon addition of the silver solution

It was determined that the exponential growth of *P. aeruginosa* started to decrease slightly at around 3 hours. *S. aureus* growth started to decrease slightly after 2 hours. Growth continued to rise for both cultures, but at a slower rate. As a result, the time of 2 hours 20 minutes was chosen as the best time point for harvesting exponentially grown *P. aeruginosa*, and the time of 2 hours was chosen as the best time point for harvesting exponentially grown *S. aureus*, for microscopy and for future experiments. These exponential time points were also selected as the best time for the addition of the silver nitrate solution. The results of the addition of silver

nitrate are included in Figure 2.4 and Figure 2.5, where it was observed that the addition of silver nitrate to both cultures resulted in rapid cessation of bacterial growth.

#### **2.4.2 TEM of Planktonic Bacteria and the Effect of Silver Nitrate on Bacterial Ultrastructure**

Preparatory methods for TEM can cause cellular damage, so various fixation protocols were examined in order to find the best method for ultrastructural preservation of the bacteria.

Fixation initially with 0.5% w/v uranyl acetate followed by 2.5% v/v glutaraldehyde resulted in a disruption of the cytoplasm causing large empty spaces to appear throughout the cell. In all other fixation methods there was preservation of bacterial cells, with the nucleoid observed as a ribosome free area within the cytoplasm and containing the DNA fibres (Figure 2.6). TEM of bacterial cells fixed with 2.5% v/v glutaraldehyde revealed a similar cellular appearance as the other fixatives (Figure 2.6) but with less background precipitation. For future TEM protocols, fixation with 2.5% v/v glutaraldehyde was chosen.





**Figure 2.6: TEM of *P. aeruginosa* and *S. aureus* with varying protocols of fixation**

**Top left** - *P. aeruginosa* fixed with 0.5% uranyl acetate followed by 2.5% glutaraldehyde – note the empty space throughout the whole cell, disrupting the structure (x40k, bar 500nm)

**Top right** – *P. aeruginosa* fixed with 5% glutaraldehyde followed by 1% uranyl acetate – ultrastructure appeared to be well preserved with preservation of the nucleoid (x100k, bar 200nm)

**Lower left** – *P. aeruginosa* fixed with 2.5% glutaraldehyde followed by 0.5% uranyl acetate – ultrastructure appeared to be well preserved with preservation of the nucleoid (x40k, bar 500nm)

**Lower right** – *S. aureus* fixed with 2.5% glutaraldehyde – ultrastructure appeared to be well preserved with preservation of the nucleoid (x100k, bar 200nm)

To distinguish bacteria and the effect of antimicrobials, silver nitrate was added to samples of both exponentially grown bacteria which were then processed for TEM. Adding silver to the bacterial cultures caused disruption of the nucleoid of both bacterial species (Figure 2.7).

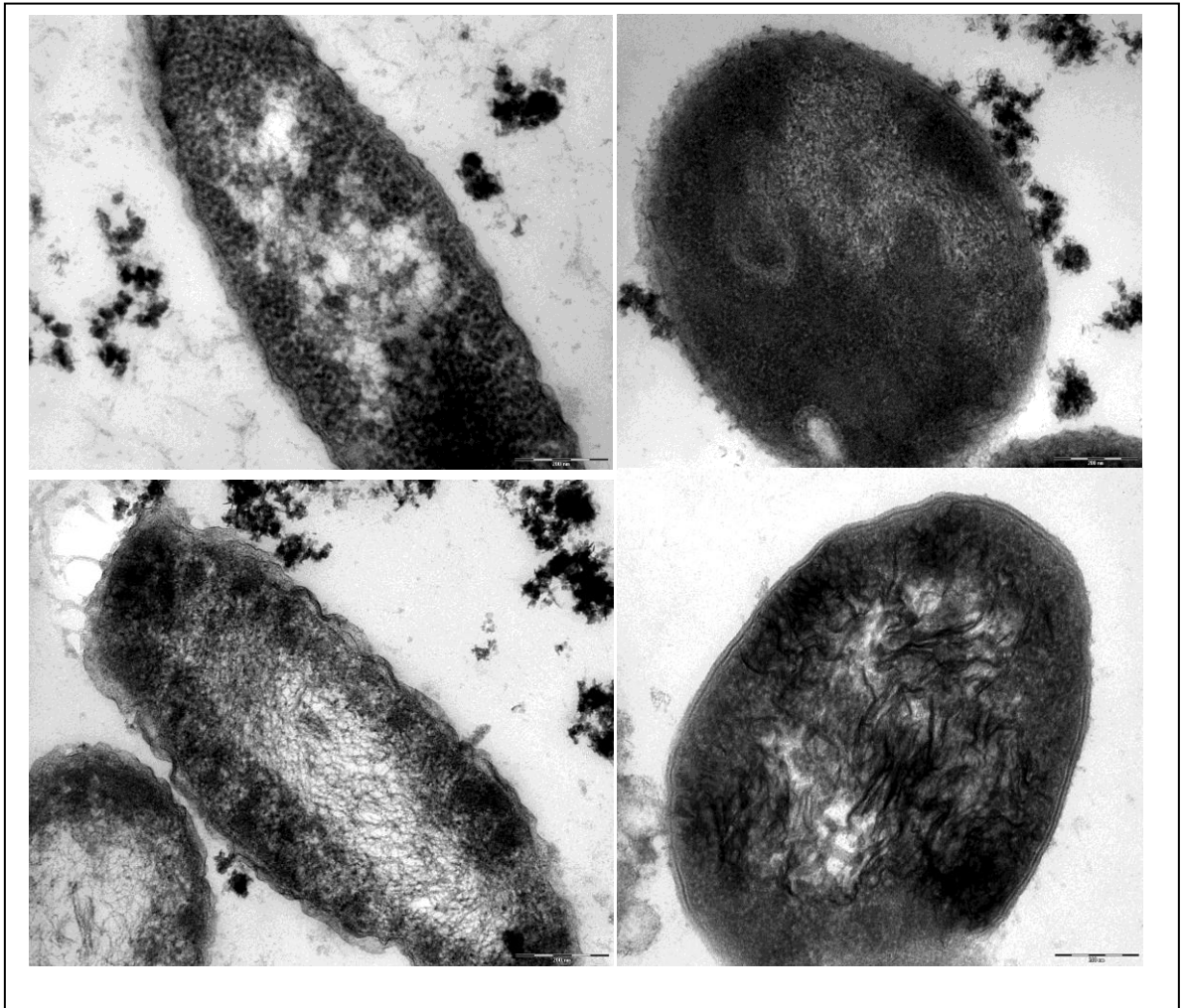


**Figure 2.7: TEM images of *P. aeruginosa* and *S. aureus* untreated and with addition of 1% silver nitrate at the the exponential point for 220 minutes, fixed in 2.5% glutaraldehyde in RK buffer and processed for TEM**

**Top - untreated *P. aeruginosa* (left) and *S. aureus* (right)**

**Lower - with addition of 1% silver nitrate, *P. aeruginosa* (left) and *S. aureus* (right)**

Note the more condensed fibrils of DNA in both treated cells. (x100k, bar marker 200nm)

The nucleoid, or ribosome free area, became more condensed in appearance and the DNA fibres were tending to become coarser and thicker.

### 2.4.3 SEM of Planktonic Bacteria

Samples of planktonic bacterial cultures were processed and viewed by SEM, in order to be able to distinguish them from biofilm bacteria in the following chapters, and to ensure the success of the preparatory methods chosen. SEM imaging showed the distinctive shapes of both the rod-like *P. aeruginosa* and the spherical, coccus shaped *S. aureus* (Figure 2.8a and b). As the bacteria were from the filtration of a planktonic culture, no EPS was evident.

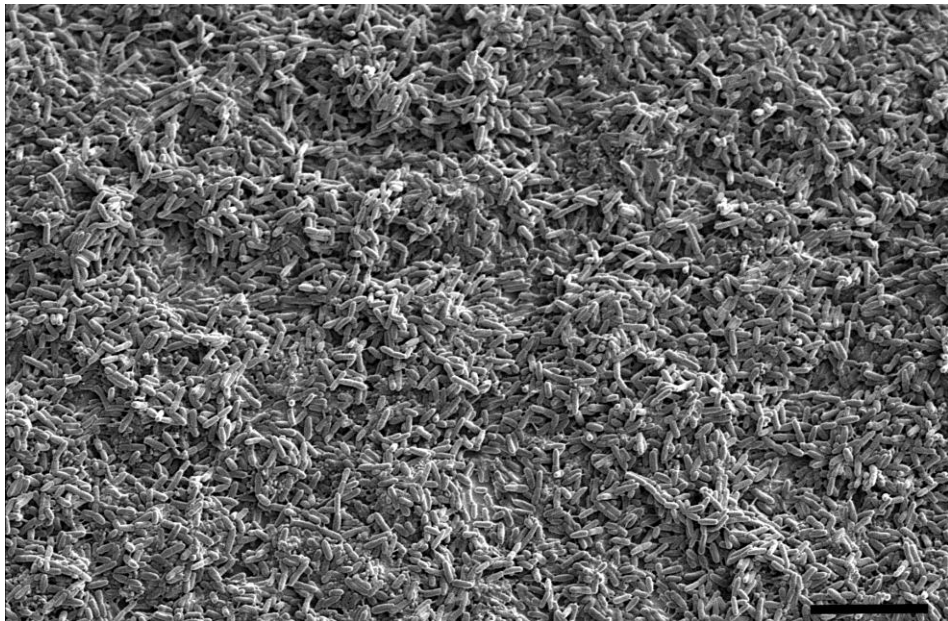


**Figure 2.8a: SEM of planktonic bacteria *P. aeruginosa*** (bar marker 10µm) bacterium appeared in clusters but showed no EPS

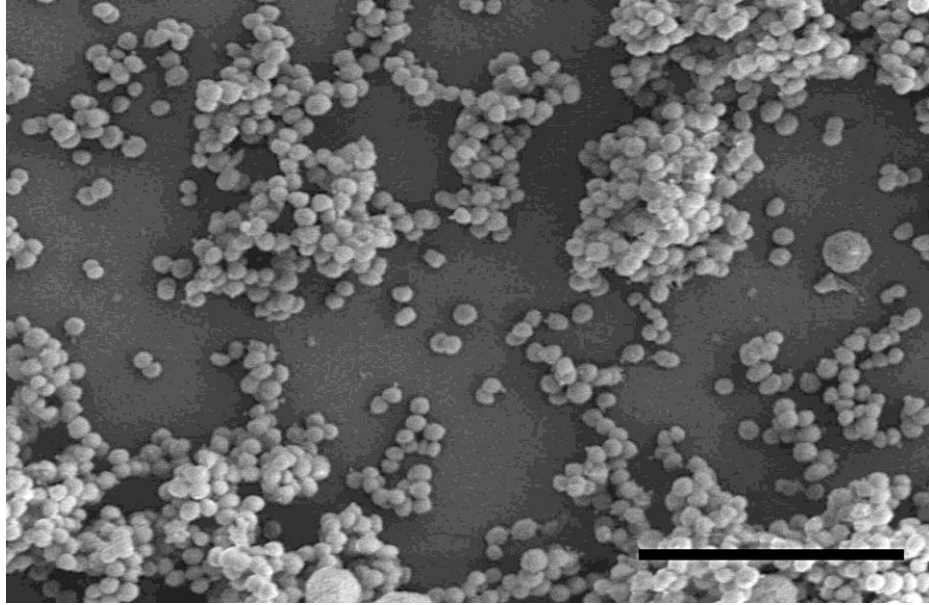


**Figure 2.8b: SEM of planktonic bacteria *S. aureus***  
(bar marker 10 $\mu$ m) bacterium appeared in clusters but showed no EPS

#### **2.4.4 Biofilm growth on glass coverslips**

Glass coverslips were chosen as the preliminary surface to start biofilm growth and examination before choosing a surface that could lend itself to all the techniques of microscopy to be used. A thick layer of biofilm development was observed on the glass surfaces. The bacteria were in a thick mat of cells with occasional bacterial clusters and the presence of faint traces of an extracellular matrix (Figure 2.9).

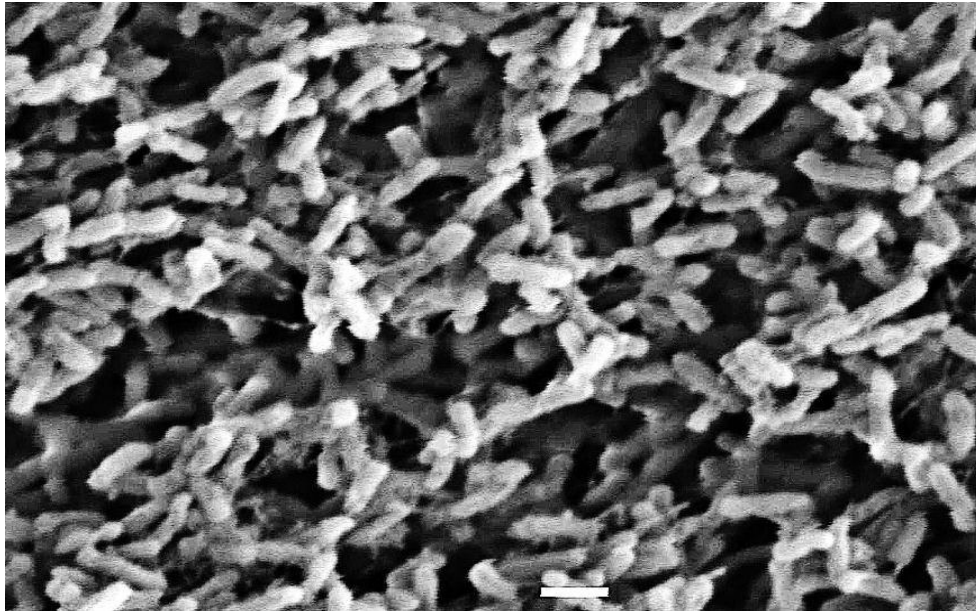


**Figure 2.9: 72 hour biofilm growth on glass coverslips by SEM**

Faint traces of EPS were present within the thick biofilm growth (bar marker 1 $\mu$ m)

Noticeably, the glass coverslips stuck to the bottom of the Petri dishes and were very difficult to remove, if at all. Removal was usually by the breakage of part of the coverslip, such that the whole coverslip could not be observed in the SEM. The larger volumes of solution and bacteria used were suited to the Petri dishes but, for ease of use and handling in multiple tests in all subsequent experiments, culture plates were used instead of Petri dishes.

#### **2.4.5 Biofilm growth on plastic coverslips**

Plastic coverslips proved more pliable than glass, and were chosen as a preferred surface. Six-well culture plates with a well diameter of 34.8 mm were preferential for use. Using culture dishes with more wells, and thus smaller well diameters,

(e.g. 12-well, diameter 22.1 mm; 24-well, diameter 15.6 mm), was not conducive to keeping biofilm adhering to the Thermanox surface. The smaller wells, upon addition and removal of solutions during SEM processing, created currents/flows that more readily removed or disturbed the biofilm than that found when using the large 6-well diameters.

Biofilm development was present in each well after 24 hours (Figure 2.10).

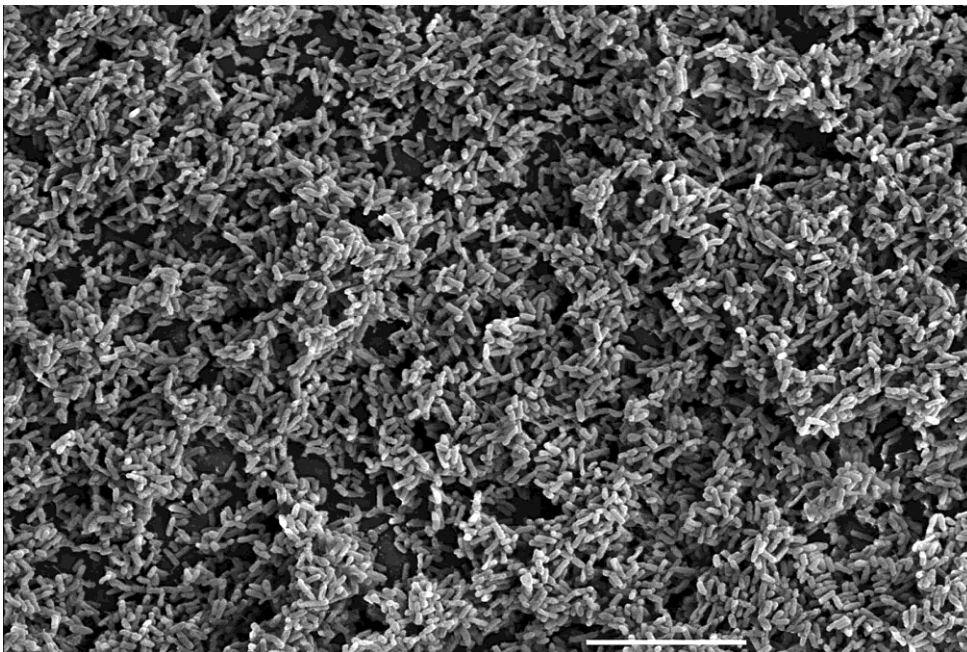


**Figure 2.10: 72 hour biofilm growth on plastic coverslips by SEM**

Biofilm was present on plastic coverslips as a thick layer of growth (bar marker 10 $\mu$ m)

When adding the fixative (glutaraldehyde in buffer) to the wells it created some swirling movement due to the thickness of the growth and the aqueous nature of the fixative. There was a variation in thickness of the biofilm formed within the wells, judged by increased opacity of the biofilm, which was visually assessed by stereo microscope. There also appeared to be some form of growth/debris on the surface of the nutrient. As the steps for SEM processing were performed the

surface growth moved up and down over the coverslips. Therefore, it was not certain if the coverslips were covered in biofilm grown on its surface below the nutrient, or if it also included this surface growth/debris.

#### **2.4.6 The effect of inoculum concentration**

Preliminary experiments were performed, to decide upon the optimum concentration for future experiments in this study, and grown for 72 hours to visualise any differences in the growth in wells of each inoculum concentration. A layer of biofilm was present in each well on the coverslip surfaces, and again surface growth/debris on the broth surface. Once fixed and processed, the biofilms were examined by SEM, to decide which dilution should be used for future biofilm growth. Surface views of bacterial coverage in all samples showed the ultrastructural appearance of individual planktonic cells in all wells, and of areas of general coverage of bacteria appearing indistinct due to being enmeshed in a matrix, i.e. biofilm (Figure 2.11).



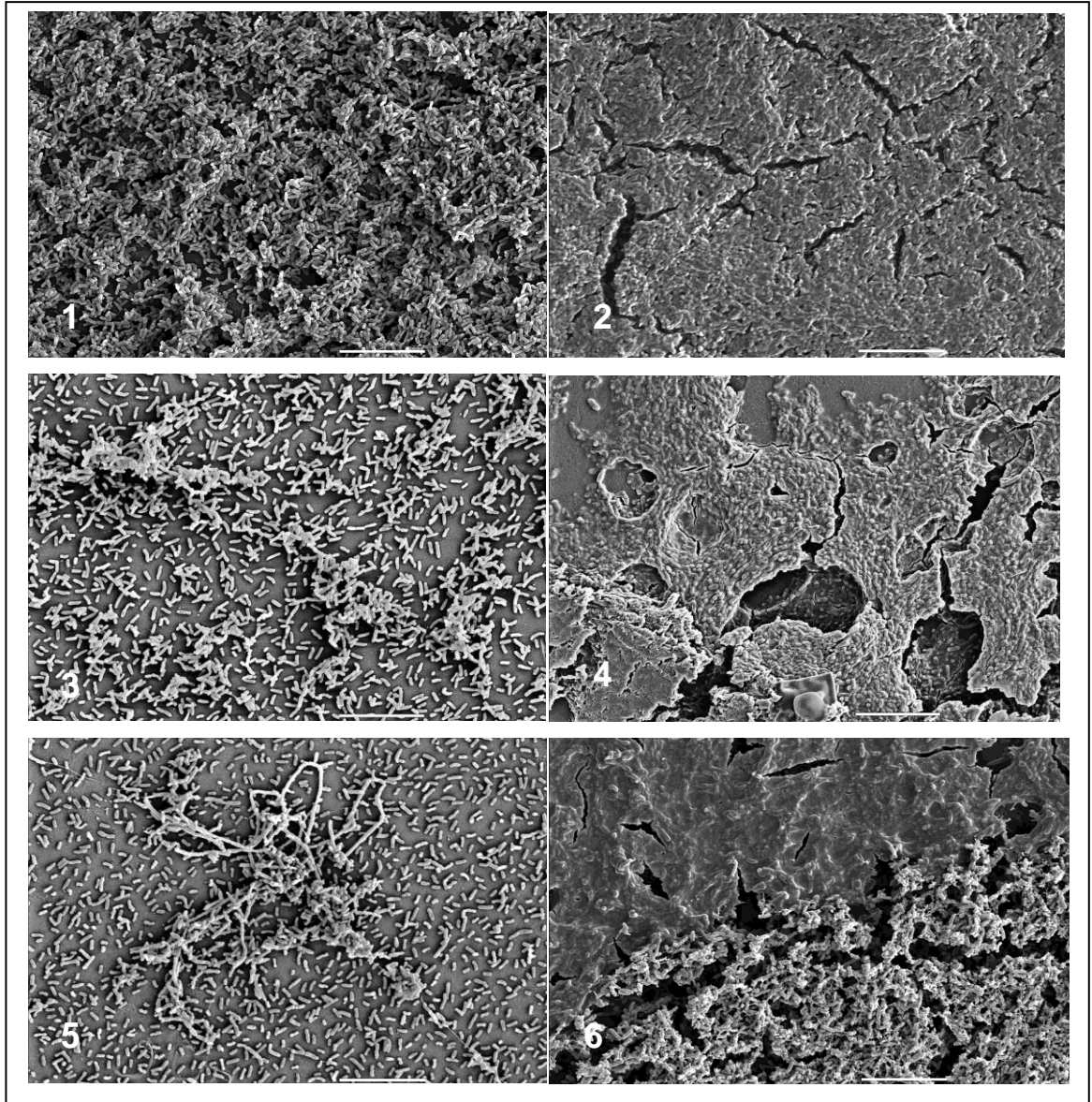


**Figure 2.11: SEM of wells 1-6 with inoculum concentrations from  $3.4 \times 10^7$  to  $3.4 \times 10^2$**   
 Images of the plastic coverslips with growth at different inoculum concentrations ( $3.4 \times 10^7$  to  $3.4 \times 10^2$ : images 1-6) Regardless of the concentration the biofilm, growth appeared similar with varying areas of thick growth plus clusters and 'mats' of biofilm (bar marker  $10\mu\text{m}$ )



### 2.4.7 Timed growth of biofilm from 1-6 hours

To ascertain how quickly bacteria start to group together in the first stages of biofilm, and present the best start for initial sampling time for future growth experiments, bacterial growth was examined during the first 6 hours (Figure 2.12).

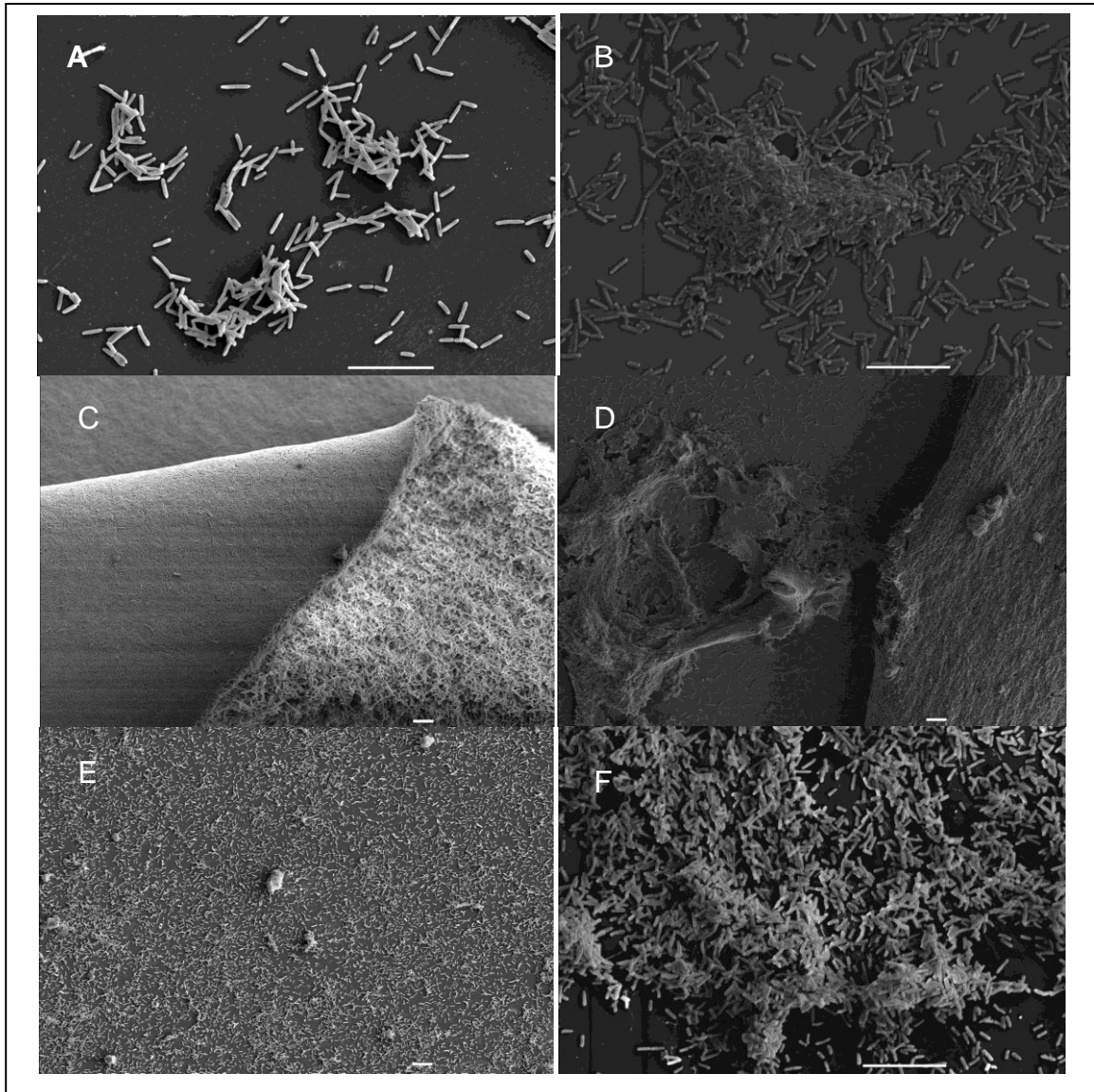


**Figure 2.12: 3-6 hour biofilm growth by SEM**

Grouping of bacteria at **3 hours** (A), **4 hours** (B), **4 hours** (C), **5 hours** (D), **6 hours** (E), and **6 hours** growth (F). Clusters of bacteria and 'mats' of biofilm growth were seen to gradually increase from the 1-6 hour period (bar marker 10µm)

This work was performed in triplicate. The first 1-3 hours showed a gradual increase in bacteria, with grouping occurring by 3 hours. Clusters of bacteria, probably immature biofilm, were present after 4 hours. There also appeared to be mats of biofilm containing numerous bacteria at 4-6 hours which appeared folded over in places. At 5-6 hours a lot of growth was apparent, with almost complete coverage within 6 hours. Calculating the mean growth from measurements of the areas of three-dimensional grouping showed a gradual increase in the grouping of bacteria with a marked increase at 5-6 hours (Figure 2.13). The dilution of glutaraldehyde in TSB prevented problems of swirling and pooling of the biofilm and was used as the method of primary fixing of the biofilm in situ.

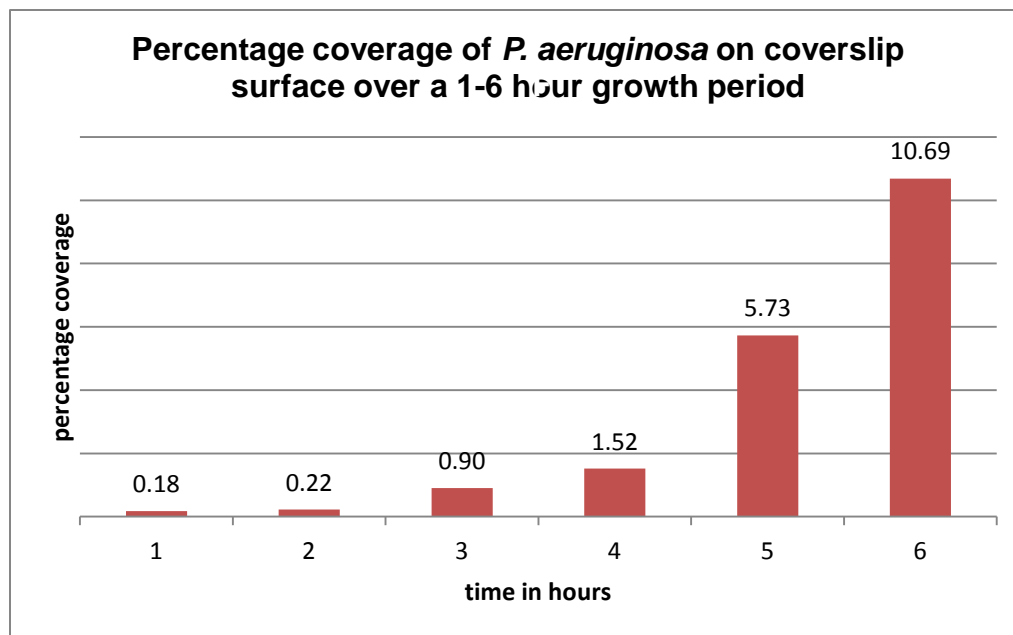


**Figure 2.13: Statistical Analysis of bacterial growth over a 1-6 hour period**

The mean areas of all three-dimensional growth present in 10 samples was measured and compared. After 4 hours it could be seen that there was a sharp increase in the presence of biofilm clusters (or colonies) and by 6 hours much of the coverslip was covered in early biofilm growth

#### 2.4.8 Surface associated material: biofilm or slough?

By comparing methods of collection of biofilm growth, biofilm on coverslips could be distinguished from biofilm/debris from the fluid surface. The plates containing coverslips which were placed into the base at the start of growth and processed *in situ*, produced clusters of bacteria, especially in the 4-6 hour. When the second set of coverslips were simply slid into the solution, dropped into the base and then processed, the resulting images showed sheets of cells as before, but also a background of planktonic bacteria.

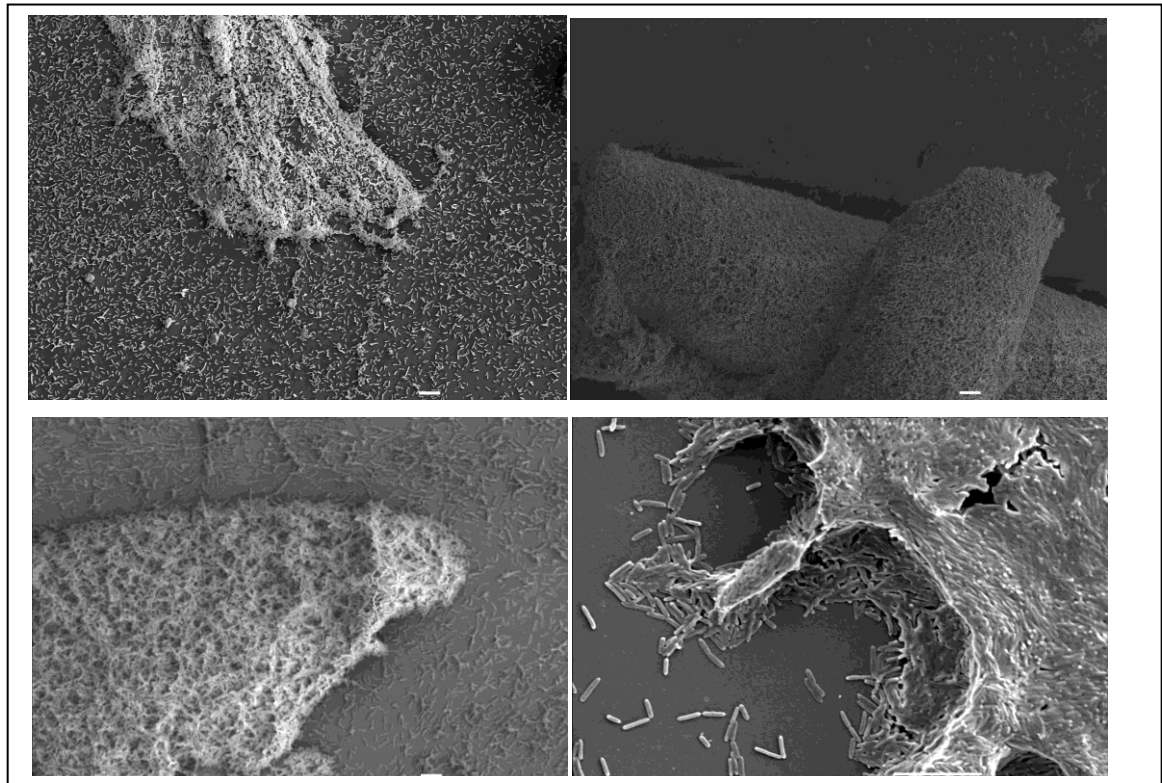


**Figure 2.14: 6 hour growth with methods of biofilm collection (bar marker 10 $\mu$ m)**

**Top left and top right** - placing coverslips in the base of the nutrient and allowing growth showed both clusters and mats after processing

**Lower left** – growing in wells then placing a coverslip in the base before processing showed a similar appearance of clusters and mats

**Lower right** – collecting the surface-associated material with a coverslip and processing revealed mats of biofilm

The third set of coverslips, which were used to scoop up the surface associated material, had a generally cleaner background, but contained sheets of cells as biofilm in 3-6 hours (Figure 2.14). Observation of the surface material using TEM showed bacteria in various stages, from live to dead, with granular material and fine fibres in between (Figure 2.15).

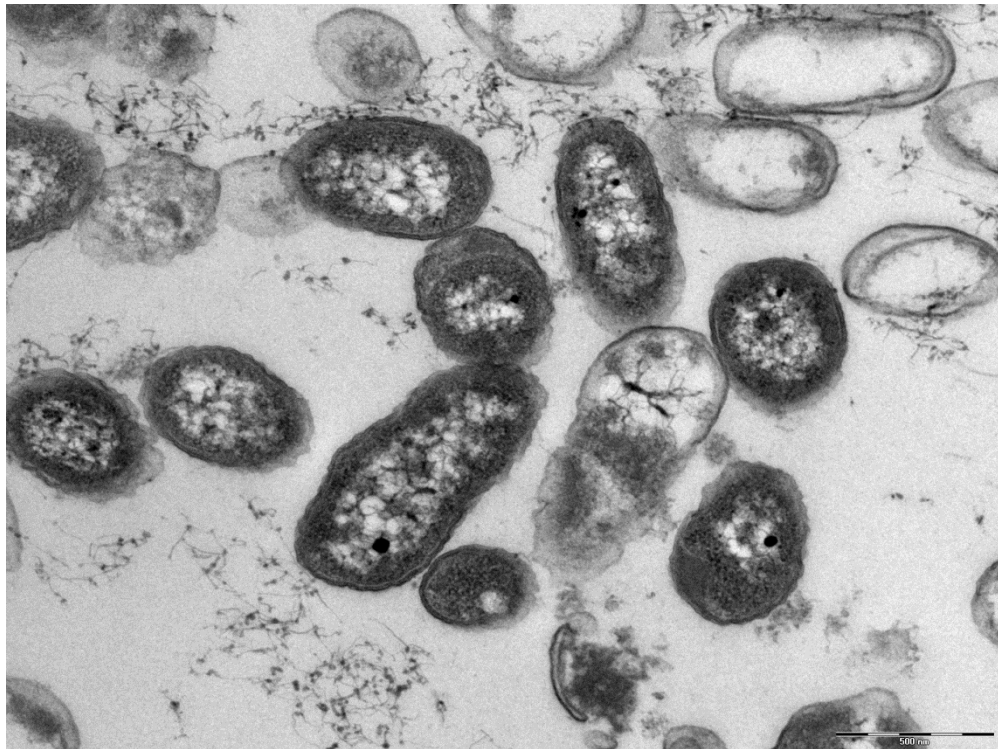


**Figure 2.15: TEM of surface-associated material after 6 hours of growth**  
Elements of biofilm were present as fine strands and granular material but appeared loosely packed. Some cells appear to have disrupted (bar marker 500nm)

## 2.4.9 Biofilm growth on surfaces for LM, TEM and SEM

### 2.4.9.1 Agar

Bacteria grown on agar plate cultures for 24 hours did not produce individual, discrete colonies, but appeared as a unified smear culture. When repeated on

thinner agar, colonies were present as discrete areas. In SEM, bacteria appeared to be in biofilm formations (Figure 2.16).

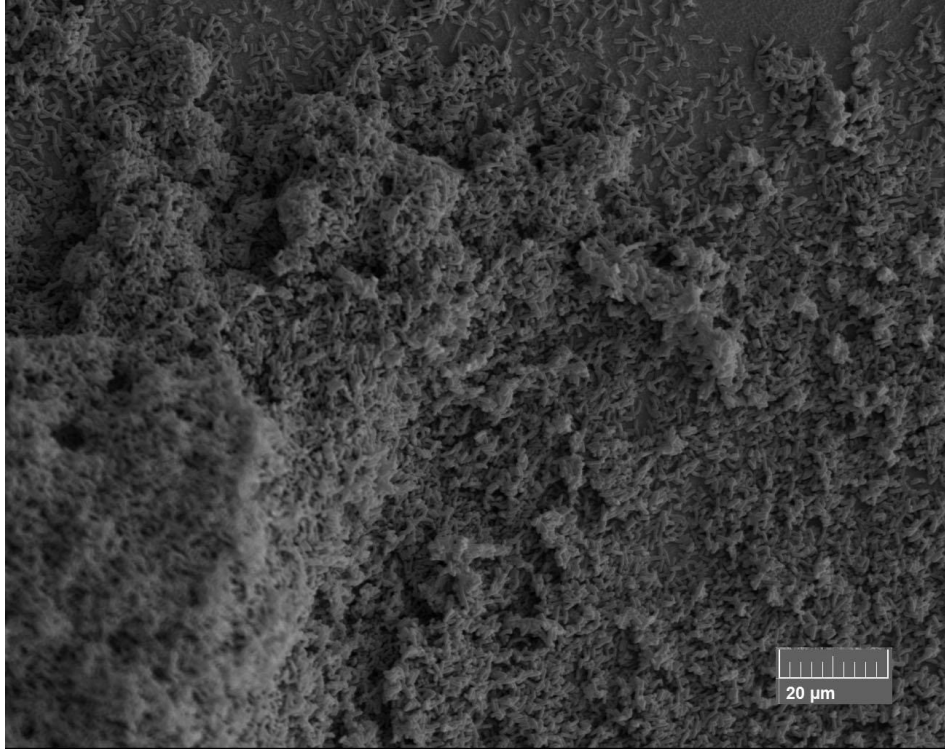


**Figure 2.16: Biofilm grown on the surface of a TSB/agar plate**  
Discrete colonies were observed plus background planktonic bacteria by SEM (x500)

Processing the small pieces of agar was extremely difficult due to it curling, so making observation in the SEM difficult. Those processed with some success looked similar to the biofilms previously produced. However, the method for producing them on agar demonstrated difficulties and so was not considered practical.

#### *2.4.9.1 Plastic coverslips*

As shown e, SEM of biofilm grown on plastic coverslips produced good images. However, for TEM, the block when cut had not sealed well at both edges and kept

coming apart, which made resin microtomy difficult. Sectioning of the coverslips was difficult even with a diamond knife, and on examination no biofilm could be visualised. Microtomy of wax blocks proved that the plastic was too hard for this method and no sections could be produced.

#### 2.4.9.2 Gauze

Cultures grown overnight on gauze, treated with a live/dead stain (*BacLight*<sup>TM</sup> Viability Kit) and viewed under the CLSM, showed small clumps of bacterial biofilm on the strands of the gauze framework. Light microscopy, also demonstrated biofilm. The tough gauze fibres within the wax blocks were sectioned during microtomy, but not without some difficulty. Viewing with SEM showed the same appearance of biofilm, with EPS around the bacteria. However, for TEM the gauze had been poorly infiltrated by the resin, which caused viewing at higher powers to cause the section to tear apart under the electron beam. Further, the sections being, by necessity for TEM, only 100 nm thick, were too thin to show much of the biofilm as the small clumps, as demonstrated by LM, were spread apart throughout the gauze surfaces (Figure 2.17).



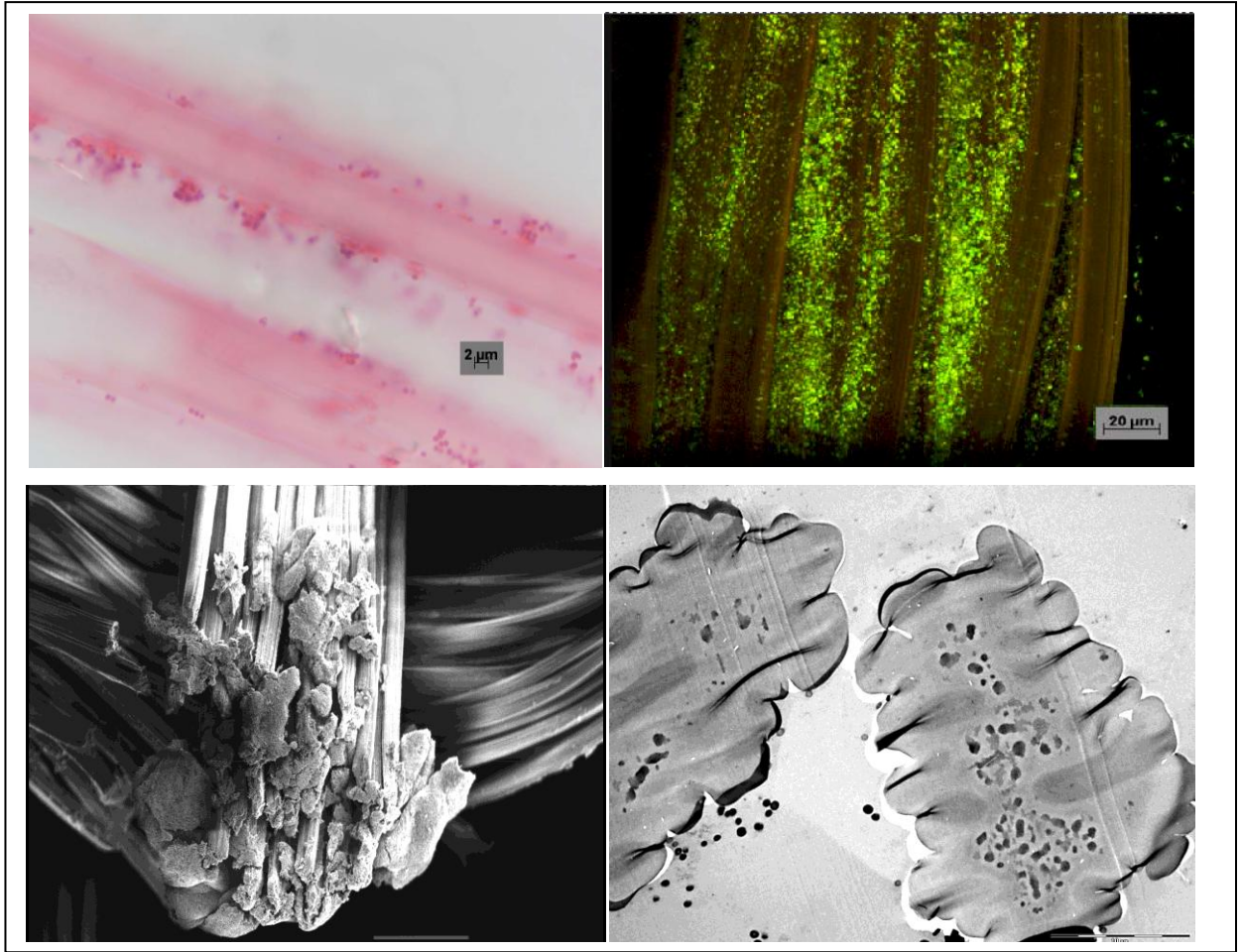


**Figure 2.17: Biofilm growth on gauze, viewed by LM, CLSM, SEM and TEM**

**Top left** - Stained with H&E, a section from a paraffin wax block viewed by LM, showing small colonies of bacterial biofilm on the gauze (x100)

**Top right** – CLSM showing mainly live bacteria (green) using a *BacLight*<sup>TM</sup> viability kit (x40)

**Lower left** – SEM showing biofilm growth within the fibres (bar 100μm)

**Lower right** - TEM of biofilm on gauze. The gauze was not infiltrated by the resin thoroughly, making it difficult to section (bar 10μm)

#### 2.4.9.1 0.4 μm PTTE cell culture inserts

The inside surface of the 0.4 μm PTTE cell culture inserts, which were constantly being provided with nutrients and moisture, appeared to allow biofilm to form.

Processing for LM and TEM necessitated the removal of the porous film from the

upright hard plastic. During processing for microscopy, the film had a tendency to curl up, causing difficulty in embedding in either wax or resin. Also this surface was not easy to cut during microtomy, as neither wax nor resin could infiltrate it. Viewing with SEM demonstrated bacteria contained within an amorphous matrix, presumably biofilm (Figure 2.18).

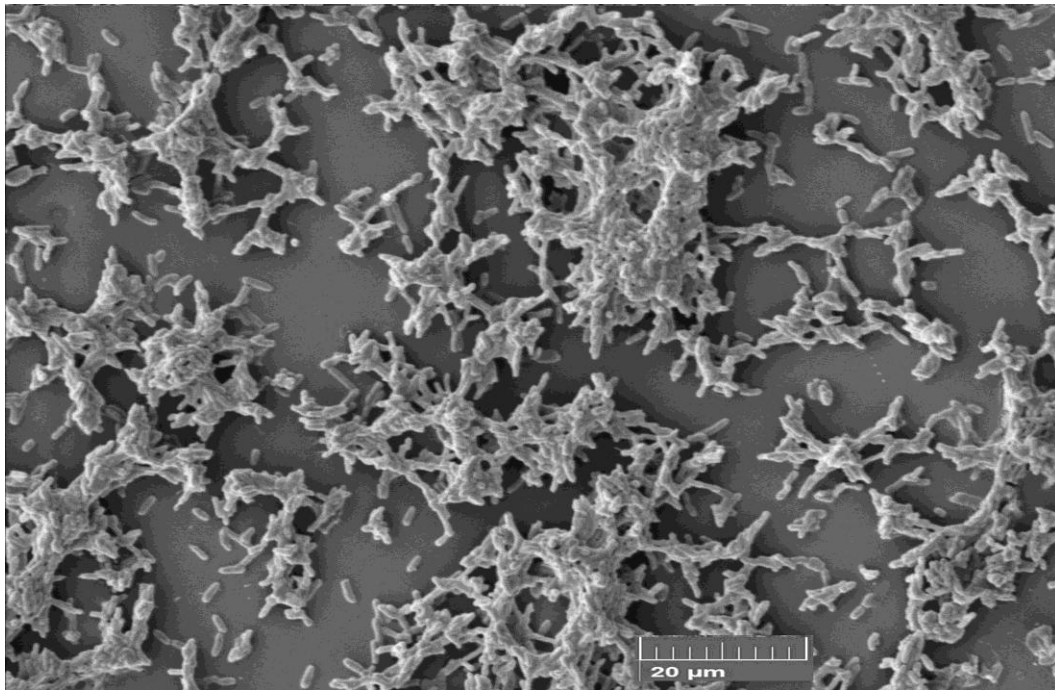


**Figure 2.18: Biofilm growth on PTTE inserts viewed by SEM**  
Clusters of biofilm growth with EPS were observed on the surface of the inserts (x2000)

#### **2.4.10 Development of an agar model to protect the delicate nature of biofilm and process it intact**

In order to prevent moving and detachment of biofilm from the insert surface, molten agar was used to envelop the biofilm. Initially, some of the bisected models split during processing. Further models were therefore processed whole and sliced upon embedding. Deep embedding moulds were used which helped minimise the



amount of slices required. Paraffin blocks were easily sectioned, although extended times on the water bath surface caused some of the sections to split. Staining by the H&E method showed a thin layer of biofilm at 24 hours, with some possible channels visible (Figure 2.19; Figure 2.20).

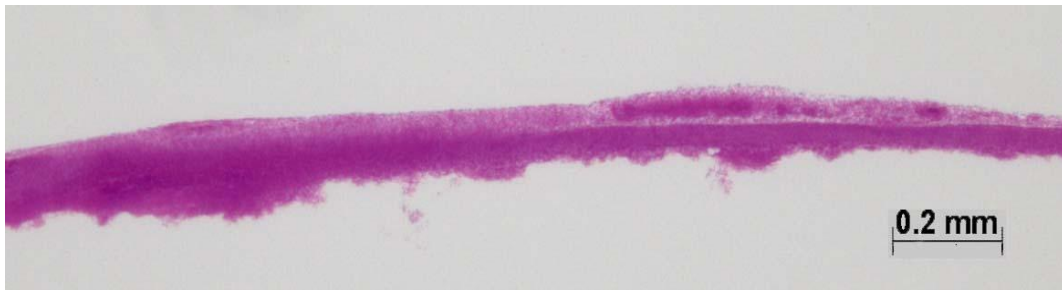


**Figure 2.19: 24 hour agar model of *P. aeruginosa* by LM**

Growth on inserts and processed using the agar model to sandwich the growth in the agar layers (x2)

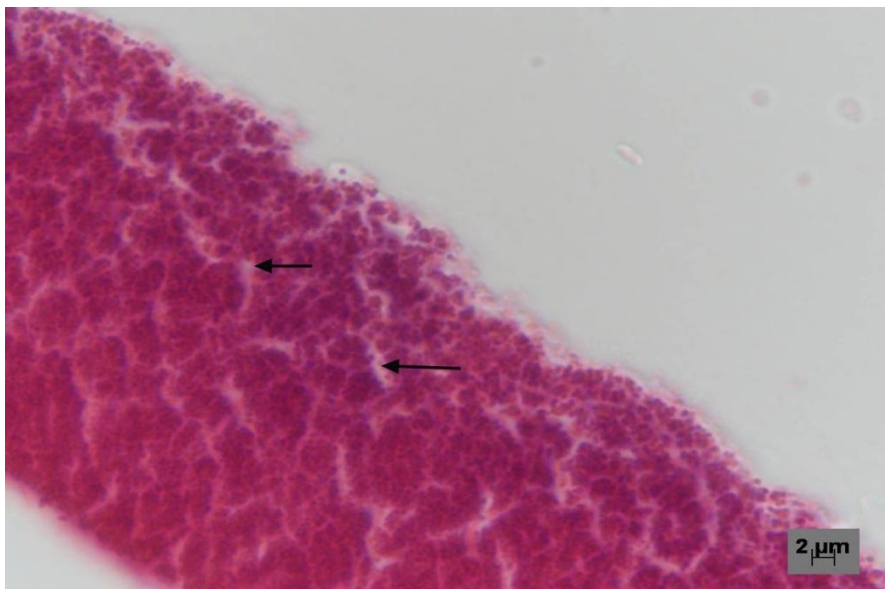


**Figure 2.20: 24 hour agar model of *S. aureus* by LM**

24 hour growth on inserts and processed using the agar. Possible channels were visible by LM (x40)

Even though some of the layers had split during section cutting, the whole of the layer was present. The sample taken from the agar, and processed to TEM showed the biofilm was mainly intact and interspersed with fine vesicles (Figure 2.21).

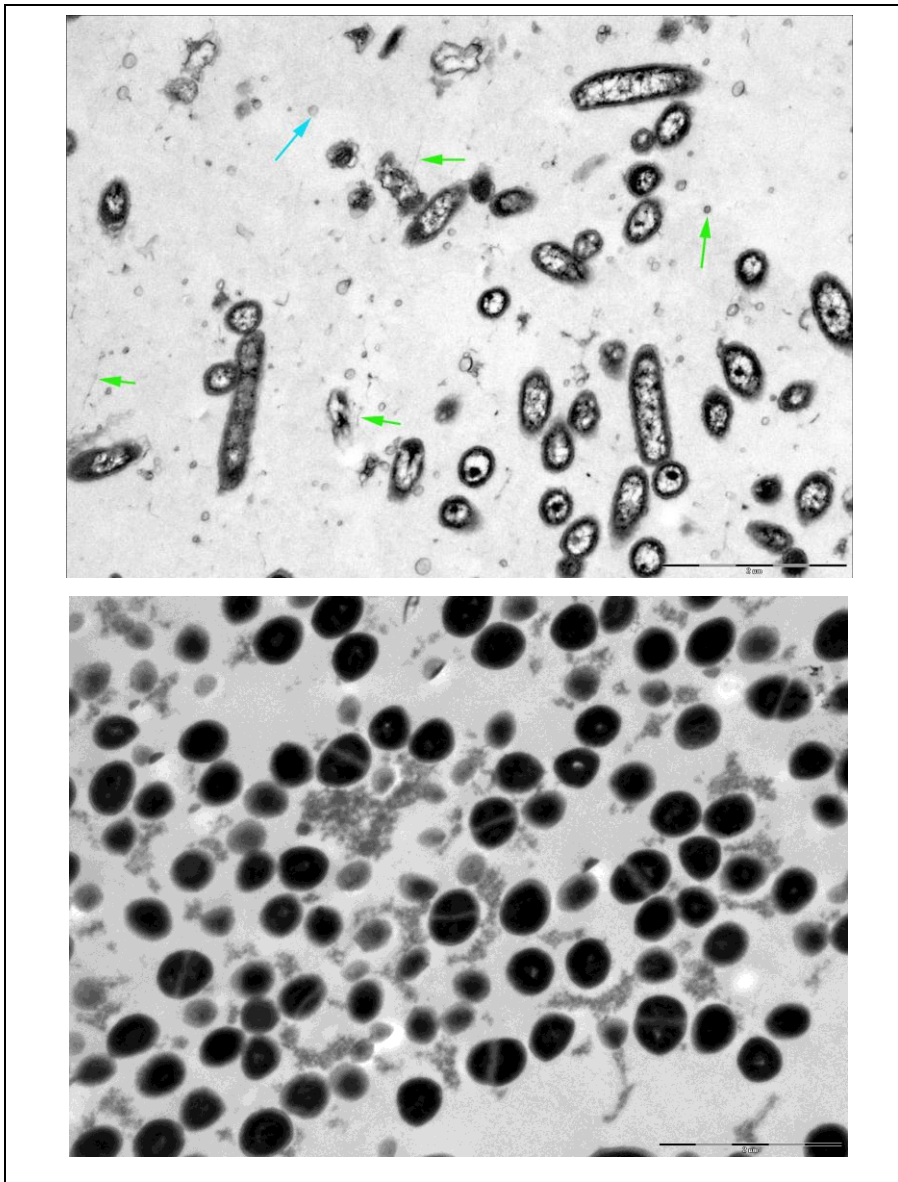


**Figure 2.21 - The 24 hour *biofilm* growth in the agar model by TEM**

**Top - 24 hour *P. aeruginosa*** Bacteria were interspersed with fine strands (green arrows) and vesicles (blue arrows) (x15k)  
**Lower - 24 hour *S. aureus*** The bacteria were interspersed with fine strands and granular material (x15k)

When repeated at 48 hours, channels and bacterial dispersal was evident. The stained sections showed what appeared to be different layers and possible microcolonies (Figure 2.22).

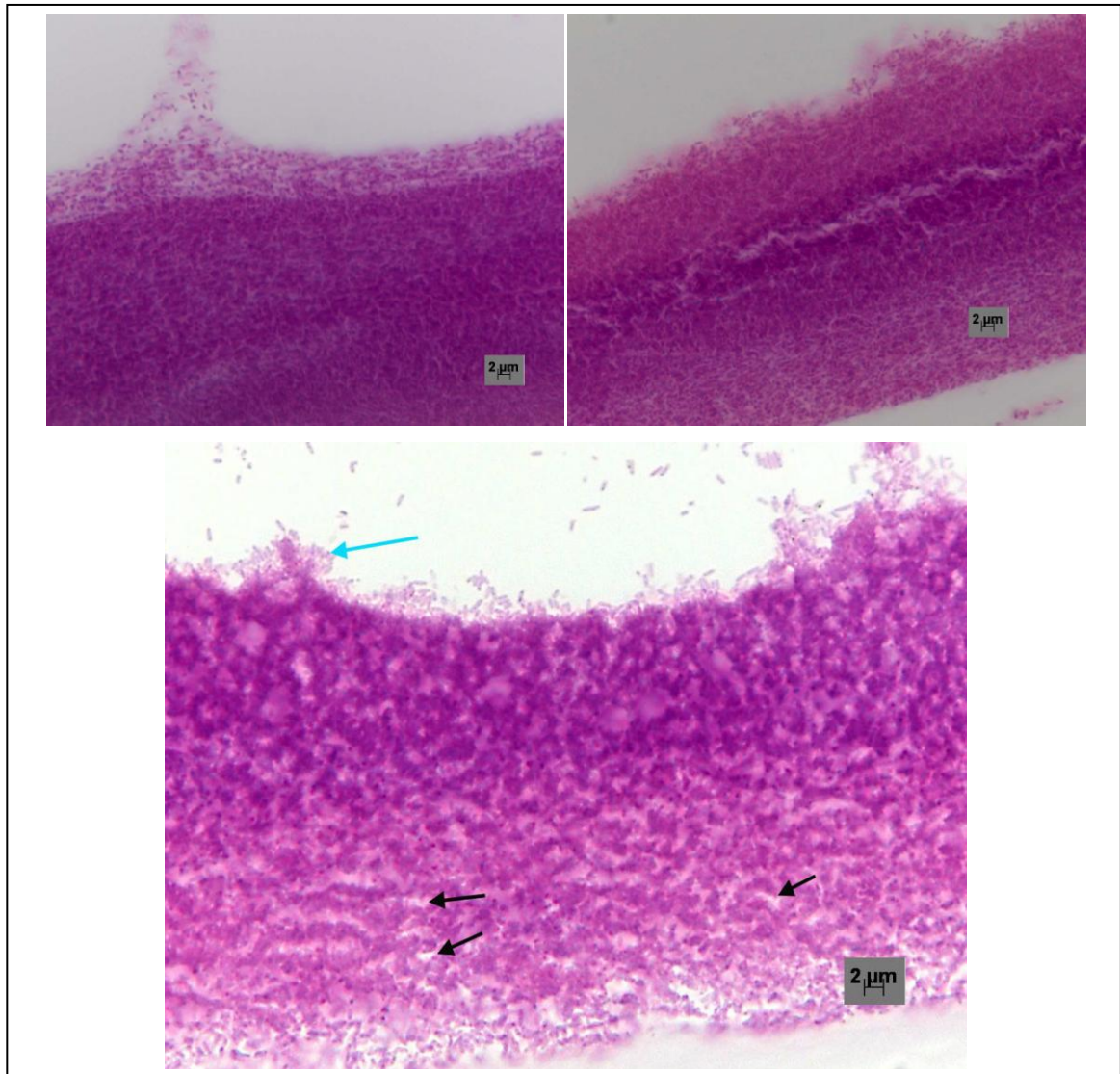


**Figure 2.22: 48 hour biofilm growth in agar models by LM**

**Top left: 48 hours of the mixed bacterial growth**

Sections showed the appearances of channels, layers and of dispersal of bacteria

**Top right: 48 hour *S.aureus***

Sections showing the appearances of channels, layers and of dispersal of bacteria (x100)

**Lower: 48 hour *P. aeruginosa***

Sections show the appearances of channels (black arrows), layers and of dispersal of bacteria (blue arrow) (x100)

These layers were present in the single cultures and in the mixed culture. Some of the layers appeared to be denser. TEM showed some bacteria to have fine strands between them. In places, fine channels could be seen within this structure which corresponded with the channels seen in the H&E sections (Figure 2.23).

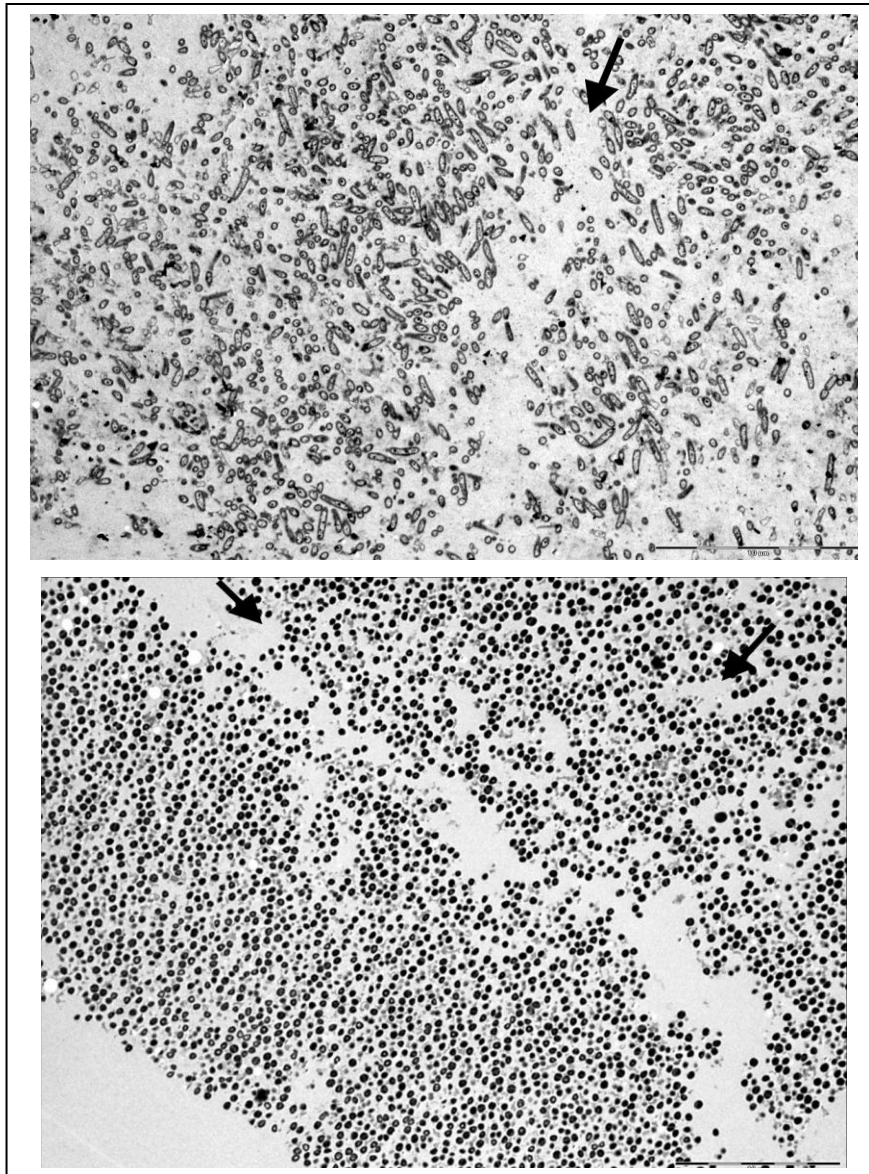


**Figure 2.23: TEM of 48 hour biofilm in the agar model with channels**  
**Top - TEM of 48 hour *P. aeruginosa* biofilm Lower - TEM of 48 hour *S.aureus* biofilm**  
Fine channels were observed within the biofilm in both biofilm models (black arrows)  
(x2500, bar 10µm)



#### 2.4.11 The meat model

Surrounding the meat and biofilm with agar afforded the delicate biofilm surface protection. In some models the paraffin wax sections split slightly when floating on the 45°C water bath. This was due to the length of time it was required to leave them on the surface, in order to straighten out the meat muscle fibres within the section. Despite this the H&E stained sections contained all the layers of biofilm and muscle, and the biofilm area could still be quantified (Figure 2.24).

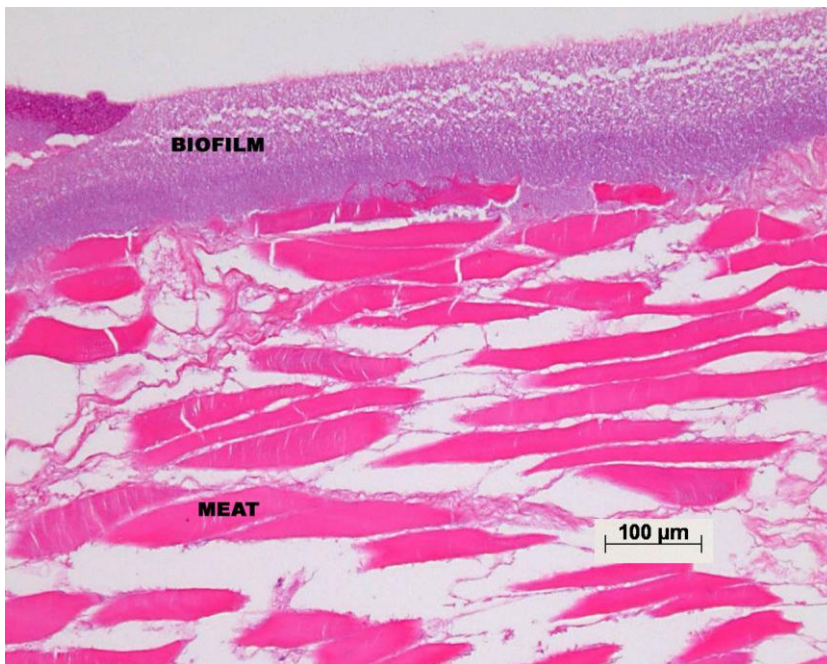


**Figure 2.24: Intact 72 hour biofilm on the meat model by LM**

Models had intact biofilm with the appearance of layers. There was also occasional invasion of the biofilm into the surface of the tissue (x10)

The 72 hour growth appeared thicker than the 24 and 48 hour layers from the agar model, as would be expected. Once again, waste/nutrient channels and areas of bacterial dispersal in *P. aeruginosa*, *S. aureus* and mixed cultures were found (Figure 2.25; Figure 2.26).

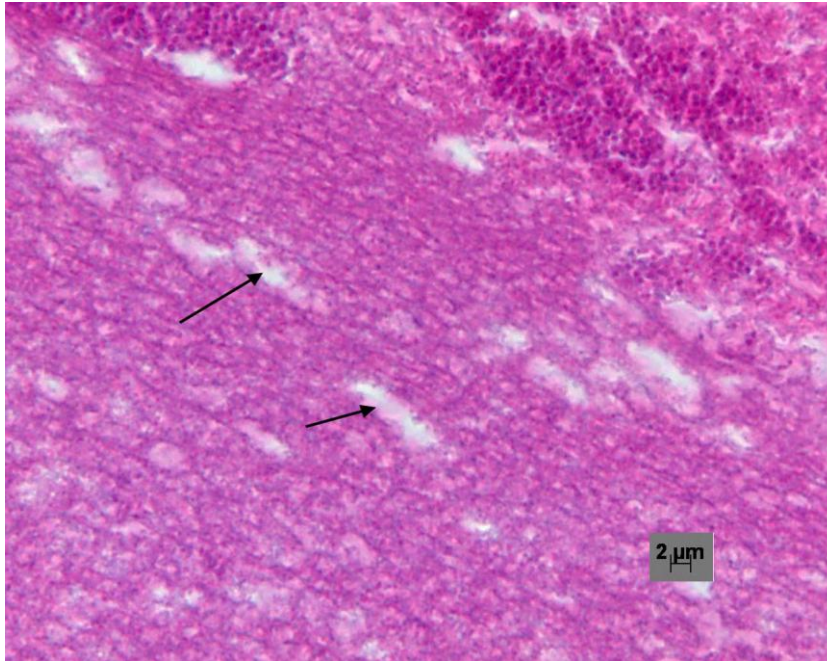


**Figure 2.25: Waste/nutrient channels in 72 hour biofilm on meat model by LM**  
Channels were visible within the layers of growth (black arrows) (x100)

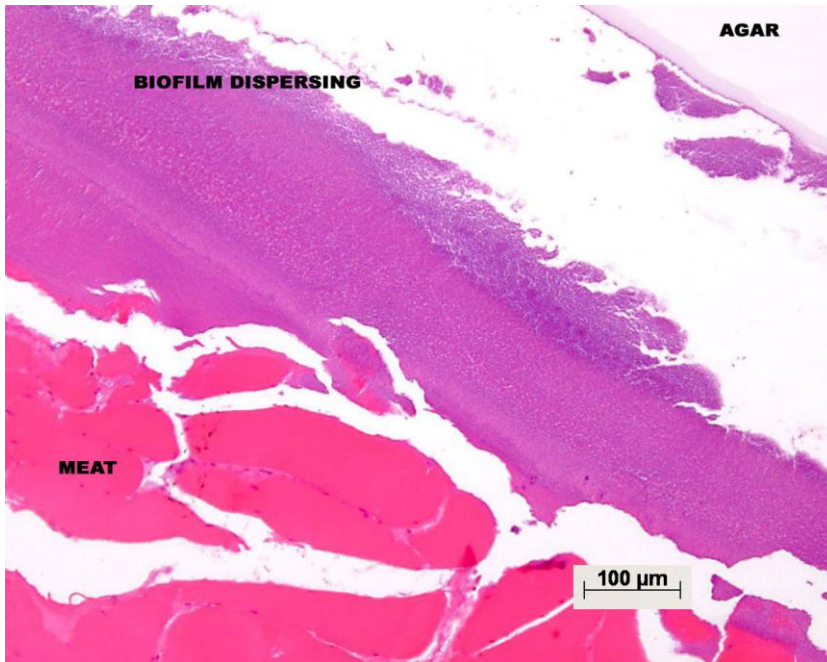


**Figure 2.26: Bacterial dispersal on 72 hour biofilm on meat model by LM**  
Layers were present within the biofilm. The surface showed looser layers and areas of bacterial dispersal below the agar covering (x20)

There appeared to be differing layers within the biofilm, the deeper layers adjacent to the meat appearing denser than the upper layers (Figure 2.27; Figure 2.28).

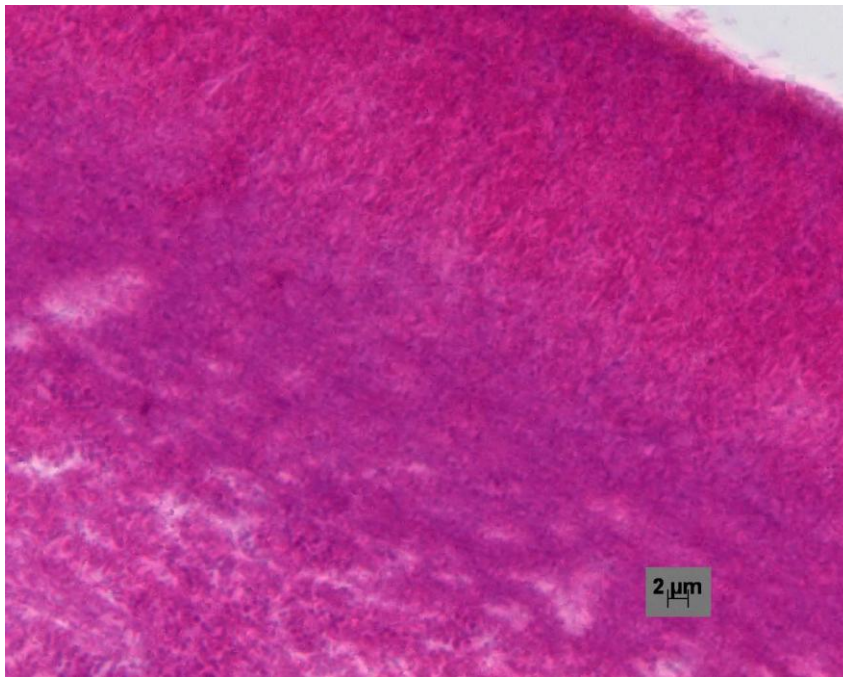


**Figure 2.27: Differing biofilm layers on the 72 hour meat model by LM**

Varying layers were seen within the biofilm growth, some appearing denser than others (x100)

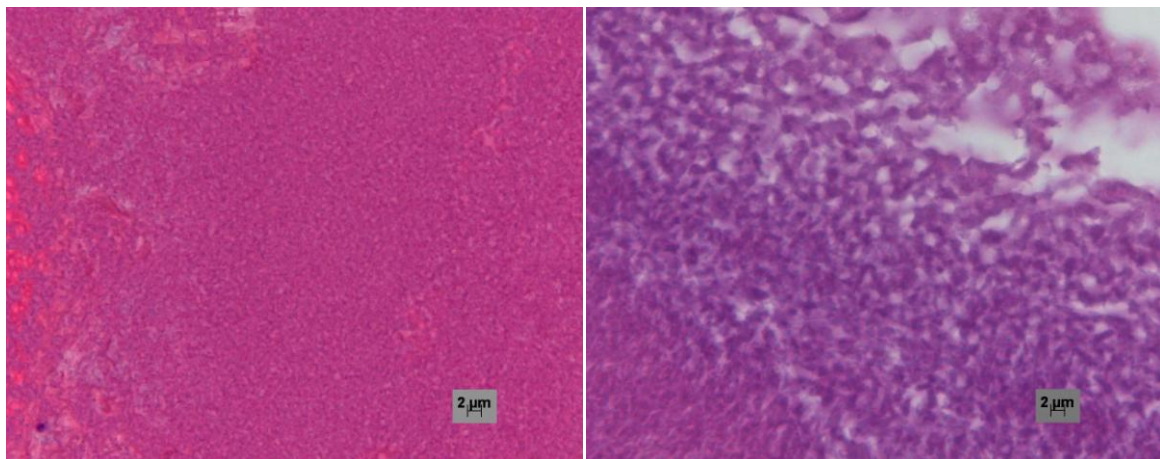


**Figure 2.28: Layers of 72 hour biofilm on meat model by LM**

Left - Showing deeper, denser layers of growth in the areas nearer to the biofilm/tissue interface. Fewer channels could be seen by LM in these layers (x100)

Right – Showing upper layers of biofilm growth which appeared more open and less dense than the lower layers of growth (x100)



Occasional groups/microcolonies of bacterial cells were found within the thick biofilm. Observation of the H&E sections showed the biofilm to be growing down into folds in the meat surface and deeper into the tissue, suggesting bacterial invasion (Figure 2.29).

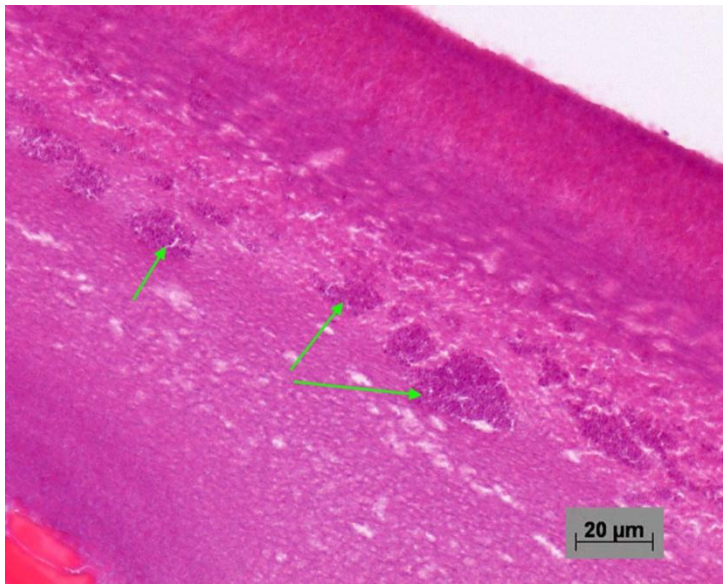


**Figure 2.29: Biofilm micro-colonies and channels in 72 hour biofilm by LM**  
Micro-colonies (green arrows), and channels were present in many areas of biofilm (x40)

The structure of the TEM images showed similar evidence of dense layers of tightly packed dormant-appearing biofilm bacteria at the meat-biofilm interface (Figure 2.30), with less tightly packed layers of bacteria further towards the surface (Figure 2.31).



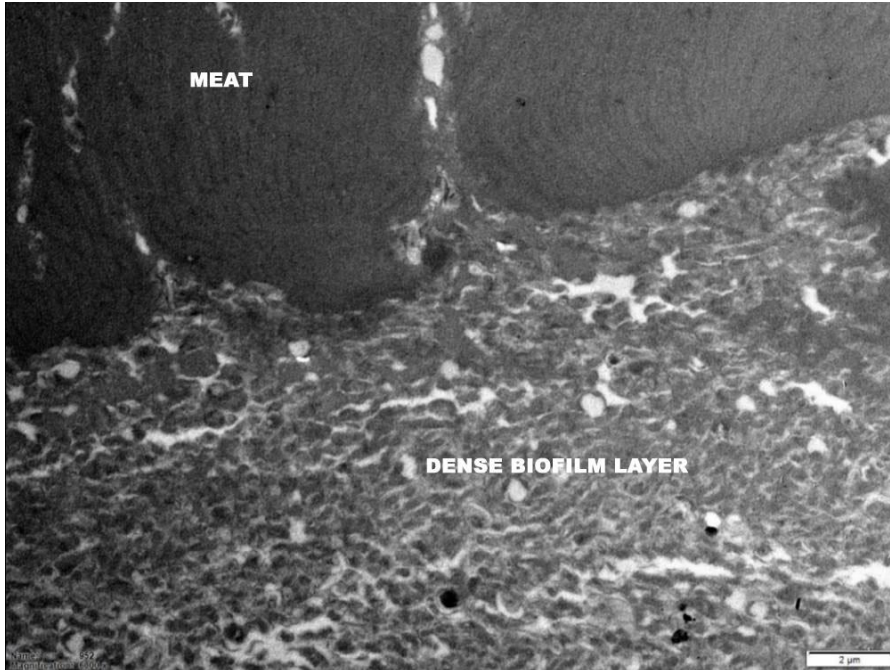


**Figure 2.30: TEM of lower dense biofilm layers at 72 hours**  
Lower layers of biofilm growth showing deeper, denser layers at the tissue/biofilm interface by TEM. Some possible channels existed but were small (15k)

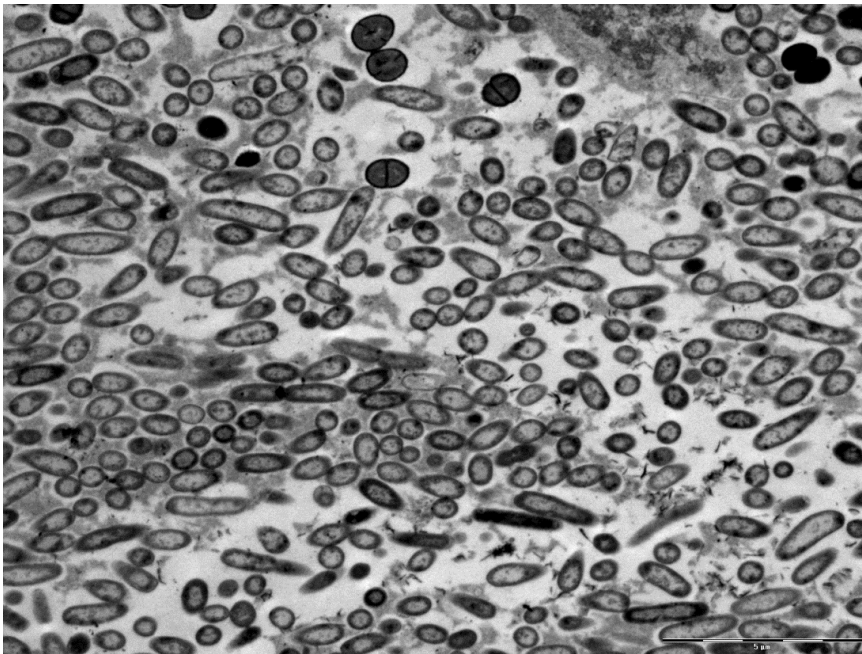


**Figure 2.31: 72 hour biofilm upper layers on meat model by TEM**  
The upper layers of biofilm growth nearer to the surface presented a looser, less densely packed appearance than the deeper layers. Fine strands of EPS were seen around the cells (bar marker 5μm)

The bacteria in the upper areas appeared to have more structure. Small channels were seen within the layers of biofilm and also larger channels containing clusters of individual bacteria (Figure 2.32).

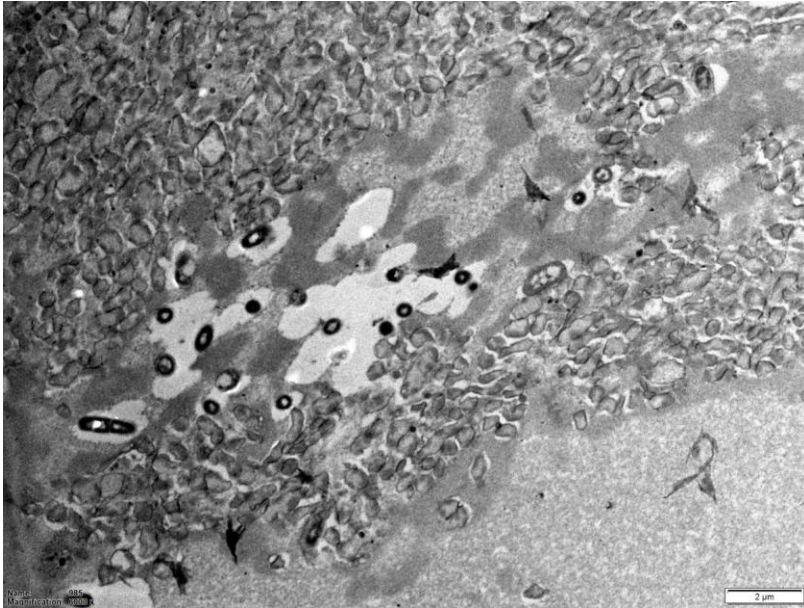


**Figure 2.32: Channel detail of the 72 hour biofilm by TEM**

Channels were observed within the biofilm, some longer than others, lined by several individual bacteria (bar marker 2  $\mu\text{m}$ )

The thickened areas contained bacteria in biofilm with EPS, when examined by TEM, some of which included bacterial budding (Figure 2.33).

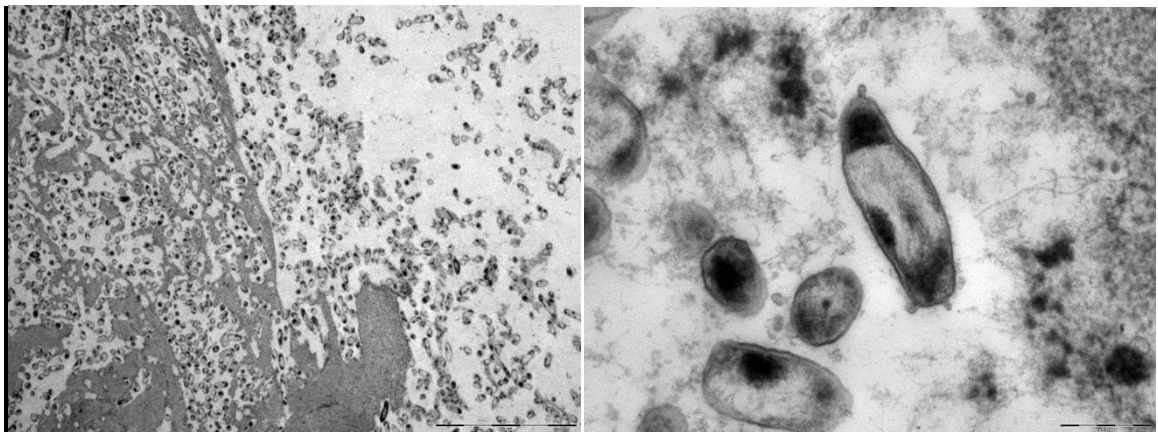


**Figure 2.33: TEM of thickened areas of biofilm in the 72 hour model**

Bacterial biofilm with EPS was present (left, bar marker 10  $\mu\text{m}$ ) and bacterial budding (right, bar marker 500nm)

Any increase in growth of the biofilm from 24 to 72 hours was confirmed quantitatively by taking LM images at x4 magnification and measuring the area of biofilm using Image J software. Two-sample t-tests and Analysis of Variance (ANOVA) statistical tests were conducted using Minitab 17 software to compare the means of biofilm areas. Statistical analysis (a two-sample t-test) of the means at 24 and 48 hour showed a significant difference ( $p= 0.000$ ), as did the 24 and 72 hours ( $p= 0.000$ ), and the 48 and 72 hour comparisons ( $p= 0.001$ ). Using a one-way ANOVA test, a Tukey Pairwise comparison of the 24 and 48 hour means of the standard deviations showed the means to be similar, but that the 72 hour growth was significantly different. An interval plot of the pooled standard deviations demonstrated that the differences between the 24 and 48 hour means were probably not significant. (Figures 2.34-36).

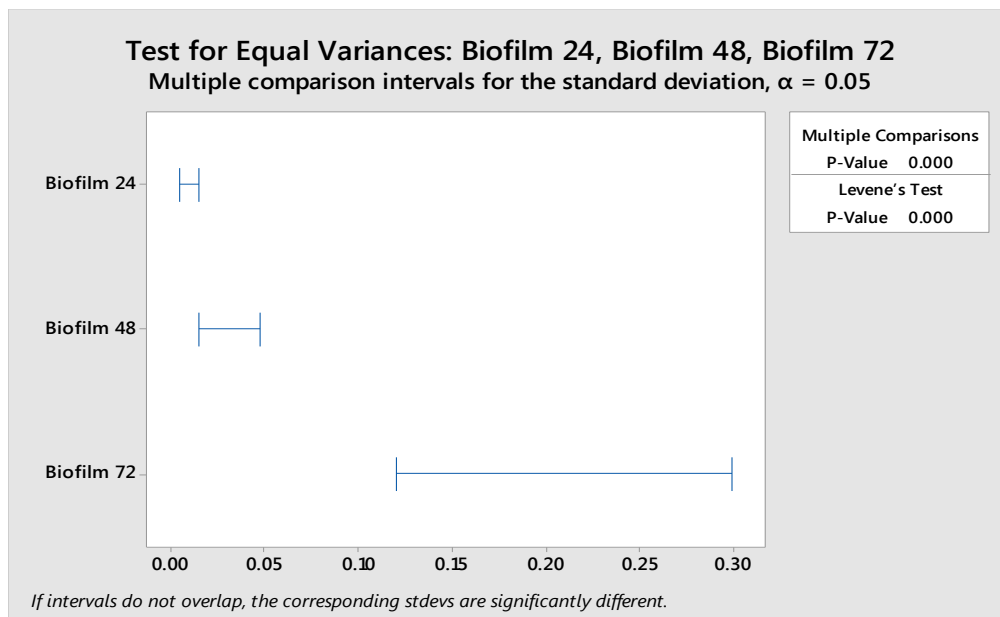


**Figure 2.34: Equal variance tests of biofilm growth at 24 48 and 72 hours**  
 The consistency in standard deviations of the biofilm growth areas showed the 24 hour growth to be the most consistent. This comparison also demonstrated that the 72 hour growth was significantly different to the 24 and 48 hour growths

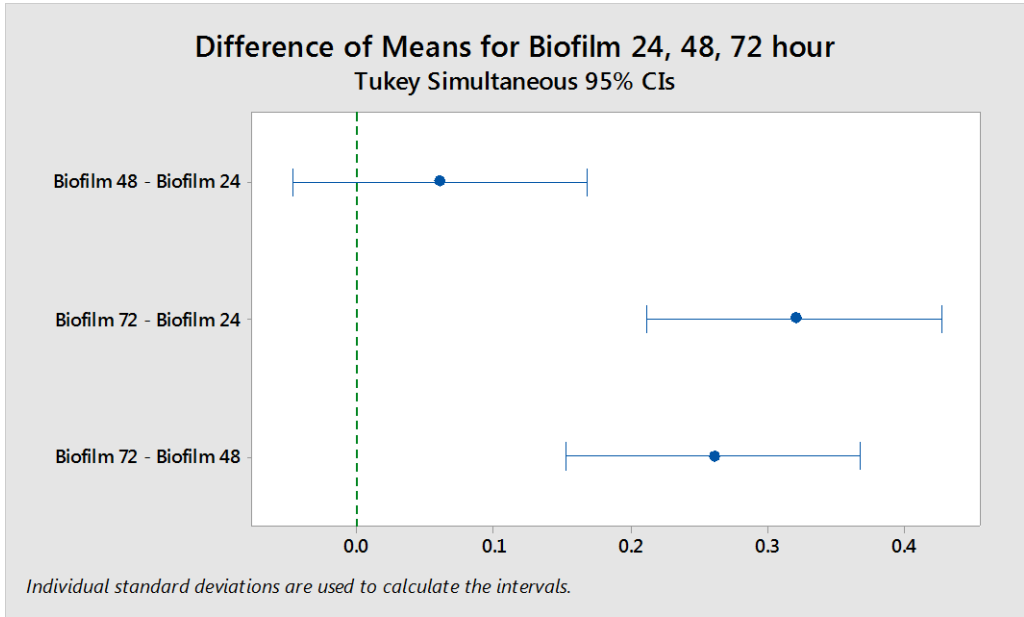
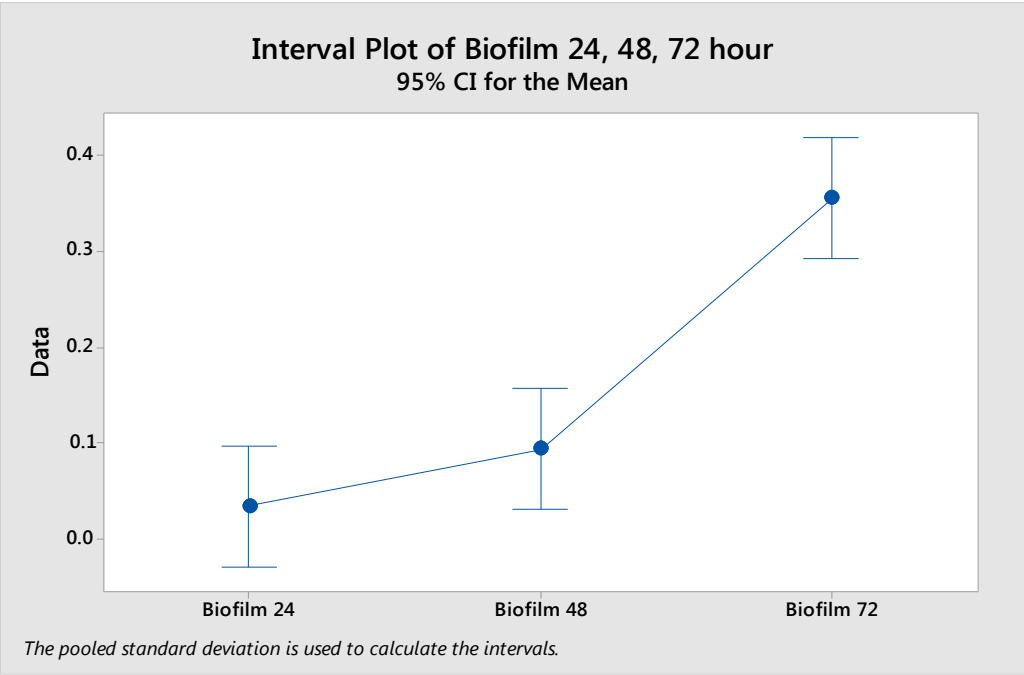


**Figure 2.35 and 2.36: Interval plot and Tukey plot of biofilm growth at 24, 48, and 72 hours**

Showing a mean increase in biofilm growth areas on the interval plot, at 24 and 48 hours the interval lines overlap showing the difference not to be significant. The 72-hour growth was significantly different from the 24 and 48-hour growth.

## **2.5 Discussion**

### **2.5.1 Growth and the Effect of Silver**

Under controlled conditions (e.g. when nutrients are plentiful and the starting number of bacteria is small), bacterial growth will be optimal and provide rapid exponential growth within a matter of hours. However, this type of environment cannot sustain an infinite population of a species and there will come a point when, as the population size increases, available nutrients and space are depleted and there will be a slowing down of growth, termed the stationary phase (Todar, 2012). To obtain a substantial sample for experimentation that is still actively growing but not slowing down, it is best to harvest a natural population at its maximum point of exponential growth (Math Insight.org). Knowing when to harvest exponentially growing cells either for the best culture of planktonic cells or for biofilm development is crucial, as it is important to have healthy and actively growing cells for any microbiological experiments. Monitoring growth of a bacterial culture allows this determination to be made accurately. The physiological experiments showed how exponential growth rates could be used to point consistently to the best time for harvesting bacteria in order to obtain a substantial sample for future experiments. This best time point for harvesting exponentially grown bacteria could be checked against the bacterial density, by taking spectrophotometer readings at the collection time points mentioned in the results section (2.4.1), so providing similar readings and hence a similar concentration of bacteria.

Bacteria readily lend themselves to study by EM and advances in specimen preparation for EM have improved the preservation of their ultrastructure (Newman

and Hobot, 2001). This has given rise to new perspectives on our understanding of the structure of the bacterial cell (Hobot, 1990; Hobot, 2015). For these studies it would be necessary to distinguish between planktonic and biofilm bacteria within wounds. Therefore, it was important to analyse bacterial structure in culture media in preparation for the more clinically relevant wound model that was one of the objectives of the study.

The addition of silver nitrate at 10 µg/ml (i.e. 1%), is known to be an effective concentration. This is the minimum inhibitory concentration (MIC), which is defined as the lowest concentration that kills at least 99.9% of a planktonic or biofilm bacterial population (Choi et al., 2008). The addition of silver nitrate to actively growing cultures resulted in a very rapid cessation of growth in both *P. aeruginosa* and *S. aureus*. This confirmed the earlier work of silver's effect on *P. aeruginosa* by Hobot et al. (2008), and the claims of the effect of silver nitrate on *S. aureus* by Jung, et al. (2008), and on Gram positive and negative bacteria by Furr, et al. (1994).

Understanding the effects of silver will be of benefit for the studies presented in Chapter 3 using different types of wound dressings on biofilm development, especially those containing silver (Newman et al., 2006).

### **2.5.2 TEM of Planktonic Bacteria and the Effect of Silver on Bacterial Ultrastructure**

Bacteria readily lend themselves to study by EM and advances in specimen preparation for EM have improved the preservation of their ultrastructure (Newman



and Hobot, 2001). This has given rise to new perspectives on our understanding of the structure of the bacterial cell (Hobot, 1990; Hobot, 2015). For these studies it was necessary to distinguish between planktonic and biofilm bacteria within wounds. Therefore, it was important to analyse bacterial structure in culture media in preparation for the more clinically relevant wound model that was one of the objectives of this study. Comparing preparatory techniques for the study of bacterial cells with TEM was important as deleterious changes to ultrastructure can occur. For example, harvesting cells by centrifugation can lead to conditions of anoxia and cause leakage of ions across the bacterial membranes (Moncany and Kellenberger, 1981). This can have consequences on the structure of the bacterial nucleoid and is why harvesting cells by filtration avoids these problems (Hobot et al., 1985). It has been found that centrifugation can affect the structure and organisation of the bacterial cell wall (Hobot et al., 1984).

Fixation with osmium tetroxide, initially introduced as part of the RK conditions of fixation by Ryter et al. (1958), has been shown to have an adverse effect on the shape of the bacterial nucleoid depending upon the salt content of the growth media (Kellenberger and Ryter, 1964). They examined the fine structure of the nucleus under different conditions and this resulted in the development of a buffering solution which obtained optimal preservation of the fine fibrillar nuclear material (RK buffer: veronal-acetate buffer, pH6.15; Ryter et al., 1958). Osmium tetroxide has also been implicated in damaging protein structures (Baschong et al., 1984). However, this has not been reported for glutaraldehyde and consequently the bacteria for TEM were harvested by filtration and fixative solutions using RK

buffer avoiding osmium tetroxide. This ensured that a similar appearance of the bacterial nucleoid under the various growth conditions, displayed a dispersed ribosome free space within the cytoplasm (Hobot et al., 1985).

Various combinations of glutaraldehyde and uranyl acetate were tried. It had been shown that uranyl acetate solutions could, *in vitro*, stabilise bacterial DNA by gelation (Schreil, 1964). Using uranyl acetate prior to fixation with glutaraldehyde was not successful, resulting in severe damage to the cytoplasm and nucleoid. Glutaraldehyde followed by uranyl acetate fixation, showed no real advantages over using 2.5% glutaraldehyde alone, which was therefore chosen as the fixative of choice for this study. The choice of LR White, an acrylic resin, which allows for a partial dehydration of cells, was based upon results indicating that this protocol was advantageous for the preservation of both cellular tissues and bacterial cell ultrastructure (Hobot, 1990; Newman and Hobot, 1987; 2001).

Addition of silver nitrate to bacterial cultures caused exponential bacterial growth to cease. This may have been due to damage to the cell structure by the silver. This was demonstrated by TEM, in the adverse effect seen on bacterial ultrastructure. Most notably the nucleoid shape changed from a more dispersed appearance to one more condensed and lying throughout the central region of the cells. This confirmed the findings of Hobot et al., (2008) for *P. aeruginosa*. The DNA fibres became coarser and thicker in *P. aeruginosa* and more so for *S. aureus*, a bacteria not studied by Hobot et al., (2008). The change in shape and appearance of the DNA fibres resembled those changes in appearance seen after fixation with osmium tetroxide (Hobot et al., 1985).



As previously discussed osmium tetroxide is known to alter the permeability properties of bacterial membranes allowing for ionic leakage to occur (Woldringh, 1973) and results in a loss of bound ions from the DNA (Moncany and Kellenberger, 1981). Similar results have been observed in the images of the effects that silver has on bacterial structure (Figure 2.7), and suggests that silver ions, upon entering a bacterial cell, can cause similar permeability changes in the bacterial membranes leading to ionic loss from nuclear areas (Hobot et al., 2008). It therefore provides an interesting hypothesis of how silver kills bacterial cells quickly and effectively, by binding to the DNA and changing its structural organisation within the cell. As silver is now a popular additive to wound dressings, and claimed to be an effective anti-bacterial agent (Newman et al., 2006; Percival et al., 2008), it is important to understand a possible mechanism by which silver ions kill bacteria. It may also lead to a better understanding of how silver may work effectively in a wound environment that could chemically impede the action of silver.

### **2.5.3 SEM of Planktonic Bacteria**

In SEM images of planktonic bacteria, the cells are clearly visible as individual entities, even though the images showed a mass of bacteria (Figure 2.8a and b). No EPS was visible throughout the bacterial populations for both *P. aeruginosa* and *S. aureus*, as would be expected in the non-biofilm phenotype. The rather short infiltration times used during the SEM preparation protocol were chosen as it was observed in previous biofilm studies, that longer infiltration times can lead to detachment of biofilm from its substrate (Fischer et al., 2013). In agreement with

the previous findings of Araujo et al. (2003), using HMDS instead of critical point drying was superior in preserving the outer appearance of the bacterial cells, and therefore was the method of choice for future SEM examination of biofilm development and structure.

Investigating and understanding the behaviour of *P. aeruginosa* and *S. aureus* in a liquid medium has been a focus in wound microbiology in the past, and consequently for many years the majority of quantitative evidence for the efficacy of antimicrobial dressings has been based upon *in vitro* studies of planktonic bacteria (Bowler et al., 1999; 2004; Jones et al., 2004). However, in chronic wounds there is increasing evidence that the wound bioburden consists of planktonic and biofilm bacteria (Malone et al., 2017; James et al., 2008; Kirketerp-Møller et al., 2008; Rhoads et al., 2008). As biofilm is defined as being microbial communities attached to a surface, or to each other, and enclosed in a matrix of EPS, it followed that the next stage of the project would be the growing and examination of biofilm attached to a surface.

#### **2.5.4 Establishing and characterizing biofilm growth**

More than a decade of evidence has discussed around how microorganisms can exist as biofilm communities in the wound environment and not as previously thought, as just planktonic microbes (Metcalf and Bowler, 2013). With such evidence it would seem that the culturing of biofilm *in vitro* should be relatively simple. However, biofilm needs certain conditions to enable them to develop, such as nutrients and a suitable surface. Once grown, flow rate, shear force, chemical

gradients, diffusional processes and surface type and topography, can all affect biofilm structure (Korber and Lawrence 2004).

Culturing the biofilm models in a TSB at 37°C with gentle agitation resulted in successful biofilm development, and it was decided that the same broth and agitation conditions would be used throughout all the remaining studies. The larger volumes of solution and bacteria used were suited to the Petri dishes but, for ease of use and handling in multiple tests in all subsequent experiments, culture plates with wells were used instead of Petri dishes. Trialling different sized culture wells showed how fluid flow and currents can affect both the growth and how biofilm can be removed/disturbed. As one of the objectives was to process a biofilm intact, larger diameter wells were used rather than the smaller well plates as they were found to create fewer disturbances to the biofilm during processing. The first of these studies, on the glass, provided thick biofilm with EPS evident (Figure 2.9), but the glass was prone to breakages and was only suitable for SEM or CLSM viewing. Plastic coverslips have been embedded in resin for thin section studies in TEM (Espinal et al., 2012), and these were tried as a different surface for the next set of studies.

Despite initial concerns over obtaining the correct optimisation of the initial bacterial concentration, this appeared not to be of great significance. Overall there appeared to be no difference to the amount or thickness of bacterial coverage on coverslips. The bacterial population, regardless of the inoculum concentration, repeatedly grew to produce a colony that quickly established itself as a biofilm community. Therefore, actual biofilm formation was independent of the initial

bacterial cell number used as an inoculum. For this reason, a starting concentration of  $1 \times 10^7$  bacteria  $\text{ml}^{-1}$  was chosen as providing a reasonable number to initiate biofilm formation and simply involving a one-step dilution from the  $1 \times 10^8$  bacteria  $\text{ml}^{-1}$  present in mid-exponential phase.

There was some early hypothesising concerning the presence of biofilm in chronic wounds (Costerton et al., 1999; Serralta et al., 2001) but most of these studies examined established biofilms only at 72 hours and did not look into the earlier times during which biofilm can form. Harrison-Balestra et al. (2003) showed, by suspending plastic coverslips in an inoculated TSB broth and staining and viewing with LM, that the EPS of developing biofilm may be visible in 5 hours after inoculation and that mature biofilm characteristics, such as a dense coating of EPS, might be found by 10 hours.

The results from the preliminary experiments (performed in 2.4.7) showed that, by viewing with SEM, bacteria were not only dividing rapidly but were starting to form small clusters of immature biofilm within only 4 hours. There were the beginnings of strands of EPS between them, with some enmeshed in EPS at 5-6 hours (Figures 2.13; 2.14). The structure at this point may not be mature biofilm, with channels and layers, but the speed with which these groups begin to form in the simplest of environments must surely reflect how quickly biofilm can start to form within a wound, if a patient is immunocompromised.

Changing the glutaraldehyde fixative diluent, from buffer to TSB, prevented the earlier problems of pooling of the biofilm and was used as the method of primary

fixing of the biofilms *in situ*. The movement of the surface associated material, during processing, made it uncertain whether the coverslips were covered in biofilm grown on its surface below the nutrient, or if it also included surface growth/debris. By placing coverslips on the base of the well, and growing biofilm beneath the nutrient, then comparing these to coverslips dropped into a well of growth, and coverslips used to scoop up the surface-associated growth, it was hoped to clarify whether the surface material was having an effect on the results.

The bacterial coverage on coverslips used to scoop up the surface-associated material contained thick folded mats of biofilm when viewed by SEM, which was probably surface-associated biofilm. To be certain of the nature of such material it was viewed with TEM. Observation of the surface-associated biofilm using TEM showed loosely grouped bacteria, with granular material and fine fibres in between (Figure 2.15). The granules and fibres between the cells were most likely extracellular DNA, a component of EPS.

The appearance of folded mats of biofilm on the other coverslips raised the question of surface-associated biofilm being present. Some of this may inadvertently have come to rest on the coverslip during processing, where there had been removal of solutions from one step to another. Webster et al. (2006) incubated coverslips half submerged in a culture of bacteria and found that biofilm formed on the submerged glass, as well as on the glass surface exposed to air. From the careful examination of the movement of the surface during processing for microscopy detailed in the results of 2.4.8, it might be concluded that some of the material in this study was biofilm. Scooping up the surface material and comparing

it to the other coverslips showed that when coverslips are submerged and then processed, they run the risk of accumulating surface biofilm and debris during processing.

The ability of bacteria to form biofilm was demonstrated clearly by growth on the array of differing surfaces trialled. Some surfaces appeared to be better than others, not for the speed of biofilm formation, but for ease of use and handling.

This study includes different types of microscopy, and the growth surfaces were tested for adaptability for use with all techniques. Therefore, the processing methods for the various techniques were applied to biofilm growth on the plastic coverslips, agar, gauze and 0.4 $\mu$  PTTE membrane cell culture inserts.

The three most common ways of growing bacteria *in vitro* are as planktonic cultures, colonies on *agar* plates, and *biofilm* in continuous-flow systems (Mikkelsen et al., 2007). Agarose, when set as a solid gel, acts as a support medium for cells in histological processing techniques into paraffin wax and electron microscopy processing techniques into resin (in-house methods). It was therefore considered that it might be possible to process biofilms grown on agar plates, for all microscopy methods. Some authors state that bacterial growth on agar is not representative of how bacteria grow in tissue sites, and that any results from tests are open to error (Costerton et al., 2003; Clutterbuck et al., 2007). It is suggested that they grow more as a smear culture. The nutrient source is thought to become eventually depleted beneath them (McBain, 2009). However, because of the nature of the agar plates and the way in which they reacted by curling during

the processing steps, it was not an ideal surface to use. Therefore, the use of the agar plates was discounted from the study.

Cotton gauze has been used to grow biofilm in various studies. Lipp et al. (2010), Rowlands et al. (2013) and Parsons (2014) all grew bacterial biofilm on gauze dressings to add to a wound model; CLSM confirmed the presence of biofilm within the gauze structure, growing around the fibres. Tachi et al. (2004) using an infected animal wound model demonstrated that by covering full thickness wounds with gauze, infections persisted. Biofilm growth on gauze provided useful images with LM, with the presence of biofilm within the gauze structure being confirmed using CLSM. Unfortunately, it did not process into the resin adequately, and gave too small a surface area to section and view with TEM. However, the growth within the gauze gave an insight into how easily biofilm may begin to grow within a gauze dressing on a wound. Despite gauze having been a traditional agent it is still used in clinics due to its low cost, sometimes as a primary dressing, but often as a secondary dressing to hold topical treatments in place. (Harding et al., 2000). Some antimicrobial dressings still use gauze as its structure (Honey - ManukaDress, TheraHoney<sup>®</sup>; PHMB - Kerlix-AMD, Curity<sup>™</sup> AMD). The rationale behind the use of gauze is that it can absorb exudate and keep the wound dry (Eaglstein, 2001) but moist healing has been advocated since the 1960s (Winter, 1962). In studies it has been shown to be ineffective in dealing with chronic infections and some consider it ethically questionable to use gauze in trial situations when it does not provide optimal healing conditions (Jones et al., 2006).

Polyethylene terephthalate track-etched (PTTE) inserts are claimed to have a higher resistance to most organic solvents than other filters making them suitable for testing with all the processing techniques (guidelines for using Falcon<sup>®</sup> cell culture inserts, PD104401 Rev. 01, Corning Life Sciences). Culture well inserts have a membrane base with regular pore size, and have been in use for some years for growing bacteria (Anderl et al., 2000; Kirker et al., 2009). Fluid seeps in gently through the pores without flooding the inside of the insert. These inserts proved the best technique for biofilm growth. The nutrient provision proved sufficient without the bacteria being fully immersed below the fluid, and being more comparable to the way bacteria might form biofilm in a wound while being supplied with wound exudate.

A wound produces exudate in response to tissue damage; it is part of the natural healing process and is present in both acute and chronic wounds. Bacteria and biofilm within these wounds are surrounded by this exudate, but are not submerged in a depth of fluid, as was also the case with the inserts. Providing the bacteria have access to a surface (i.e., the insert's membrane) that is, or can become, conditioned by a thin nutrient layer, it facilitates accessibility and anchorage of bacteria to it, and biofilm may form (Garrett et al., 2008). Fluid can also evaporate from a wound causing the exudate concentration to increase, which may affect its viscosity (Cochrane et al., 1999). Insert surfaces were also subject to evaporation, even though constantly supplied with nutrient from fluid through the pores. Inserts therefore seemed to provide a close comparison to the conditions that might be expected for biofilm to experience in a chronic wound. Further, they were



supportive of growth and supplied the bacteria with nutrients (TSB) but did not submerge them in too deep a layer of the broth, eliminating the possibility of false measurements due to surface associated biofilm coming to rest on the surface during processing, as had been previously encountered (2.4.8).

Protecting bacterial growth and biofilm with agar proved successful, providing there was enough growth of biofilm to stay in the upper layer of agar before the insert film was removed. There was no guarantee that the entire biofilm layer had been removed from the plastic film, but viewing of the 24 hour growth showed a good layer of biofilm and examining the insert film by stereomicroscopy showed no visible remnants of growth. Biofilm grown for 48 hours presented with channels, the development of which may allow flow of waste and nutrients, and are therefore thought of as a simple system of fluid transport (Wilking et al., 2013; Proal, 2008). The biofilm appeared to be thicker than the 24 hour growth, and was forming layers of differing densities with occasional clusters of cells. This was even more pronounced in the mixed cultures.

### **2.5.5 A novel model**

The 24 and 48 hour models were grown and placed in agar successfully, however the meat model was considered the best model due to its ability to demonstrate biofilm growing into lower tissue layers. After 72 hours of growth on the meat model, the resulting images showed how the bacteria grew gradually into the crevices in the meat which, if in a clinical wound, would make the biofilm more difficult to access for debridement. This demonstrates the accepted theory that it is

unrealistic to believe that a wound can be completely debrided and kept sterile (Bjarnsholt et al., 2008). Biofilm covered the entire upper meat surface to the edges, and although there was some infiltration deeper into the meat, the bacteria had not seeped from the edges to the underside of the meat, which would mean that there would not be false growth in the model from the base up, when tested against dressings.

The structure within the biofilm under LM appeared to be in discrete layers, with occasional microcolonies of bacteria present. Some studies have demonstrated that *P. aeruginosa* are frequently located in aggregates or microcolonies within biofilm or tissue (Kirketerp-Møller et al., 2008). Fazli et al. (2009) found using PNA-FISH analysis that *S. aureus* aggregates were located close to a wound surface, whereas *P. aeruginosa* aggregates were located deeper in the wound bed. This would suggest that *P. aeruginosa* are capable of colonising deeper into the wound bed, although viewed by TEM in this study *P. aeruginosa* were observed throughout the biofilm thickness. Each biofilm grown using this meat model had a similar structure, whether it was single or two- species biofilm, with evidence of dense layers of tightly packed biofilm bacteria at the meat-biofilm interface, with less tightly packed layers of living bacteria further towards the surface. This would suggest the upper layers contain more metabolically active biofilm versus the denser and less active biofilm beneath.

This layered structure could represent what may be an optimal arrangement of structure to allow the transfer of nutrients and waste. In TEM, there were channels lined with a few single cells. It has been demonstrated that biofilm channels permit

the flow of fluid around and over cell clusters (Stoodley and Lewandowski, 1994). Cells such as these may be active due to the nutrient transport in these channels, or newly divided cells. However, these cells may be present due to nutrient depletion/limitation deep within the biofilm layers, causing biofilm to revert to planktonic forms and travel down the channels to disperse (Delaquis et al., 1989; Sauer et al., 2004). Several *P. aeruginosa* cells were producing what are sometimes termed extracellular or membrane vesicles (Stubbs et al., 1999). The presence of membrane vesicles would suggest a possible stress response. McBroom et al. (2007) found that release of vesicles increased directly with the level of protein accumulation in the cell envelope, which occurs under stress conditions. Membrane vesicles are spherical and formed from the outer membrane without loss of its integrity (Schwechheimer et al., 2013). They are thought to transport bacterial products to the biofilm environment, and have been suggested in the delivery of proteins, hydrolytic enzymes (such as phospholipase C, proteases, hemolysin and alkaline phosphatase), quorum-signalling molecules, lipids, virulence factors in pathogenesis, and to affect proteolytic activity and antibiotic binding (Kulp and Kuehn, 2010; Kadurugamuwa and Beveridge, 1995). They allow the delivery of such to reach distant targets in a concentrated, protected and targeted form. Membrane vesicles are also thought to differ in planktonic and biofilm forms. Once liberated, those from the planktonic bacteria parent cell migrate, whereas membrane vesicles found in biofilm tend to accumulate in groups (Schooling and Beveridge, 2006).

When the biofilm area measurements for 24, 48 and 72 hours were compared using two-sample T-tests, these demonstrated that the different growth periods were statistically significant from each other (with greater than 95% confidence). Performing a one-way ANOVA test using the Tukey confidence intervals confirmed that it was necessary to have grown the biofilm to 72 hours to differentiate it from shorter time periods, as 72 hours resulted in significantly more biofilm development (Figures 2.35-2.37). The interval plot performed showed that the differences between the 24 and 48 hour growth were probably not significant due to the overlap of the interval bars. A test for equal variances revealed that the 24 hour growth, which had a close grouping, was more consistent.

## **2.6 Conclusion**

All of the objectives were achieved, as covered in the discussion, and from this there are several conclusions. The preliminary experiments showed how exponential growth provided a constant and consistent supply of bacteria that could be readily reproduced throughout the undertaken study periods. The best time point for harvesting exponentially grown bacteria was confirmed by the bacterial density by taking spectrophotometer readings at selected time points. The growth curves served as a guide to the estimated number of organisms in cultures, in order to estimate more accurately the exponential growth point for each experiment. The growth rate was monitored by estimation of optical density, to provide similar readings and hence a similar concentration of bacteria.

All these experiments were essential for learning microbiology techniques, and gaining an insight into the structure of bacteria, the best protocol of fixation, and why a 2.5% glutaraldehyde in RK buffer should be employed for the remaining sets of experiments. The effect of an antimicrobial was demonstrated upon the exponential growth and by ultrastructural examination after using silver nitrate, showing how growth of planktonic cells can be effectively inhibited if its concentration is sufficient.

Growth of biofilm developed with 6 hours which confirmed that any analysis of the effect of antimicrobials in dressings should include the time points starting from 3 hours, and the statistical analysis demonstrated that biofilm should be grown to 72 hours to visualise any significant difference in further models. The initial bacterial concentration was, however, not significant when examined by SEM.

The growth of biofilm on inert, non-biological surfaces is less likely to accurately reflect the growth found in wounds, despite the apparent success of utilising surfaces such as poloxamer hydrogel in various models (Gilbert et al., 1998; Percival et al., 2007). Inert surfaces use non-biological substrata for biofilm attachment, and Luppens and Ten Cate (2005) demonstrated that biofilm development can be regulated by the type of substrata to which it attaches. A study of biofilm in wound healing is more likely to benefit from an *in vitro* model that more closely mimics the physiology of human wounds. Some have evaluated dressings using cell lines such as epithelial cells and fibroblasts (Cochrane et al., 1999; Walker et al., 2011) but these are limited in size for use in many experiments, and are complex and expensive. An *in vivo* meat model facilitates multiple sample

collection from a standard, more controllable surface, over variable time points.

The surface of a wound is also complex. However, a meat model can more closely reflect this topography compared to non-biological surfaces. Using this porcine meat model allowed for multiple tests, and an endless supply of material, for use in this study.

Architectural analysis of any biofilm is impractical unless the whole structure can be kept intact. Although there have been some justified comments that CLSM is the best way to view biofilm without treatment-induced structural changes (Lawrence et al., 1991), the agar model with its sandwiching technique presented in this chapter, has helped to maintain whole biofilm layers together in both LM and TEM methods. This makes it a good model, not only for further LM and EM comparative studies, but also for the next chapter of studies on wound dressings and their effectiveness at preventing bacterial biofilm growth. This chapter has already confirmed that bacteria can begin to form a biofilm within hours, and that it will try to invade into the surrounding host tissue. Debridement of biofilm in a wound cannot be guaranteed, and neither can a wound area be made completely sterile. Hence there will always be some small clusters of biofilm or planktonic cells present, even with the most careful debridement of a wound. Demonstrating that some of these dressings are indeed effective against planktonic growth and early biofilm formation could help to provide evidence of how they can help a wound to heal, to the extent that the patient/host is able to 'kick-start' the normal healing process and eliminate the bacterial infection.

# **Chapter 3**

## **Testing the Efficacy of a Selection of Antimicrobial Dressings using the *In Vitro* Model**

### 3.1 Introduction

The deleterious effects of microbes in wounds have been recognized for many years, and it is becoming more widely recognised that bacteria do not exist simply as solitary cells, but as communal organisms. The presence of biofilm is becoming increasingly recognised by clinicians as a primary cause of delayed wound healing and wound infection. Consequently, this type of wound is both detrimental to the patient, as well as a major drain on health budgets.

The cost to the NHS of wound care is substantial (as explained in more detail Chapter 1.12) due to the length of time wounds can exist. The Government's Quality, Innovation, Productivity and Prevention agenda 2012, focused on reducing harm and expenditure in wound care, especially around pressure ulcer formation, estimated to cost over £140,000 per case. A quicker healing wound reduces the need for more dressings and nursing care (Harding et al, 2001). The primary wound contact dressing can have an extremely important effect on a wound and ultimately on the cost of patient care. Most modern dressings have been developed to incorporate an element of moisture retention to the wound, in keeping with Winter's theory on moist wound healing (Bryan, 2004).

The addition of antimicrobial agents to wound dressings continues to be used to reduce the risk of wound infection, yet the presence of protective mechanisms adopted by biofilm bacteria means it is much more difficult to penetrate through this defence and reduce increasing wound chronicity (examples of some of the dressings used today are found in Appendix 10). The *in vitro* simulated chronic



wound model developed and discussed in Chapter 2, has now been used to evaluate current wound dressings containing antimicrobials, including silver, iodine and polyhexamethylene biguanide to demonstrate how effective they were against prevention and removal of a bacterial infection.

## **3.2 Control dressings chosen for the wound model study**

### **3.2.1 Gauze**

Gauze, originally made from silk, has been produced for centuries (Daunton et al., 2012). By the early 20<sup>th</sup> century it was developed with substances such as petroleum jelly (Pinnegar and Pinnegar, 1986). More commonly made today from open weave cotton or viscose, these dressings often resulted in trauma to the healing epidermis at dressing changes (Jones, 2005). Gauze is now often used as a primary dressing beneath many of the medical dressings produced, or as a secondary dressing helping to hold some antimicrobials in place (Blome-Eberwein et al., 2009). Some modern dressings have been designed using gauze impregnated with an antimicrobial and claim success in reducing the polymicrobial burden (Motta et al., 2004). Consequently, gauze (Systagenix, Gatwick, UK) was chosen as one of the non-antimicrobial wounds dressings included in this study.

### **3.2.2 A non-silver Hydrofiber<sup>®</sup> dressing (NSHD)**

Another non-antimicrobial control dressing is NSHD, (AQUACEL<sup>®</sup>, ConvaTec, Deeside, UK) which is composed of sodium carboxymethyl cellulose fibres that form a gel on contact with fluid. It is produced as flat non-woven pads and may be

applied to exuding lesions or granulating wounds. This dressing was chosen as a second non-antimicrobial dressing for direct comparison to two silver containing Hydrofiber dressings and as a comparison with the gauze control. A literature review by Barnea et al., (2004) has suggested that patients treated with this dressing experienced significantly less pain and a rapid rate of epithelialisation. The dressing has been shown to remain in place for 7 days, which was a lower frequency of changes than most dressings, and hence was more cost effective (Armstrong et al., 1997).

### **3.3 Silver antimicrobial dressings chosen for the wound model study**

#### **3.3.1 Silver Dressings**

Silver is a well-known antimicrobial. It has existed in the metallic form for thousands of years for use in vessels, and as a covering for surfaces to protect against infection (Rovee et al, 2003). However, in the metallic (or elemental) form silver cannot kill bacteria as it is un-reactive. It is in the positive, ionic form that silver demonstrates more effectiveness against microbes (Demling and Desanti, 2001). When exposed to aqueous environments, silver ions can become detached rapidly from their respective salts (e.g. silver sulphate, silver chloride). Elemental silver needs to form an intermediate stage, usually silver oxide, which dissociates to form silver ions. This can occur when exposed to air or fluid. Silver ions are thought to be transported into the cell and cause disruption of the cell's energy

production by binding to proteins and interfering with enzyme function and cell replication (Lansdown, 2002).

There have been Cochrane reviews performed on the widespread use of silver dressings. Two reviews, one by Bergin et al., (2006) and another by Storm-Versloot (2010), concluded that there was insufficient clinical trial evidence, despite the widespread use of silver, to evaluate its effectiveness. Neither could they determine cost effectiveness or establish whether silver-containing dressings or topical agents promoted wound healing or prevented wound infection. In 2011 a review by Toy et al., stated that there was emerging but not conclusive evidence of antimicrobial efficacy, with silver type dressings, because there are limited large, well-designed random controlled trials. Despite this apparent lack of absolute evidence, there are many dressings available containing antimicrobials including silver, that are used to manage a wide range of wounds. Below are the list of those chosen for the study.

### **3.3.2 A silver containing Hydrofiber dressing – SCHED**

SCHED (AQUACEL Ag, ConvaTec Deeside, UK) has been designed for exuding wounds, as it combines Hydrofiber Technology with the antimicrobial action of ionic silver (1.2% w/w). In the Cochrane review of Storm-Versloot, 2006, the conclusion was that of the six trials of silver-containing dressings, there was only one that showed a significant difference in healing times associated with diabetic foot ulcers (Jude et al., 2007), and the dressing used was AQUACEL<sup>®</sup> Ag. Research has been performed upon this dressing using planktonic bacteria to show the sequestering

and antibacterial effect (Newman et al., 2006), and also various studies on its effect on biofilm (Percival et al., 2007) and in clinical trials (Caruso et al., 2004). The primary reason for including this dressing was to compare it to the newer next-generation antimicrobial silver dressing as described below.

### **3.3.3 A next-generation antimicrobial dressing - NGAD**

Termed as a next generation antimicrobial dressings ( AQUACEL Ag<sup>+</sup> Extra™, ConvaTec, Deeside, UK), this dressing claims to be nine times stronger and to have up to 39% greater absorbency than its predecessor (ConvaTec.com). This dressing is also a carboxymethylcellulose dressing with 1.2% ionic silver, but unlike the SCHED, it is designed with two dimensional sets of fibres in layers of the Hydrofiber. The theory of the mode of action is that, upon contact with a fluid, the Hydrofiber forms a gel that surrounds the layers of fibres. The action of the gel still allows the dressings to lock in the exudate and fill the wound bed, and the two-dimensional fibres give strength to the dressing, for easier removal from a wound. A combination of a metal chelator to help sequester divalent metal ions found in biofilm structure, a surfactant and pH control to help ionic silver move more rapidly, are all combined in this dressing (Metcalf et al., 2016), to aid in the disruption of biofilm and allow the action of the silver to have greater effect.

### **3.3.4 A cellulose ethyl sulphonate fibre silver dressing - CES-SD**

To compare the effect of gelling fibre dressings, another fibre dressing DURAFIBER<sup>◇</sup> Ag (Smith & Nephew, Hull, UK) was included in the study. This dressing is composed of cellulose fibres combined with cellulose ethyl sulphonate

fibres, to form a non-woven dressing that forms a clear gel on contact with fluid. This dressing is designed for exudating wounds, to help maintain appropriate moisture levels, to help facilitate healing (Forlee et al., 2014). It contains ionic silver as an antimicrobial, to prevent or reduce infection, which it claims starts to kill bacteria within 30 minutes of contact, and to sustain antimicrobial activity for up to 7 days (Bullough et al., 2015).

### **3.3.5 An alginate carboxymethylcellulose nylon silver dressing – ACN-SD**

Fibrous wound dressings have the potential problem of shedding fibres. To prevent this Silvercel<sup>®</sup> Non-Adherent (Johnson & Johnson, Wokingham, UK) has been designed with a perforated outer layer of ethylene methyl acrylate, which it claims prevents the inner fibres from sticking to the wound (Wounds International, 2012). Alginate, a derivate of seaweed has been used to treat wounds as dressings for just over 30 years. The high absorption is achieved via strong hydrophilic gel formation. Alginate, on its own, is a natural wound dressing and as such the gel can be rinsed away by irrigation with saline. The holes in the ACN-SD perforated outer layer allow fluid to seep through and be absorbed by a pad composed of a high G (guluronic acid) calcium alginate, carboxymethylcellulose, and silver coated nylon fibres. This type of dressing is suited to wounds that produce a lot of exudate (Clarke, 2012).

### **3.3.6 A nanocrystalline silver dressing NC-SD**

This is a five layered high-density polyethylene mesh dressing, coated with nanocrystalline silver (Acticoat 7™, Smith & Nephew, Hull, UK). The coating is performed using a vapour deposition process and the layers are welded together. The nanocrystals measure 15 nanometres across and are between 30 and 50 atoms, and form a lattice structure resulting in a high energy, meta-stable form of elemental silver (Dunn, 2004). This type of dressing requires constant moisture for the oxidation process to take place and release the silver cations (Kostenko et al., 2010), it should therefore suit an exudating wound ([www.smith-nephew.com](http://www.smith-nephew.com) accessed 10/11/16). The manufacturers suggest that a constant moist environment helps to release a constant flow of silver ions for up to seven days, but that the dressing must not dry out, and recommends moistening the dressing with sterile water.

## **3.4 Other non-silver antimicrobial dressings chosen for the wound model study**

### **3.4.1 A Polyhexamethyl biguanidine dressing - PHMBD**

A PHMB dressing (Suprasorb® X+PHMB, Activa Health Ltd/Lohmann-Rauscher, Burton on Trent, UK.) was included in this study. PHMB, sometimes called polyhexamide, is a polymer which exerts little toxicity. It has been used for over 60 years as an antiseptic, and has been used in contact lens solutions, and to sanitise swimming pools (Moore et al., 2007).

PHMB works by binding to the bacterial cell membrane. As an antimicrobial, it is thought to cause complex reactions in the bacterial cell wall, which allows entry of the PHMB, reducing wall strength (Hübner et al., 2010). It causes fluidity and permeability of the outer membrane, releasing lipopolysaccharides and hence causes cell death (Gilbert et al., 1990).

#### **3.4.2 A Cadexomer iodine dressing - CID**

Iodoflex™ is part of a range of Cadexomer iodine dressings (Smith & Nephew, Hull, Uk). Iodine is thought to be antimicrobial by causing disruption of the protein and nucleic acid structure and its synthesis (Rutala et al., 2008). Cadexomer iodine is classed as an iodophor, as it contains iodine complexed with a solubilising agent. This is a water-soluble modified starch polymer containing 0.9% iodine (w/w) and is produced by the reaction of dextrin with epichlorhydrin coupled with ion-exchange groups and iodine. CID consists of cadexomer iodine paste incorporating sterile, beads 0.1- 0.3 mm in diameter. The dressing is presented as a paste between two layers of a gauze fabric. The theory behind its action is that when placed in an aqueous environment the beads take up liquid and swell. As they swell the beads release the iodine.

### **3.5 Aims and Objectives**

Due to the work already performed (Chapter 2), it was evident that clusters of bacteria were observed after 3 hours and biofilm growth was visible within 6 hours.. Studies of the biofilm growth on the meat model had already been performed at 24, 48 and 72 hours, viewed qualitatively and quantified statistically. It was therefore

decided that similar time points should be used to perform tests on the antimicrobial dressings chosen, in order to compare with the model.

The specific objectives proposed were:

- To grow biofilm on the wound model beneath the selection of test dressings and view at 3, 6, 12, 24, 48, and 72 hours by LM and SEM
- To grow biofilm beneath test dressings and view at 24 and 48 hours by TEM and CLSM
- The following would be used as test dressings
  - A gauze control
  - A non silver Hydrofiber
  - A silver containing Hydrofiber
  - A silver containing 'next generation' Hydrofiber
  - A silver containing cellulose ethyl sulphonate fibre
  - A silver containing alginate with carboxymethylcellulose
  - A nanocrystalline silver polythene mesh
  - A polyhexamethyl biguanidine cellulose
  - A cadexomer iodine

### **3.6 Materials and Methods**

*P.aeruginosa* and *S.s aureus* were grown to the exponential point (as in 2.3.2) and a 1:10 dilution was prepared from each culture in sterile Tryptone Soya Broth (TSB). 0.4µ Polyethylene Terephthalate (PET) track-etched membrane cell culture



inserts were placed inside the wells of 6 well culture plates. On the inside film surface of each insert was placed a thin slice (3mm) of meat cut from a piece of sterile back bacon using a sterile number 8 (13mm diameter) cork borer. 50 µls of each culture was mixed then pipetted onto the surface of the meat to give a mixed culture.

A smaller sterile number 7 (11mm diameter) cork borer was used to cut out pieces of dressings into discs, one for each insert. 5 minutes after applying the bacteria, a dressing disc (treated per manufacturer's instructions) was placed on top of each piece of meat in the inserts and flattened gently down, so that the dressing was in full contact with the culture and tissue (meat) surface (Figure 3.1).

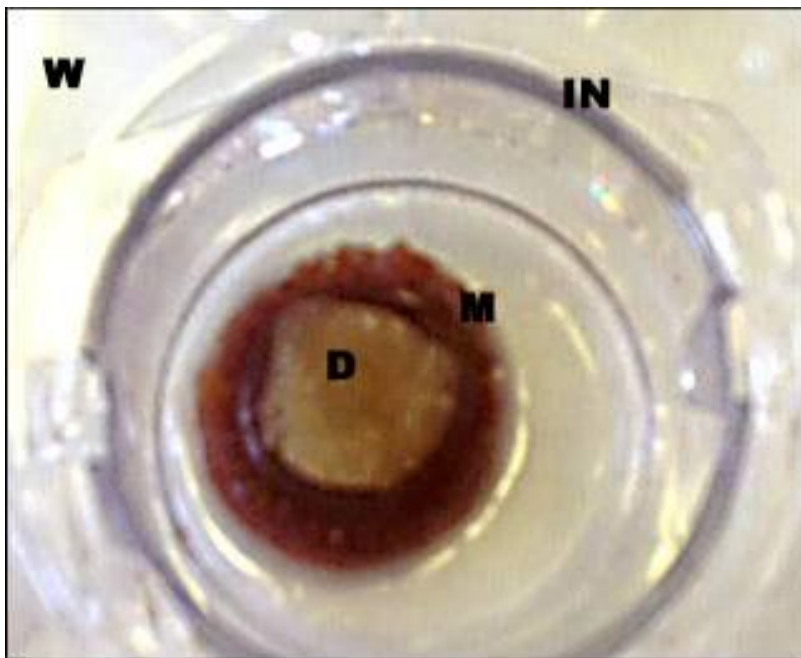


**Figure 3.1: Preparing a meat model with dressing**

A dressing disc (**D**) placed on top piece of a larger disc of meat (**M**) in an insert (**IN**) in a well (**W**) and flattened gently, so that the dressing was in full contact with the meat

The outer well area of each insert was filled with 2-3 ml of TSB broth until the insert was about to float. The plates were incubated with gentle agitation on a flatbed mini orbital shaker (50 rpm), at 37°C for 3, 6, 12, 24, 48 or 72 hours. For the longer time periods of 24, 48 and 72 hours, each morning the TSB culture was topped up in the well outside the insert. After each time was ended the models were prepared for examination.

Models for examination by Confocal Laser Scanning Microscopy (CLSM) were removed from the wells at selected time points (24 and 48 hours). These samples were rinsed gently in sterile distilled water, and then stained with *BacLight*<sup>TM</sup> Viability Kit and viewed on a Leica TSC SP2 DM IRE2 Confocal Laser Scanning Microscope as described in 2.3.14. Samples were examined and images taken.

Samples to be prepared for Light Microscopy (LM), Transmission Electron Microscopy (TEM) and Scanning Electron Microscopy (SEM) at each time point had the remaining TSB fluid removed by pipette from the outer well area and replaced with 2.5% v/v glutaraldehyde in TSB. This fixative solution was also added into the insert, to gently flood the inside but not disturb the meat/dressing model *in-situ*. This was then left for 24 hours at 4°C before it was gently replaced by RK buffer (as per 2.3.17) (Figure 3.2; Figure 3.3).



**Figure 3.2: A meat model with gauze dressing after 12 hours of growth**  
Model sat in an insert within a well of a clean plate with remnants of TSB culture, ready for fixation and processing



**Figure 3.3: A meat model with NSHD after 24 hours of growth**  
Meat with dressing in an insert within a well of a clean plate, with remnants of TSB culture

For SEM specimens, the RK buffer was carefully pipetted from the outside and inside of the insert, with as much excess fluid as possible removed from inside the insert. The meat/dressing model was lifted out of the insert, and placed back into

the well of a clean plate. The model was viewed under a stereo-microscope and the dressing carefully removed and placed in an adjacent well.

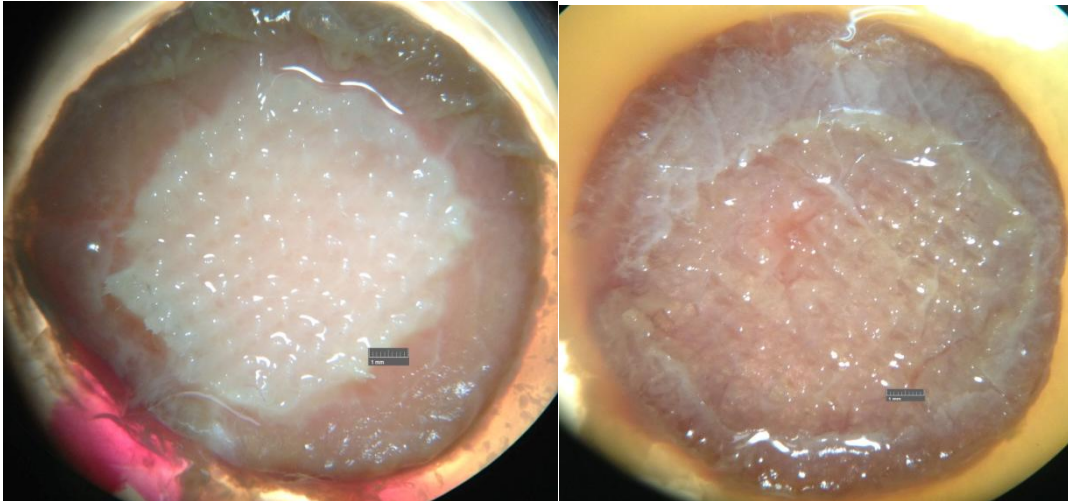


**Figure 3.4: Gauze on meat model viewed under a stereo microscope**

The left image shows the gauze on the meat after 12 hours growth, with the dressing in place. Gauze was carefully removed from the model ready for the addition of agar (right image) bar 1mm

Representative pictures of the meat before and after dressing removal are shown in Figure 3.4 (gauze) and Figure 3.5 (NSHD).

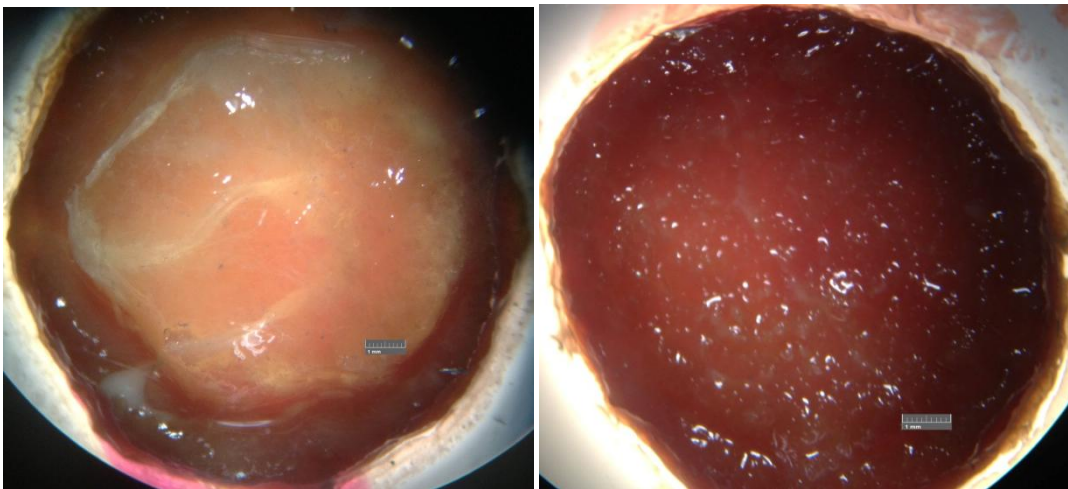


**Figure 3.5: NSHD on meat model viewed under a stereo microscope**

The left image shows the gauze on the meat after 12 hours growth, with the dressing in place. Gauze was carefully removed from the model ready for the addition of agar (right image) bar 1mm

Both meat and dressings were processed *in-situ* for SEM (Figure 3.6).





**Figure 3.6: Meat and dressings processed *in-situ* for SEM**

Once processed, samples were placed on to self adhesive carbon tabs which were stuck to aluminium SEM stubs, ready for sputter coating and SEM examination

For the LM and TEM culture plates a 3% w/v Agarose solution was prepared and allowed to cool but not set. The RK buffer was carefully pipetted from the outside and inside of the inserts and as much excess fluid as possible was removed. The slice of meat was carefully removed and the base placed on the absorbent material to remove excess fluid. Using fine-forceps the meat was carefully tilted and the base finely coated with a thin layer of tissue marking dye, using an orange stick, before placing back on to the absorbent tissues for a few minutes to absorb the excess ink. The dye would help to distinguish the base from the biofilm surface after processing, to aid correct embedding. Under a stereo microscope the dressing was carefully removed from each model. Whilst still fluid, the agar solution was gently poured inside a watch-glass, taking care not to include bubbles, and the meat was placed into the agar biofilm side down, but not touching the base of the

glass. The agar was allowed to start to set, before more agar was poured over to totally cover the meat (Figure 3.7).



**Figure 3.7: Agar models – meat set in an agar surround**

Meat models were placed in a watch glass and carefully covered with agar which was allowed to set. Models were then processed for LM and TEM

This whole model was left until set then removed from the watch-glass and placed in 2.5% v/v glutaraldehyde in RK buffer. This was allowed to fix for 24 hours at room temperature before processing for LM or TEM. For TEM, a punch biopsy was performed from the centre of 24 and 48 hour models for each dressing, using a 6mm Stiefel biopsy punch, and pieces processed for TEM. Sections were cut and stained as per section 2.3.5 (TEM) and 2.3.6 (LM).

Growth with all dressings was for 3, 6, 12, 24, 48 and 72 hours. Imaging was taken at all times for paraffin wax sectioning. SEM was performed on all hours and relevant imaging taken. TEM and CLSM imaging was performed on 24 and 48 hour models.

Growth beneath the dressings, at 24, 48 and 72 hours, was confirmed quantitatively by taking LM images at x4 magnification and measuring the area of

biofilm using Image J software. Two-sample t-tests and Analysis of Variance (ANOVA) statistical tests were conducted using Minitab 17 software to compare the means of biofilm areas remaining on the LM models.

## 3.7 Results

### 3.7.1 3-6 hour dressing treated models

There was little bacterial growth seen by histological examination in any of the dressing treated models, all of which had a similar appearance in the 3 – 6 hour growth phase at LM, although some had occasional dressing fibres (Figure 3.8 ) which had remained stuck to the surface.



**Figure 3.8: 6 hour ACN-SD model by LM with fibres**

Occasional dressing fibres were visualised (black arrows) which had remained stuck to the surface of the tissue (x4)

The meat model beneath the NC-SD appeared to have intermittent layers of black deposition on the surface (Figure 3.9).

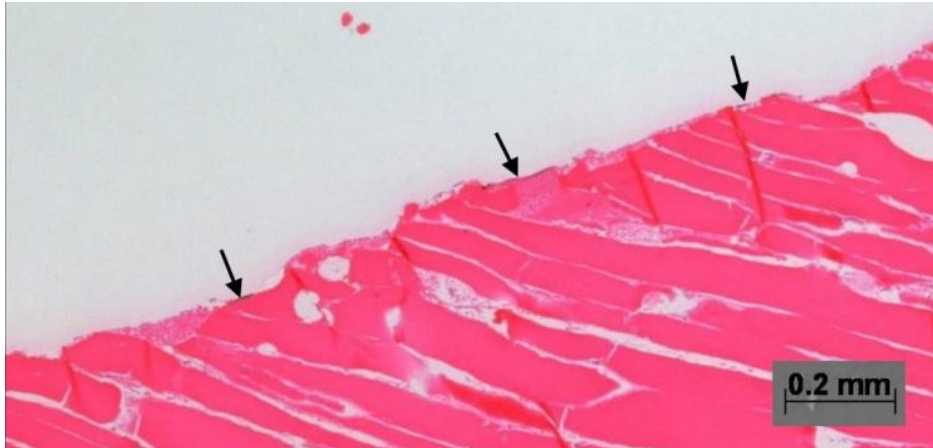


**Figure 3.9: The tissue beneath the 6 hour NC-SD stained with silver**  
It appeared to have intermittent layers of black deposition on the surface (black arrows) (x4)

There was little difference in the dressings when viewed by SEM, apart from the CID, where crystals were present amongst the cadexomer beads appearing almost as spikes. These had the characteristic appearance of iodine crystals. (Figures 3.10-3.13).

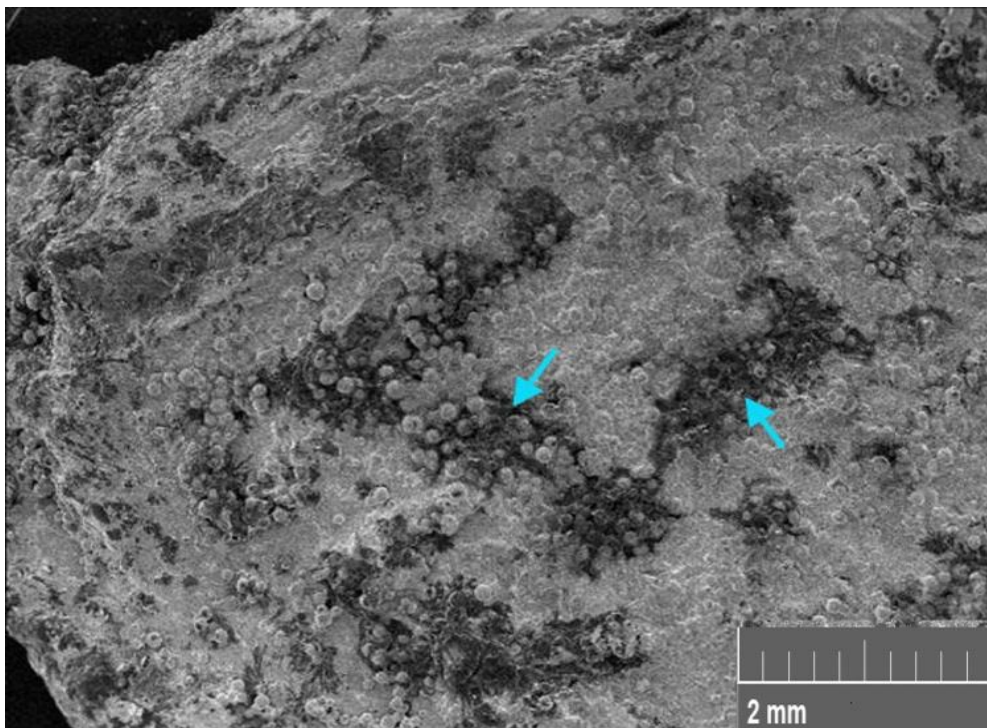


**Figure 3.10: 3 hour CID treated model by SEM**  
Iodine crystals could be seen as dark patches on and within the cadexomer beads (arrows)



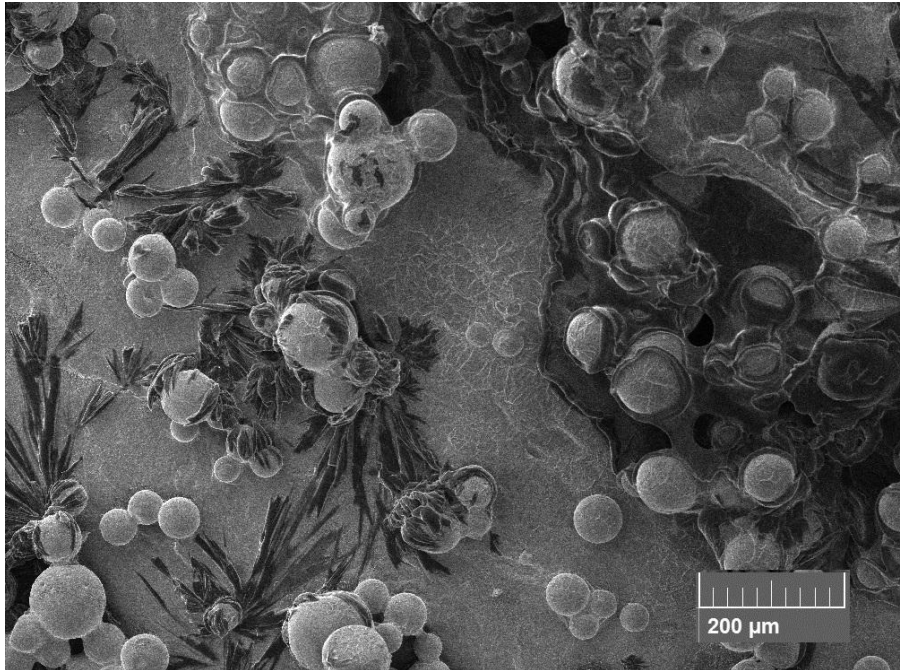


**Figure 3.11: 3 hour CID treated model with iodine crystals by SEM**  
At higher magnifications the structure of the crystals could be seen amongst the cadexomer beads appearing almost as spikes

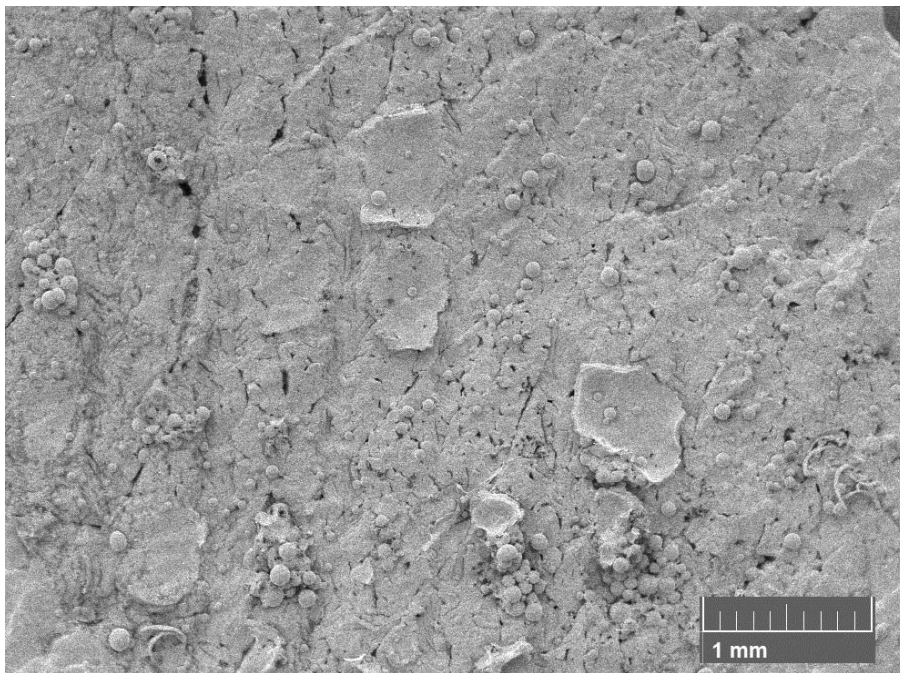


**Figure 3.12: 6 hour CID treated model examined by SEM**  
After 6 hours only a few dark patches of iodine crystals could be seen (x50)

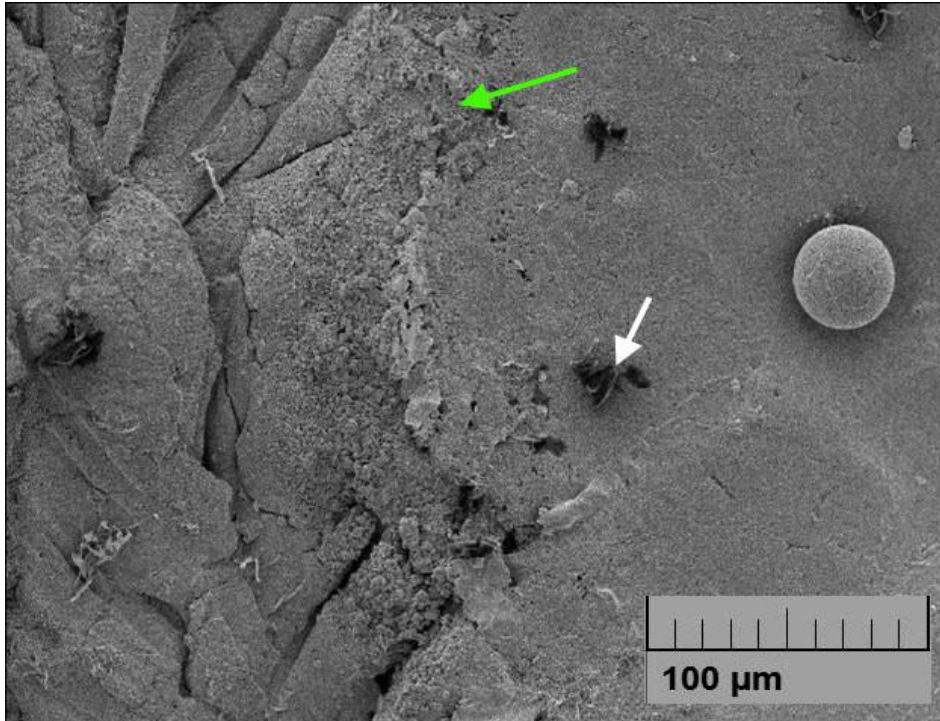


**Figure 3.13: 6 hour CID treated model by SEM showing a lack of iodine**  
The iodine crystals were almost depleted (white arrow) and possible biofilm was noted (green arrow) (x500)

### 3.7.2 12 hour dressing treated models

Incubation for 12 hours showed an increase in the presence of bacteria in the gauze control model (Figure 3.14) but very little in the Hydrofiber dressings tested (Figure 3.15) or the PHMBD.

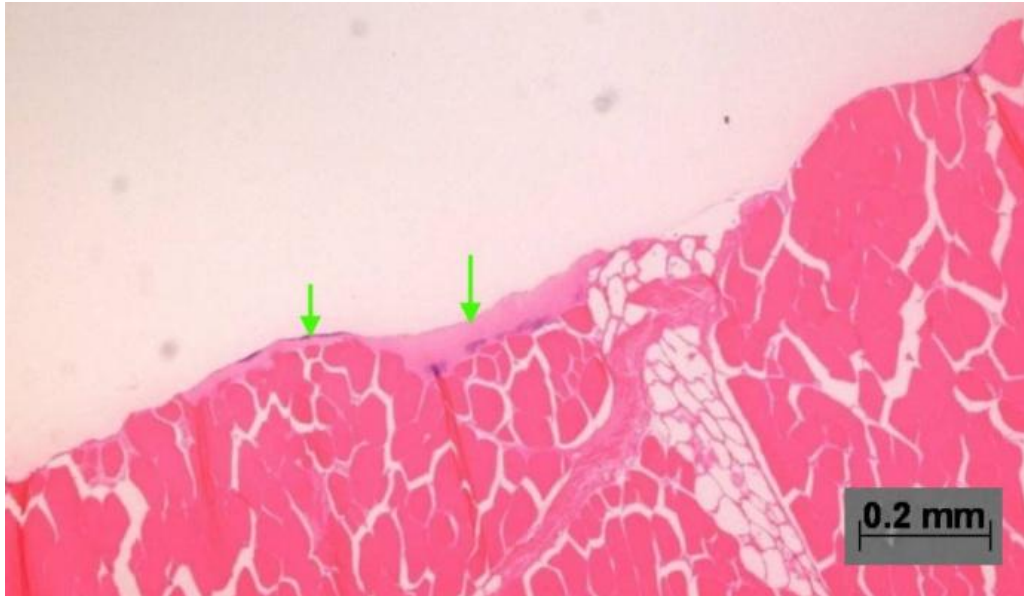


**Figure 3.14: Biofilm growth beneath gauze at 12 hours by LM**

There was an expected increase in the presence of bacteria in the gauze control model (green arrow) (x4)

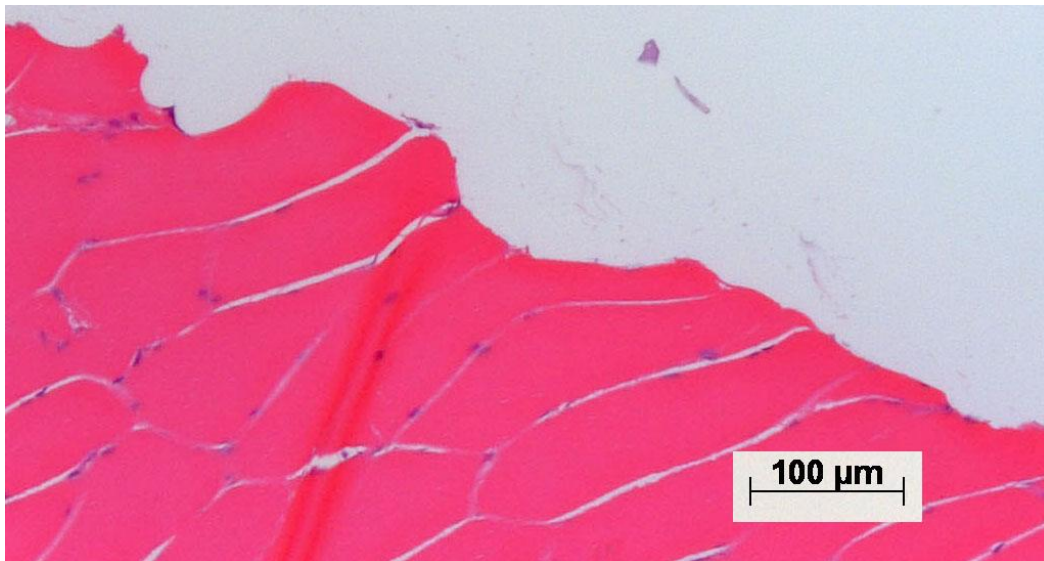


**Figure 3.15: 12 hour NGAD showing no visible growth by LM**

The surface of the tissue showed no bacterial growth (x10)

The gauze appeared to have a higher content of biofilm growth on its surface at SEM (Figure 3.16), with a few of the fibres attached to the surface. SEM of the NSHD showed evidence of some gelling property of the colloid fibres (Figure 3.17).

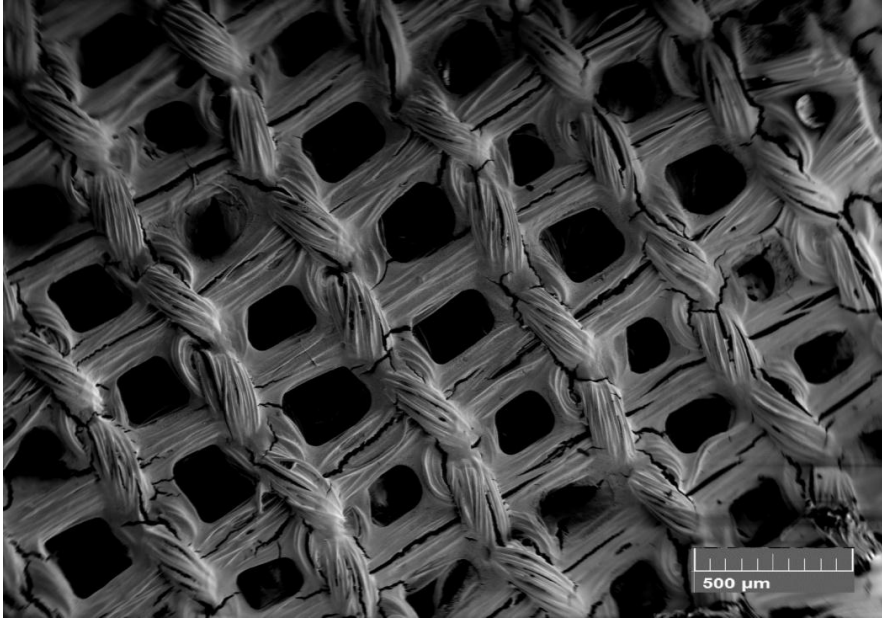


**Figure 3.16: SEM of 12 hour gauze dressing surface**  
The gauze appeared to have bacterial growth at 12 hours between its fibres (x20)

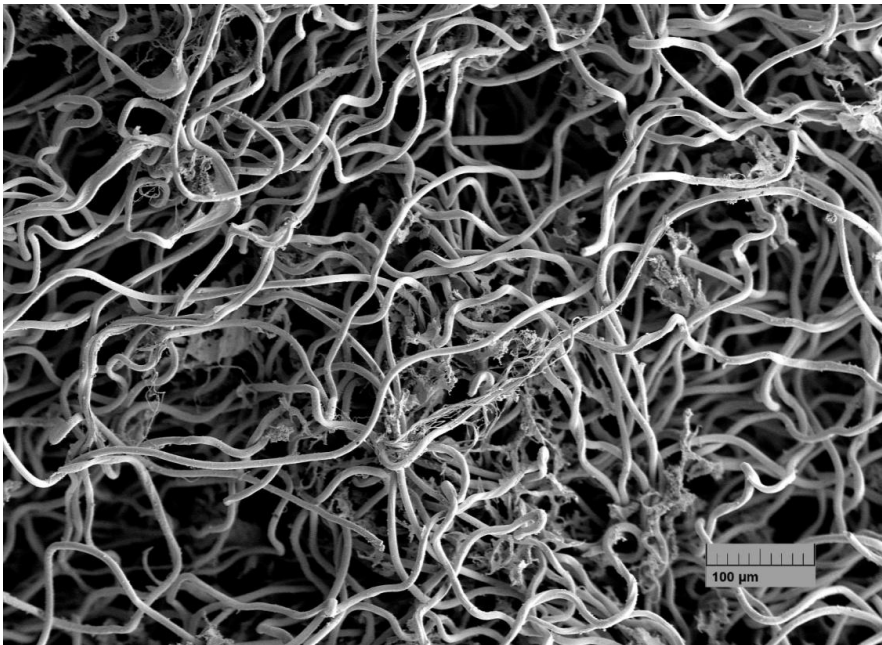


**Figure 3.17: SEM of 12 hour NSHD with slight gelling of fibres**  
NSHD showed evidence of some gelling property of the colloid fibres (x100)



The surface of the tissue under NSHD had several of the looser fibres from the dressing stuck to the surface, although the central area was clearer of these fibres (Figure 3.18).

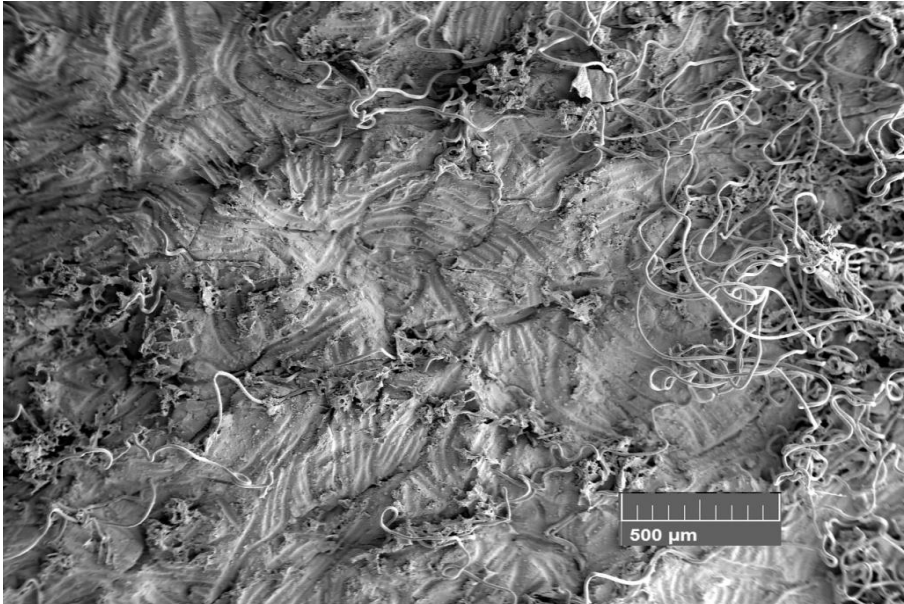


**Figure 3.18: The surface of the tissue below the 12 hour SCD**

Several of the looser fibres from the dressing stuck to the surface, although the central area was clearer of these fibres (x50)

The CES-SD model had a scattering of growth across the whole surface by 12 hours (Figure 3.19).

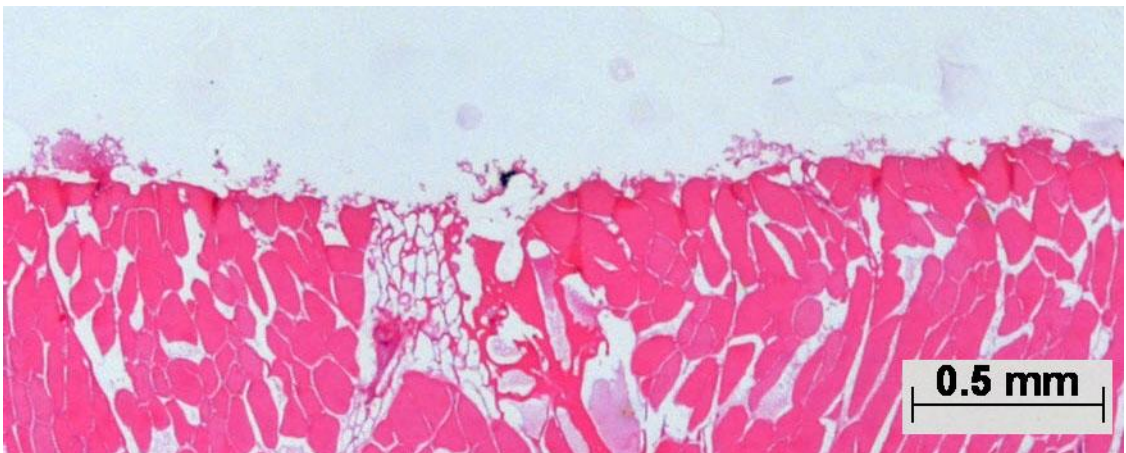


**Figure 3.19: The 12 hour CES-SD by LM**

This model had a scattering of growth across the whole surface by 12 hours (x2)

The 12 hour NC-SD model had surface deposition of silver on LM, similar to the 6 hour model. Between these patches of silver, however, there was an appearance of an increase in the presence of bacterial growth (Figure 3.20).

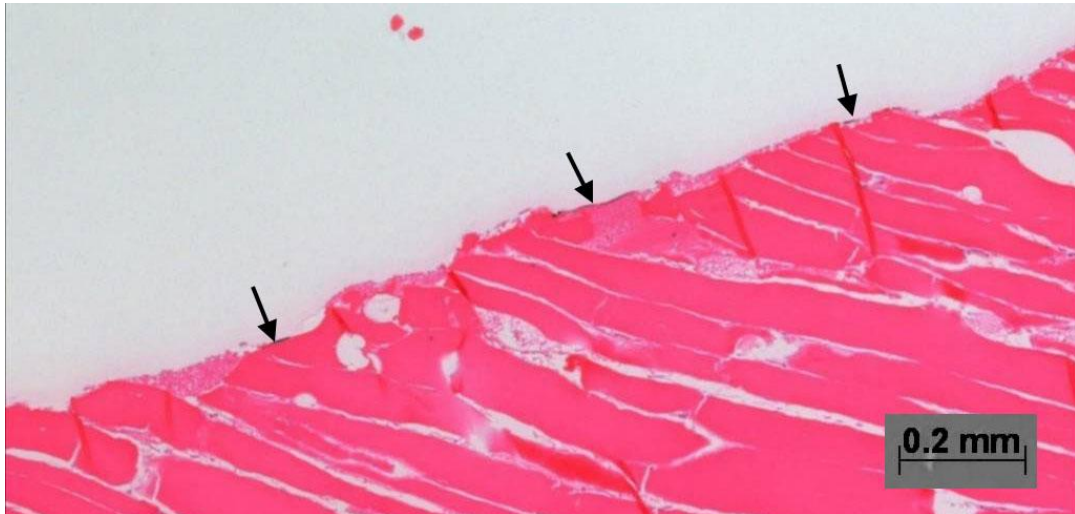


**Figure 3.20: The 12 hour NC-SD model with more silver deposition**

Surface deposition of silver, similar to the 6 hour model. There was an appearance of an increase in biofilm growth between patches of silver (black arrows) (x4)

The CID model had no iodine crystals remaining on the surface and there were groups of bacteria around the beads. Occasionally these formed sheets or mats, similar to those found on the surface of the nutrient fluid above coverslip growth in 2.4.8 (Figure 3.21; Figure 3.22).

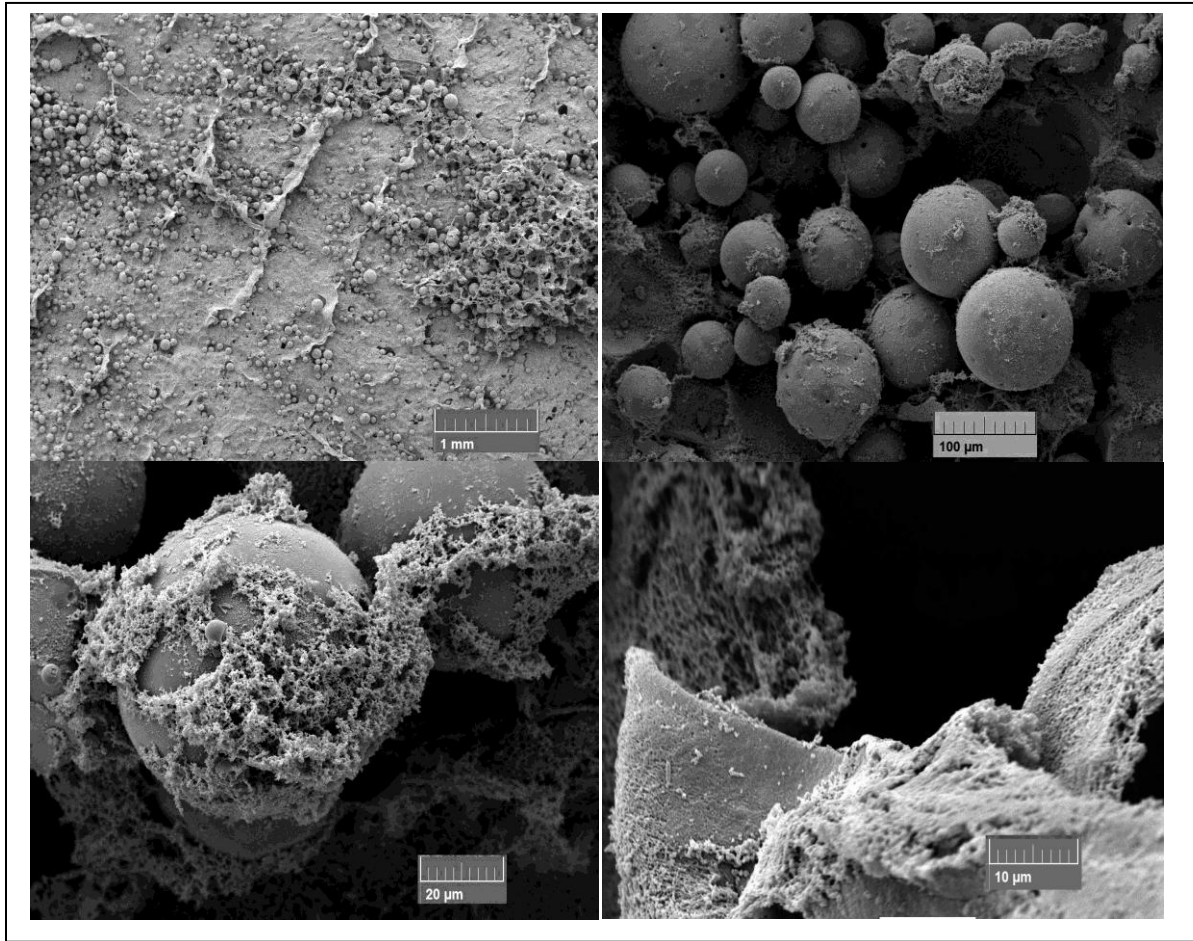


**Figure 3.21: Tissue surface and cadexomer beads of CID at 12 hours by SEM**

Top left – the surface of the tissue was covered with a scattering of beads on the surface but no iodine crystals (x50)

Top right - Cadexomer beads were covered in possible biofilm growth (x500)

Lower left – individual cadexomer beads were shown to have a layer of debris and possible biofilm wrapped around them (x2000)

Lower right - Biofilm 'mats' between cadexomer beads, which appeared similar to biofilm surface growth in 2.4.8 – Figure 2.14 (x4300)

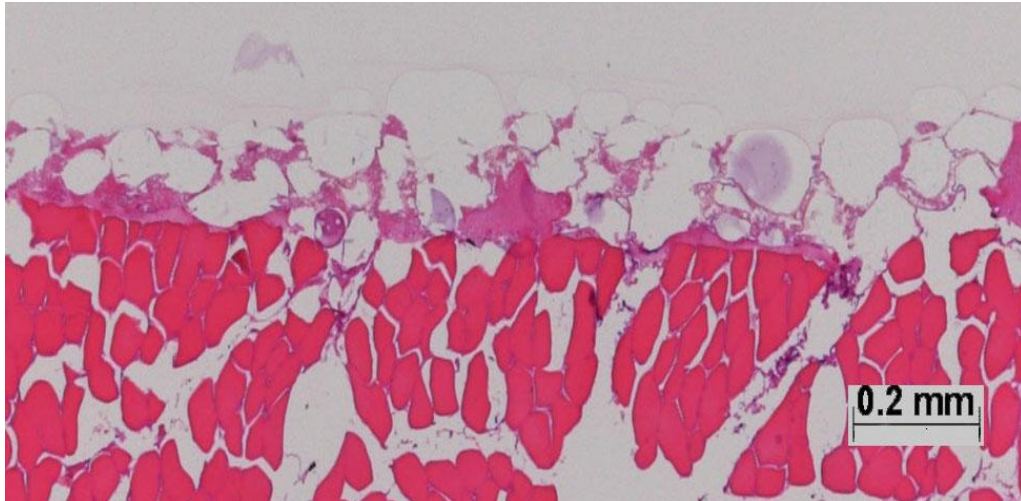


**Figure 3.22: 12 hour CID with cadexomer beads and growth**

CID at 12 hours had bacterial growth around the beads and on the surface of the tissue (x2)

### **3.7.1 24 hour dressing treated models**

24 hour incubation showed a marked difference between the dressings. The bacterial growth beneath the gauze was easily visualised with LM as an almost continuous layer (Figure 3.23), and bacteria and EPS were evident with SEM (Figure 3.24).



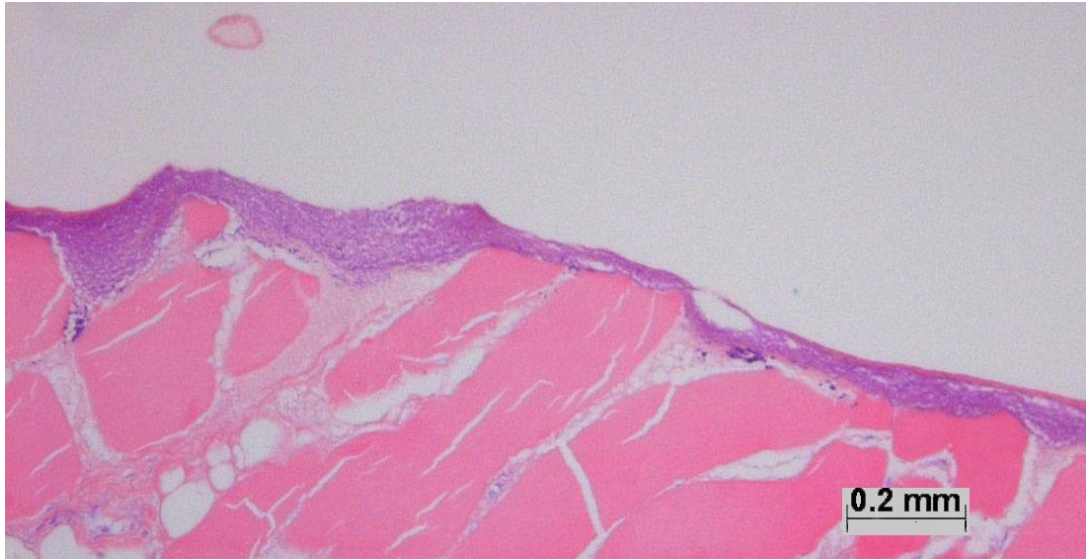


**Figure 3.23: The 24 hour gauze with a continuous layer of biofilm by LM**  
24 hour incubation showed bacterial growth, visualised with LM as an almost continuous layer (x10)

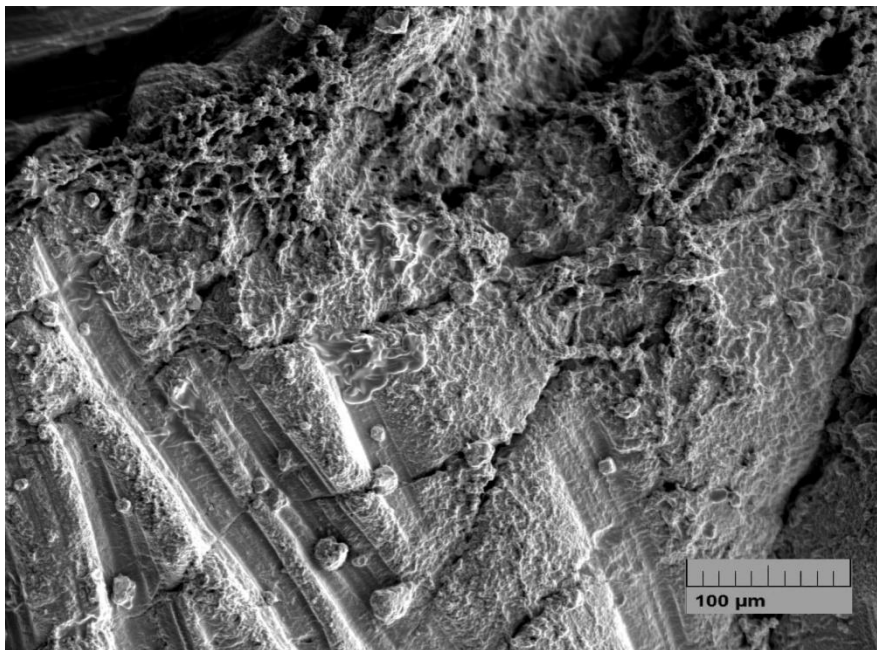


**Figure 3.24: 24 hour gauze model with SEM with areas of biofilm**  
Bacteria in EPS were evident on the surface (x100)

The NSHD control model had a few small groups of bacteria remaining on the surface of the tissue (Figure 3.25) which were also present with SEM (Figure 3.26).

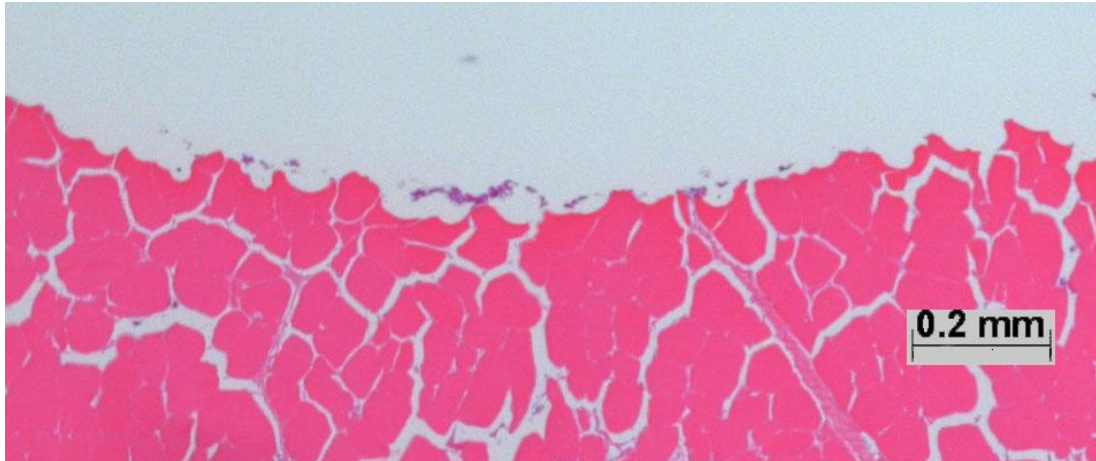


**Figure 3.25: The 24 hour NSHD model by LM**

A few small groups of bacteria remained on the surface of the tissue (x4)

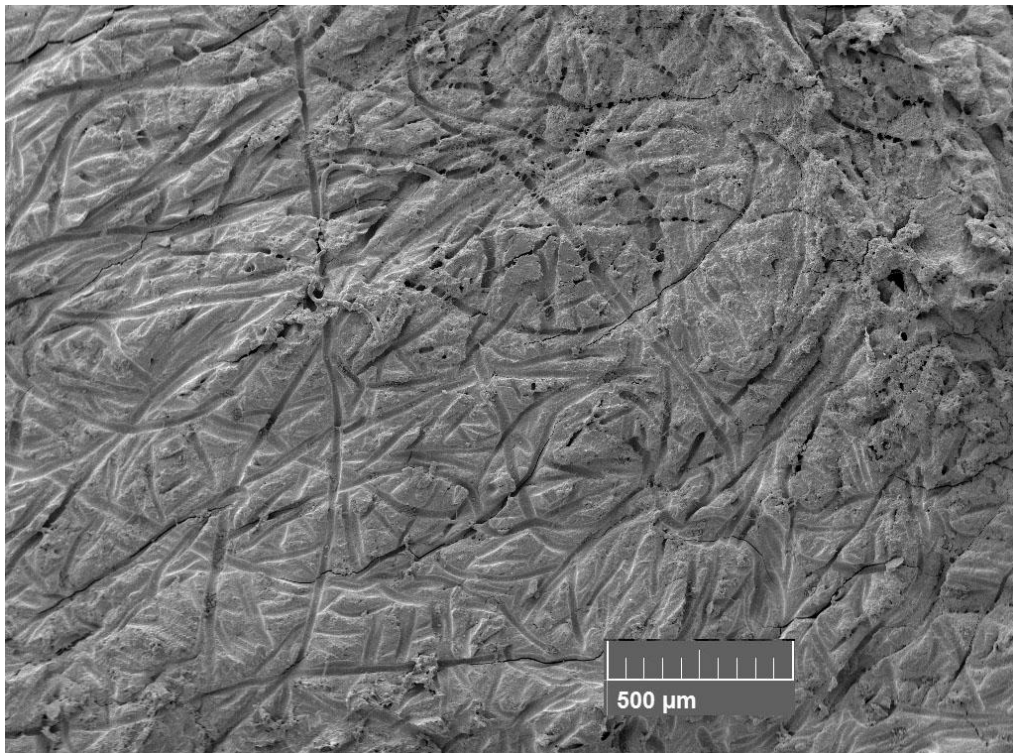


**Figure 3.26: The 24 hour NSHD tissue surface by SEM**

A few small groups of bacteria were present with SEM (white arrows) (x100)

The dressing showed further swelling of the fibres and bacteria were trapped within them (Figure 3.27).



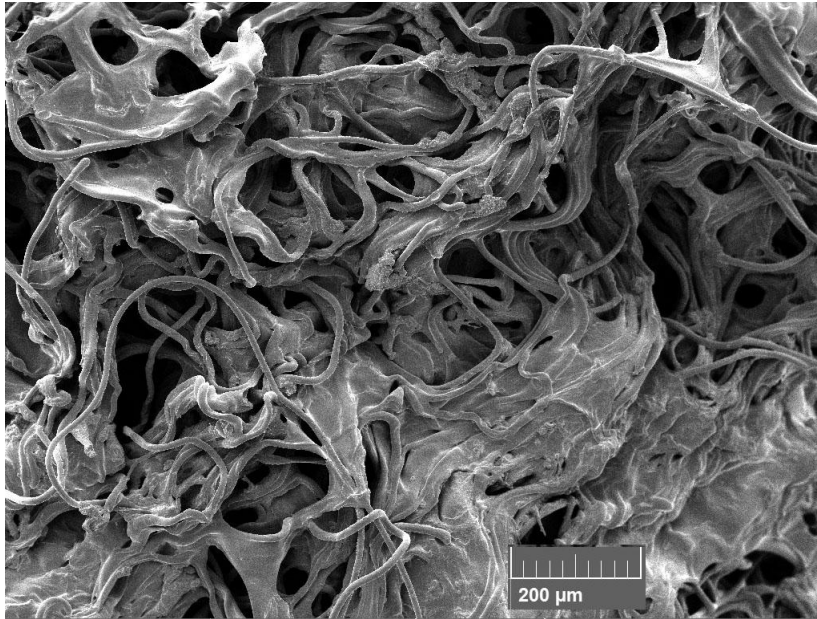


**Figure 3.27: The 24 hour NSHD by SEM**

Further swelling of the fibres. Swelling of fibres is designed to enable the trapping of bacteria within them (x200)

The SCHD and NGAD had very few visible bacteria when viewed with LM (SCHD shown in Figure 3.28), although the occasional cluster of bacteria was present on SEM (Figure 3.29) and TEM (Figure 3.30) with the SCHD, with apparent extracellular polymeric substance (EPS).

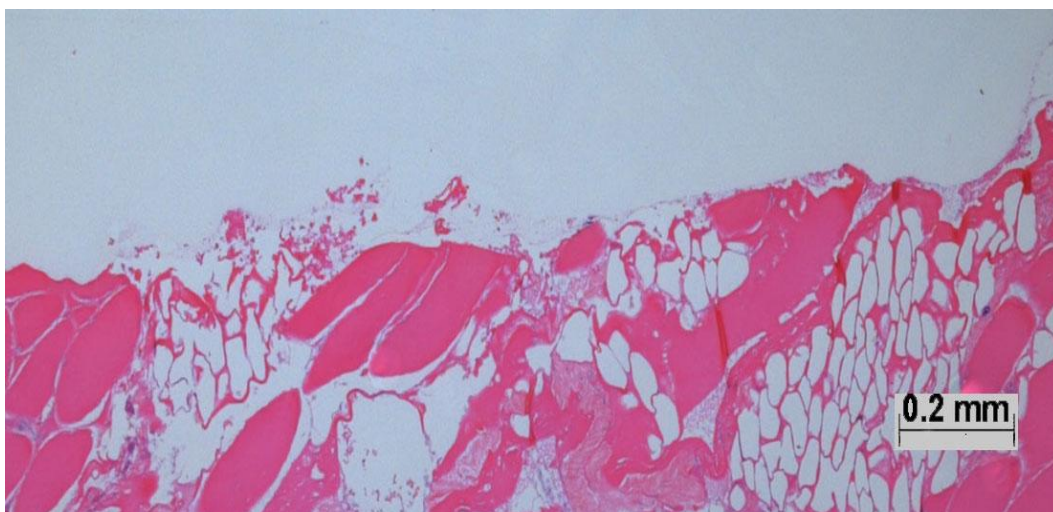


**Figure 3.28: The 24 hour SCHD by LM**

The surface of the tissue appeared to have very few visible bacteria (x4)

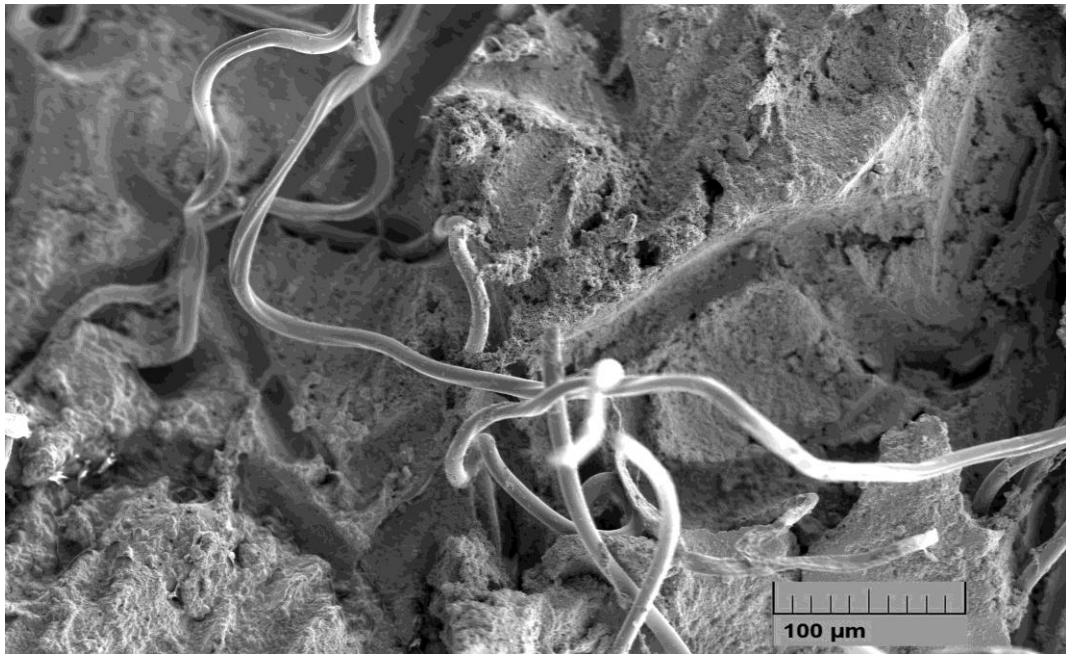


**Figure 3.29: The 24 hour SCHED by SEM showing occasional bacterial clusters**  
The occasional cluster of bacteria present on SEM and the occasional small fibre (x200)

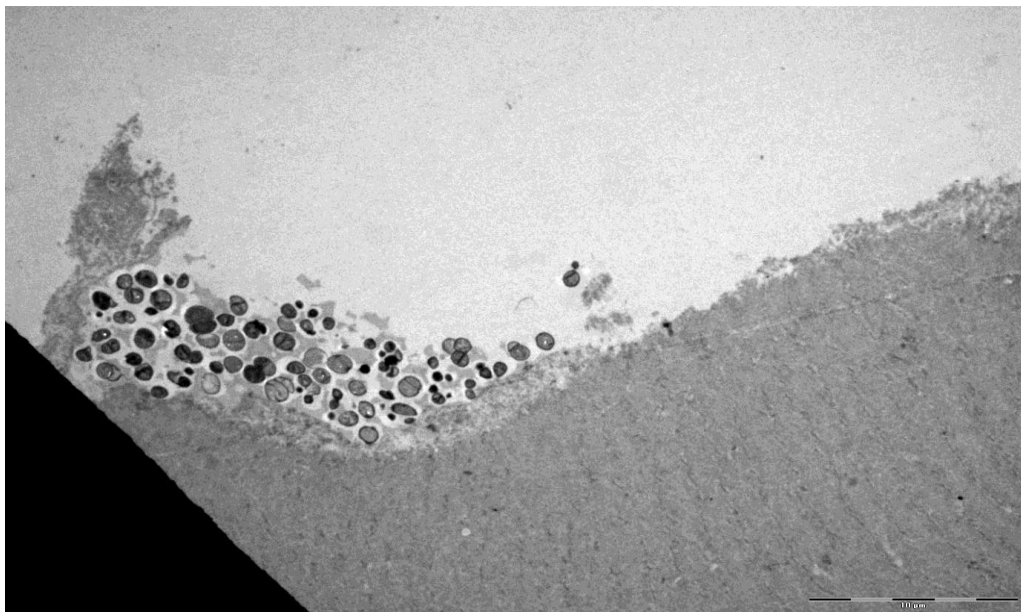


**Figure 3.30: The 24 hour SCHED by TEM with bacterial clusters**  
The occasional cluster of bacteria was present also on TEM models (x 2500)

Closer inspection of the bacteria by TEM showed that many were disrupted (Figure 3.31).

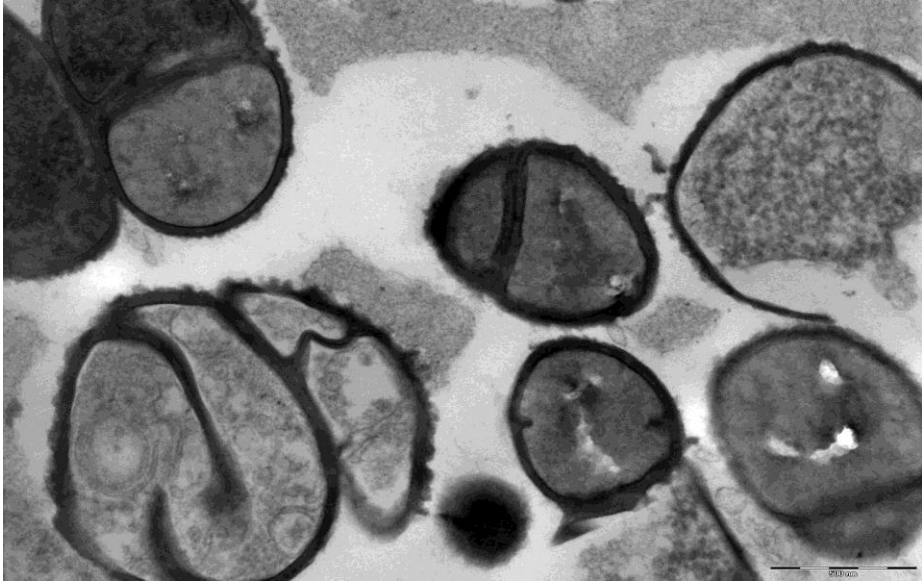


**Figure 3.31: Bacteria being disrupted in the 24 hour SCHED by TEM**

The occasional cluster of bacteria was present but closer inspection showed many of the bacteria were disrupted (x 40k)

The NGAD model had a few bacteria present, but by viewing with TEM it could be seen that these bacteria were planktonic and not surrounded with EPS (Figure 3.32).

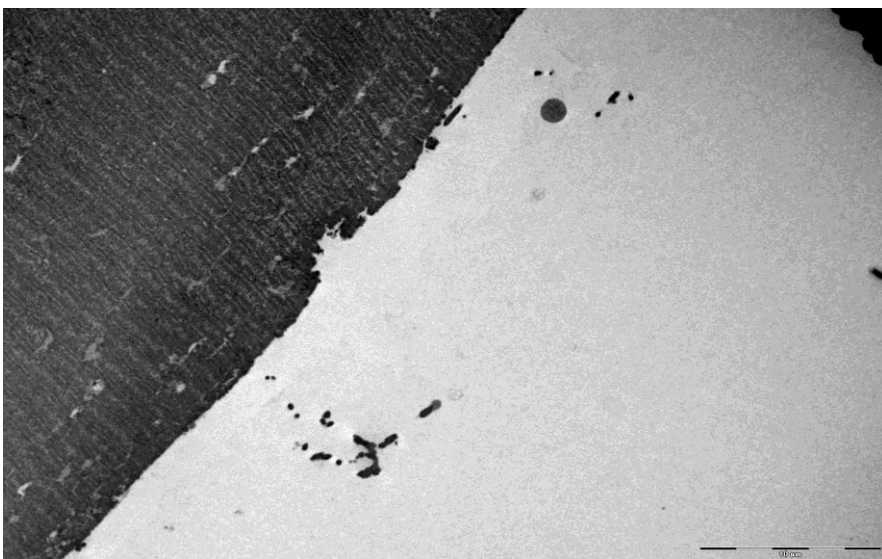


**Figure 3.32: The 24 hour NGAD with virtually clean surfaces by TEM**

A few bacteria present, but by viewing with TEM it could be seen that these bacteria were planktonic and not surrounded with EPS (white arrow) (x2500)

CLSM also demonstrated a few small clusters on the SCHED (Figure 3.33) but not on the NGAD (Figure3.34).

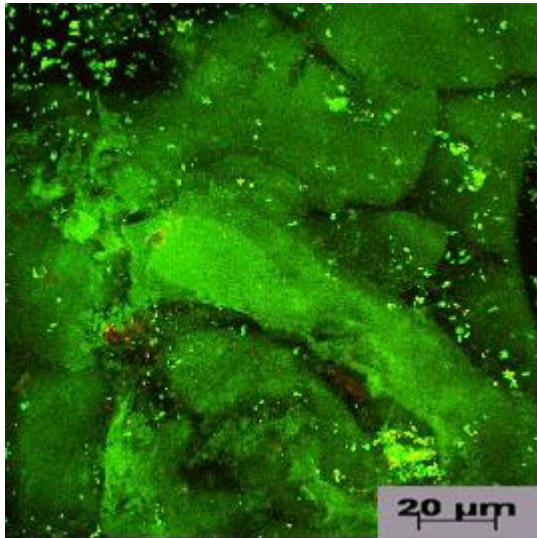


**Figure 3.33: CLSM of the 24 hour SCHED tissue surface**

A few small clusters were present on the tissue beneath 24 hour SCHED staining green (live bacteria), with a combination of red and yellow representing dying bacteria (x40)

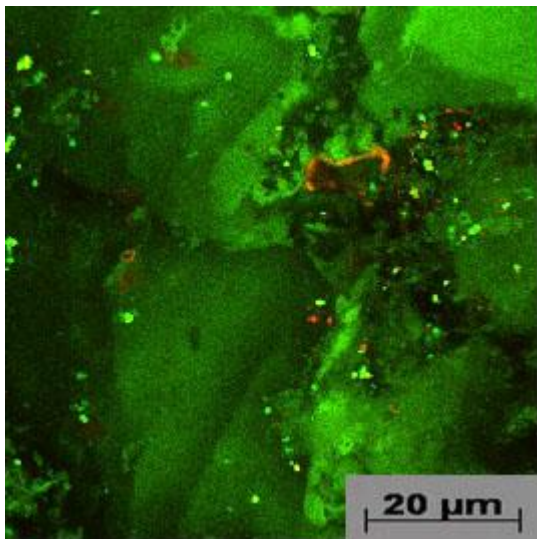


**Figure 3.34: CLSM 24 hour NGAD tissue surface with no biofilm**

No visible biofilm was present on the tissue beneath 24 hour NGAD, only the occasional planktonic cell was present, some live (green), some dead (red)(x80)



The fibres of the Hydrofiber dressings were seen to gel and sequester bacteria within them on SEM (Figure 3.35).

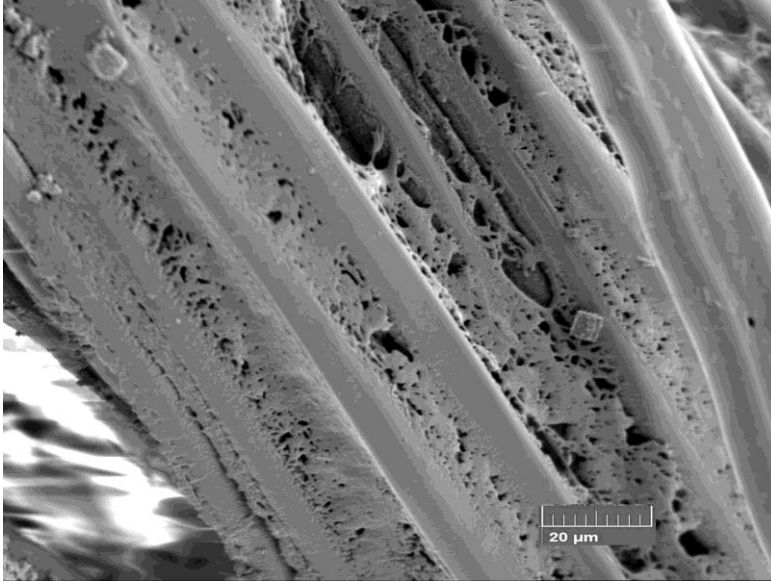


**Figure 3.35: The sequestering effect of 24 hour Hydrofiber dressings**  
Fibres of the Hydrofiber dressings could be seen beginning to swell and sequester bacteria (x500)

The LM of the CES-SD model showed a layer of bacteria with occasional groups (Figure 3.36).

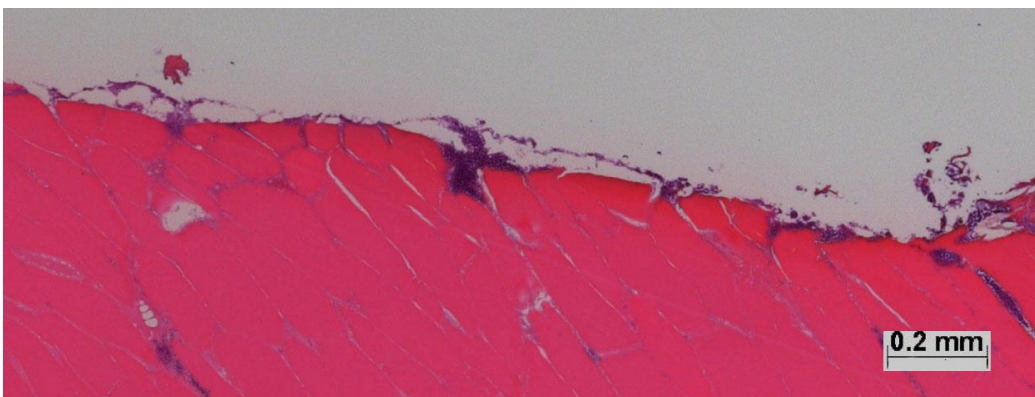


**Figure 3.36: The 24 hour CES-SD model by LM**  
A layer of bacteria was observed across the tissue surface with occasional groups of bacterial biofilm (x4)

The dressing contained a few bacterial clusters visible within it with SEM (Figure 3.37), and fibres were again left on the surface of the tissue with bacterial groups amongst these (Figure 3.38).

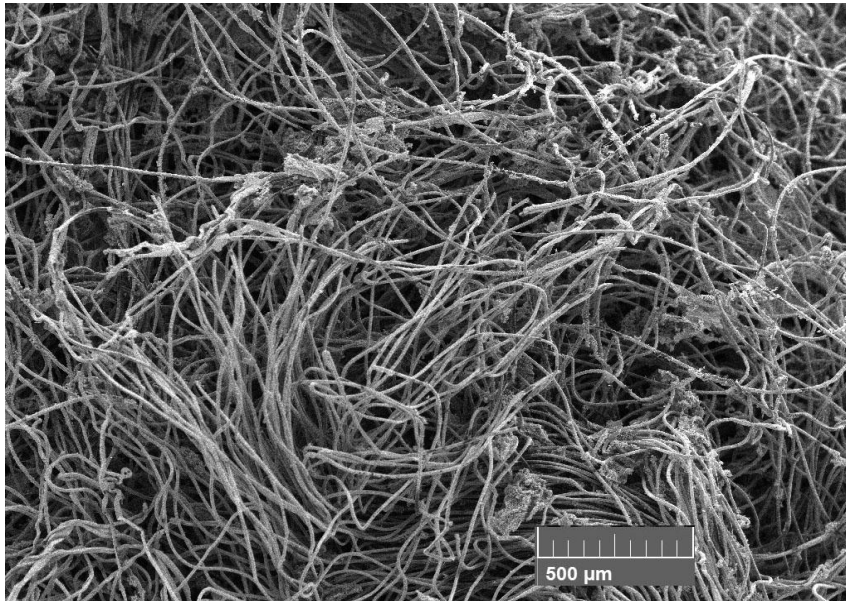


**Figure 3.37: The 24 hour CES-SD with bacteria**  
A few bacterial growths were matted within the dressing (white arrows) (x100)

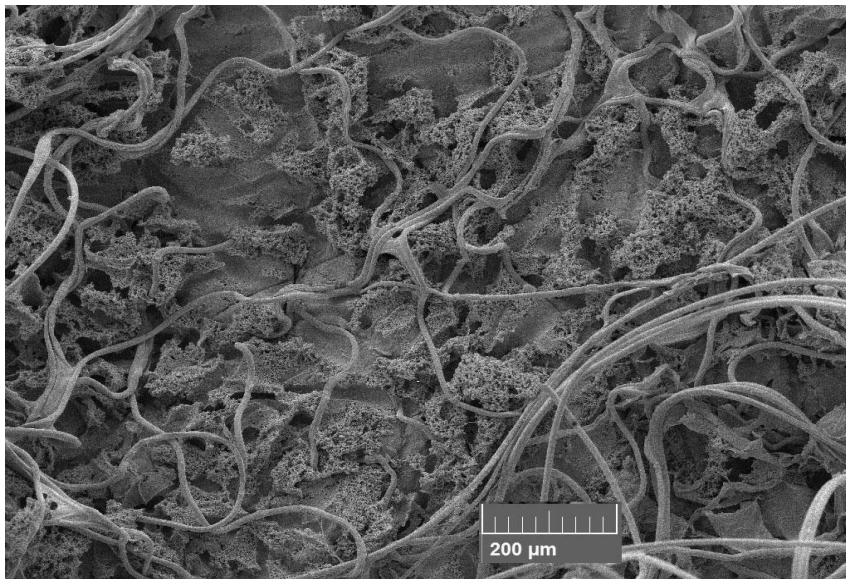


**Figure 3.38: The 24 hour CES-SD tissue surface by SEM**  
Fibres were again left on the surface of the tissue with bacterial groups amongst these (x200)



CLSM imaging showed areas of live bacteria in groups around fibres, with minimal dead staining (Figure 3.39).

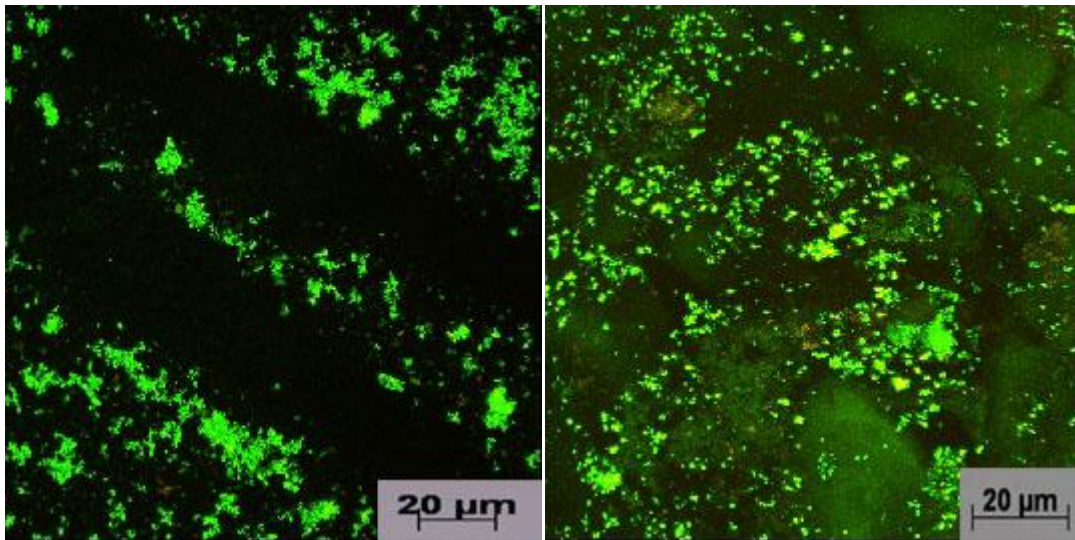


**Figure 3.39: CLSM imaging of 24 hour CES-SD and tissue surface**  
Areas of live bacteria were found around fibres (left) and biofilm on the tissue surface (right) , with mainly live bacteria (green) and minimal dead staining of bacteria present (red) (x40)

A few small groups were present on the surface of the ACN-SD model (Figure 3.40) but much of the area appeared to be free of bacteria with LM. There was a similar appearance with SEM (Figure 3.41) and TEM (Figure 3.42).

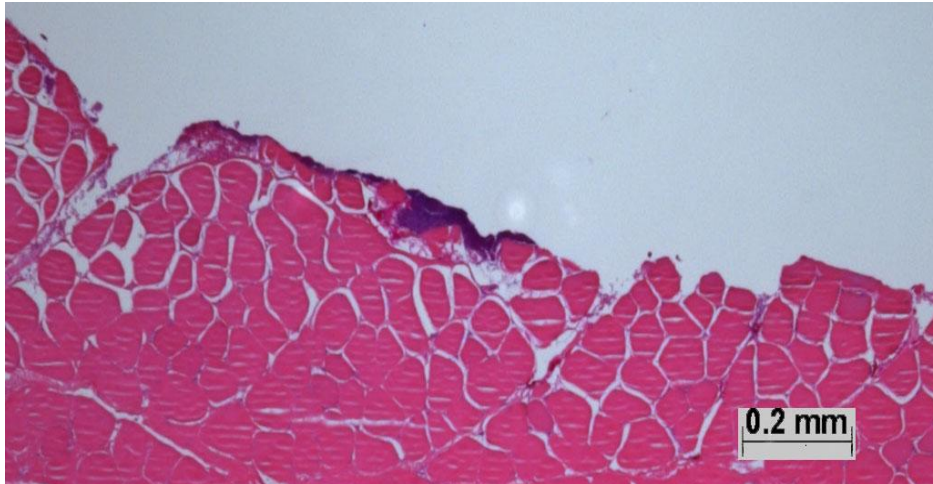


**Figure 3.40: 24 hour ACN-SD model by LM**

A few small groups were present on the surface of the tissue, but much of the area appeared to be free of bacteria when viewed by LM (x4)

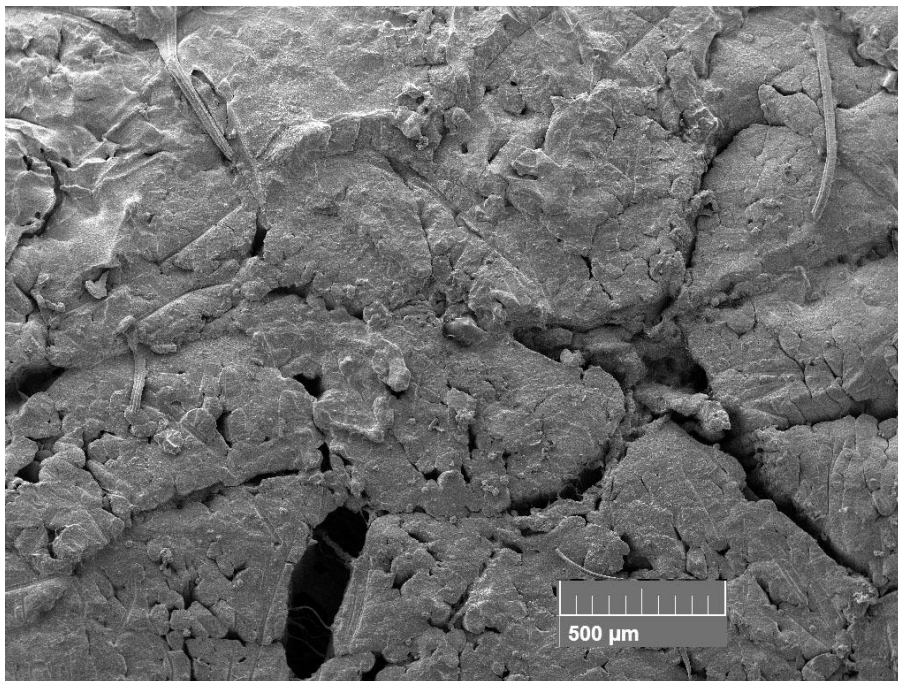


**Figure 3.41: SEM 24 hour ACN-SD tissue surface by SEM**

Much of the area appeared to be free of bacteria, similar to the LM (x100)

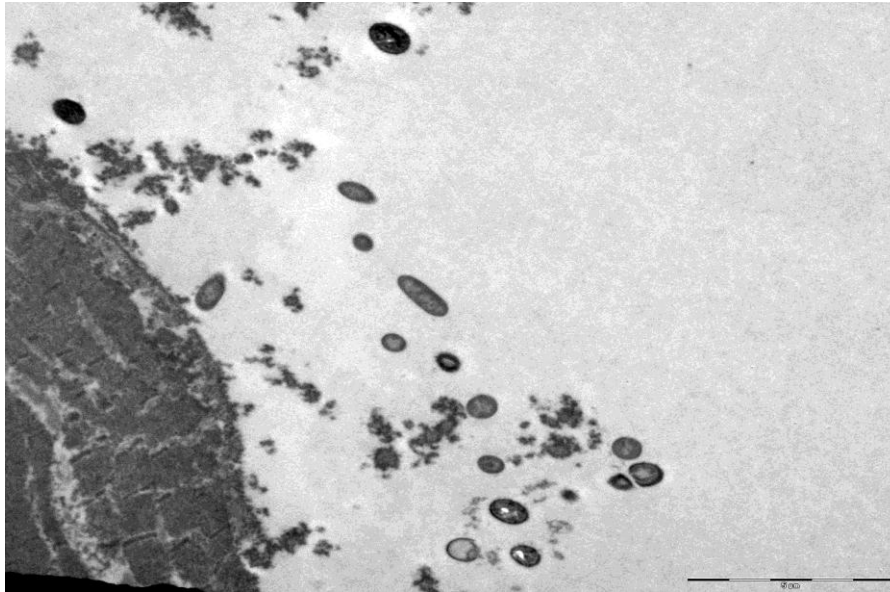


**Figure 3.42: TEM 24 hour ACN-SD tissue surface (x100)**

Only a few bacteria seen on the tissue surface with only the occasional possible EPS

Bacteria could be seen within the fibres of the dressing and a minimal amount on the outer dressing surface (Figure 3.43). CLSM images of the tissue showed the presence of bacterial clumps within with live and some dead staining (Figure 3.44)

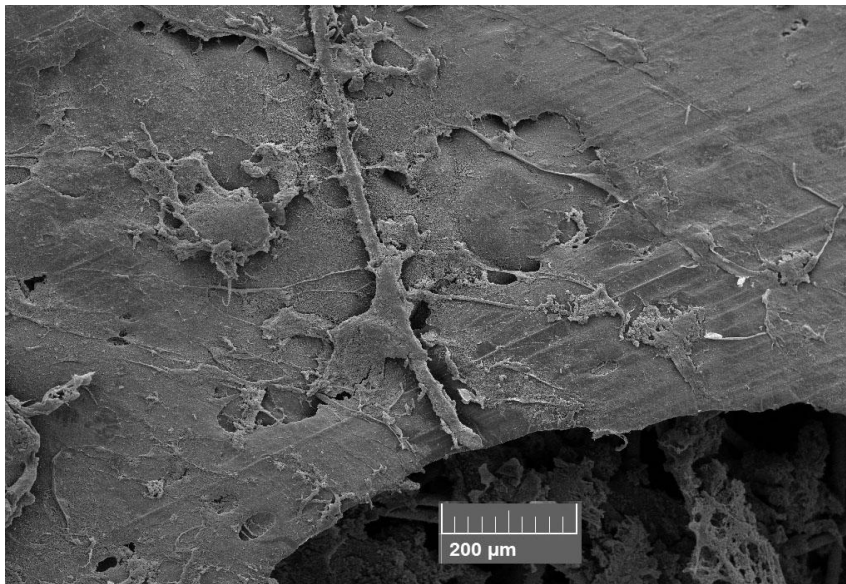


**Figure 3.43: 24 hour ACN-SD surface on SEM**

Bacteria could be seen within the fibres beneath the outer surface layer of the dressing (x200).



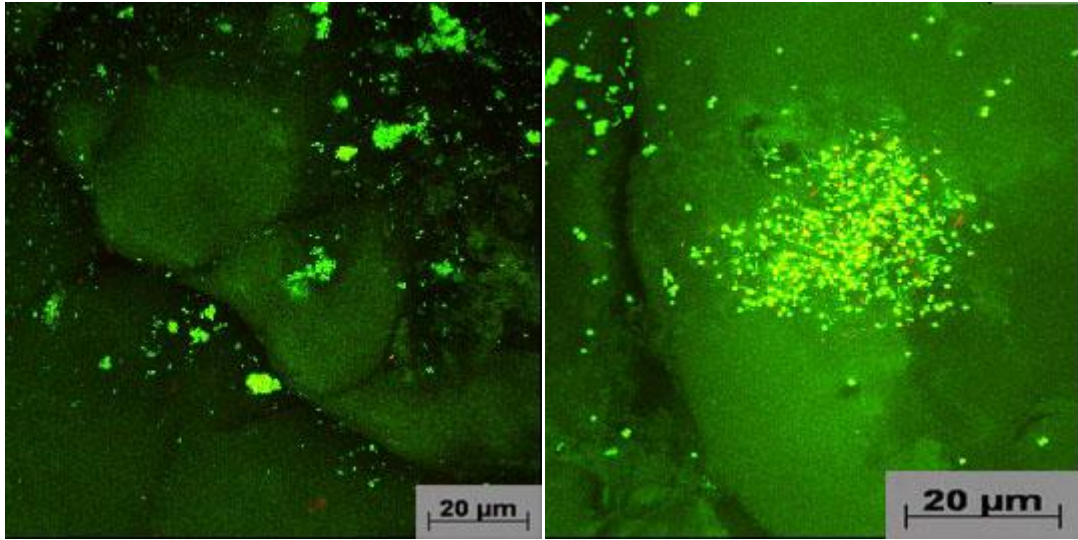


**Figure 3.44: CLSM images of the tissue beneath the 24 hour ACN-SD**

A presence of bacterial clumps were found, with live bacteria visible (green) and some dead (red) (left x40, right x80)

LM of NC-SD showed black areas of silver deposition on the surfaces much increased from the 12 hour appearance. Bacteria were present in a few places on the surface and groups of bacteria were present below the surface (Figure 3.45).



**Figure 3.45: LM of NC-SD treated model at 24 hours with darkening of the tissue surface**

Areas of silver deposition were increased (black arrows). Bacteria were still present in a few places on the surface and groups of bacteria were present in the tissue below the surface (green arrows) (x4)

The layers of silver and bacterial groups could be seen with TEM, some of the bacteria were encased in extrapolymeric substance (EPS) (Figure 3.46; 3.47).

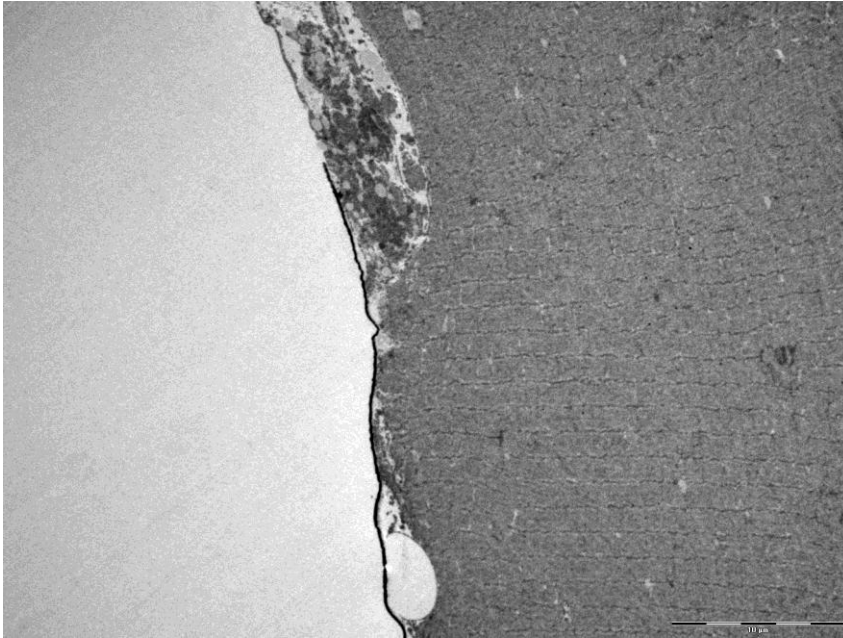


**Figure 3.46: TEM of 24 hour NC-SD with silver deposition**  
Layers of silver were present as thin black lines with bacterial groups beneath (x2500)

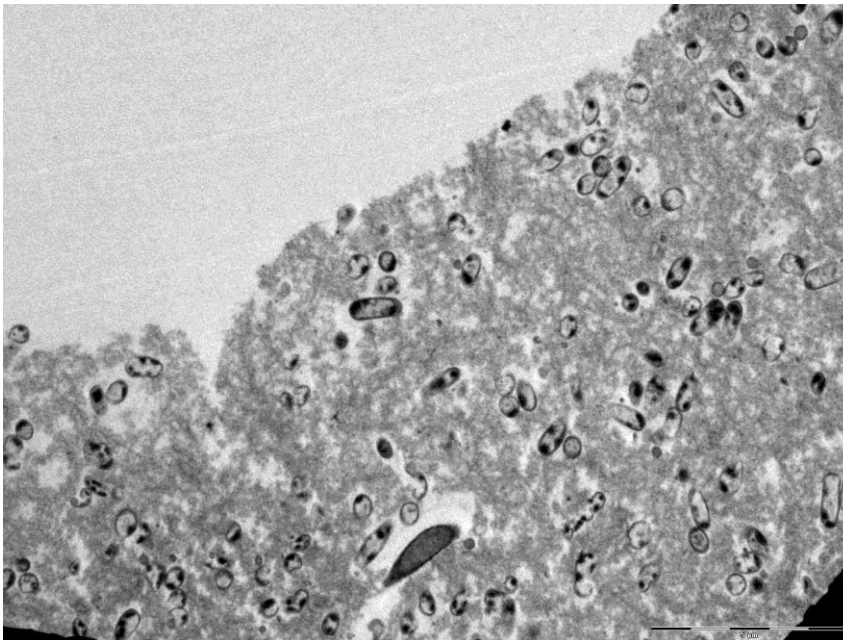


**Figure 3.47: Biofilm under the NC-SD at 24 hours by TEM (x6000)**  
Biofilm was found on the tissue surface showing bacteria encased in EPS

SEM of the tissue surface showed the impression of the dressing structure in some areas, with minimal bacteria where the dressing made contact with the tissue.

Where there was no dressing contact, bacteria were present in the form of biofilm (Figure 3.48; Figure 3.49).

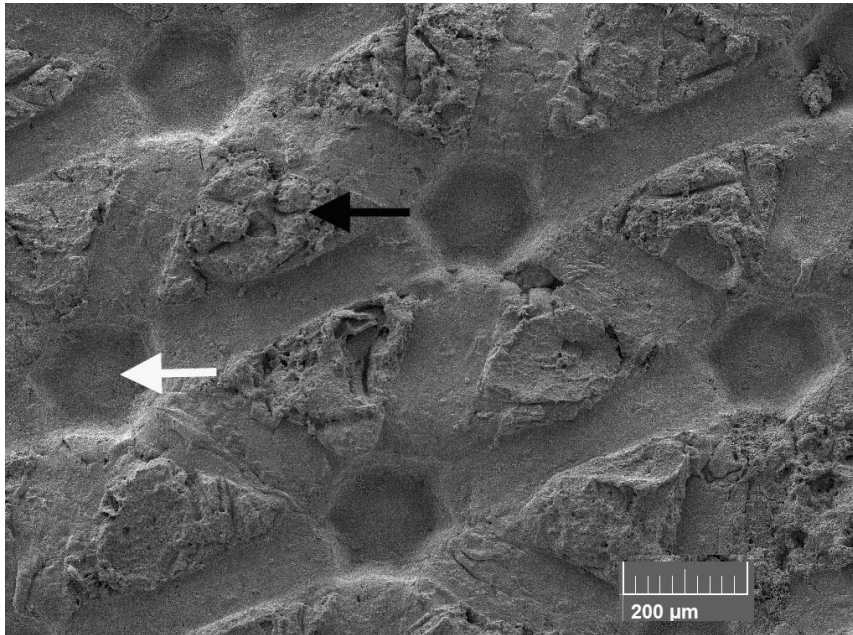


**Figure 3.48: 24 hour NC-SD tissue surface by SEM**

The impression of the dressing was seen in some areas of the tissue surface with lack of bacteria (white arrow). Other areas contained biofilm where there was a lack of dressing contact (black arrow) (x200)

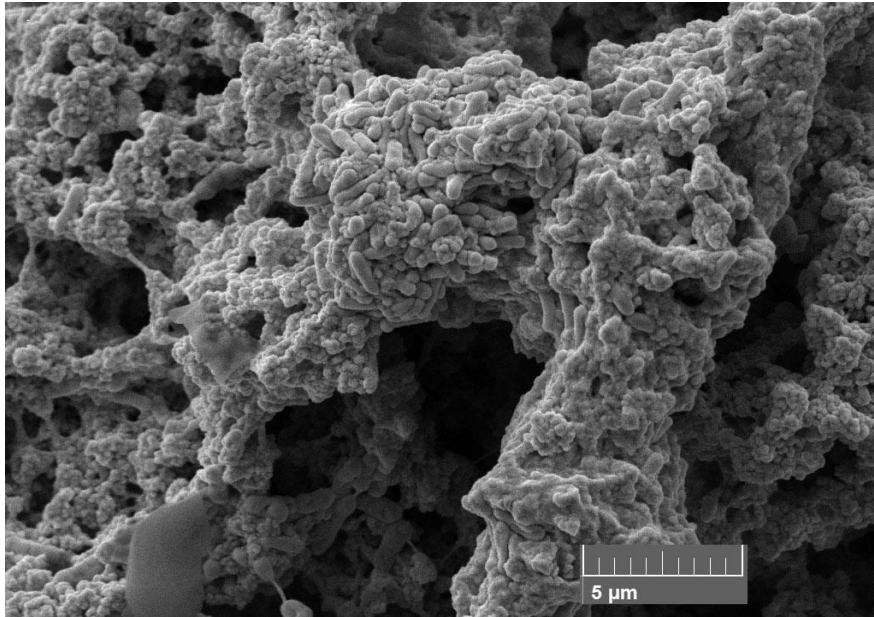


**Figure 3.49: 24 hour NC-SD SEM biofilm on tissue surface**

Where the dressing was not in contact with the tissue, a mixture of both bacteria was present (x10k)

The surface and lower fibre layers of the dressing were coated with bacteria

(Figure 3.50).

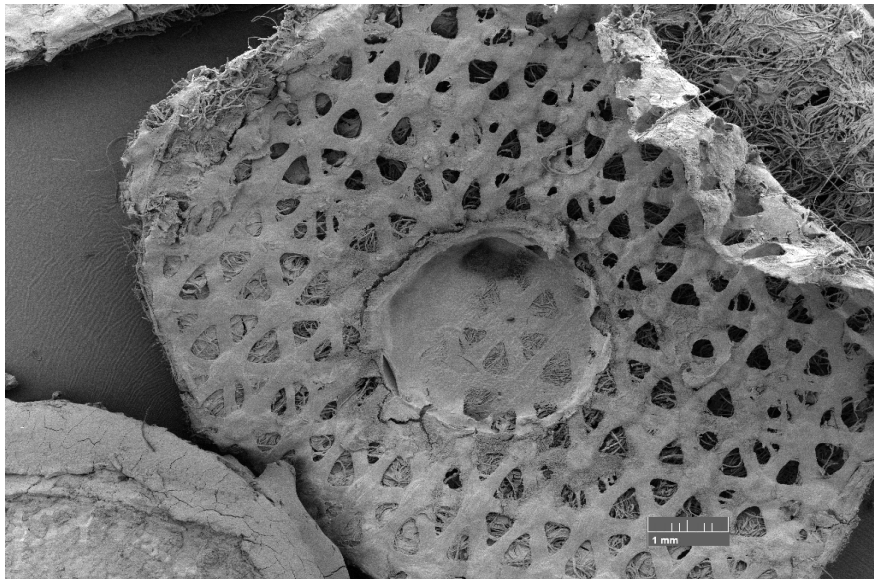


**Figure 3.50: The surface and lower fibre layers of the NC-SD at 24 hours**

Dressings were coated with bacteria on the surface and also into the dressing structure (x20)



CLSM of the tissue and the dressing showed the presence of many live bacteria (Figure 3.51).

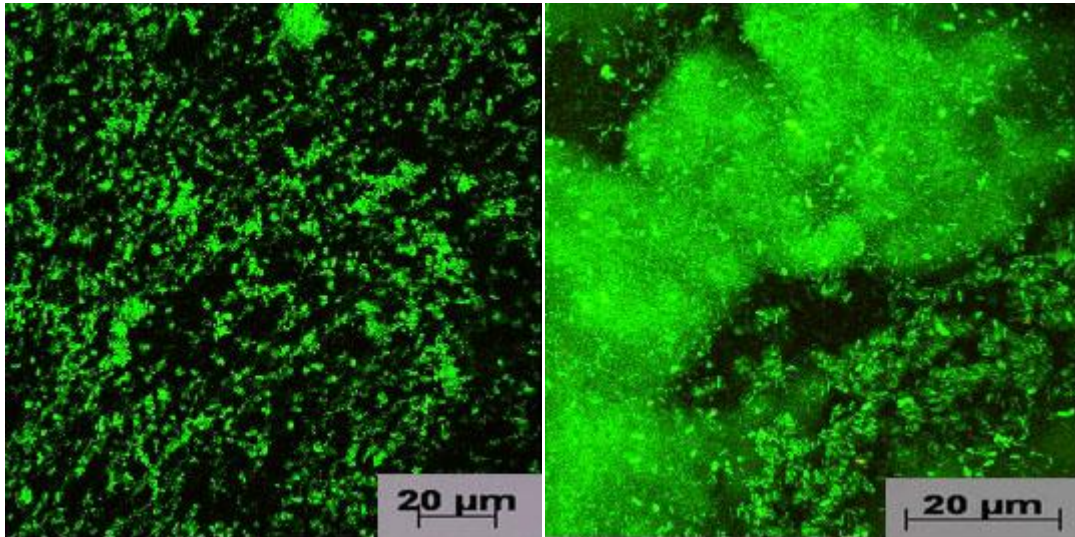


**Figure 3.51: CLSM at 24 hours of the NC-SD and tissue**

Live bacteria present on the NC-SD (left x40) and on the tissue (right x80) below 24 hour NC-SD, showing the presence of many live bacteria in the form of biofilm

PHMBD at 24 hours had few bacteria observed under LM with only the occasional small group or thin layer of bacteria (Figure 3.52).

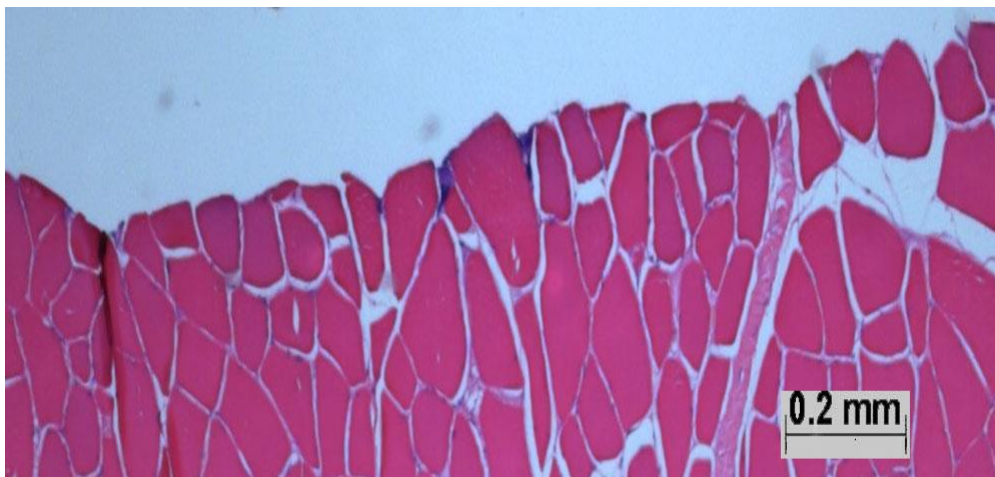


**Figure 3.52: PHMBD treated model at 24 hours with few bacteria apparent in LM**

Only the occasional small group of bacteria were present on the surface between a few muscle fibres (x4)



This was mirrored in the SEM model (Figure 3.53; Figure 3.54) and TEM model (Figure 3.55).

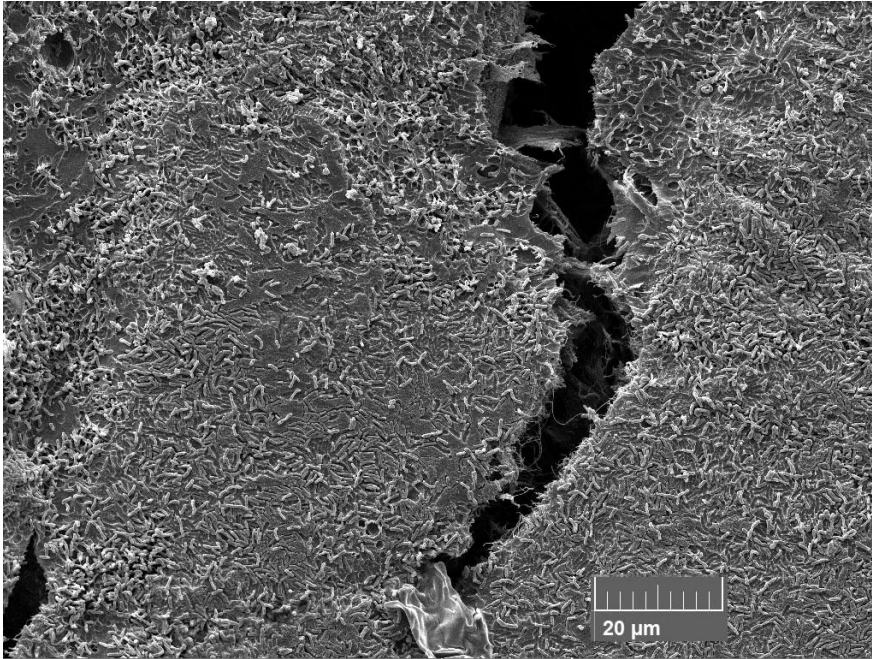


**Figure 3.53: Tissue surface below the PHMBD at 24 hour by SEM**  
A thin, flat layer of bacteria was present on the tissue surface (x2000)

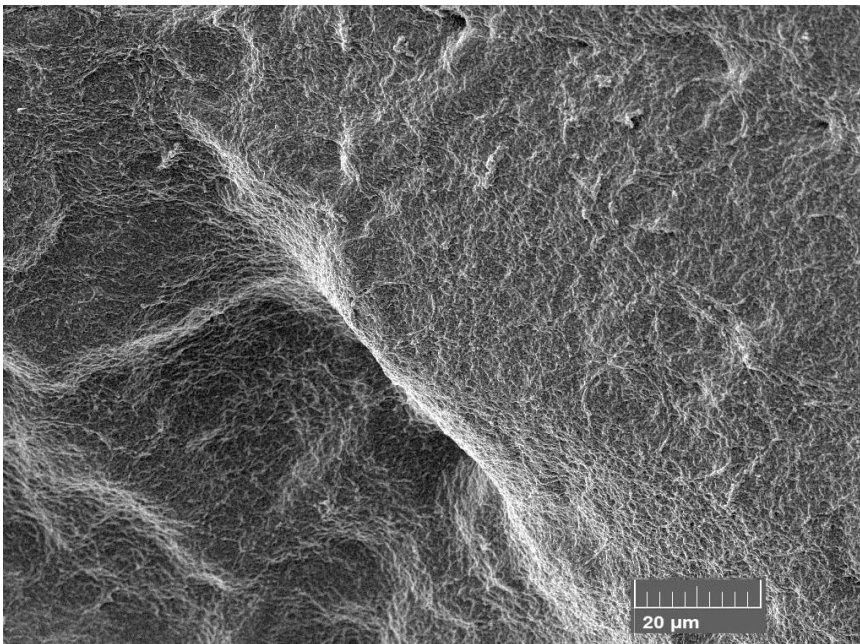


**Figure 3.54: PHMBD surface at 24 hour SEM**  
Bacteria did not appear to be attached/sequestered on to the dressing (x2000)

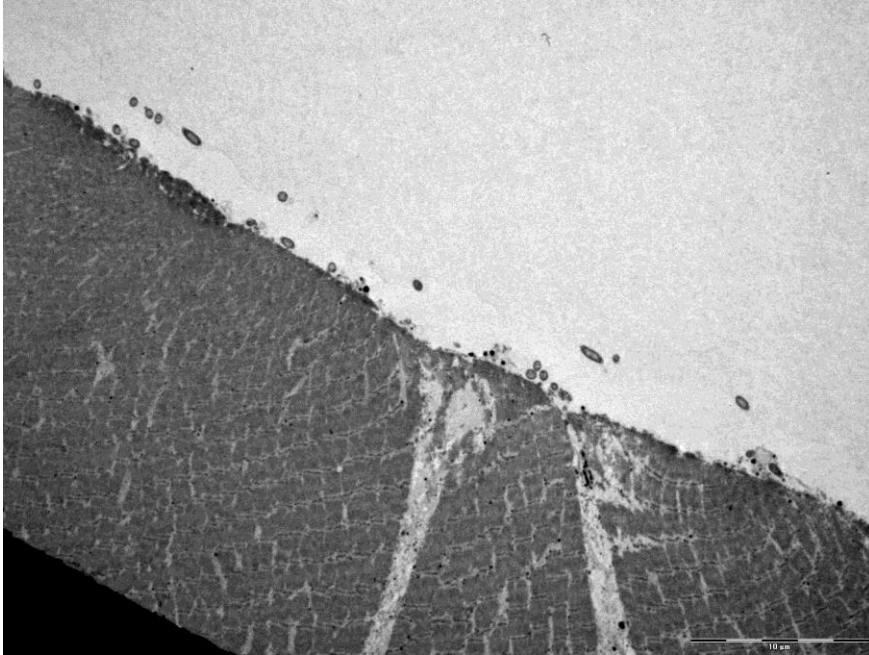


**Figure 3.55: Tissue surface below the PHMBD at 24 hour by TEM**  
A thin line of minimal bacteria was present with no apparent EPS (x2500)

No EPS was seen on TEM. Areas of live and dead bacteria were present with CLSM (Figure 3.56).

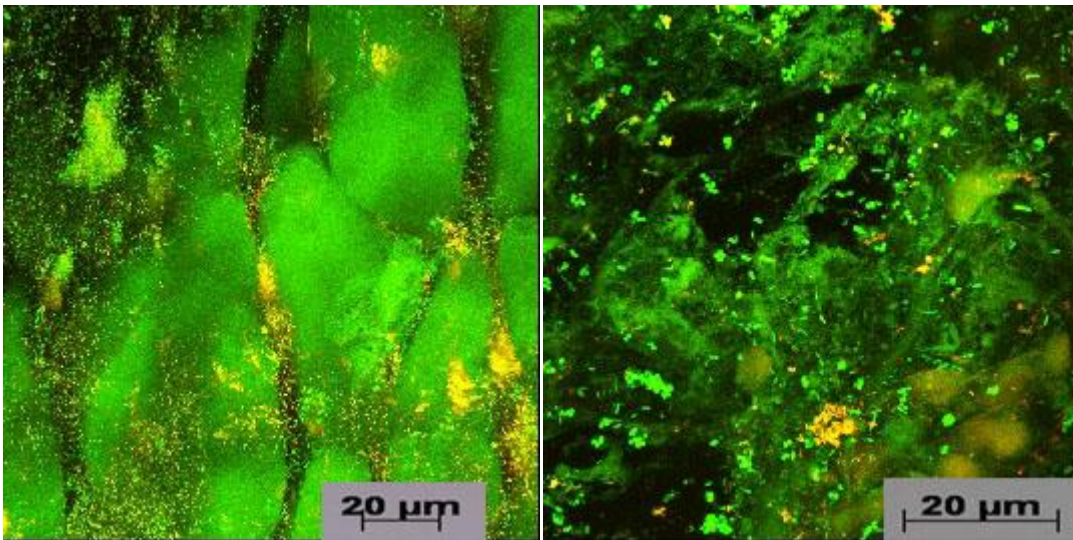


**Figure 3.56: PHMBD tissue surface and dressing at 24 hours by CLSM**  
A few live bacteria (green) present on the tissue surface (left) or the dressing (right) but most were dying (yellow and red) (x40)

The iodine crystals of the CID model were not present after 12 hours and in the 24 hour model the bacterial growth appeared to have increased. Beads were present surrounded by bacteria and EPS in LM, SEM and TEM imaging (Figure 3.57; Figure 3.58; Figure 3.59; Figure 3.60).

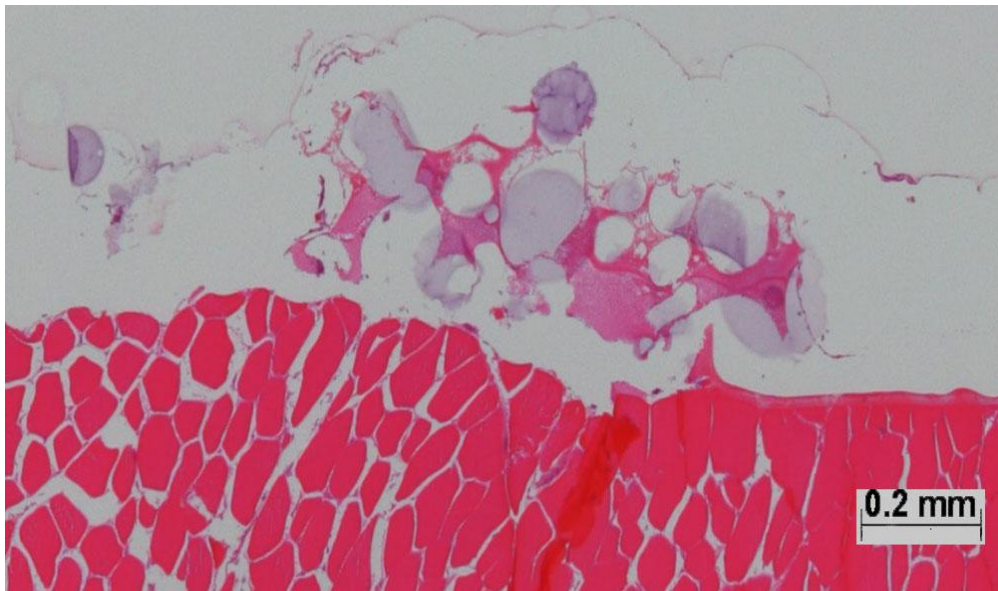


**Figure 3.57: The CID tissue surface at 24 hour by LM**

The model appeared to have an increase in bacteria. Beads (blue arrow) could be seen surrounded by biofilm (green arrow) on LM (x4)



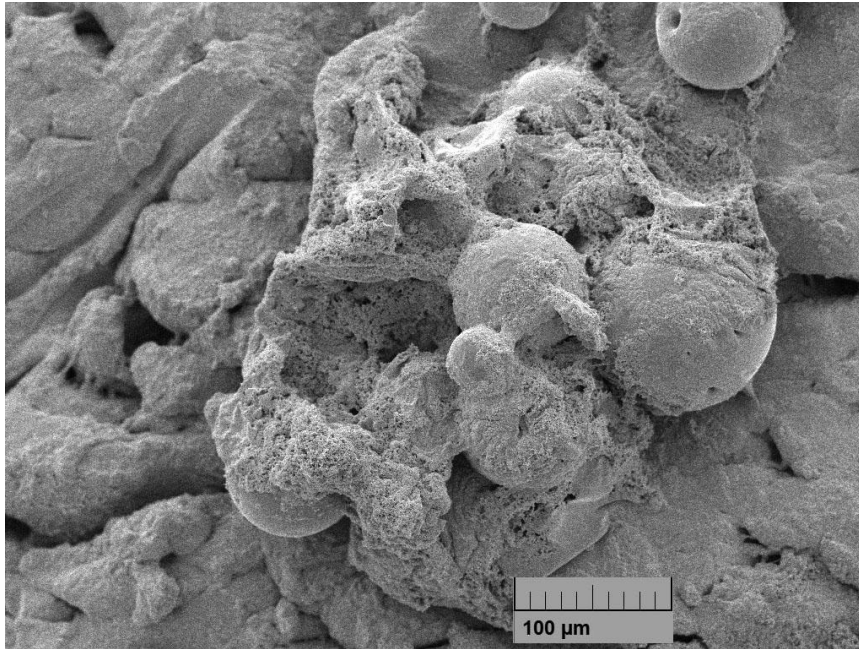


**Figure 3.58 The CID 24 hour model by SEM with cadexomer beads**  
Most of the beads were enmeshed in biofilm (x500)

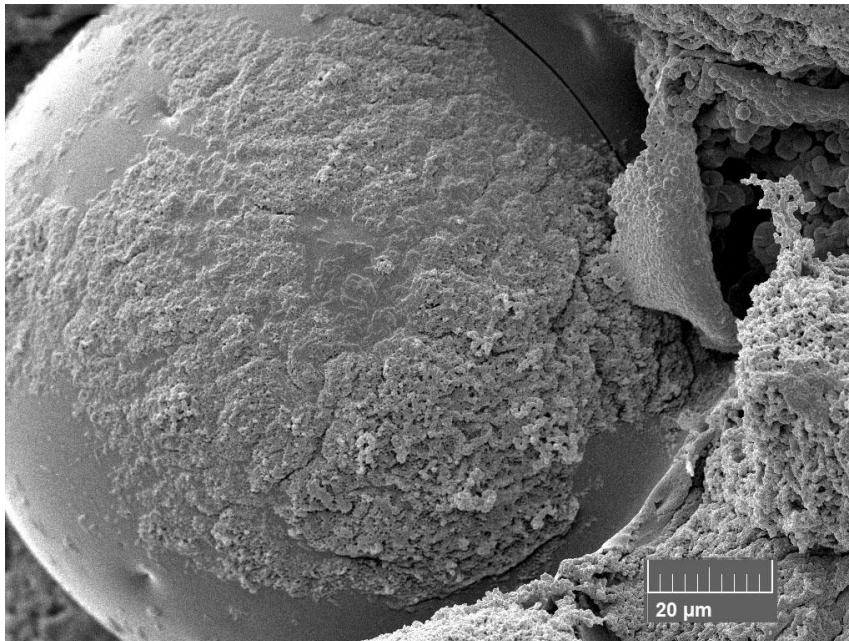


**Figure 3.59: An individual cadexomer bead from the 24 hour CID model by SEM**  
Even the larger beads had biofilm attached and mats of biofilm in-between (x2000)

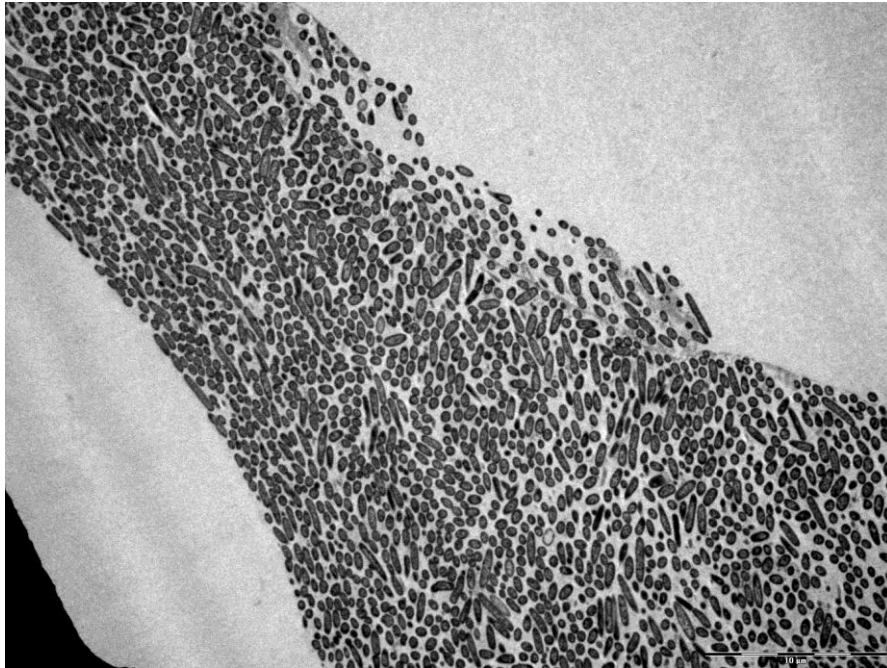


**Figure 3.60: Biofilm growth in the CID 24 hour model by TEM**  
Bacterial biofilm was seen between the beads (x2500)

Imaging by CLSM also showed live bacteria between the beads (Figure 3.61).

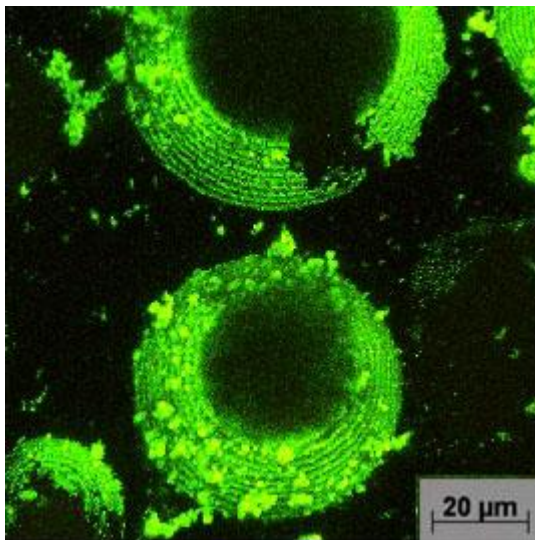


**Figure 3.61: Imaging of cadexomer beads by CLSM of 24 hours**  
CID showed live bacteria on and around the beads forming biofilm (x40)

### 3.7.2 48 Hour dressing treated models

In the 48 hour models, bacterial growth below the gauze was mainly continuous (Figure 3.62), with some areas slightly variable on the surface and some penetrating into the lower layers of muscle.

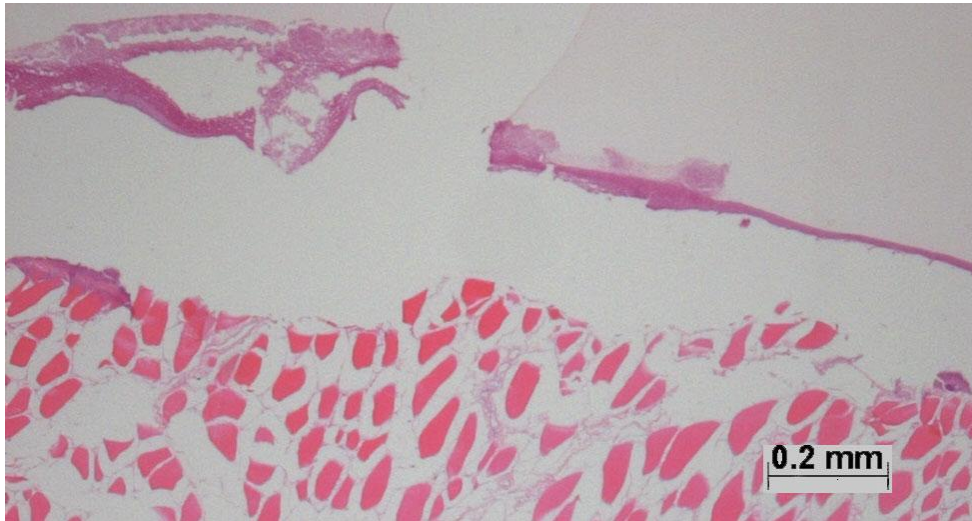


**Figure 3.62: The 48 hour gauze models with thick continuous growth by LM**  
Bacterial growth below the gauze was mainly continuous (x4)

This could also be seen in the TEM models where the bacteria were present in a thick layer containing EPS (Figure 3.63).

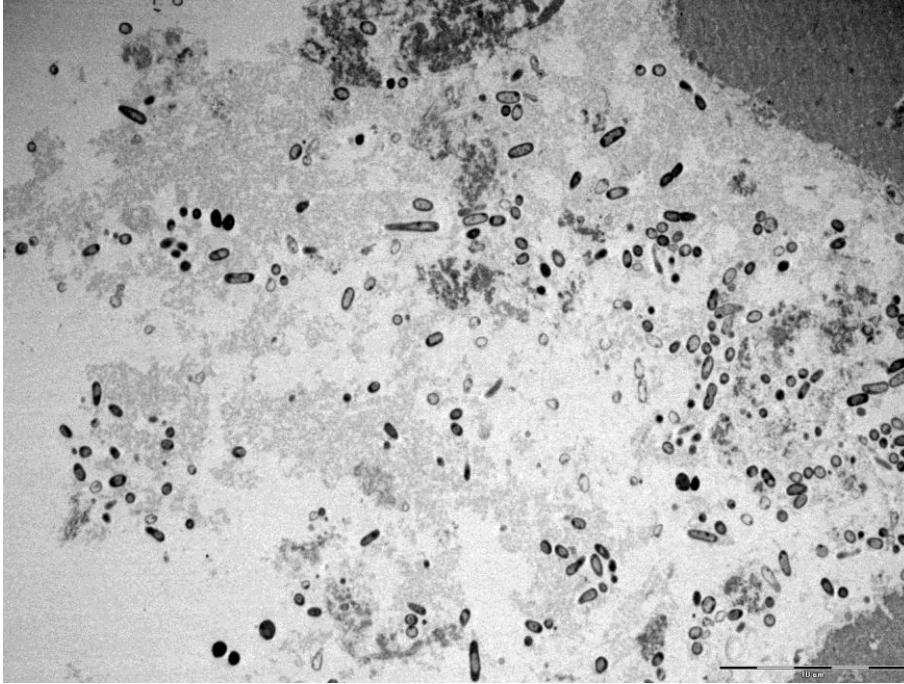


**Figure 3.63: 48 hour growth beneath gauze viewed by TEM**  
Bacteria in EPS was found in a thick layer upon the tissue surface (x2500)

The gauze dressing was coated in a thick layer of biofilm when viewed with SEM (Figure 3.64).

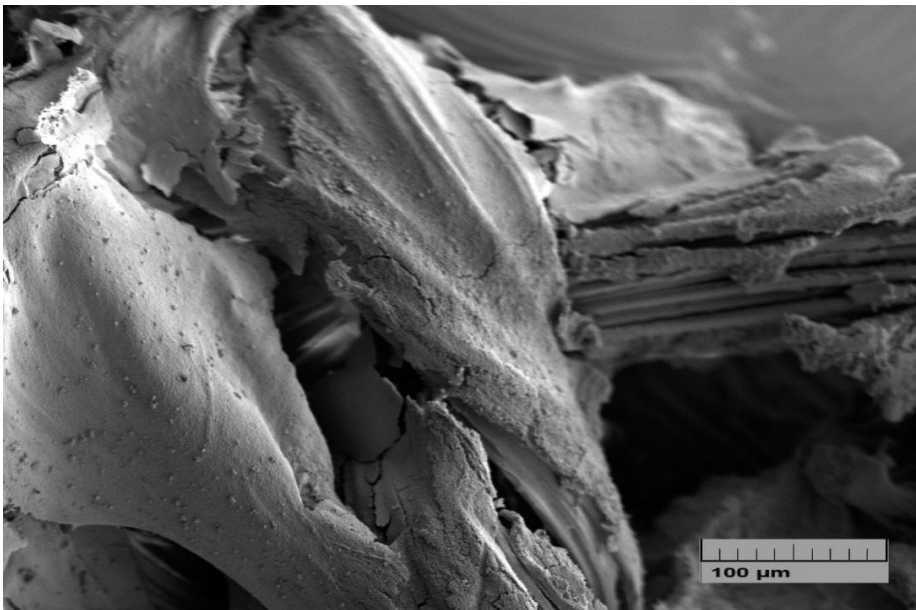


**Figure 3.64: The 48 hour gauze dressing by SEM**  
Dressings were coated in a thick layer of biofilm (x100)



The surface of the tissue, when viewed with SEM, was coated in a layer of biofilm so thick in most areas, that the tissue was not visible beneath it (Figure 3.65).

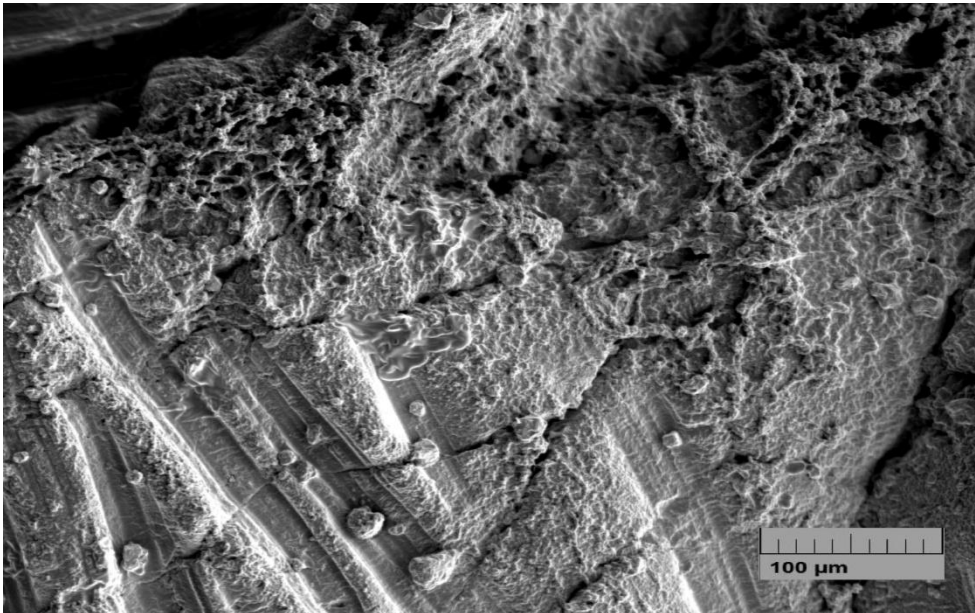


**Figure 3.65: 48 hour gauze tissue surface by SEM**

The tissue surface was coated in an almost continuous thick layer of biofilm such that it was difficult to see the tissue surface (x200)

Statistical analysis (a two-sample t-test) of the means at 24 and 48 hour for gauze showed no significant difference ( $p= 0.063$ ).

The NSHD control model had small groups of bacteria remaining on the surface of the tissue (Figure 3.66), which was also seen on TEM (Figure 3.67) and SEM (Figure 3.68).



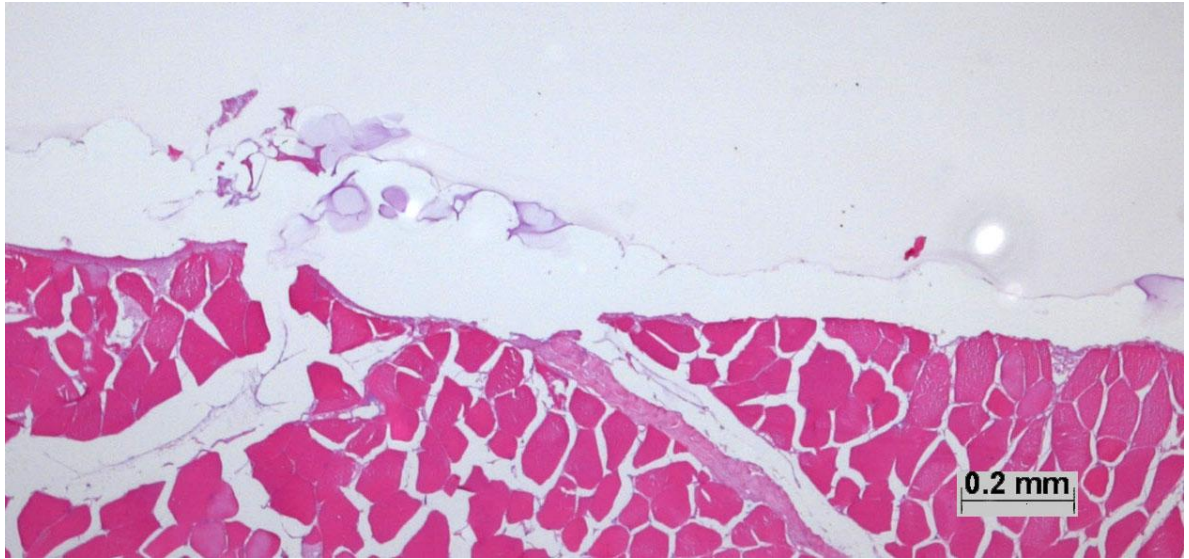


**Figure 3.66: LM of 48 hour NSHD**  
Small groups of bacteria remained on the surface of the tissue (x4)

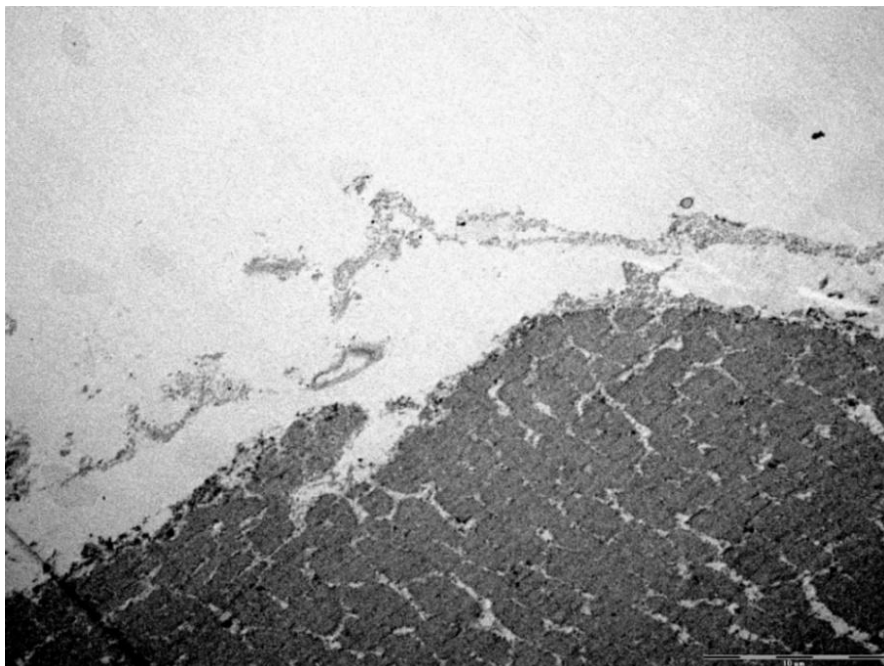


**Figure 3.67: 48 hour NSHD by TEM**  
Small groups of bacteria remained on the surface of the tissue with possible EPS (x2500)

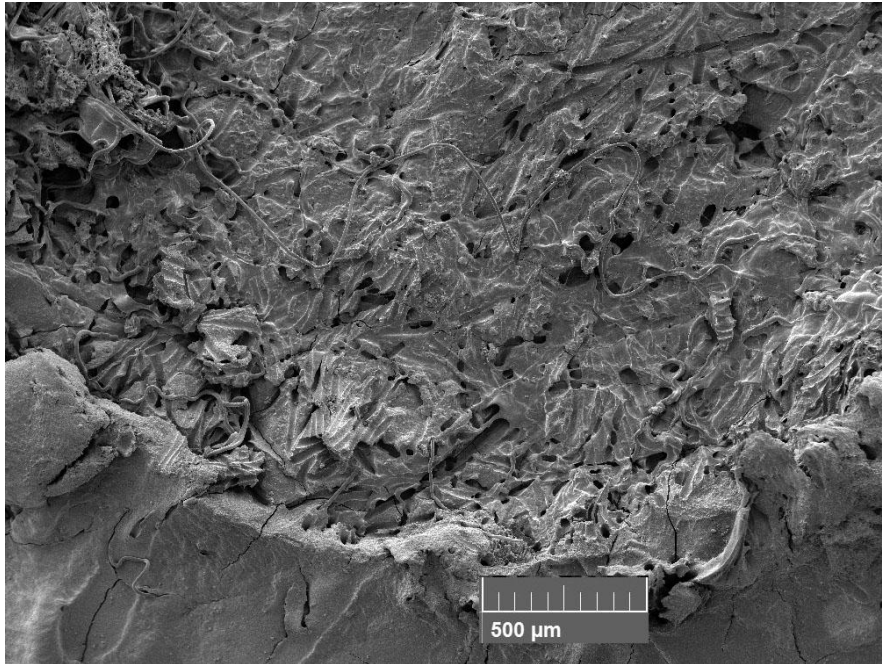


**Figure 3.68: The 48 hour NSHD by SEM including model edge**

Small groups of bacteria remaining on the surface of the tissue. Here the edge can be viewed on the lower part of the model, where the circular dressing did not cover the surface and thick biofilm was able to grow (x100)

The dressing showed some bacteria sequestered within the gelled fibres under SEM (Figure 3.69). There was a significant difference ( $p=0.007$ ) between the means at 24 and 48 hours.

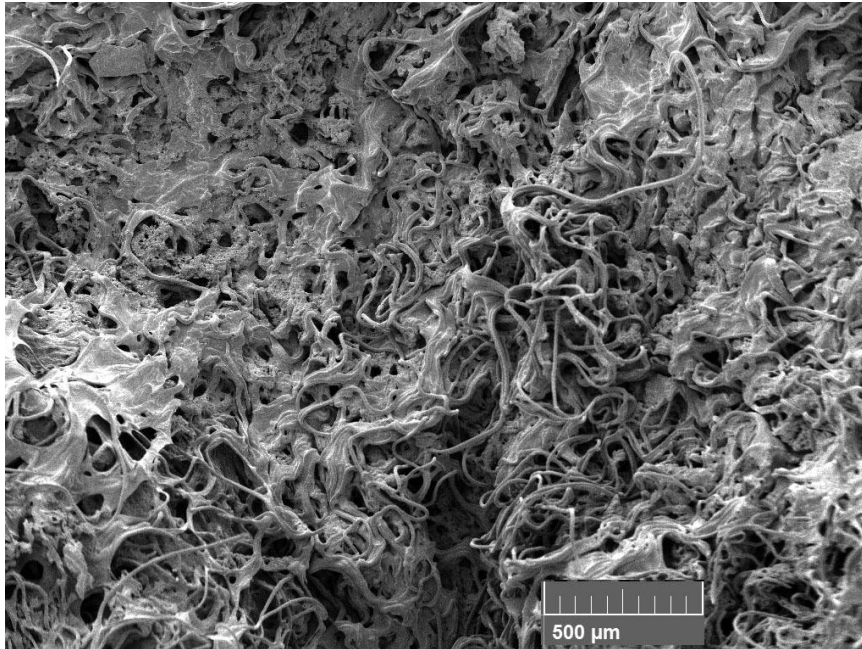


**Figure 3.69: The 48 hour NSHD with swelling of fibres**

Dressings showed fibres sequestering bacteria, with some groups of bacteria on the surface (x100)

The SCHED with LM showed the occasional cluster of bacteria especially around a few fibres left on the surface of the tissue (Figure 3.70).

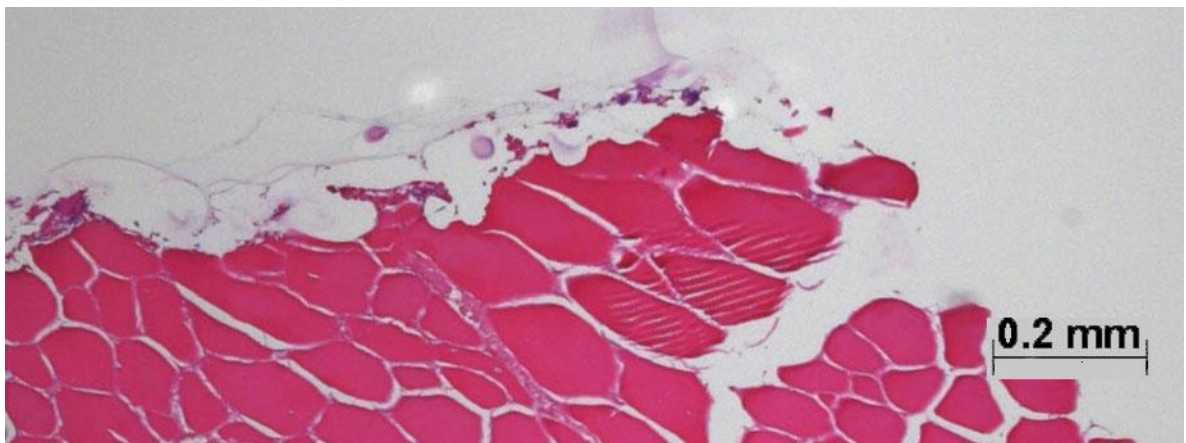


**Figure 3.70: SCHED at 48 hours by LM**

The occasional cluster of bacteria was present, especially around a few fibres left on the surface of the tissue (x4)

A few fibres on the model surface visualised by SEM, gave a similar picture of bacteria attached to the fibres (Figure 3.71). TEM showed these groups to contain



possible EPS, but with few viable bacteria within it (Figure 3.72). The two-sample t-test of the 24 and 48 hour means showed a significant difference ( $p=0.004$ ).

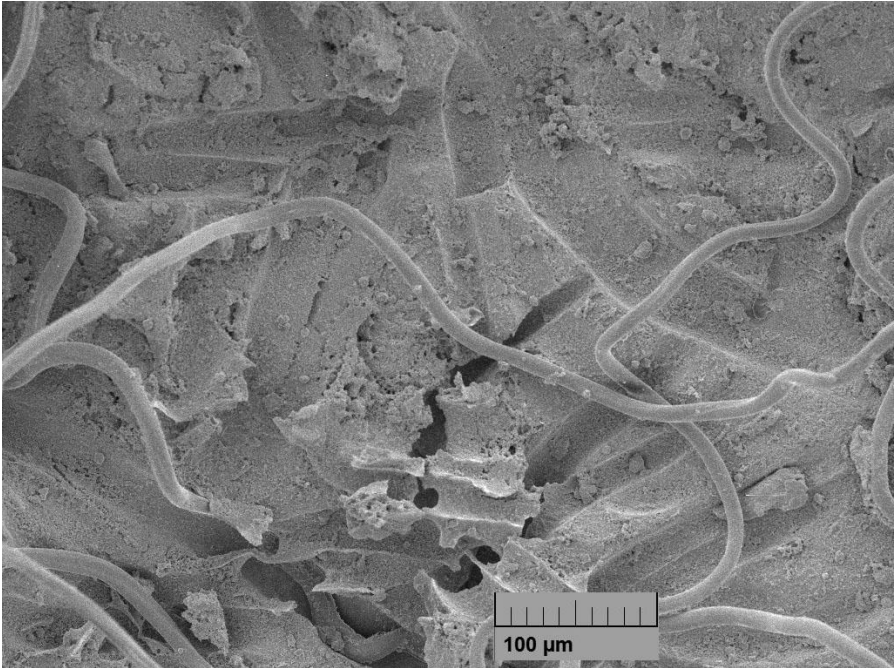


**Figure 3.71: A few fibres on the 48 hour SCHD tissue surface**  
Surfaces visualised by SEM, showed bacteria attached/sequestering into the fibres (x500)

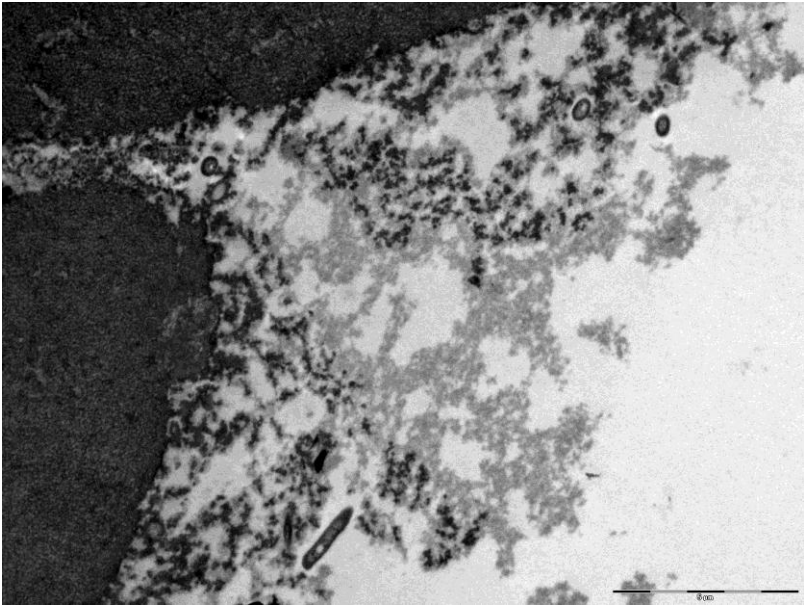


**Figure 3.72: TEM 48 hour SCHD model surface**  
This contained possible EPS, but with very few viable bacteria within it (x6000)

The NGAD model had minimal bacteria present under LM (Figure 3.73), and this was confirmed by TEM. The few bacteria present appeared to be disrupted with no viable nuclear material (Figure 3.74).

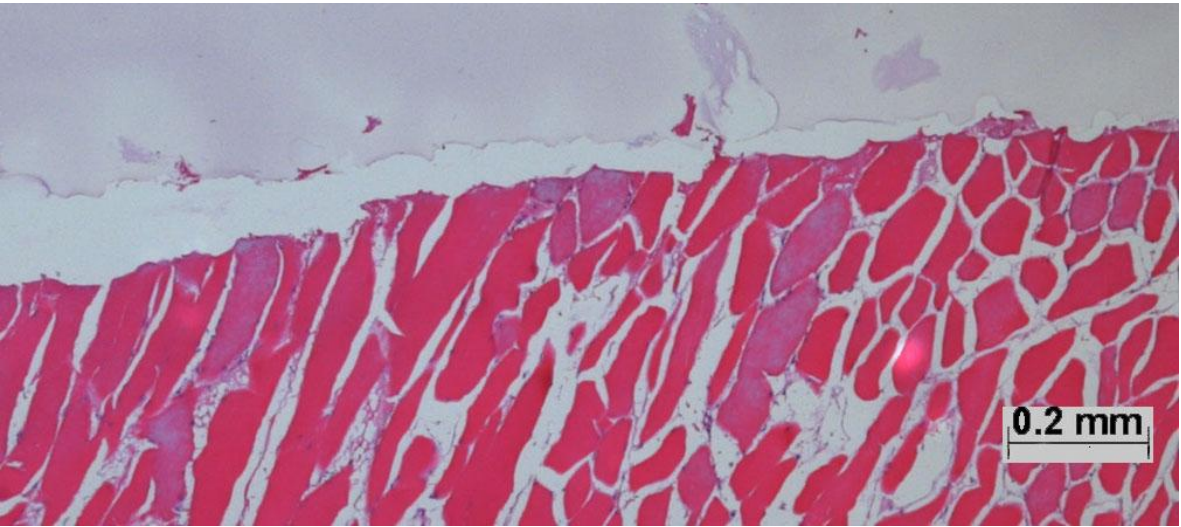


**Figure 3.73: The 48 hour NGAD model with clean surfaces below the agar**  
Minimal bacteria was seen by LM. The surfaces appeared almost clean (x4)

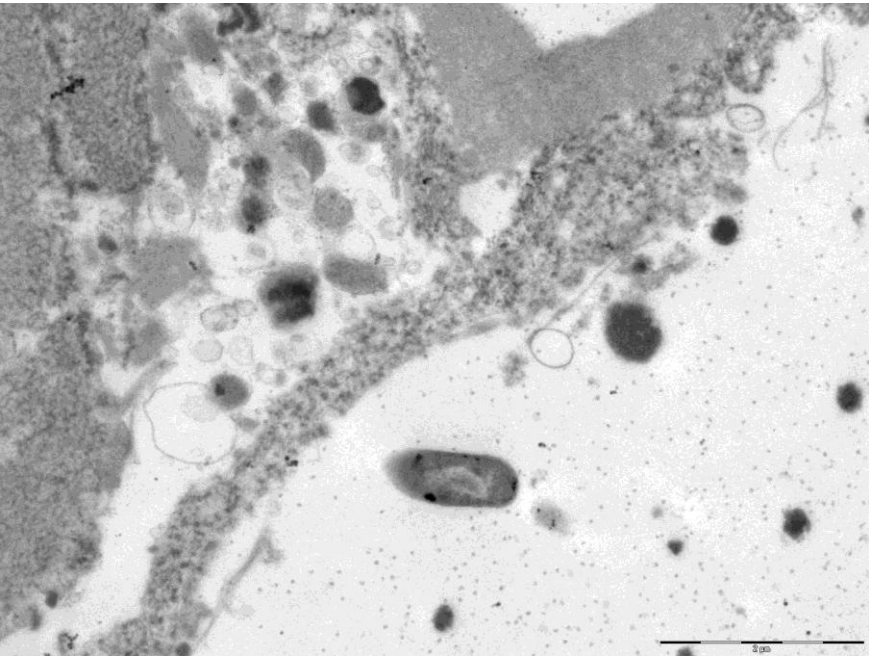


**Figure 3.74: The 48 hour NGAD model by TEM**  
TEM showed very few bacteria. Those present were mostly disrupted (x15k)

SEM models showed almost clean surfaces (Figure 3.75).

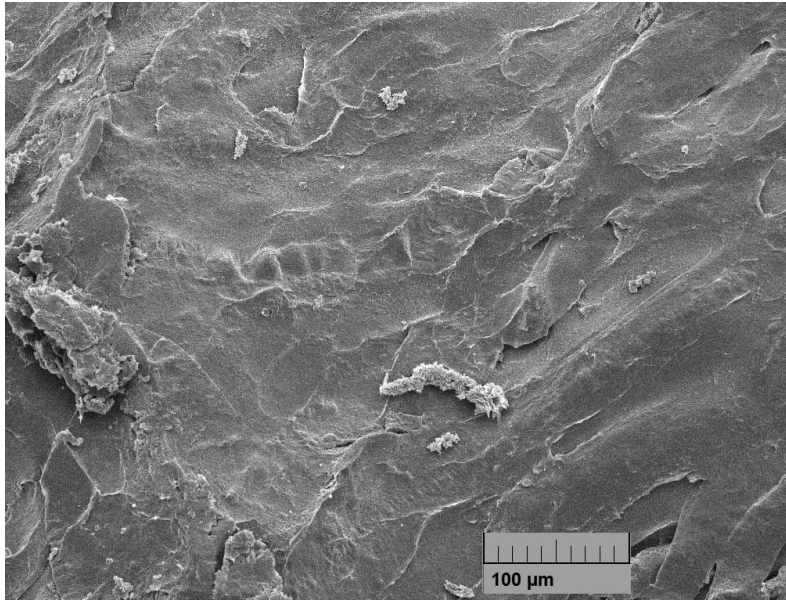


**Figure 3.75: 48 hour NGAD tissue surface by SEM**

SEM showed tissue surfaces which appeared to be clean of any biofilm growth (x500)

The means showed no significant differences in 24 and 48 hours ( $p= 0.201$ ).

Viewing under CLSM the SCHD and NGAD showed very few viable bacteria present on the tissue surface, either live or dead. Similar results were obtained in the dressings. (Figure 3.76; Figure 3.77).



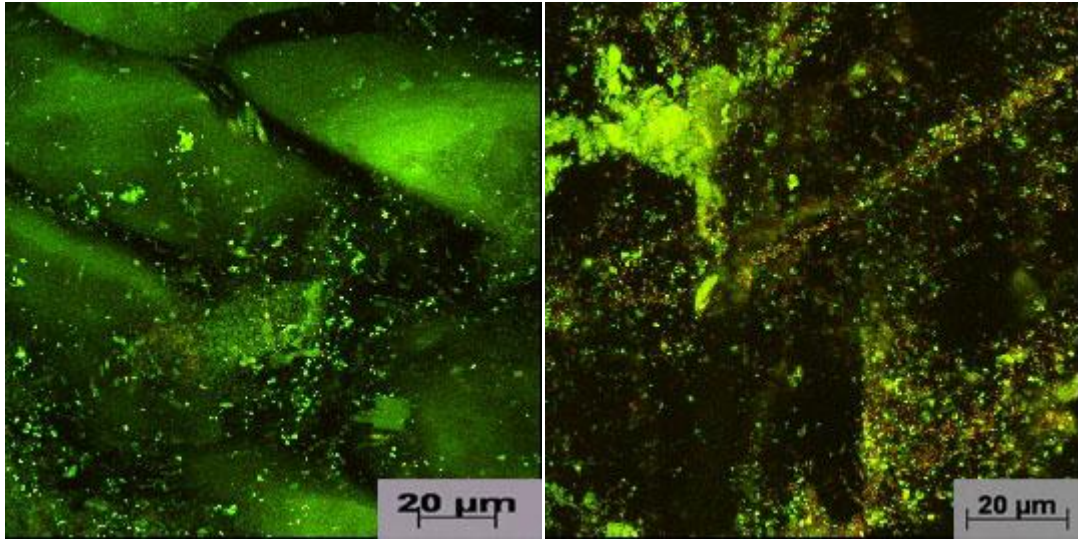


**Figure 3.76: 48 hour SCHED tissue surface and dressing by CLSM**

Left - CLSM of tissue beneath SCHED showed no visible bacterial biofilm although a few live bacteria were noted (x40)

Right - The dressings contained bacteria in both live (green) and dead (red) (x40)

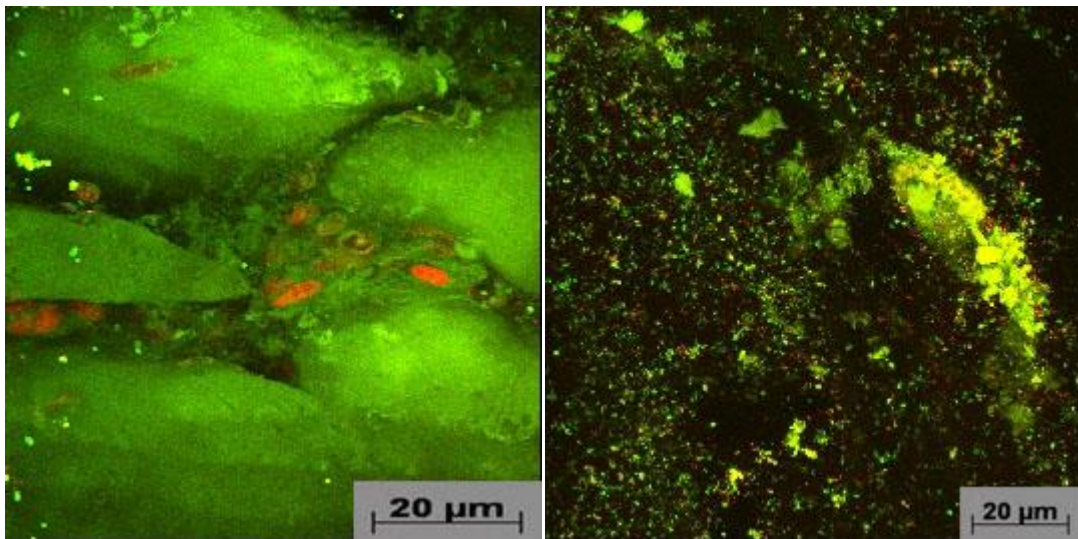


**Figure 3.77: 48 hour CLSM of NGAD tissue surface and dressing by CLSM**

Left - Tissue beneath NGAD showed no visible bacterial biofilm (x40)

Right - NGAD showed no visible bacterial biofilm and contained bacteria in both live, dying and dead (green, yellow and red) (x40)

The CES-SD model had some groups of bacteria present in the lower layers of the tissue, with occasional surface groups of bacteria when viewed by LM (Figure 3.78) and TEM (Figure 3.79).

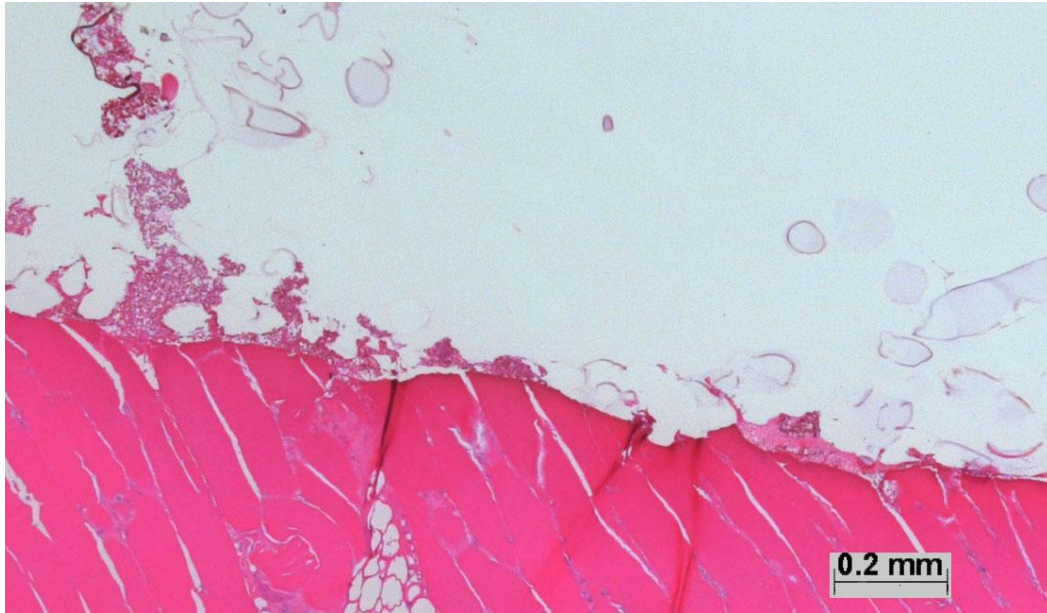


**Figure 3.78: CES-SD 48 hour model by LM**  
Groups of bacteria were present as occasional surface groups (x4)

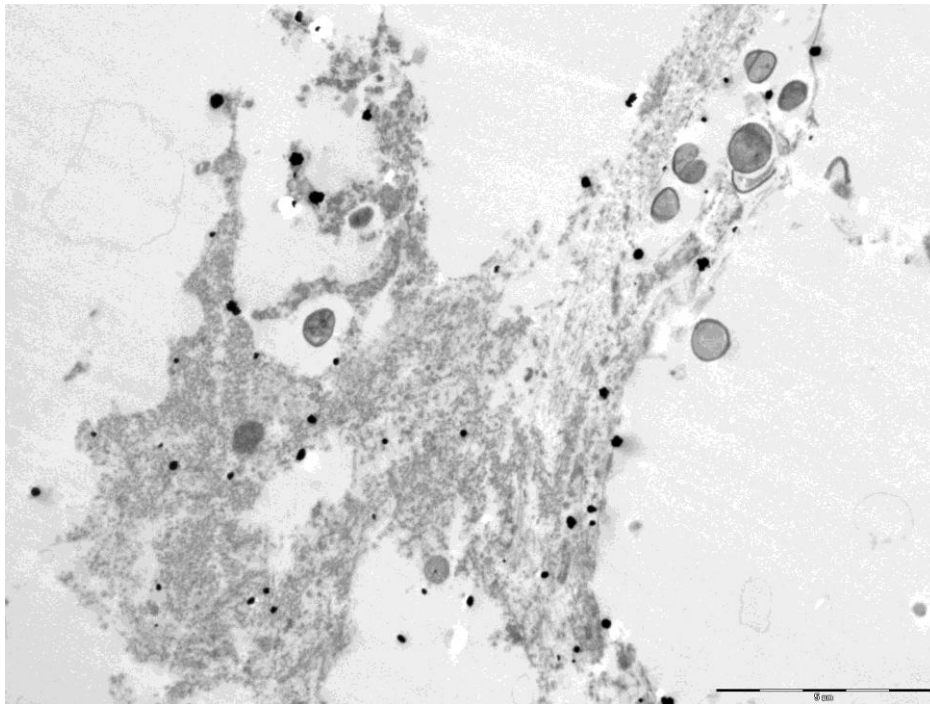


**Figure 3.79: 48 hour CES-SD hour model by TEM**  
Groups of bacteria were present which appeared to be surrounded by EPS (x6000)



Under SEM the dressing contained a few bacterial growths, but the dressing fibres were so attached to the surface of the tissue that it was impossible to view the tissue surface in any of the samples (Figure 3.80). The 24 and 48 hour means were not significantly different ( $p=0.148$ ).

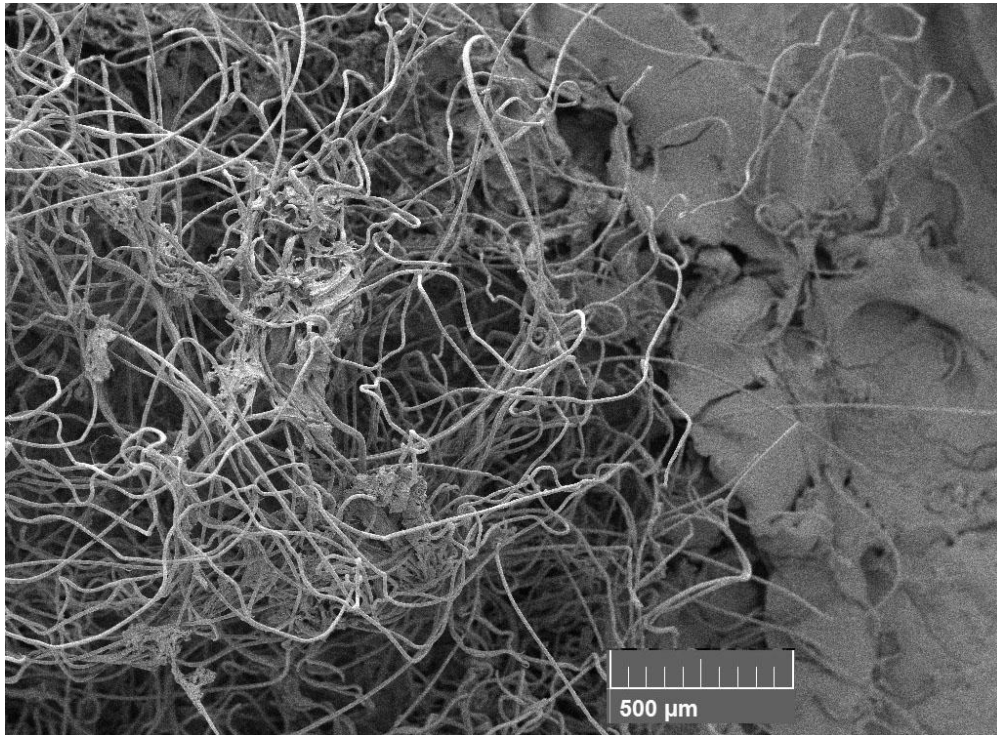


**Figure 3.80: The CES-SD tissue surface at 48 hours by SEM**

CES-SD was so attached to the surface of the tissue that it was impossible to view the tissue below it (x100)

Viewing by CLSM showed fibres, with live bacteria visible around them, with very few apparently dead (Figure 3.81).

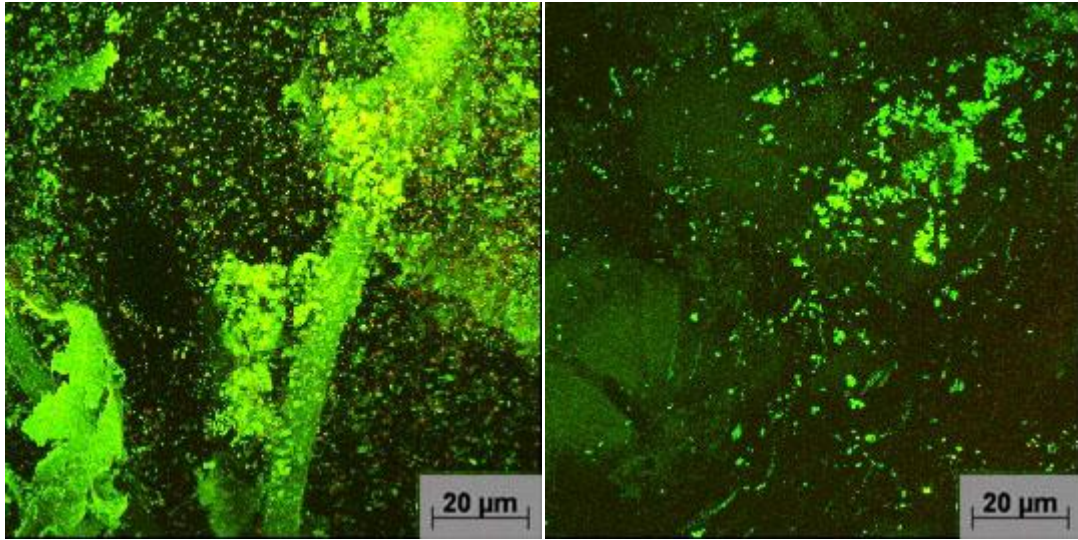


**Figure 3.81: CES-SD at 48 hour and tissue surface by CLSM**

Fibres, some coated with bacteria (left x80), mainly live but some dead, were found on the model surface, and clusters of biofilm were found on the tissue surface (right x40)

A few pockets or thin lines of bacteria were present on the surface of the ACN-SD model (Figure 3.82). Some dressing fibres remained, visible by LM, some of which showed release of silver into the immediate surrounding area (Figure 3.83).

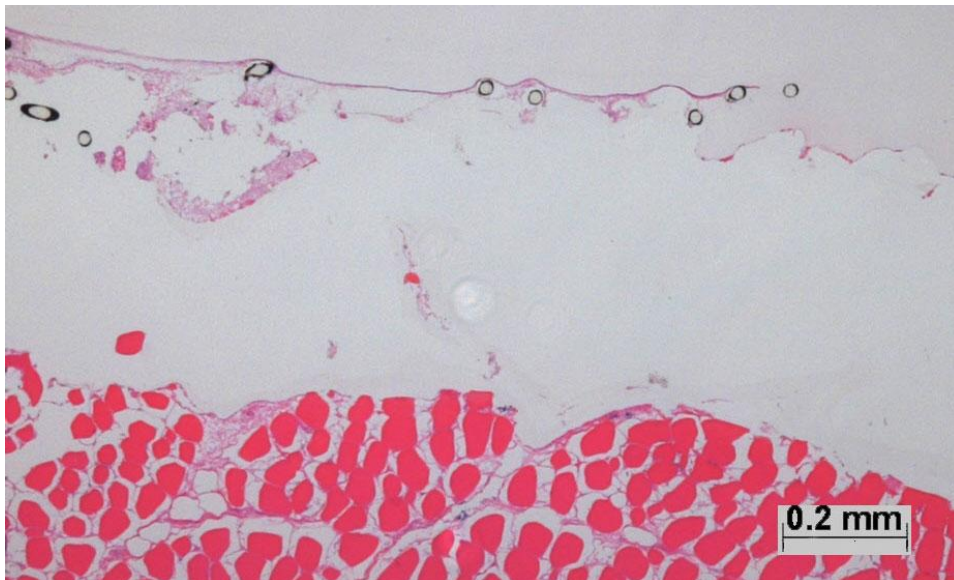


**Figure 3.82: 48 hour ACN-SD model by LM**

A few pockets or thin lines of bacteria were present on the surface and some dressing fibres remained on one model (x4)



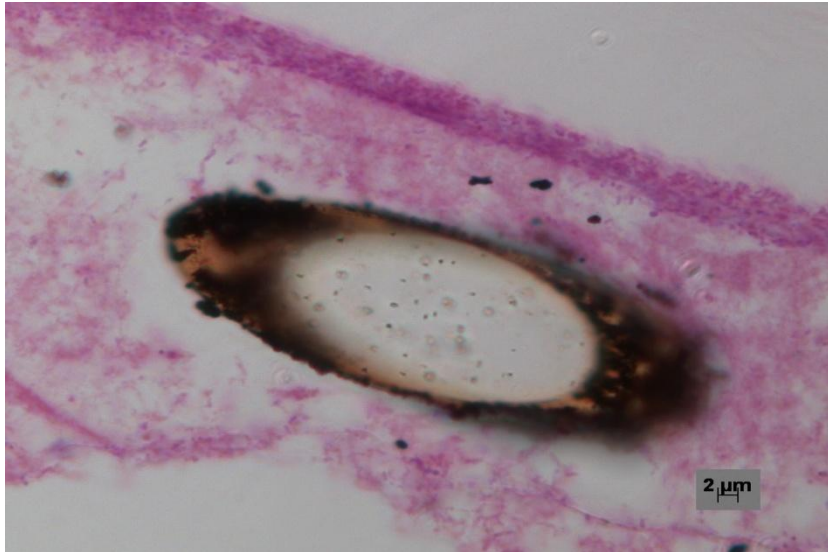


**Figure 3.83: 48 hour ACN-SD fibres by LM**

A silver containing fibre shed from the 48 hour ACN-SD with small black dots of silver release (x100)

This was a similar appearance with SEM (Figure 3.84), but TEM demonstrated that some of these small groups were viable biofilm (Figure 3.85).

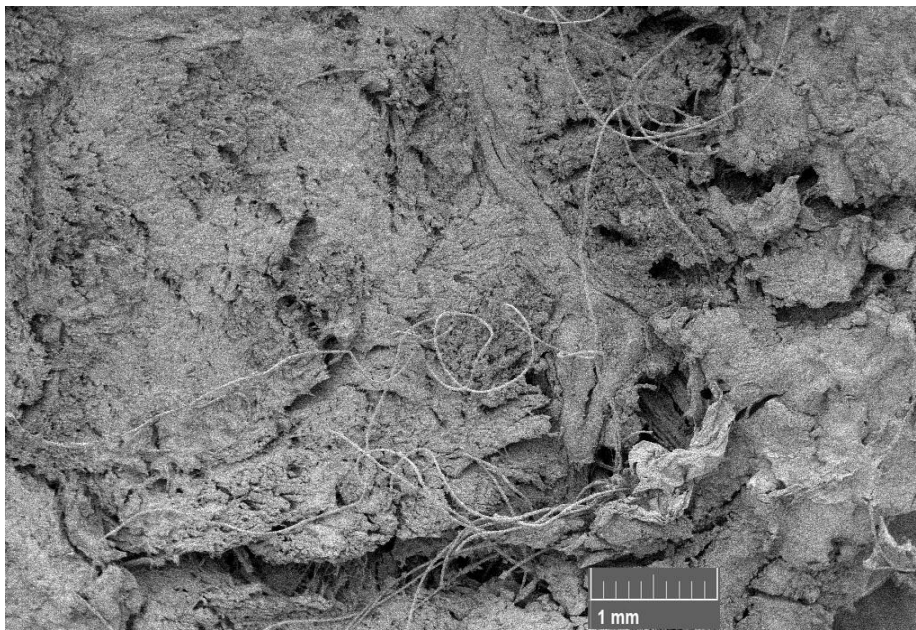


**Figure 3.84: SEM 48 hour ACN-SD model**

A few pockets of bacteria were present with a few dressing fibres (x40)

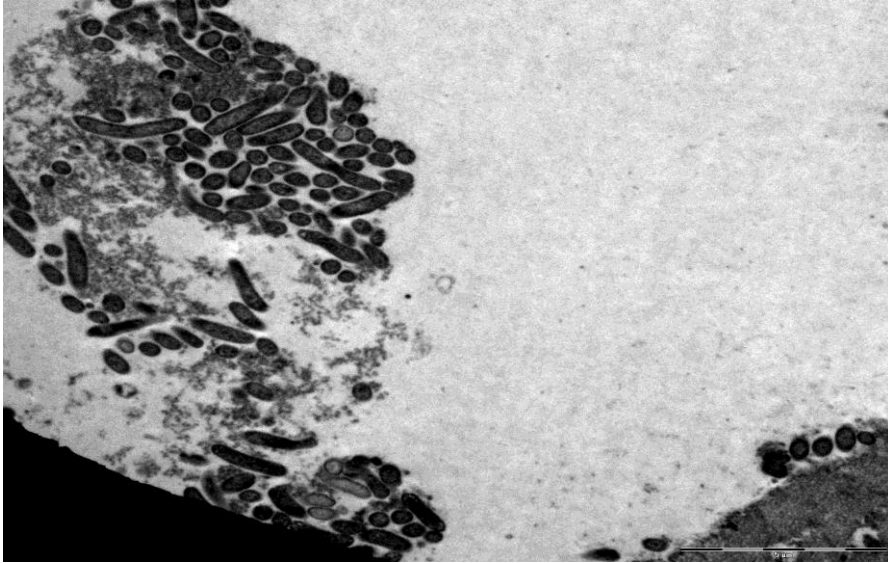


**Figure 3.85: TEM 48 hour ACN-SD model**

A few small groups of biofilm were found on the tissue surface (x6000)

Some possible absorption of surface material could be seen within the fibres of the dressing (Figure 3.86). Statistical t-tests of this silver dressing found the means of biofilm areas of 24 and 48 hours not to be significantly different ( $p= 0.135$ ).

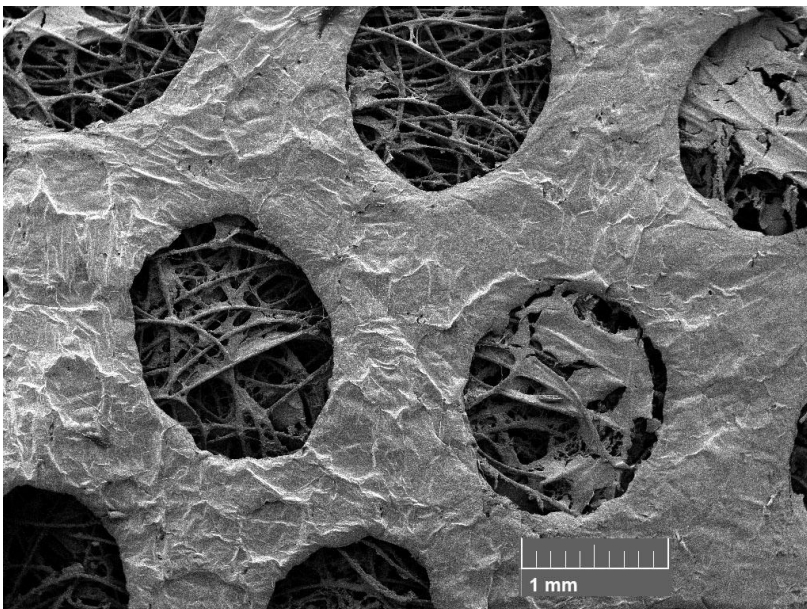


**Figure 3.86: SEM 48 hour ACN-SD model**

Some possible absorption of surface material could be seen within the fibres of the dressing (x50)



There was a similar appearance with CLSM, demonstrating that some of these small groups were viable biofilm (Figure 3.87).

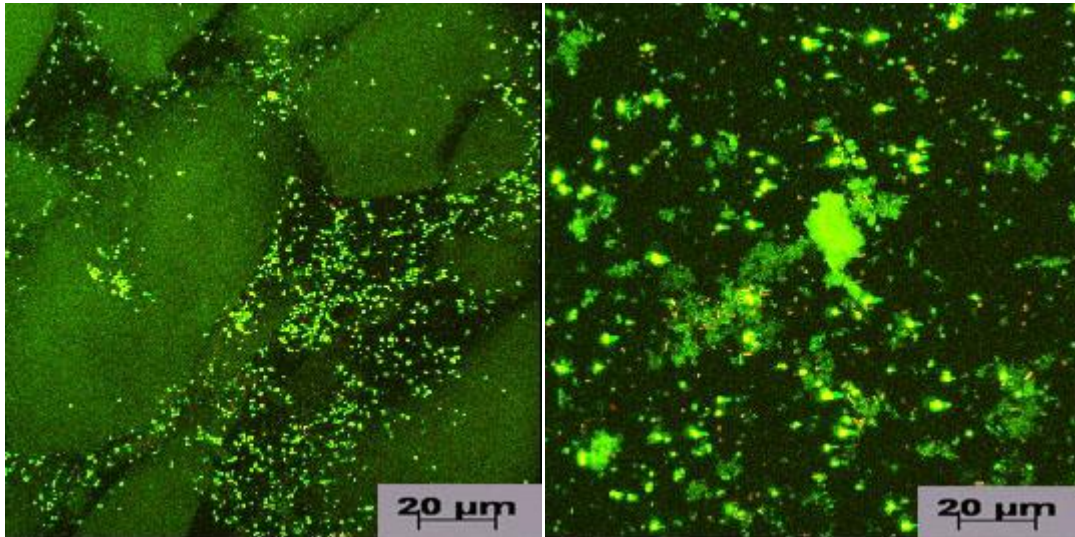


**Figure 3.87: CLSM 48 hour ACN-SD model**

A few pockets of bacteria were present on the tissue and the dressing surface

LM of NC-SD showed silver deposition on the surfaces, with bacteria present in a few places on the surface and in the tissue layers below the surface (Figure 3.88).

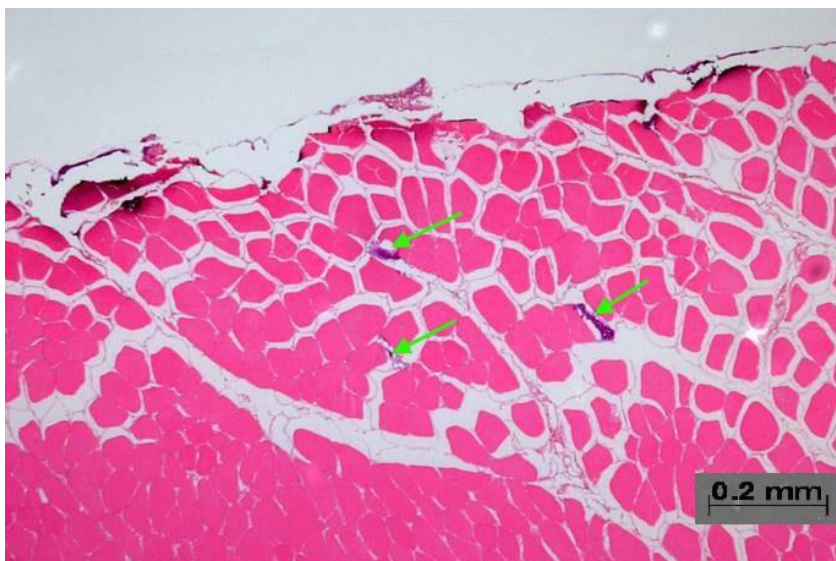


**Figure 3.88: LM of NC-SD at 48 hours (x4)**

Silver deposition (black) on the surface and bacteria in the tissue layers below (arrows)

Some of these bacteria could be seen with TEM as viable dividing bacteria, surrounded by EPS, although there was some nuclear disruption (Figure 3.89).

SEM of the NC-SD showed the surface and lower fibre layers of the dressing were coated with bacteria (Figure 3.90).



**Figure 3.89: TEM of NC-SD at 48 hours**

Dividing bacteria could be seen surrounded by EPS, but with some nuclear disruption (x6000)

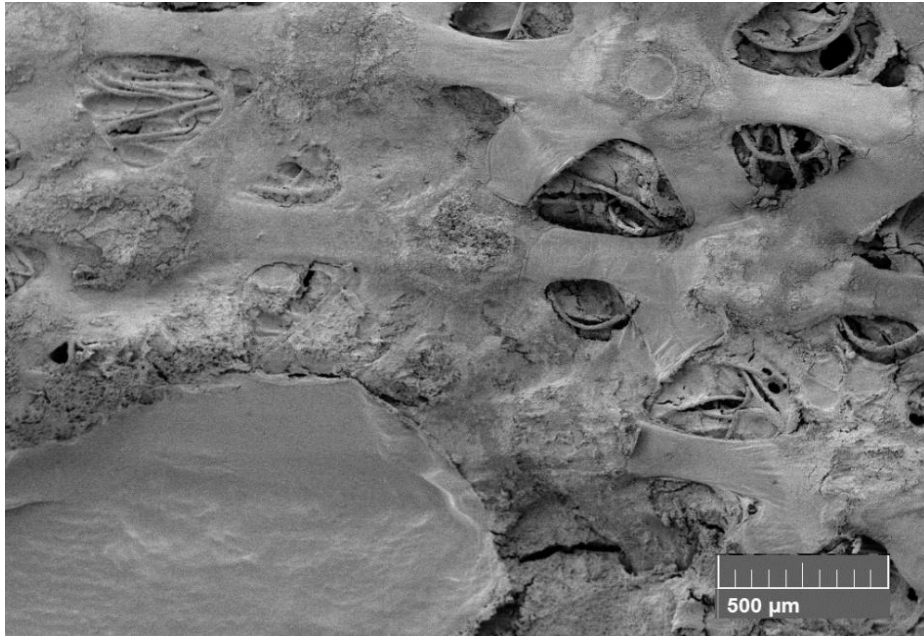


**Figure 3.90: NC-SD surface by SEM**

The surface and lower fibre layers of the dressing were coated with bacteria (x100)

The tissue had patches of bacteria on the surface (Figure 3.91).

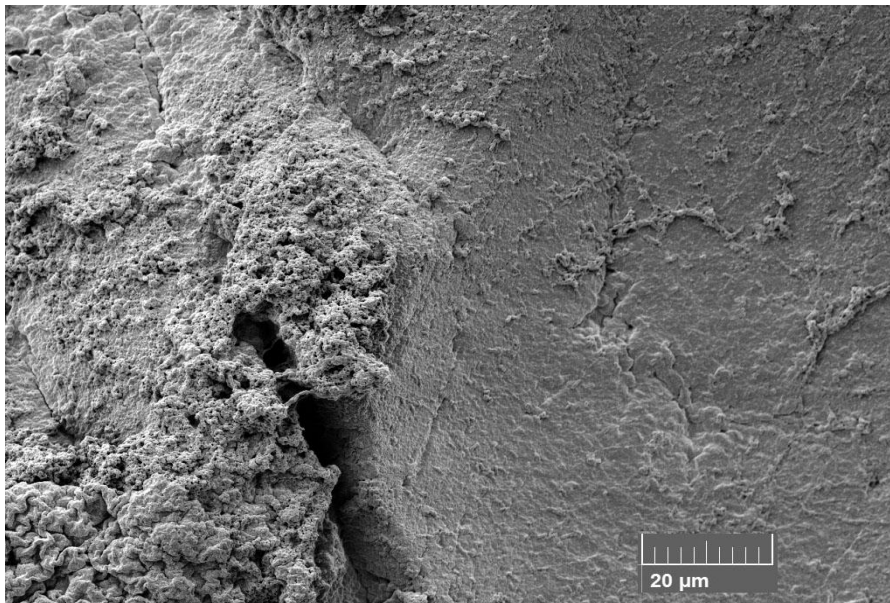


**Figure 3.91: SEM of NC-SD tissue surface at 48 hours**

The surface of the tissue had patches of bacteria upon it (left)(x2000)

There was no statistical significance ( $p=0.63$ ) between the means at 24 and 48 hours. CLSM demonstrated a few groups of live bacteria present in the tissue with very little evidence of dead bacteria (Figure 3.92). Similar results were shown with the dressing.

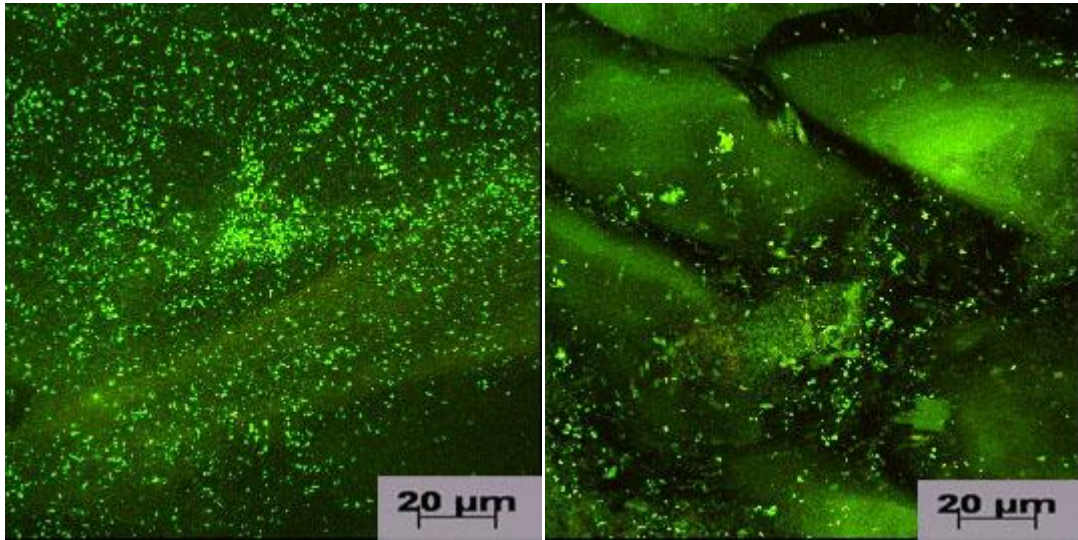


**Figure 3.92: CLSM demonstrated NC-SD and tissue at 48 hours**

A few groups of possible biofilm was seen with more live bacteria than dead within them

PHMBD showed bacteria apparent in LM as thin, continuous lines (Figure 3.93) but no clusters of bacteria were evident.



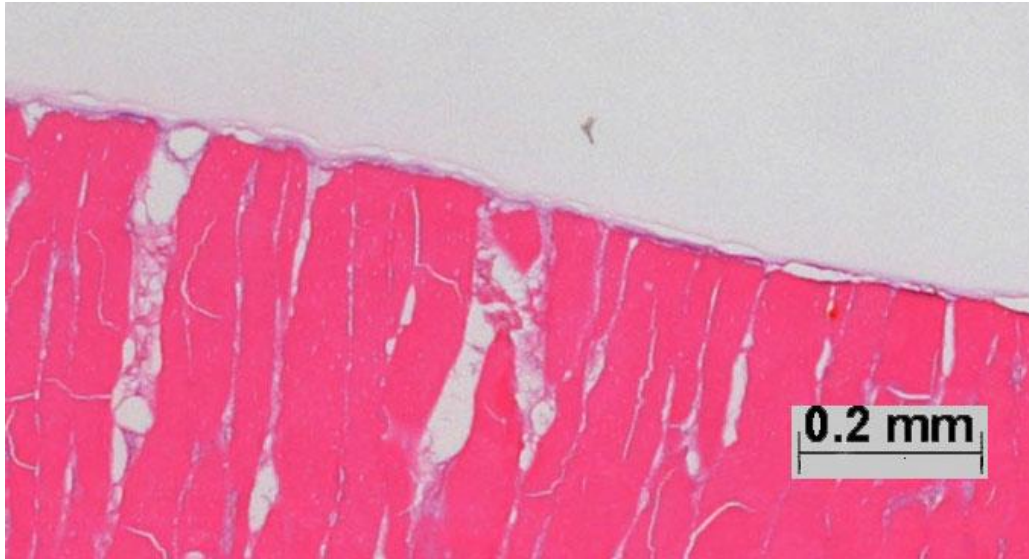


**Figure 3.93: PHMBD at 48 hours by LM**

Occasional thin lines of bacteria were apparent on the surface in LM (x4)

This was confirmed with SEM which showed a thin layer of planktonic bacteria on the surface of the tissue and the dressing respectively (Figure 3.94; Figure 3.95).

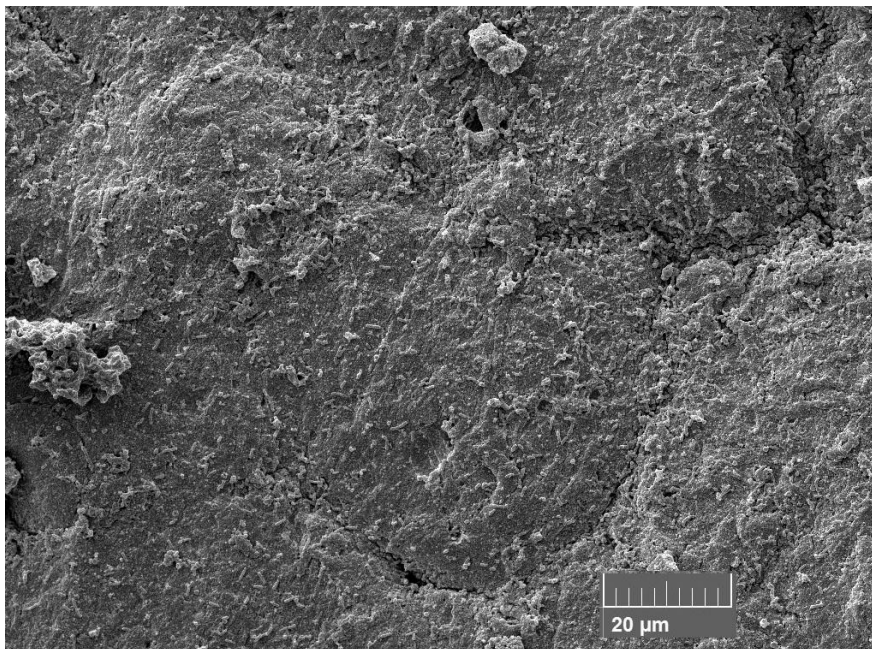


**Figure 3.94: SEM of 48 hour PHMBD tissue surface**

Single bacteria were present on the surface of the tissue (x2000)

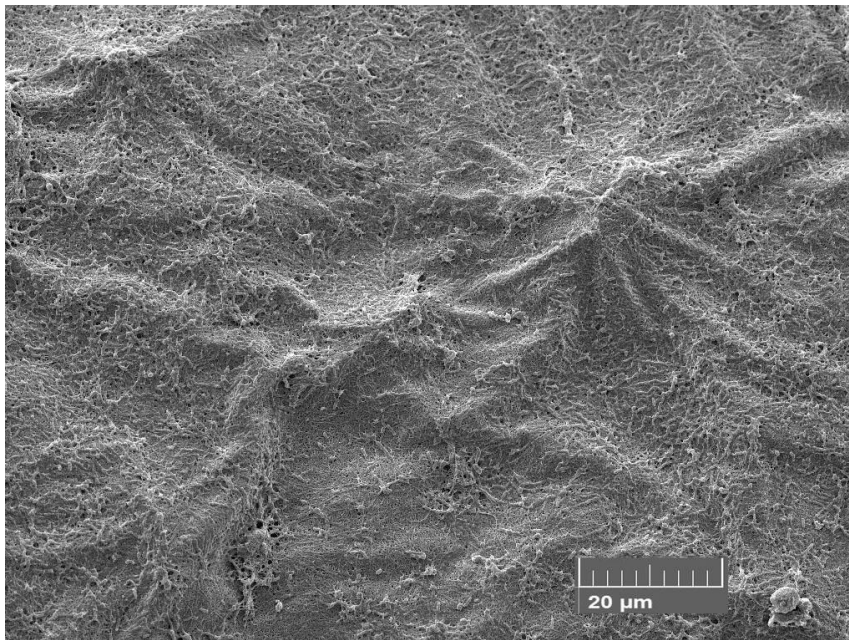


**Figure 3.95: SEM of 48 hour PHMBD surface**

Thin layers of single bacteria were present on the surface of the dressing (x2000)

This was a similar appearance in the TEM sample (Figure 3.96) such that there was no significant difference in the 24 and 48 hour samples ( $p= 0.079$ ).

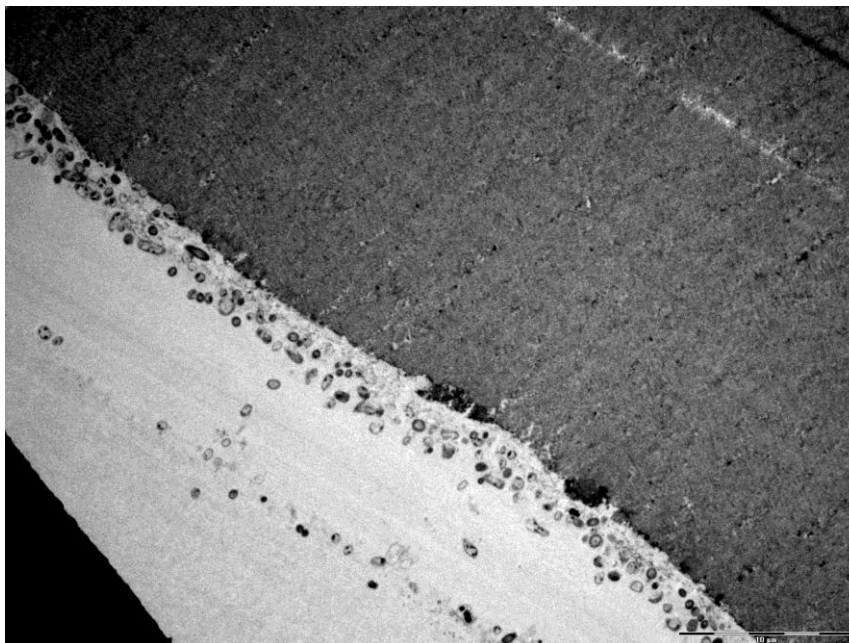


**Figure 3.96 TEM of 48 hour PHMBD model surface**

A thin layer of bacteria was found on the surface of the tissue (x2500)



CLSM showed what appeared to be some planktonic cells in the tissue and the dressing, and groups of cells which appeared to be dying (Figure 3.97; Figure 3.98).

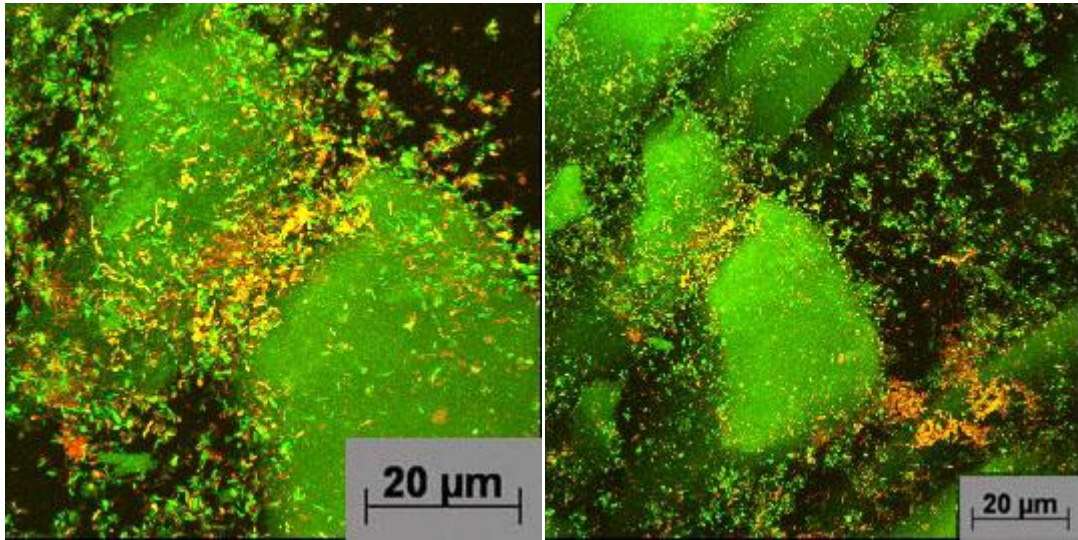


**Figure 3.97: Tissue surface under 48 hour PHMBD with CLSM**

Planktonic cells were present on the tissue with groups of cells which appear to be dying (yellow and red)

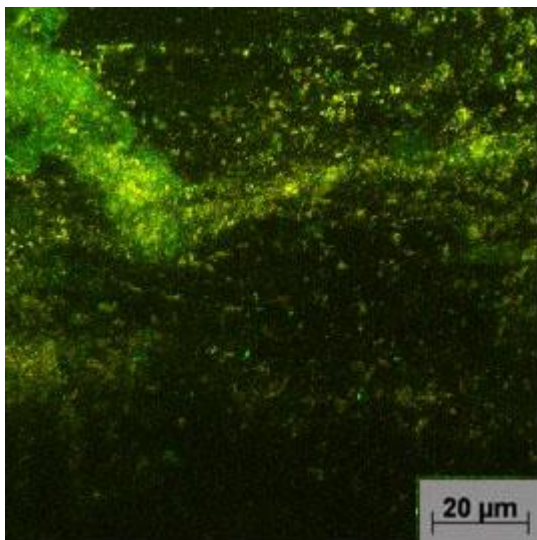


**Figure 3.98: 48 hour PHMBD surface with CLSM**

Bacteria attached to the dressing which appeared to be dying (yellow and red)

The CID model at 48 hours demonstrated an increase in the bacteria and biofilm growth in the apparent absence of iodine. Beads were present surrounded by bacteria and EPS in LM, and SEM images respectively (Figure 3.99; Figure 3.100).

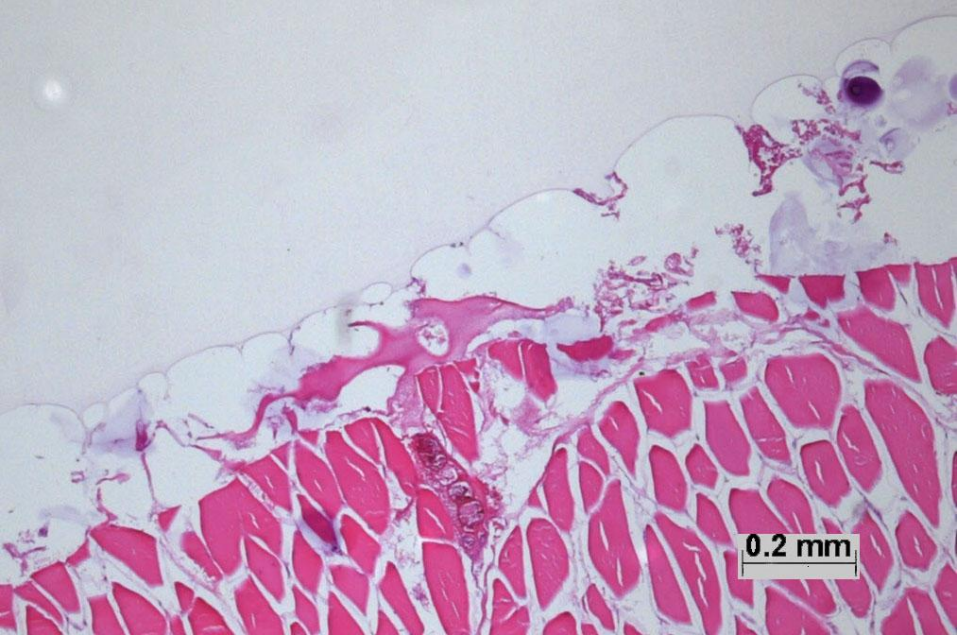


**Figure 3.99: The CID sample at 48 hours by LM**  
Bacteria and biofilm growth were apparent. Beads were present surrounded by bacteria and EPS (x4)



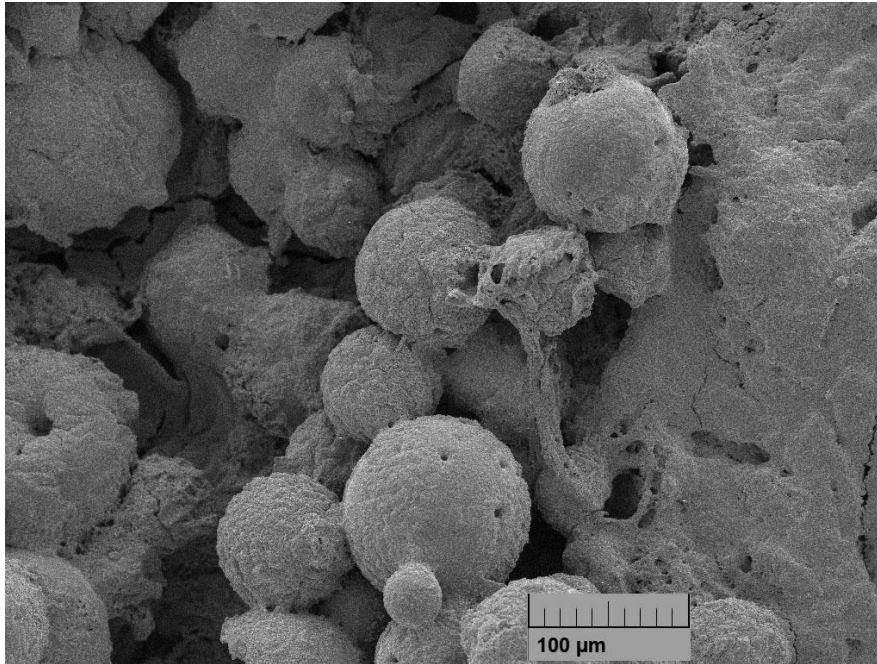


**Figure 3.100: The 48 hour CID sample with beads by SEM**

Beads were surrounded by bacteria in biofilm and the biofilm extended to the tissue layer below(x500)

Beads were present surrounded by bacteria and EPS with TEM and CLSM

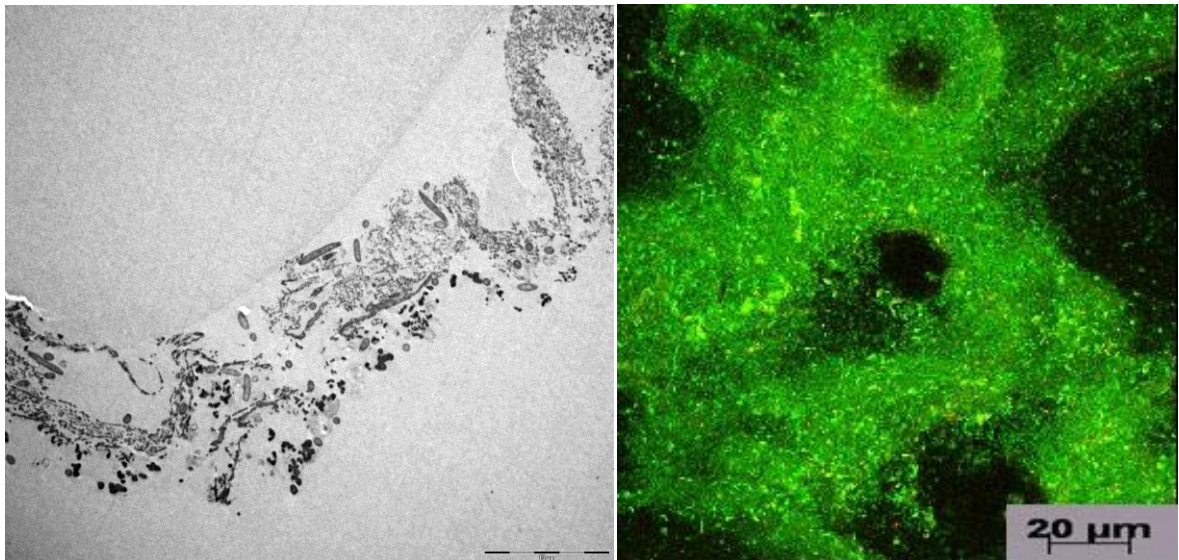


**Figure 3.101: TEM and CLSM of 48 hour CID showing biofilm around the beads**

Beads were covered in a layer of biofilm viewed by TEM (left, x2500) and CLSM (right, x40) showed this biofilm to contain mainly live bacteria

The cadexomer beads were clearly visible within a thick layer of biofilm, with live bacteria within it. Minimal dead bacteria were present (Figure 3.101). No significant difference ( $p=0.256$ ) was shown in the 24 and 48 hour samples.

### 3.7.3 72 hour dressing treated models

Gauze control models had a variable thickness of biofilm on the surface, sometimes appearing in peaks by LM. In some areas biofilm appeared to have been removed. Where the gauze dressing had remained stuck to the specimen, biofilm was found to be growing within it (Figure 3.102).

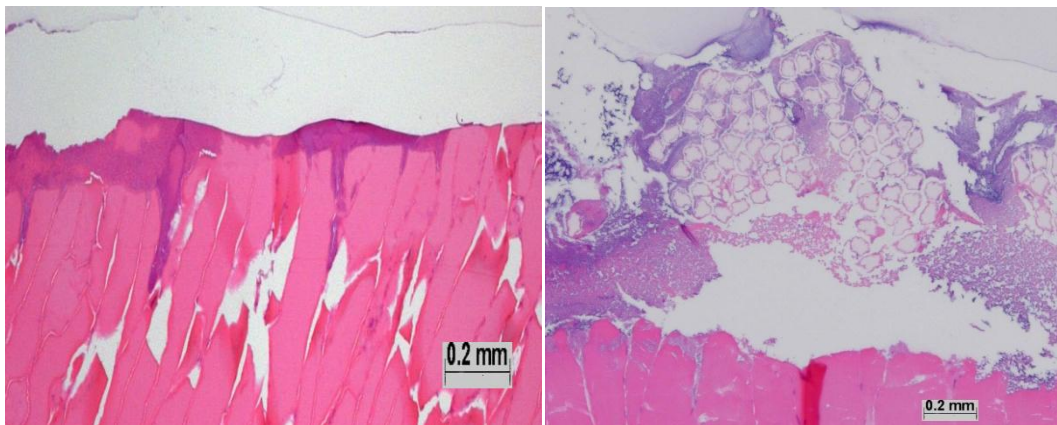


**Figure 3.102: 72 hour gauze control models**

There was a variable thickness of biofilm on the surface. In some areas biofilm appeared to have been removed (left, x2). Gauze was occasionally stuck to the specimen with biofilm growing within it (right, x4)

SEM revealed a layer of thick biofilm on the tissue surface, and a gauze dressing covered in biofilm (Figure 3.103).

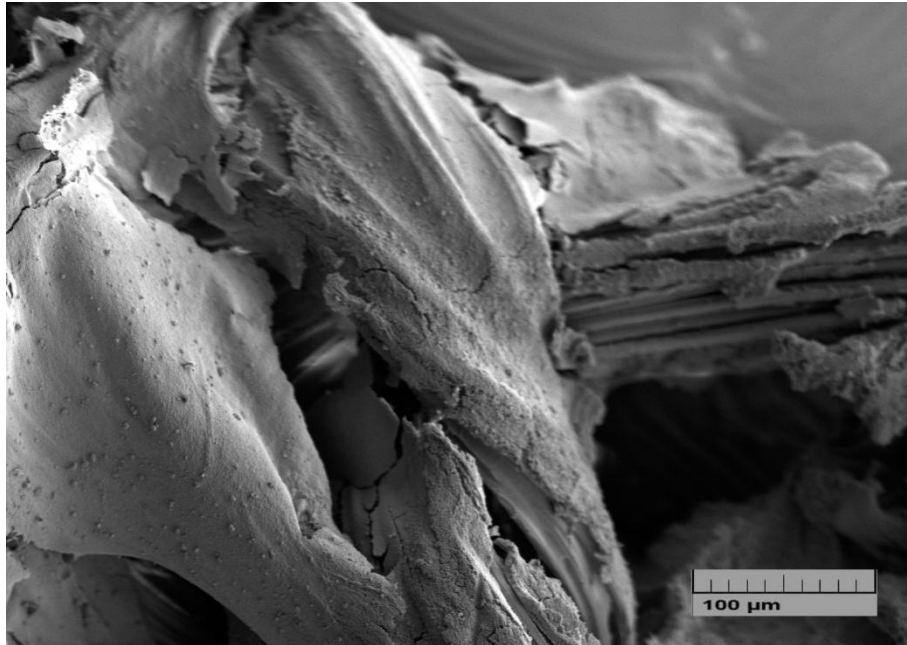


**Figure 3.103: SEM of 72 hour gauze model surface and dressing**

A thick layer of biofilm covered the tissue surface and was covering the whole dressing (right, x100)

Statistical analysis at 48 and 72 hours found there to be no significant difference ( $p=0.552$ ), but comparisons at 24 and 72 hour were significantly different ( $p=0.011$ ). Using a one-way ANOVA test, a Tukey Pairwise comparison also showed similar results. The amount of bacterial growth on the surface of the model dressed with gauze was found to gradually decrease between 24 and 72 hours (Figure 3.104). The difference between the area of biofilm at 24 and 72 hours was statistically significant ( $p=0.022$ ), but not between 24 and 48 hours, or between 48 and 72 hours.

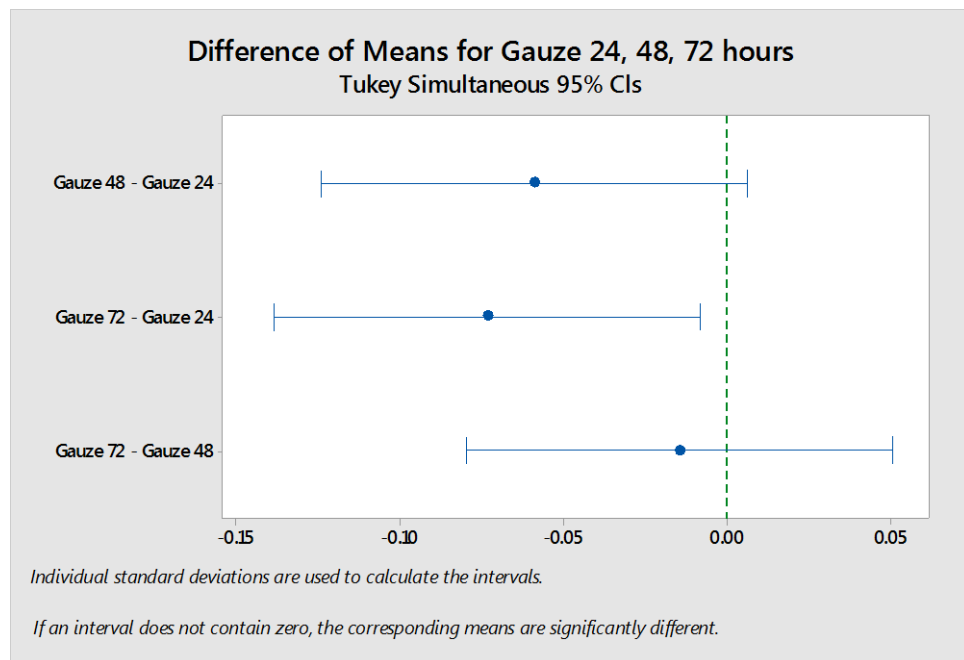
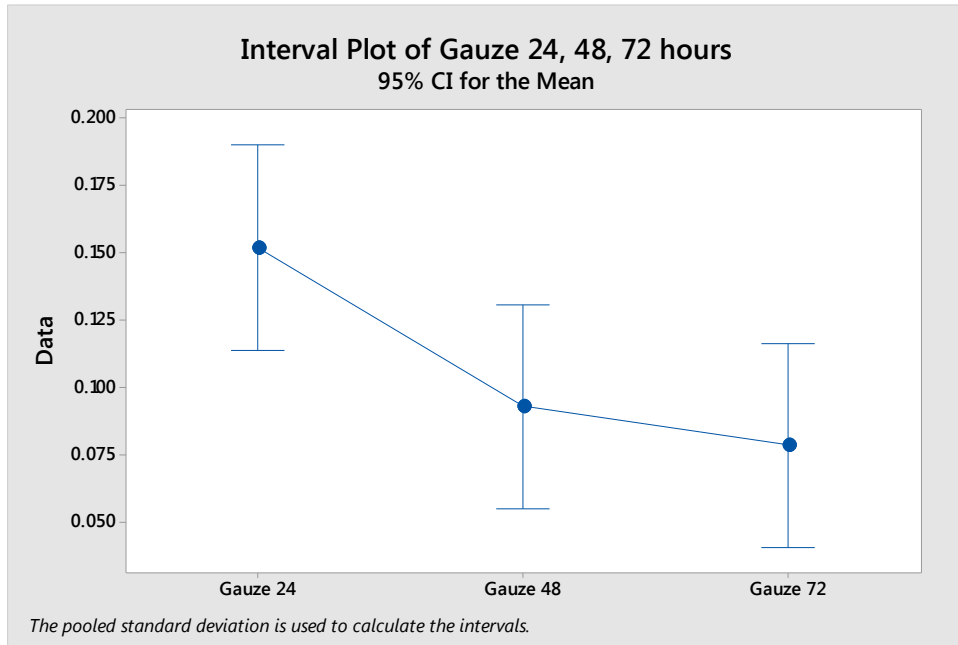


**Figure 3.104: Interval plot and Tukey plot of 24 - 72 hour Gauze models**

An interval plot demonstrated how the biofilm growth decreased over time, possibly due to debridement of the gauze. Although the 24 and 72 hours pooled standard deviations overlap slightly in this figure they were statistically different ( $p=0.022$ ) A Tukey plot showed that with the gauze biofilm growth only the 24 and 72 hour differences was statistically significant



Bacterial growth on models of NSHD controls had increased, with areas of continuous staining of biofilm on the surface by LM (Figure 3.105), which were visible with SEM (Figure 3.106).

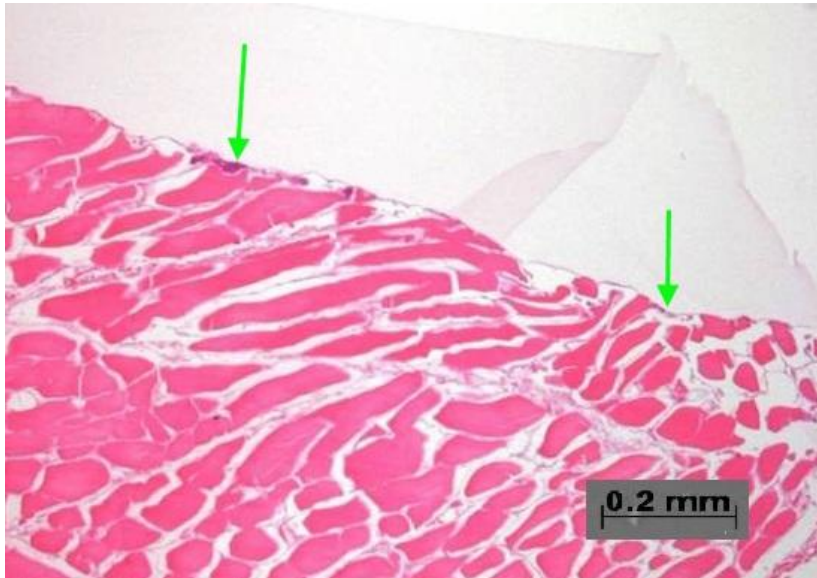


**Figure 3.105: Increased growth on models of 72 hour NSHD controls**  
Occasional clusters of bacteria were beginning to form (arrows) (x4)

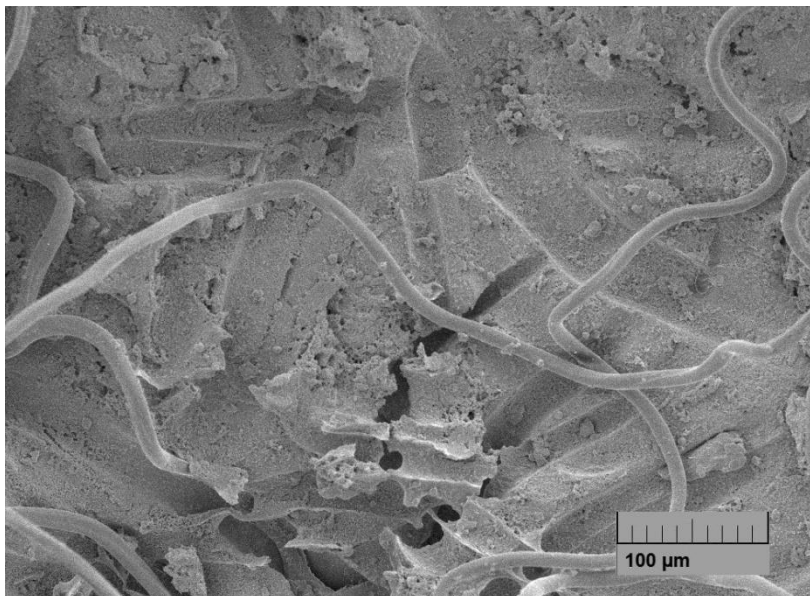


**Figure 3.106: SEM of 72 hour NSHD tissue surface by SEM**  
SEM showed increased bacterial growth on the surface of samples with small clusters of biofilm appearing (x500)

The 72 hour growth was significantly less than the 48 hour growth by Tukey pairwise comparison ( $p=0.005$ ) and with the t-test ( $p=0.052$ ). The 24 and 72 hour comparison were found not to be of significant difference ( $p=0.230$ ), and the mean grouping showed the 24 and 72 hours to be similar (Figure 3.107).

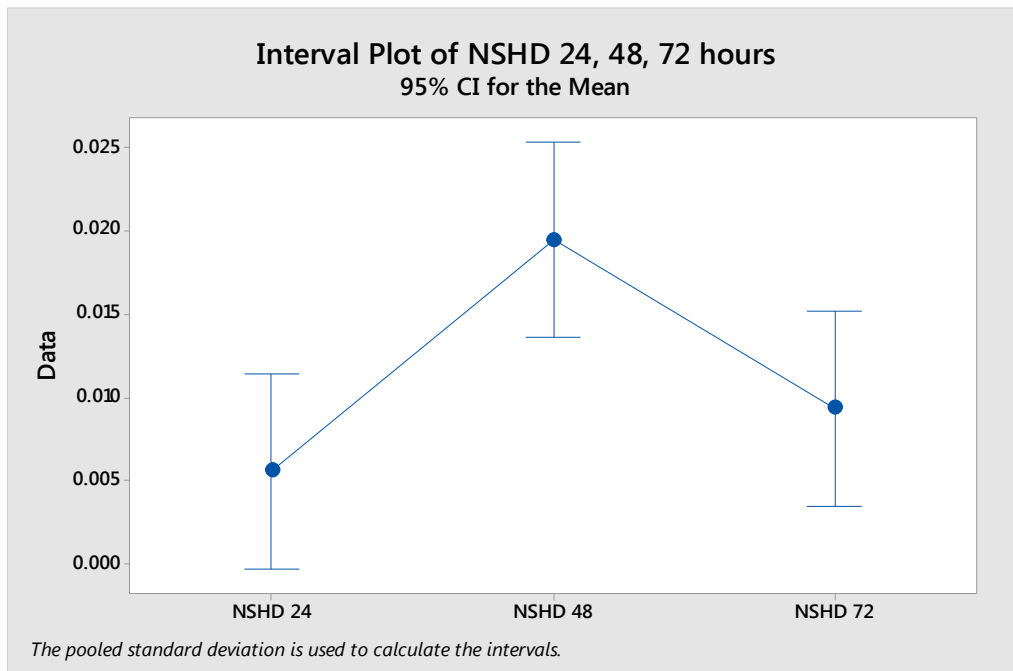


**Figure 3.107a: Interval plot of 24 - 72 hour NSHD models**

Although not containing an antimicrobial, growth was shown to decrease at 72 hours. This was likely due to the dressing sequestering the bacteria

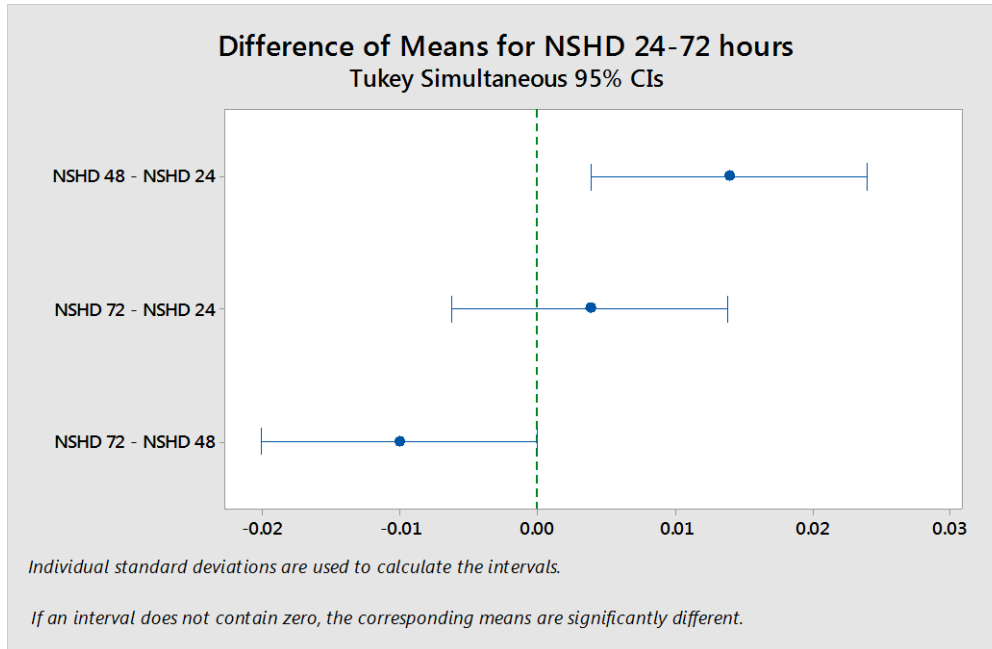


**Figure 3.107b: Tukey plot of 24 - 72 hour NSHD models**

72 hour growth was significantly less than the 48 hour growth by Tukey pairwise comparison ( $p=0.005$ ), but the 24 and 72 hours were similar ( $p=0.230$ )

The SCHD showed a similar picture with LM to the 48 hour model with occasional clusters of bacteria and a few fibres on the surface of the tissue (Figure 3.108).

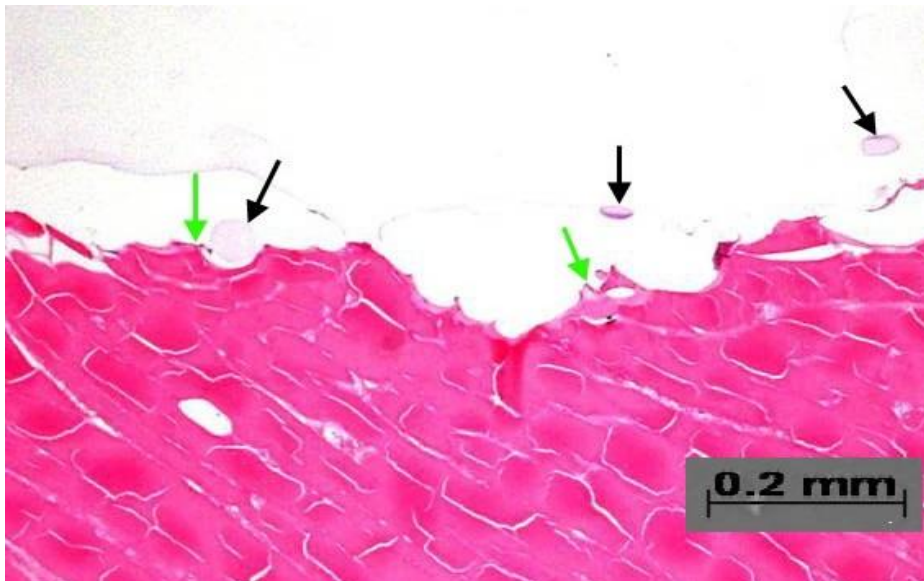


**Figure 3.108: SCHD at 72 hours by LM with fibres and beginnings of growth**

Occasional clusters of bacteria were present (green arrows) and a few fibres (black arrows) on the surface of the tissue (x4)

A few fibres on the model surface visualised by SEM, gave a similar picture to the LM, with attached bacteria amongst them (Figure 3.109).

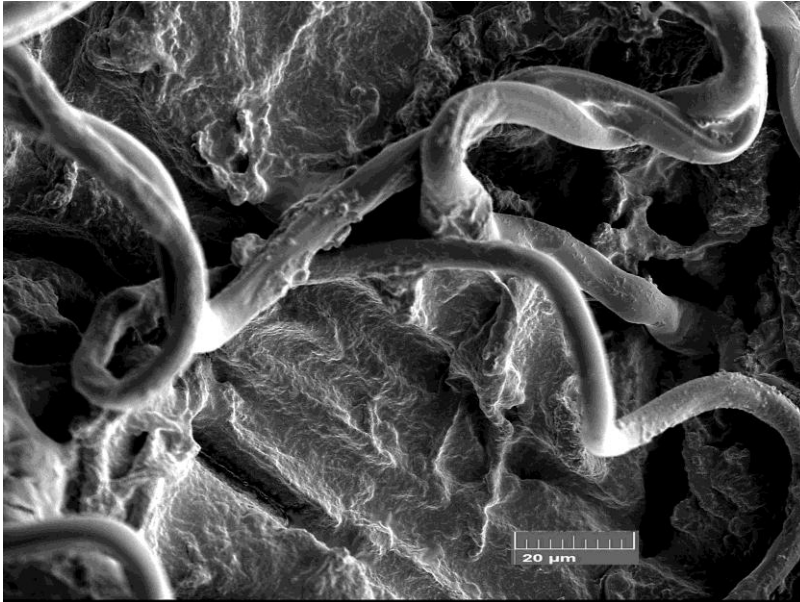


**Figure 3.109: The SCHD tissue surface at 72 hours by SEM**

A few fibres on the model surface were visualised by SEM, with sequestered bacteria amongst them (x3000)

The analysis showed the 72 hours not to be significantly different from the results of the 48 hour ( $p=0.160$ ) or the 24 hour ( $p=0.544$ ) models (Figure 3.110).

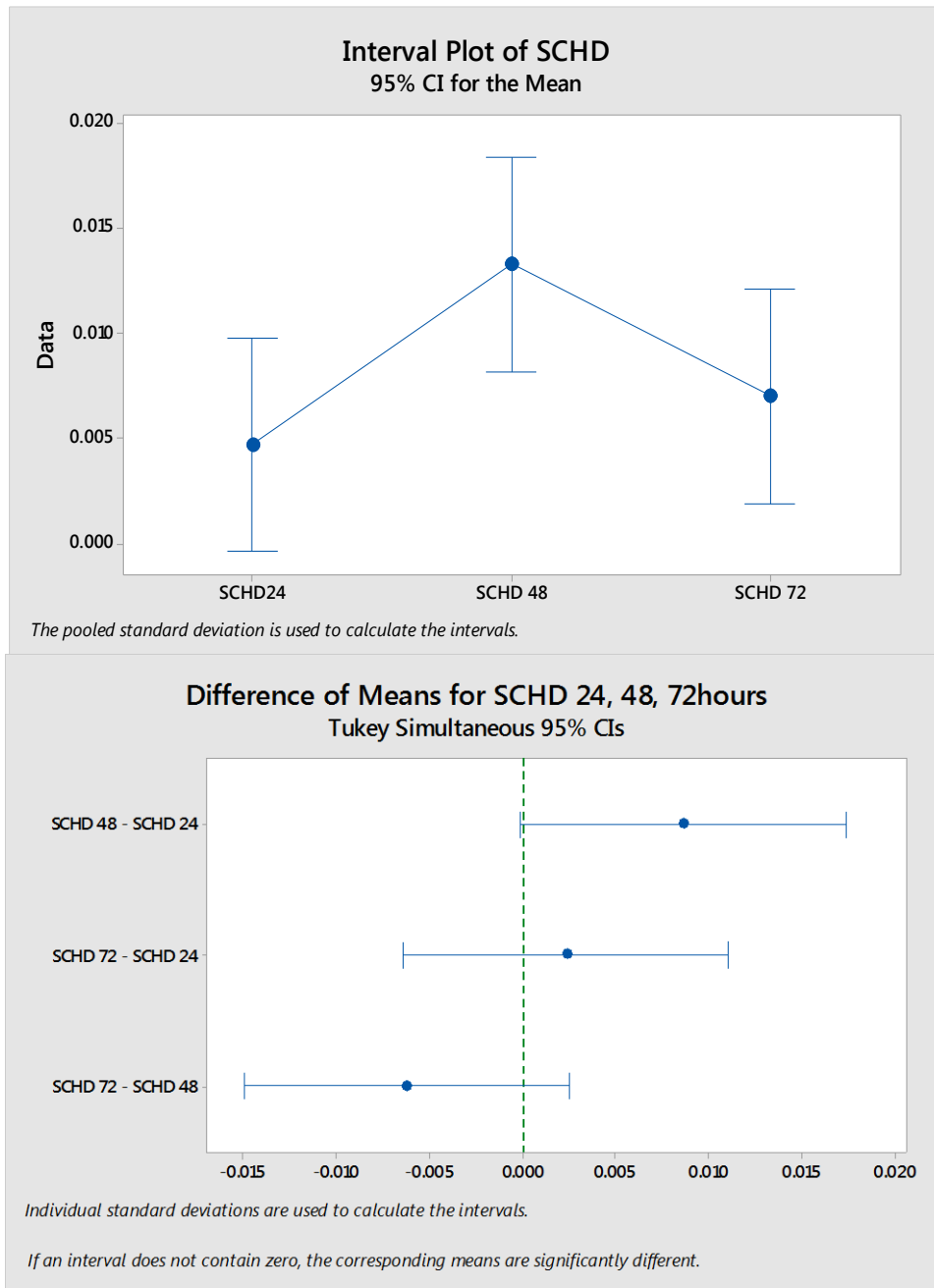


**Figure 3.110: Interval plot and Tukey plot of 24- 72 hour growth of SCHD models**

No significant difference was found between the 24, 48 or 72 hour models

The interval plot of the SCHD showed a similar pattern to the NSHD with reduced amounts of biofilm by 72 hours



The NGAD model showed almost clean surfaces on LM and SEM (Figure 3.111; Figure 3.112).

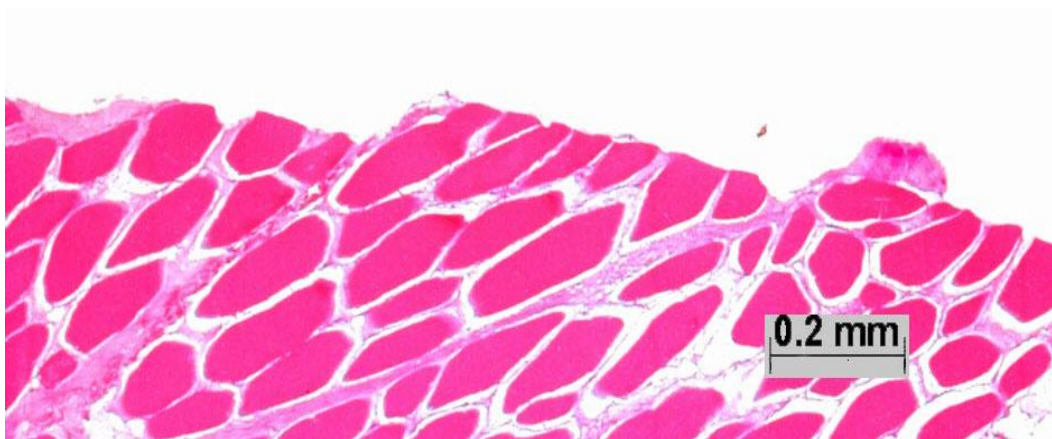


**Figure 3.111: The NGAD 72 hour model by LM**  
The model showed surfaces clear of bacteria (X4)

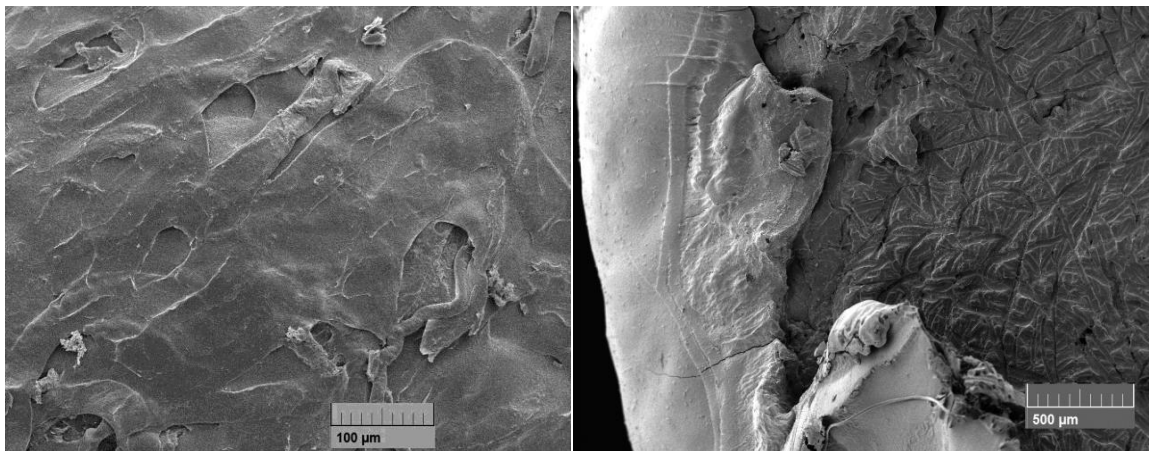


**Figure 3.112: 72 hour SEM of central area of NGAD model after dressing removal**  
SEM and showing the debriding and antimicrobial effect. NGAD models showed almost clean surfaces (left, x500) where the dressing was removed. At the edge where there was no dressing coverage the biofilm growth could be seen (right, x100)

The analysis showed the 72 hours not to be significantly different from the results of the 48 hour ( $p=0.061$ ) or the 24 hour ( $p=0.456$ ) models (Figure 3.113).

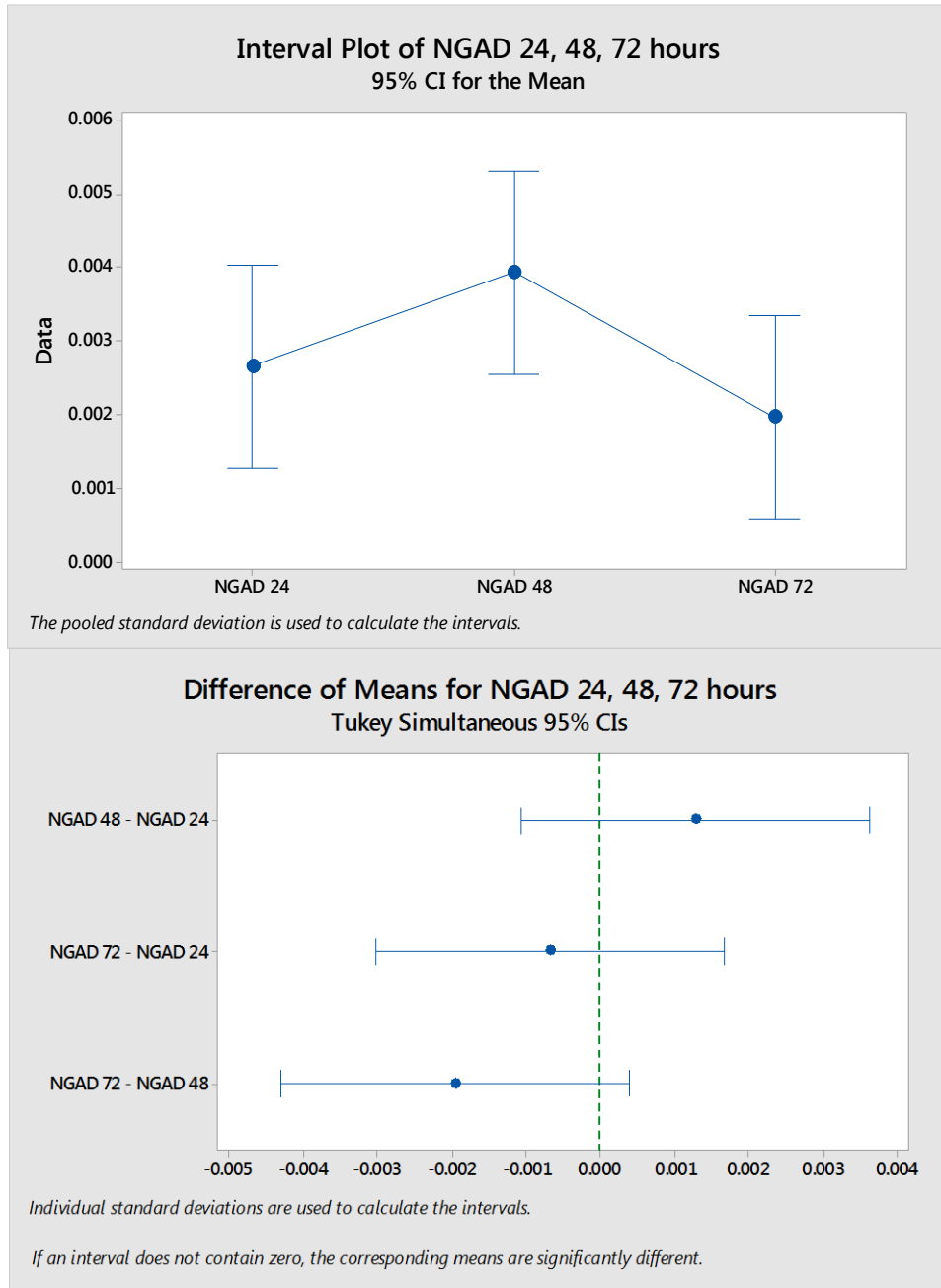


**Figure 3.113: Interval plot and Tukey plot of 24- 72 hour growth of NGAD models**  
As with the SCHD the NGAD had no significant difference between the 24, 48 and 72 hour biofilm growth. An interval plot showed what little growth there was on the model was reduced by 72 hours



The 72 hour CES-SD samples had groups of bacteria present in the lower layers of tissue on each model with LM, combined with a black staining of silver from the dressing. On the surface, small clusters of bacteria and fibres were observed by LM (Figure 3.114) and SEM (Figure 3.115).

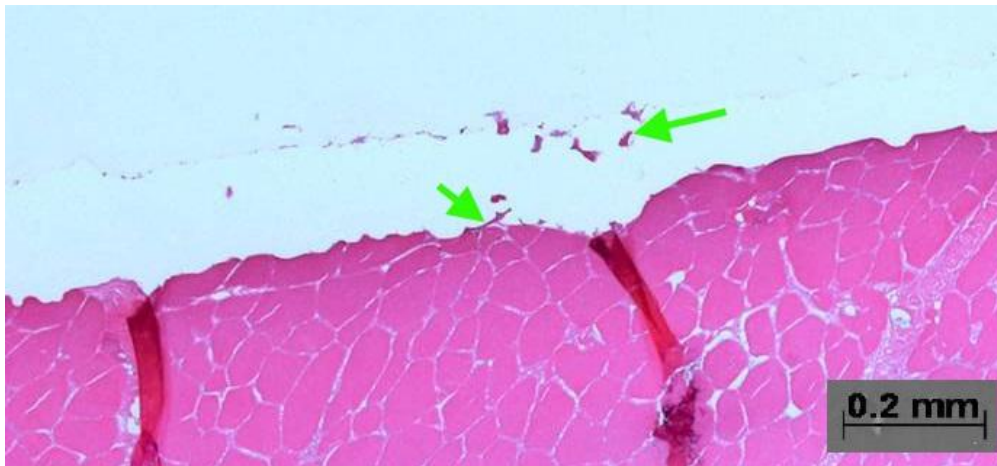


**Figure 3.114: 72 hour CES-SD model by LM (x4)**

On the surface, small clusters of bacteria and fibres were observed by LM (green arrows)

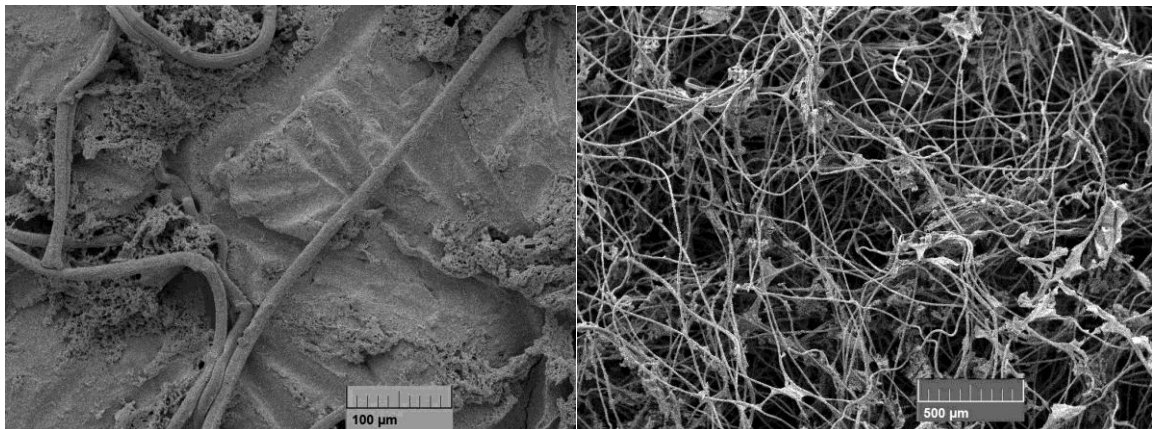


**Figure 3.115: 72 hour CES-SD surface and dressing by SEM**

On the surface, small clusters of bacteria and fibres were observed by SEM (left, x500)

A few groups of biofilm were present in the dressing with a little fibre swelling (right, x100)

The dressing contained a few mats of biofilm and some probable swelling of the fibres. Two sample t-tests concluded that the 72hour growth was significantly different from both the 24 ( $p=0.007$ ) and 48 hour ( $p=0.011$ ) growths with a gradual decrease in the amount of biofilm area remaining on the surface. As with gauze, CES-SD had 24 and 48 hour showing similar grouping, with Tukey pairwise comparison, as did the 48 and 72 hour models (not significantly different), but the 24 and 72 hour growth were found to be significantly different ( $p=0.003$ ). (Figure 3.116)

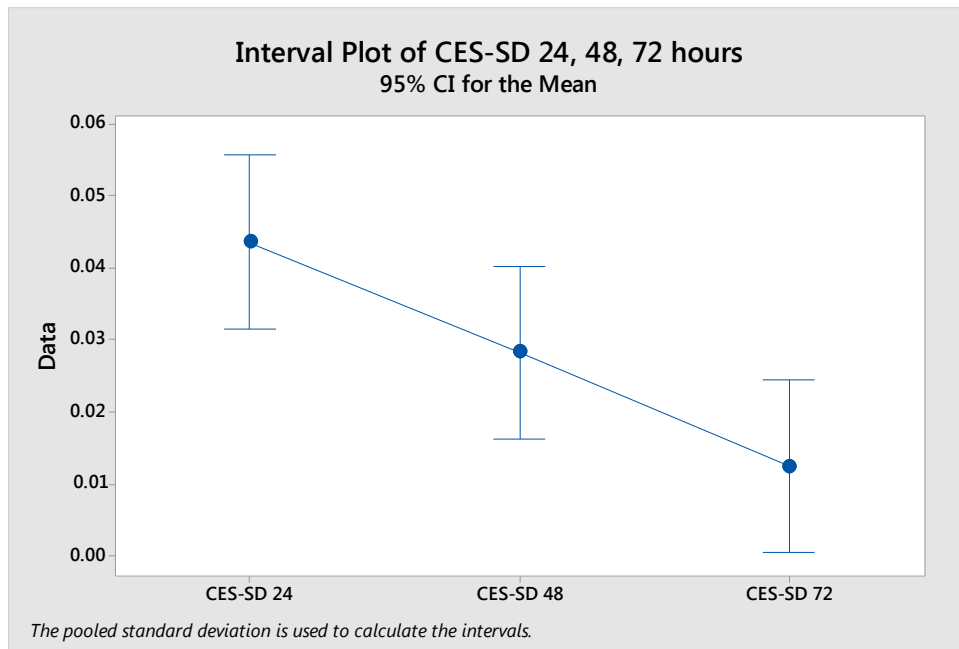


**Figure 3.116a: Interval plot of 24- 72 hour growth of CES-SD models**

The CES-SD 24 and 72 hour growth were significantly different, with a gradual decrease in the presence of biofilm.

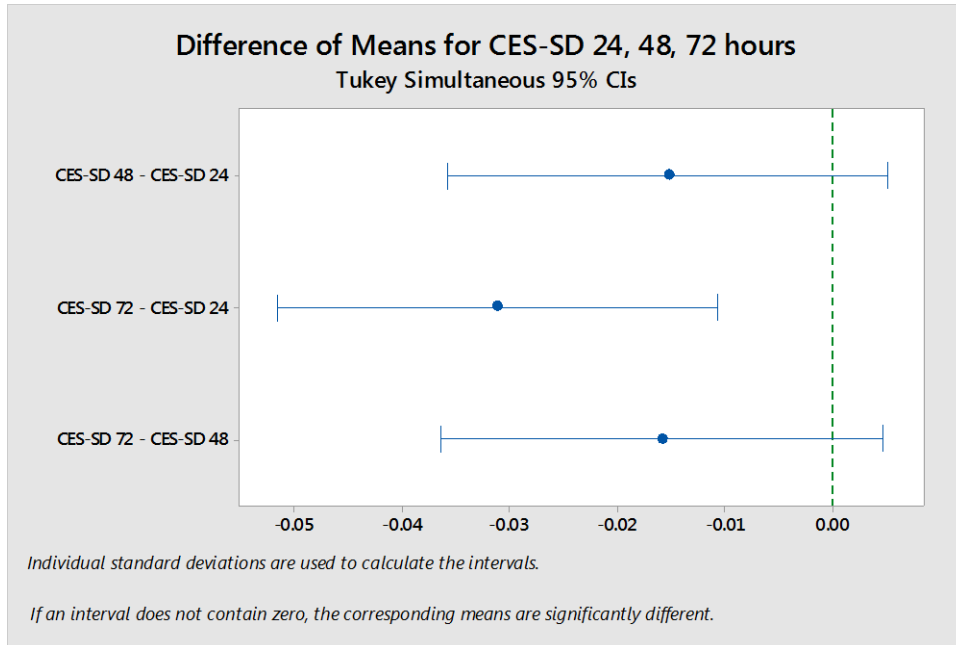


**Figure 3.116b: Tukey plot of 24- 72 hour growth of CES-SD models**

Growth gradually decreased so that the 24 and 72 hour growths were significantly different ( $p=0.003$ )

A few thin lines of bacteria were present on the surface of the ACN-SD model (Figure 3.117), and a few dressing fibres were found in some sections

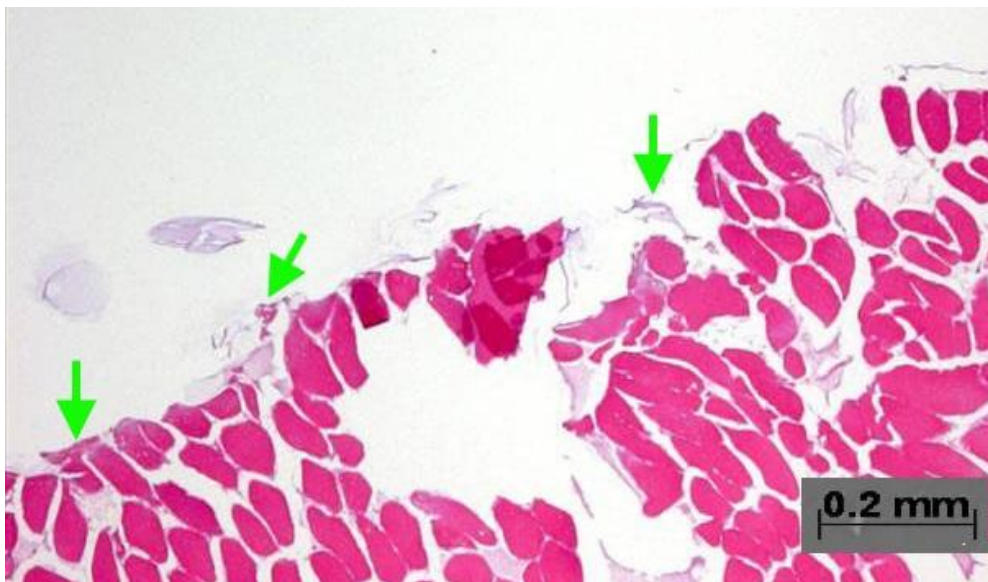


**Figure 3.117: 72 hour ACN-SD model by LM**

A few thin lines of bacteria were present on the tissue surface (arrows) (x4)

. A clear imprint of the dressing on the surface of the model was observed with SEM, the bacterial growth being present in the imprint of the holes of the dressing (Figure 3.118).

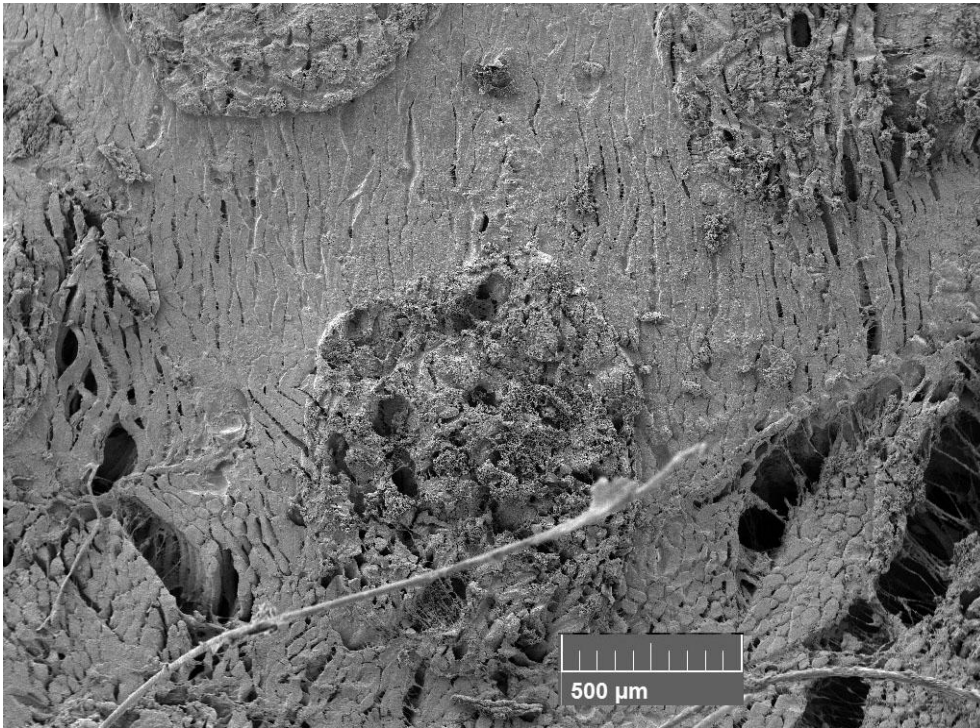


**Figure 3.118: 72 hour ACN-SD tissue surface by SEM**

An imprint of the dressing on the surface was observed with SEM, bacterial growth being present in the imprint of the holes as circular areas (x100)

Statistical analysis of this silver dressing found the means of biofilm areas of 24, 48 and 72 hours not to be significantly different (48 and 72 hour  $p=0.833$ ; 24 and 72 hour  $p=0.173$ ) (Figure 3.119).

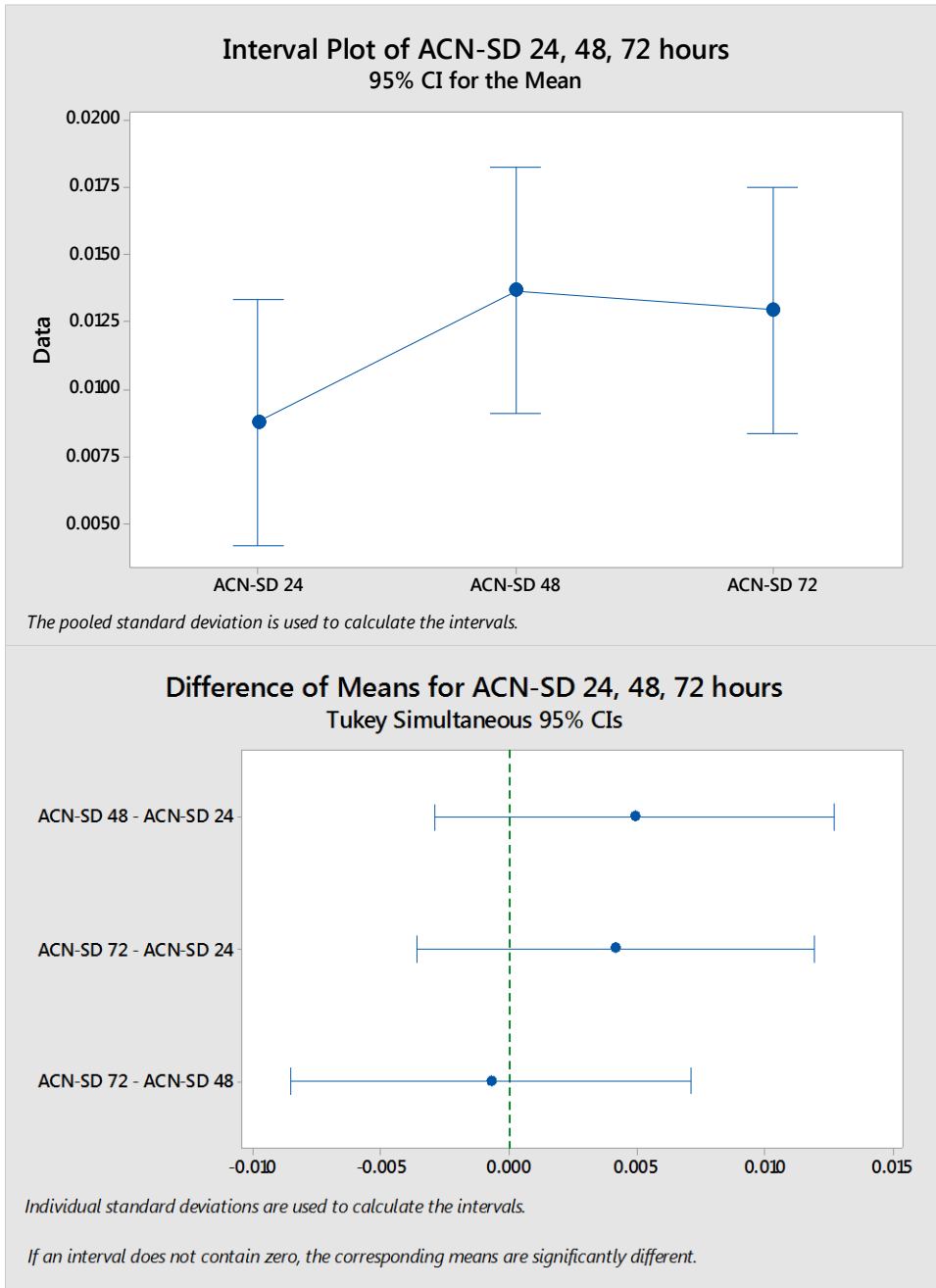


**Figure 3.119: Interval plot and Tukey plot of 24- 72 hour growth of ACN-SD models**  
Although an interval plot demonstrated that there was a slight increase in growth from 24 - 48 hours which remained almost unchanged, the 24, 48 and 72 hour growths were shown not to be significantly different by Tukey plot



72 hour growth areas under NC-SD showed bacteria present in a few places on the surface in thin layers and silver staining deep into the tissue layers below (Figure 3.120).

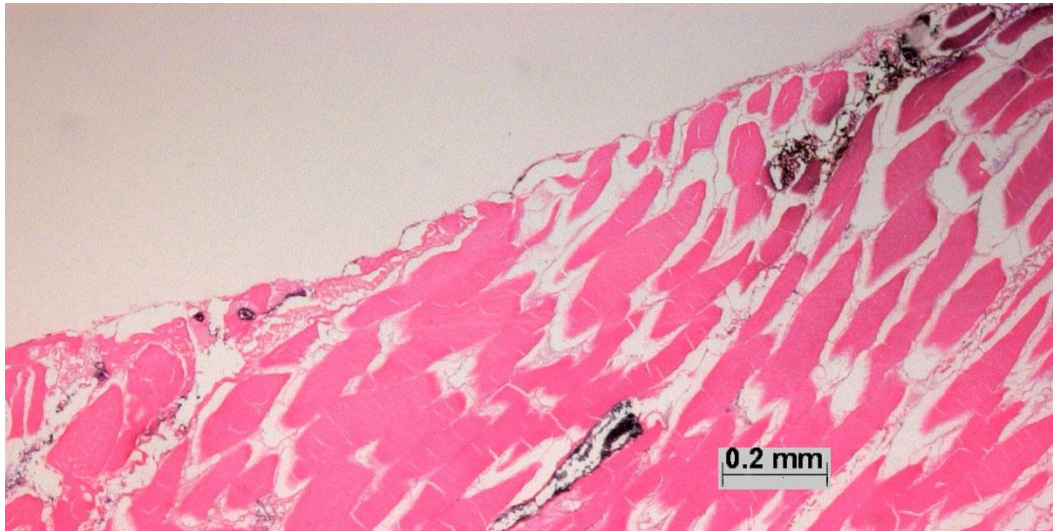


**Figure 3.120: 72 hour growth and silver deposition under NC-SD by LM**

Bacteria were present on the surface in thin layers on the surface and black silver staining was observed near the surface and deeper into the tissue (x4)

SEM showed the surface of the dressing to be covered, and some of the holes to be blocked, by biofilm. The tissue was observed to have the pattern of the dressing imprinted on the surface and, where the uppermost surface of the dressings were not in contact with the tissue, there were pockets of bacterial on the surface (Figure 3.121).

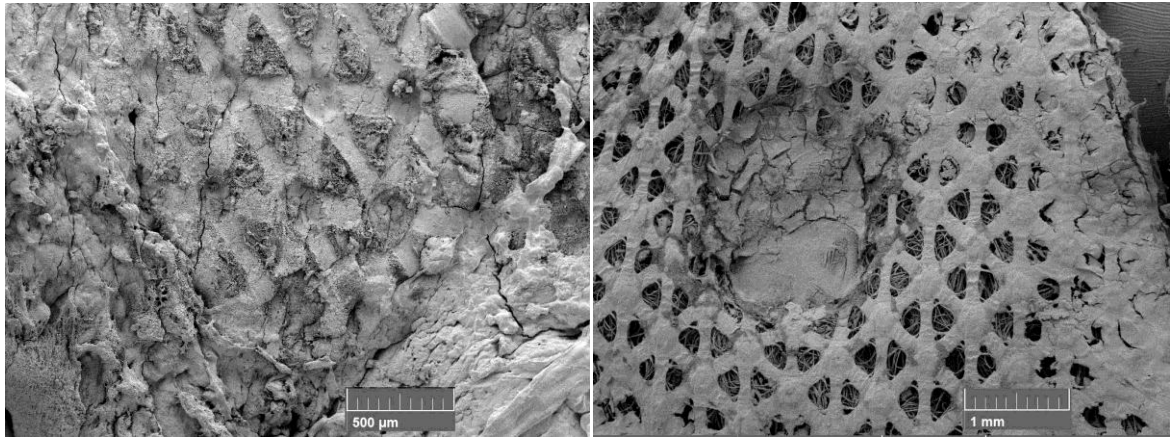


**Figure 3.121: 72 hour growth under NC-SD and on the NC-SD by SEM**

The tissue was observed to have the pattern of the dressing on its surface which, when not in contact with the tissue, showed pockets of bacterial biofilm (left, x100) as can be seen in these images.. SEM showed the surface of the dressing to be covered and blocked by biofilm (right, x50)

Statistical analysis showed the 24, 48 and 72 hour areas of bacterial growth not to be significantly different (48 and 72 hour  $p=0.390$ ; 24 and 72 hour  $p= 0.201$ ), and this was confirmed by Tukey Pairwise comparisons (Figure 3.122). The NC-SD treated models showed a gradual decrease in biofilm area over the 24 to 72 hour period.



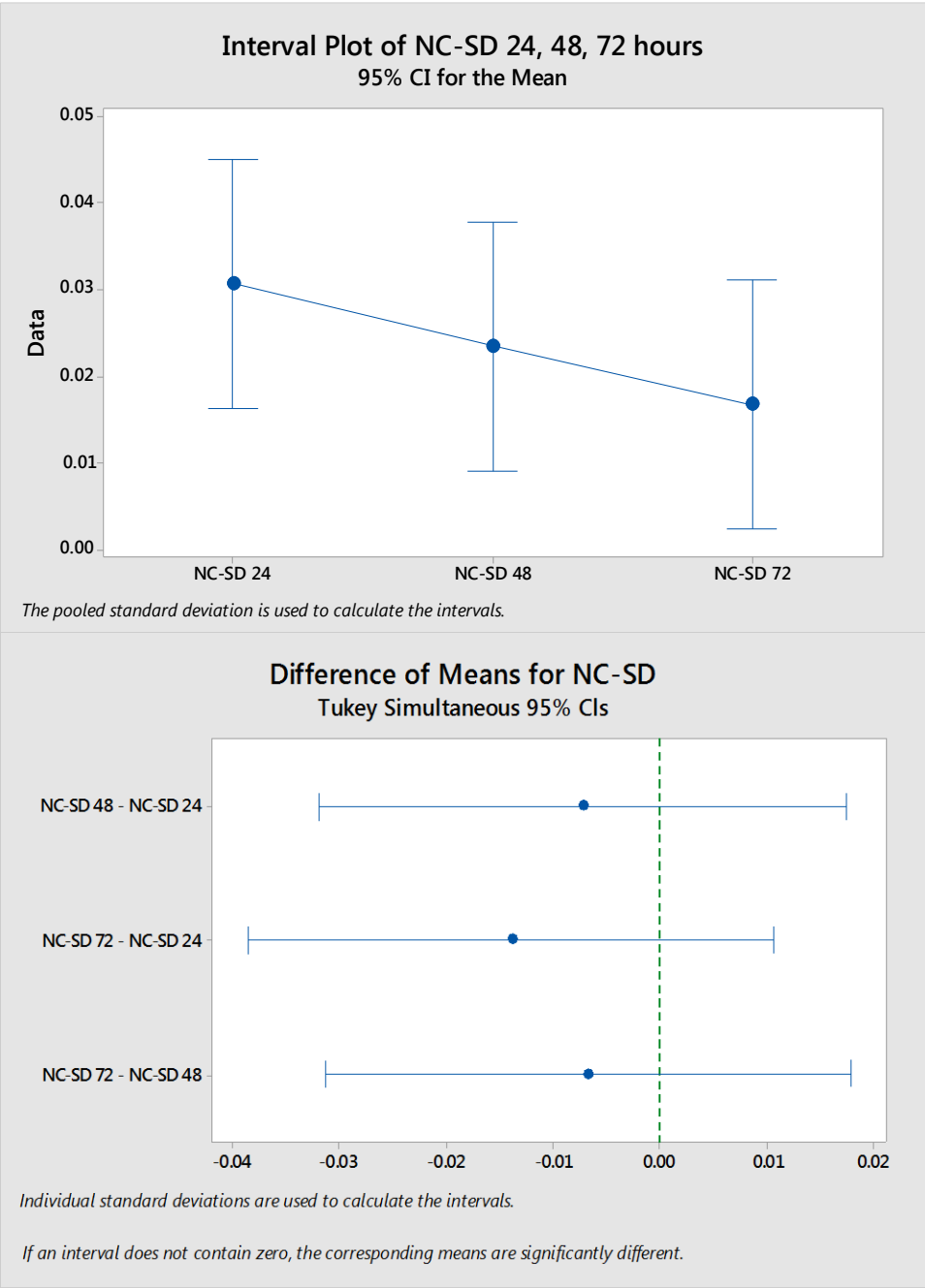


**Figure 3.122: Interval plot and Tukey plot of 24 - 72 hour growth of NC-SD models**  
An intervals plot showed all 24, 48 and 72 hour growth to be similar even though it slightly decreased over time. Tukey pairwise showed the 24, 48 and 72 hour areas of bacterial growth not to be significantly different (48 and 72 hour  $p=0.390$ ; 24 and 72 hour  $p= 0.201$ )

PHMBD at 72 hours had few bacteria apparent in LM with only an occasional thin line of bacteria, but was mainly clean of bacterial growth (Figure 3.123).



**Figure 3.123: PHMBD at 72 hours by LM**

Only an occasional thin line of bacteria appeared on the surface of the tissue (x2)

A similar appearance was observed on the SEM models of tissue, and minimal bacterial growth was present on dressings (Figure 3.124).

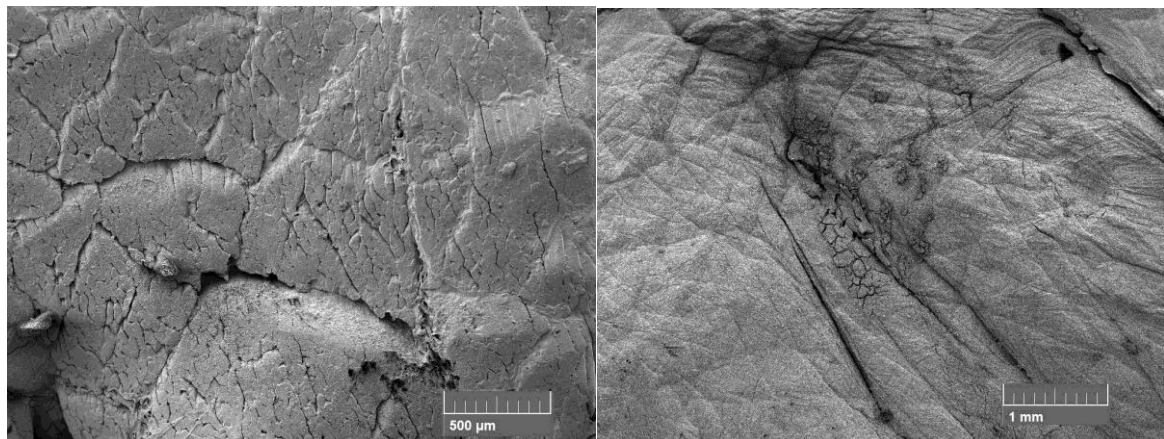


**Figure 3.124: PHMBD tissue surface and dressing surface at 72 hours by SEM**

The tissue (left, x100) and the dressing surface (right, x50) were mainly clear of bacterial growth

All the 24, 48 and 72 hour models were shown to be of no significant difference from each other (48 and 72 hour  $p=0.104$ ; 24 and 72 hour  $p=0.771$ ) (Figure 3.125).

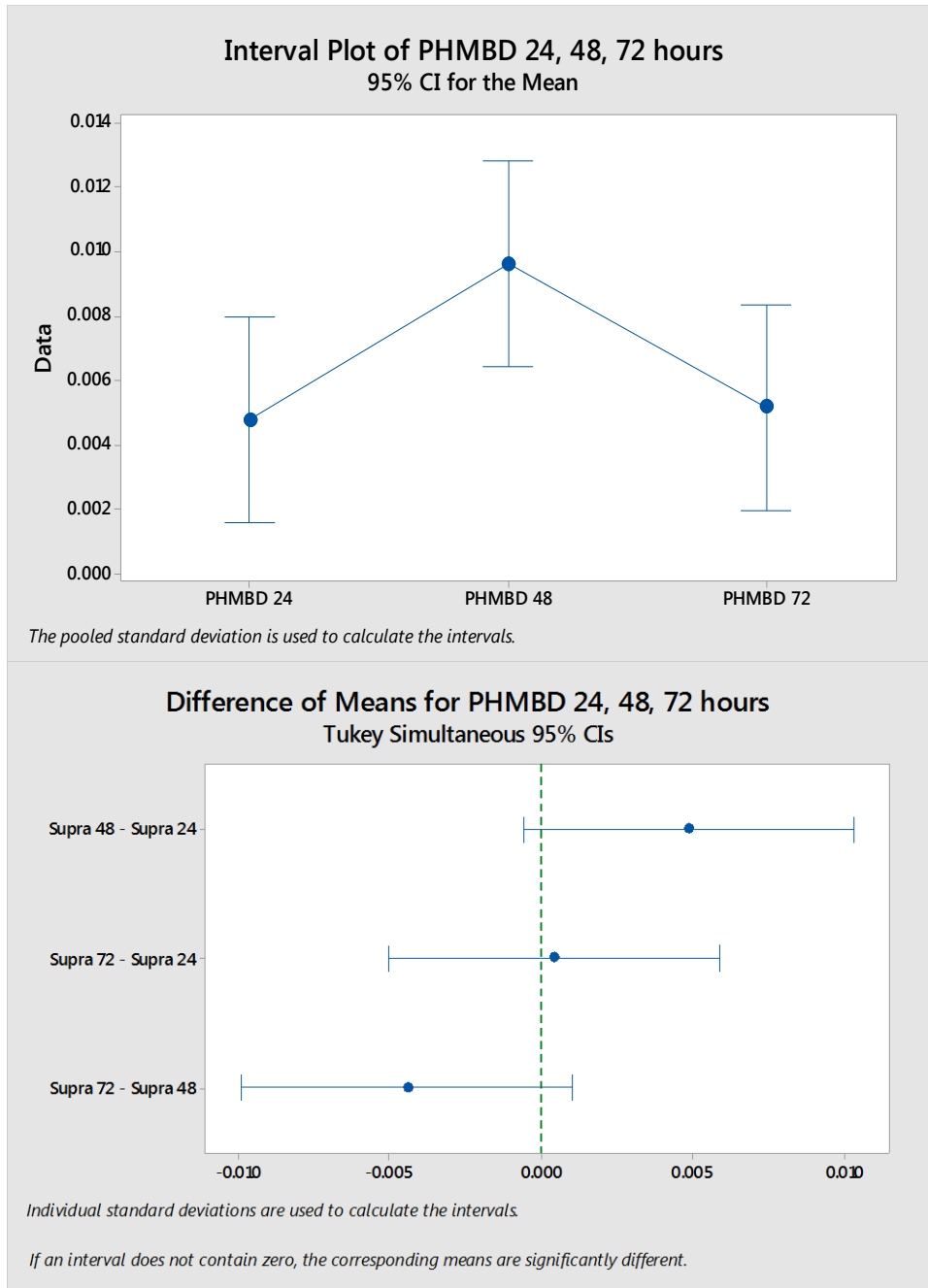


**Figure 3.125: Interval plot and Tukey plot of 24- 72 hour growth on PHMBD models**  
Although there was minimal growth and no significant difference between the hours the interval plot showed a similar pattern to the NSHD, SCHD and NGAD with a slight increase from 24 to 48 hours then a decrease to 72 hours. This and a Tukey plot confirmed there was no significant difference (48 and 72 hour  $p=0.104$ ; 24 and 72 hour  $p=0.771$ )

The CID model at 72 hours demonstrated a continued increase in the amount of bacteria and biofilm growth. Beads were still present and observed as surrounded by bacteria and EPS in LM and SEM imaging (Figure 3.126; Figure 3.127).

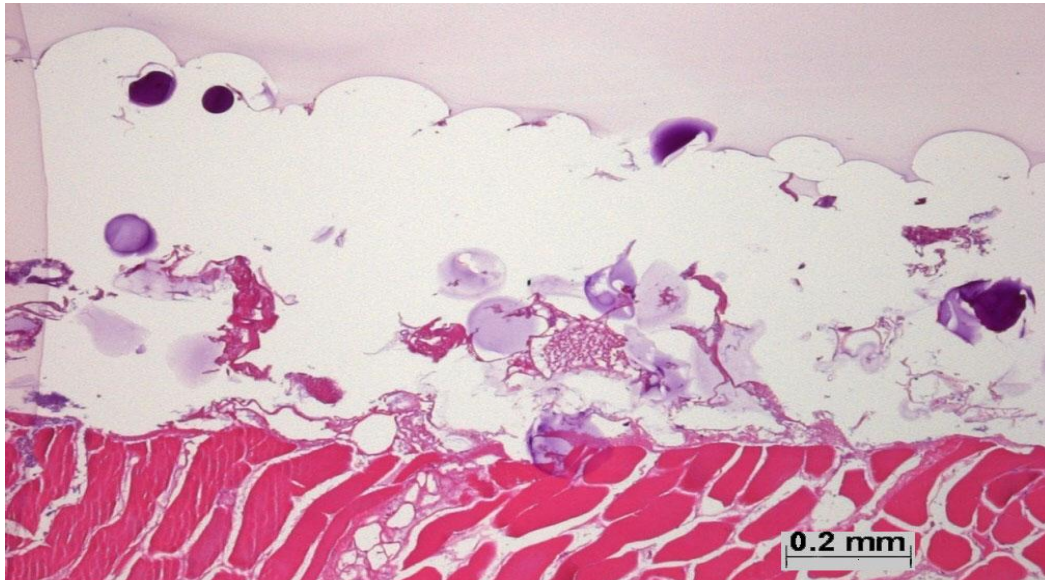


**Figure 3.126: LM of 72 hour CID showing thick growth**

Bacteria and biofilm growth was much increased with beads present surrounded by EPS (x4)

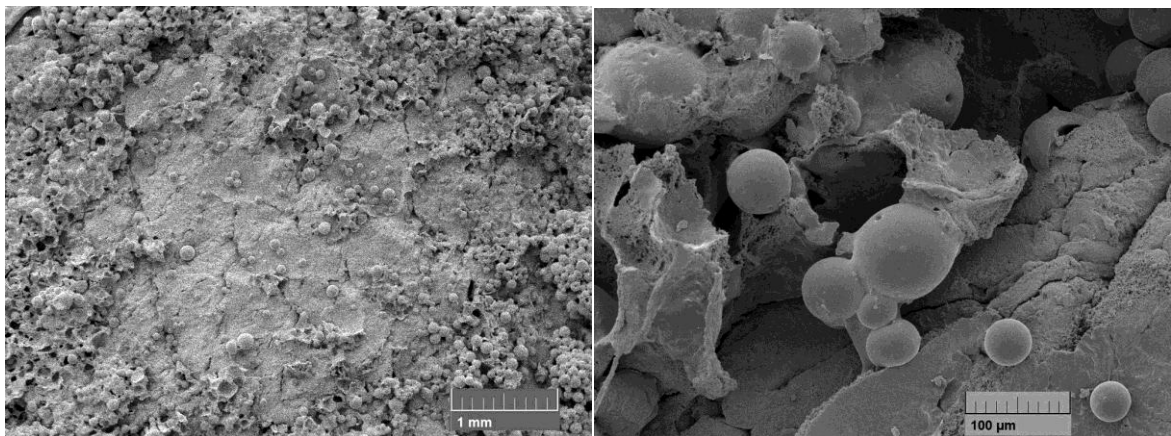


**Figure 3.127: 72 hour CID by SEM**

Many beads were present (left, x50) which were surrounded by bacteria and biofilm (right, x500)

According to ANOVA and Tukey analysis there was no significant difference in the compared results for 24, 48 and 72 hours, although the two sample t-test showed

significant difference between the 24 and 72 hour growths (48 and 72 hour  $p=0.924$ ; 24 and 72 hour  $p=0.026$ ) (Figure 3.128).

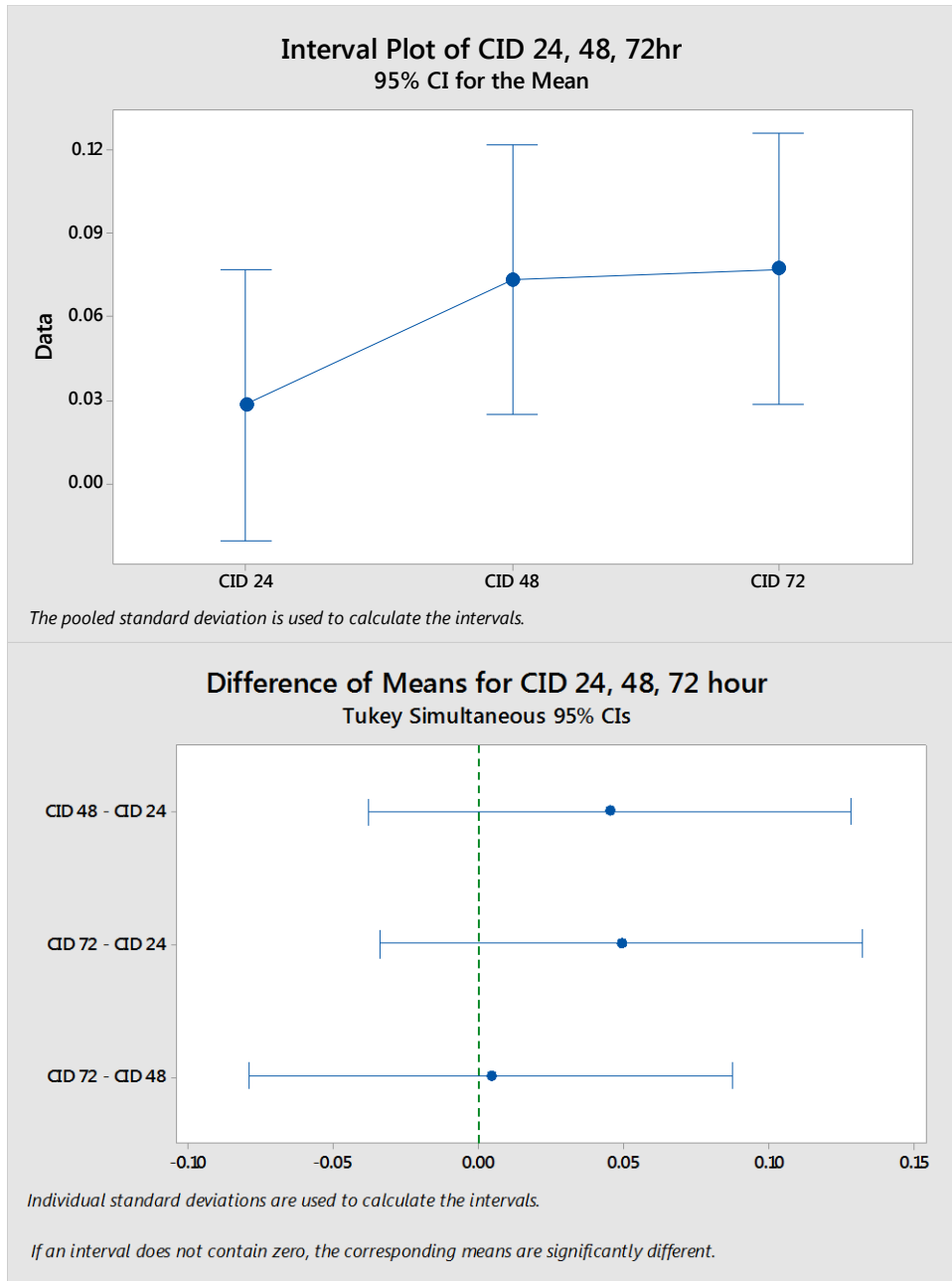


**Figure 3.128: Interval plot and Tukey plot of 24- 72 hour growth of CID**  
CID biofilm was much thicker than in the other dressings and by interval plot and Tukey analysis there was no significant difference in the 24, 48 and 72 hours. The two sample t-test showed significant difference between the 24 and 72 hour growths (48 and 72 hour  $p=0.924$ ; 24 and 72 hour  $p=0.026$ )



Dressings statistics were compared using a test for equal variances to look for consistency using standard deviations at each of the time points of 24, 48 and 72 hours (Figure 3.129; 3.130; 3.131).

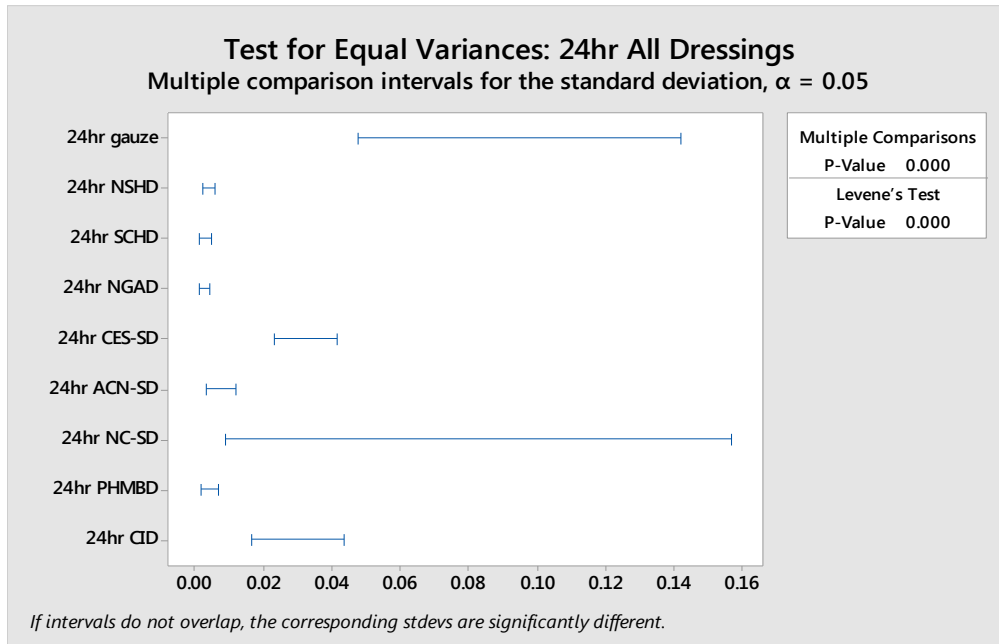


**Figure 3.129: At 24 hours, comparing tests for equal variances**  
The least consistent dressings were NC-SD, then gauze and then CID  
The most consistent were the NGAD, then SCHED and then NSHD

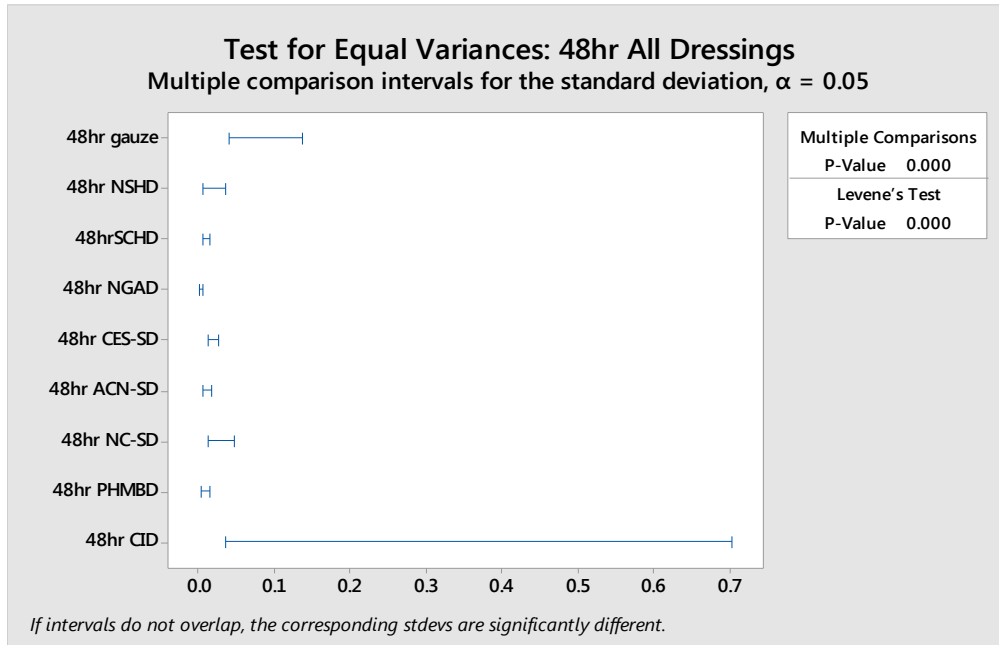


**Figure .130: At 48 hours, comparing tests for equal variances**  
 The least consistent dressings were CID, then gauze and then NC-SD  
 The most consistent were the NGAD, then SCHD and then ACN-SD

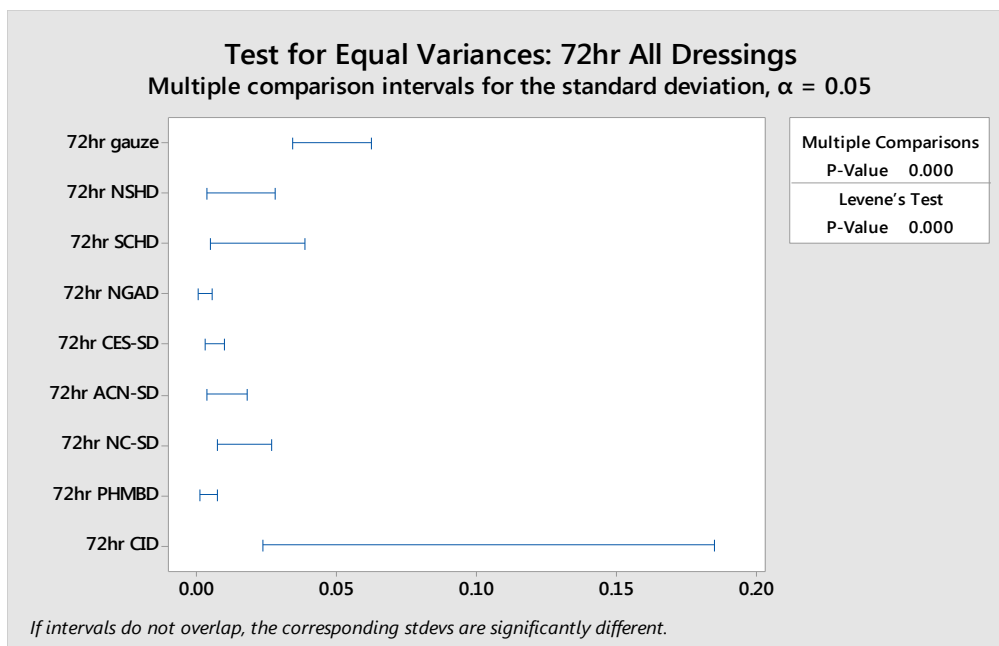


**Figure 3.131: At 72 hours, comparing tests for equal variances**  
 The least consistent dressings were CID, then SCHD and then gauze  
 The most consistent were the NGAD, then PHMBD, then CES-HD



The dressings varied in consistency with some performing better than others depending on the length of time the dressing was applied. Some, such as the NGAD and PHMBD were consistent throughout, others such as the gauze and CID were inconsistent. The gauze control, the best and the worst dressing from these results, at 72 hours, were compared (Figure 3.132).

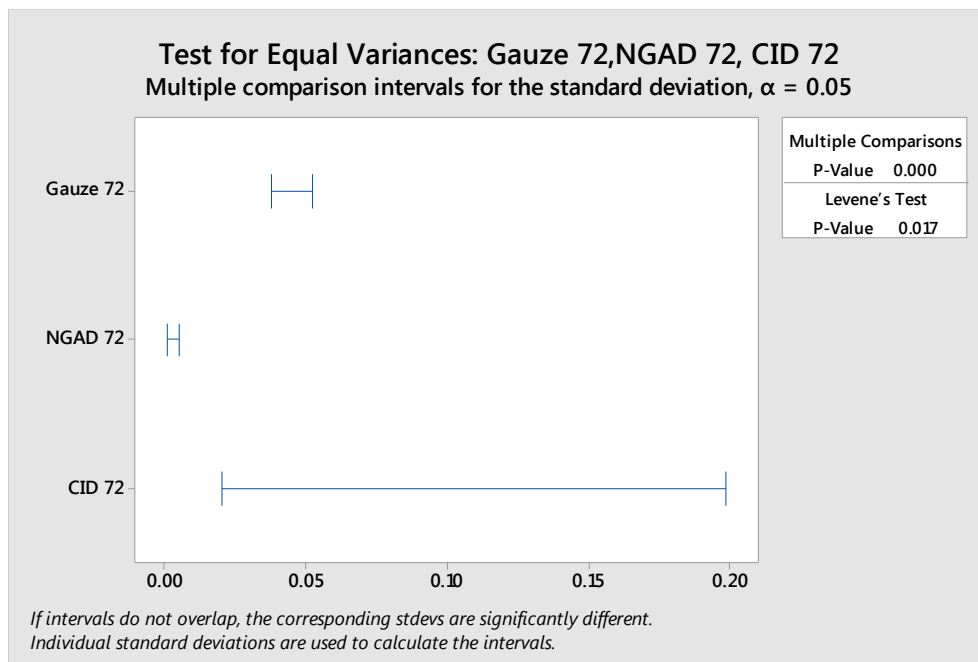


**Figure 3.132: At 72 hours; the control, the best and the worst performing dressings' tests for equal variances**

Compared to show the consistency, or otherwise, in the dressings' performance. The NGAD variance is small so it performed consistently well. The CID had a large variance, performing generally poorly and inconsistently (more inconsistent than the gauze)

Comparative interval plots were done to show the consistency and performance of the dressings on the same axes for a clearer comparison at each of 24, 48 and 72 hours (Figure 3.133).

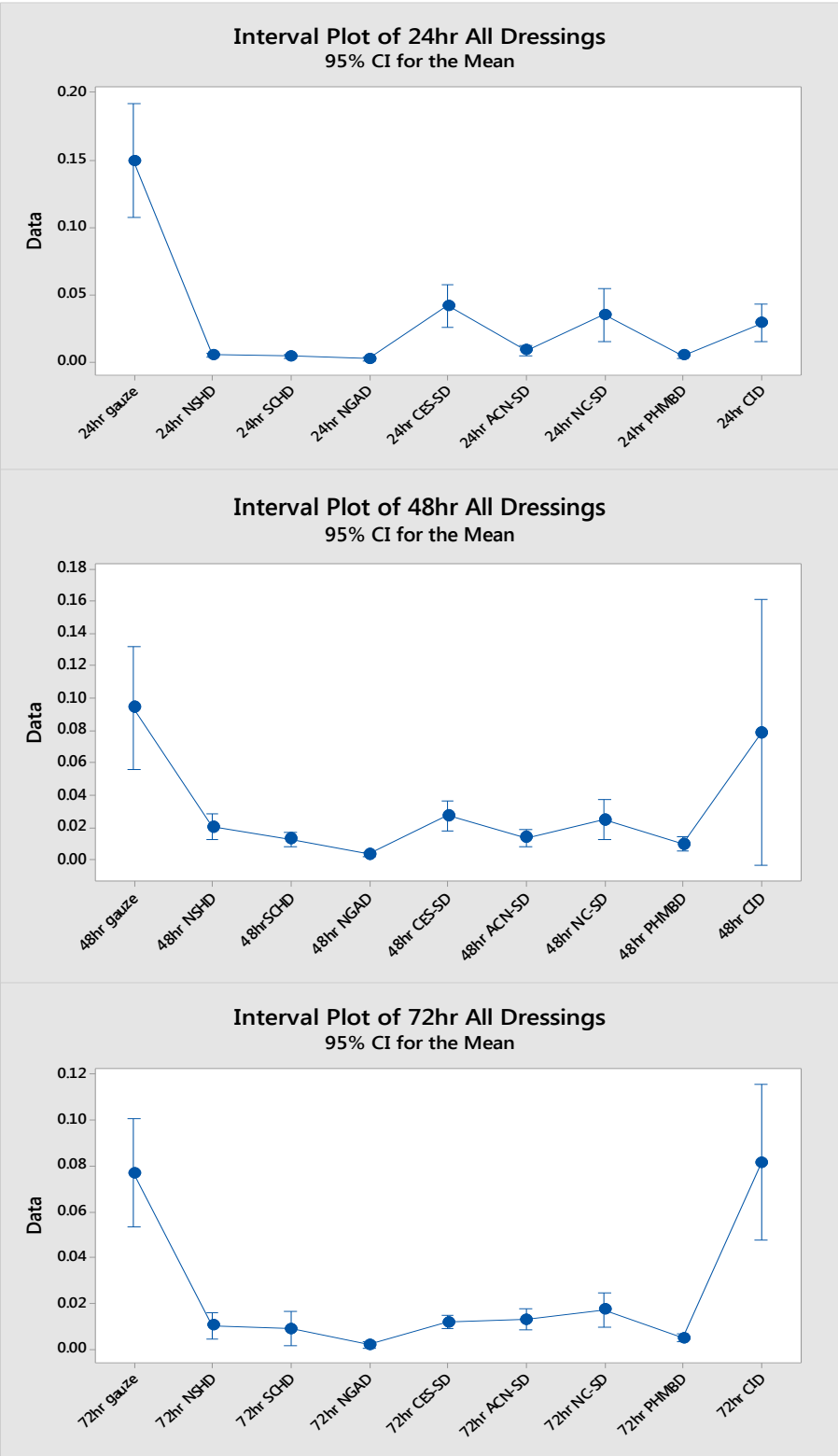


**Figure 3.133: Comparative interval plots of all dressings at 24, 48 and 72 hours**  
Comparative interval plots demonstrating performance and consistency of dressings, seen on the same axes. (Individual standard deviations are used to calculate the intervals)

And finally a bar chart was created to compare the Tukey pairwise Comparison Means for each dressing at each of the 24, 48 and 72 hours, with dressings put in order of the amount of biofilm growth areas beneath dressings. Overall the best performing dressings were NGAD, PHMBD ACN-SD, SCHD in this decreasing respective order, as shown in Figure 3.134.

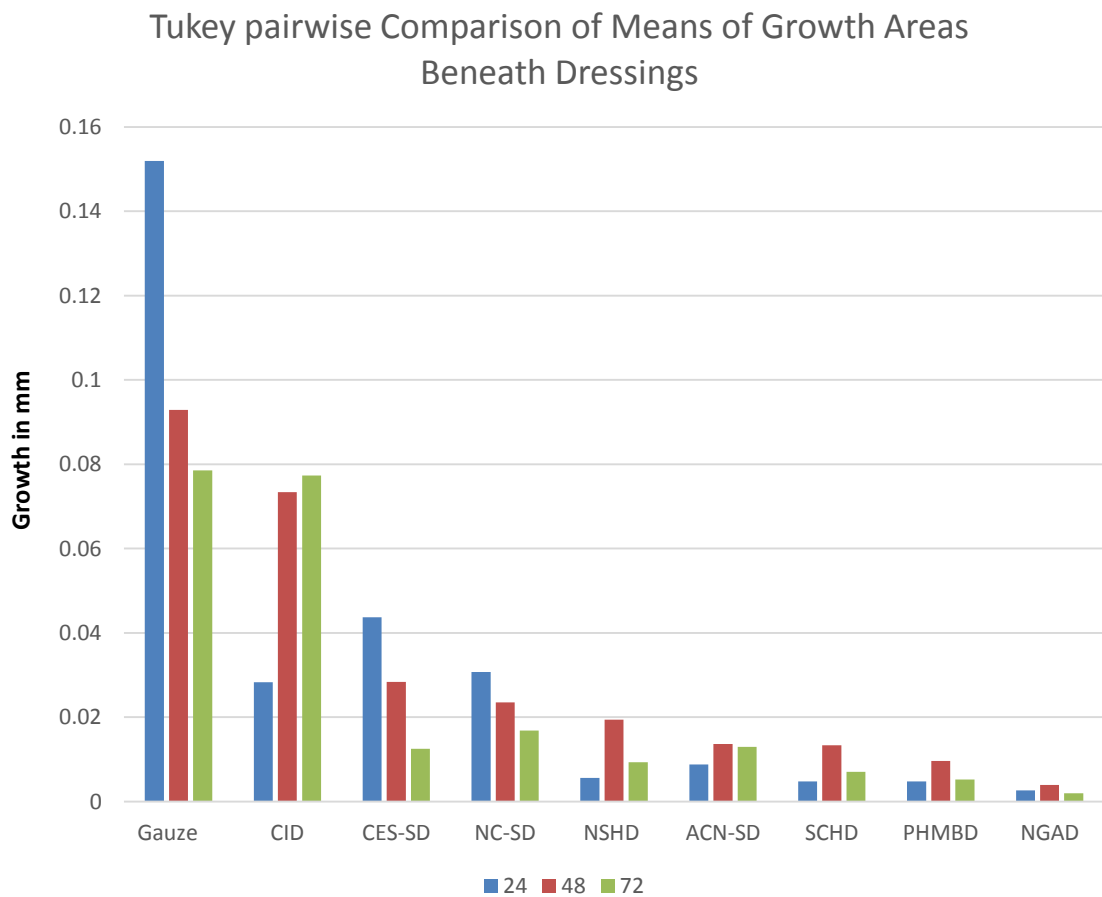


**Figure 3.134: Bar Chart of Tukey pairwise Comparison Means of Biofilm Growth Areas Beneath Dressings**

This shows the worst performing (gauze and CID) to best performing in this study (PHMBD and NGAD). It also demonstrates that all the dressings except CID had a decrease in growth at 72 hours (green bar)

## 3.8 Discussion

A greater understanding of biofilm presence in wounds is important in wound care for the effective treatment and improvement in patient management. Observations from this *in vitro* study demonstrated which dressings were the most effective against biofilm formation, when employed on moist tissue surfaces inoculated with *S. aureus* and *P. aeruginosa* and incubated from 3-72 hours.

The results from the preliminary experiments on the bacteria, performed in 2.4.7, showed that bacteria were starting to form small clusters within 6 hours when viewed under SEM. When grown on the surfaces of the tissue models beneath dressings, this was very difficult to observe at the LM level, and even with SEM much of the growth was incorporated into the surface of the dressings. Whether the bacteria were alive was demonstrated in the later time points (e.g. 24-72 hours) using CLSM and *BacLight* staining following 24 and 48 hours of growth, and TEM. These overall observations highlight the importance of understanding wound dressing structure, which are used to help explain the results obtained throughout these studies.

### 3.8.1 6 hour models

It was apparent that within the first 6 hours little bacterial growth was observed under the NC-SD although, even within that time, some apparent deposition of silver was visible under the dressing (Figure 3.9). Similar silver deposition has been observed when this dressing was applied to human skin both *in vitro* (Walker et al., 2006) and *in vivo* (Trop et al., 2006). This would suggest that this dressing

does not have the capacity to maintain its silver content once in contact with moisture, which may result in excessive amounts being made available that can stain wound tissue and be deleterious to wound healing (Ahamed et al., 2008; Atiyeh et al., 2007). Further observations at these early time points showed that some of the dressings had several fibres left on the model surface (Figure 3.8). The other observation was that the CID samples showed a marked loss of iodine, with visible iodine crystals released from the cadexomer beads (Figures 3.10-3.13).

### **3.8.2 12 hour models**

After 12 hours incubation, it was not surprising to see bacterial growth in the gauze control model, but there was hardly any growth visible within the other control dressing (NSHD). This was probably due to the differences in the respective dressing structures. Gauze is essentially 100% cellulose, having very little absorbency, due to the cellulose fibres being tightly bound to each other thus producing effectively 'open' spaces, which as demonstrated allow the bacteria to proliferate (Walker and Parsons 2010).

On the other hand, the NSHD, and indeed all the Hydrofiber-based dressings, provide a much less tightly bound structure, and individual fibres can increase their thickness by ten-fold before being gelled with neighbouring fibres (Newman et al., 2006). This gelling capacity also means that the bacteria which are present on the wound surface become sequestered within the gelled dressing, resulting in reduced bacterial growth (Walker et al., 2003).

A similar finding to the gauze, with respect to bacterial growth, was observed with the CES-SD, but this growth was more even and may be due to the inability of this dressing to gel and conform completely to the tissue surface. There was increased silver deposition evident with the NC-SD, as well as areas of increased bacterial growth, which may again be due to the relatively inflexible dressing material not allowing good intimate contact to take place.

In the CID samples after 12 hours, no iodine crystals were visible. The CID contains 0.9% molecular iodine, physically bound to the cadexomer matrix of a 3-D cross-linked polysaccharide starch matrix. The product information for use provided (IFU, Smith & Nephew UK. product website) states that exudate is thought to cause the beads to swell and release iodine until an equilibrium is reached. Each time this equilibrium changes, the iodine will be released until it becomes depleted. At this point the dressing would need to be changed.

Unfortunately, an exuding wound is in a constant state of producing fluid (similar to the model used) which may shift the equilibrium, exhausting all the iodine, potentially rapidly, if exudation is consistent. If exhausted by 6-12 hours, the dressing would have to be replaced on a highly frequent basis to be fully effective. If this occurred in a clinical setting, it would increase the expense in terms of dressings and patient visits.

### 3.8.3 24 hour models

24 hour incubation showed a marked difference between the dressings. Due to the mesh-like structure acting as a support surface, the bacteria grew within the gauze to form a well-established biofilm, wrapping itself around the fibres and gradually filling the holes over time. The NSHD at 24 hours however was observed to have a few small groups of biofilm growth on the tissue surface, which is likely due to its ability to sequester bacteria within the gelled dressing, even though no antimicrobial agent is present (Walker et al., 2003). It was therefore expected that the silver-containing Hydrofiber dressings should be more efficient in eradicating the bacteria than this NSHD, having both a sequestering and antimicrobial effect. Both the SCHD and NGAD were even more effective at bacterial control at 24 hours. The fibres were shown to sequester bacteria, and both had minimal amounts of bacteria remaining on the tissue sample that could be visualised by any of the microscopical methods, with the NGAD performing marginally better. The bacteria viewed by TEM were found occasionally as small clusters in the SCHD, but were observed to have poor structure and appeared to be internally disrupting. This would be comparable to the findings of the disruption of the nucleoid by the addition of silver nitrate to planktonic bacteria, as performed in Chapter 2.4.2.

The CES-SD results for 24 hours presented fibres stuck to the tissue surface on most models, which impeded viewing of some of the SEM models. Although a stereo microscope was used to lift off the dressings, some of the fibres were difficult to remove from the moist surface of the tissue. Without the stereo microscope, the extent of the quantity of these fibres was difficult to visualise. This



dressing is designed for one-piece dressing removal due to dressing integrity, ensuring that there is no residue left (Barrett, 2012). The product Instructions For Use states that it may adhere to lightly exuding wounds, yet this model was provided with a constant supply of fluid, and raises the question of how much fluid has to be present for the fibres to be to gel.

The ACN-SD at 24 hours also shed a few fibres, but these were minimal in comparison to the CES-SD. There was biofilm-like material within the small inner fibres of the dressings, below the outer coverings. There was presence of bacteria in patches on the tissue samples beneath these dressings. The outermost surface of this dressing has been designed to be a non-adherent layer of hydro-alginate to help reduce trauma and pain when removed (Gray, 2009). The silver ions should be released through the perforations of the non-adherent layer, from the silver-coated nylon fibres. However, bacteria were managing to grow in these areas. The nylon fibres are amongst alginate fibres, and alginates have been demonstrated to swell to varying extents in the presence of fluid (Walker et al., 2006; Walker and Parsons, 2010). This would once again suggest the issues of contact with the tissue surface, where the openings in the weave of the dressing allowed bacteria to grow in the lack of contact, and a lack of sufficient quantity of silver release. It may also suggest that the alginate fibres swell and prevent the silver reaching the surface.

The 24 hour NC-SD released silver, but in even more pronounced patches of silver deposition, which stained the surfaces of the models. There were groups of bacteria present on the surface, in-between these areas of silver deposition.

Metallic silver (elemental silver) is a neutral form of silver and is not an antimicrobial. It is only in the positively charged form (ionic silver) that it can release cations to bind to sites on bacterial cells, and hence become antimicrobial (Ovington, 2004). Nanocrystalline dressings require constant moisture for the oxidation process to take place and release the silver ions (Kostenko et al., 2010). They should therefore suit an exuding wound. It was possible that this silver technology, being nanocrystalline, was not releasing sufficient silver ions with which to kill the bacteria, and the bacterial load was beginning to increase to such an extent that biofilm was now beginning to form. Compared to the other antimicrobial dressings, the NC-SD was taking longer to initiate its antimicrobial effect, which could be detrimental to wound healing due to biofilm having the opportunity to begin to form.

The PHMBD is recommended for light to moderately exuding wounds (Glover and Wicks, 2009), and those critically colonised and infected (Haemmerle et al., 2012), and claims to have a cooling and soothing effect with less wound pain (Kingsley et al., 2009). The theory of its action is to absorb exudate over the wound but to supply moisture to the drier parts of the wound edge, to promote hydration. At the same time, it releases the PHMB to kill the bacteria present. The bacteria were observed to be in thin lines beneath the dressing, with no apparent EPS by TEM. The quantity of bacteria on the surface was more visible on the SEM due to LM and TEM being only the equivalent of a representative thin slice across the surface. The bacteria were numerous but only in a flat layer, which would suggest that bacteria were present in a planktonic form, possibly surface attached, but not

as biofilm clusters. It would also suggest that the gap between the dressing and the tissue was minimal, only allowing bacteria to grow in the smallest of areas.

CID beads, although not submersed in a fluid but in a moist environment, became pale within 24 hours, and the iodine was shown by SEM to have been apparently exhausted. This therefore showed that there was no visible antimicrobial remaining amongst the beads. The structure of the iodine-exhausted beads appeared to be acting in the same manner as the gauze, in that it was providing a support structure on which the bacterial biofilm could grow.

#### **3.8.4 48 hour models**

48 hour growth showed a variation in results in the dressings. Beneath gauze dressings, the tissue was covered in a thick biofilm when viewed by SEM. The LM sections showed that in some areas the biofilm was thinner in appearance and this may have occurred when the gauze was removed by lifting it off the tissue surface. The gauze dressing viewed with SEM was coated thickly by the biofilm, so the mesh structure had slightly debrided the samples due to the biofilm being wrapped around it, demonstrating that even a basic dressing can have a debriding effect. The amount of growth was such that there was no significant difference between the mean growth areas of the 24 and 48 hour biofilm ( $p=0.063$ ).

The NSHD had a larger presence of bacteria than at 24 hours, but still had nothing like the quantity present in the gauze. Similarly, the SCHED had a slight increase in the presence of bacteria which were mainly seen in a few of the fibres remaining

on a few models. This increase was reflected in the statistical data with a significant difference ( NSHD  $p=0.007$ ; SCHED  $p=0.004$ ).

The tissue beneath the NGAD appeared to be almost clean. Only a few bacteria were seen under the dressing at TEM and these did not appear to be viable bacteria from the structure. CLSM demonstrated that at 48 hours the tissue was free of clusters of bacteria and that the dressing contained what appeared to be individual live and dead bacteria, and there was no significant increase with statistical analysis ( $p=0.201$ ). This observation would confirm that the dressing was, by this time point, sequestering the bacteria away from the tissue. It would also support the theory that the Hydrofiber component of the NGAD can debride wounds (Queen, 2010). Sibbald (2005) trialled a four week application of the SCHED and found it to have a desloughing action. NGAD consists of two layers of Hydrofiber stitch-bonded together to provide 50% more absorbency and 9-times greater strength than the SCHED (Bugedo et al., 2012). It also contains a metal chelator (EDTA), a surfactant (benzethonium chloride) and pH control. The clean tissue surfaces would appear to support the claims of this NGAD structure and formulation being improved upon compared to the SCHED. Recent studies on surfactants have shown the reduction in bacteria and biofilm with their use (Schultz et al., 2016). EDTA has been demonstrated to have antimicrobial activity and to be useful as an anti-biofilm agent (Percival et al. 2005; Al-Bakri et al., 2009).

The structure of the CES-SD had not improved by 48 hours ( $p=0.148$ ) and many fibres were still attached to the tissue surface. If the fibres had gelled more effectively, then the dressing may have been removed more easily. As such it was

virtually impossible to see the tissue surface by SEM, but what could be seen were groups of bacteria and possible biofilm around them. Some of the fibres viewed by CLSM confirmed this with evidence of growth around the fibres. The growth could be followed along individual fibres, which would again confirm that these fibres had still not gelled.

Due to the outer covering of the ACN-SD it was more difficult to view the inner fibres. Only a few of these fibres were found attached to the tissue, showing that the dressing was mostly intact. The few fibres on the surface showed silver deposition, so these were likely to be nylon fibres that had been shed from the dressing. There was an increase in growth in the 48 hour ACN-SD, but it was not significantly different from the 24 hour growth ( $p= 0.135$ ).

The NC-SD growth at 24 and 48 hour was also of no significant difference ( $p=0.63$ ), which would suggest that the silver ions were finally being released from the dressing by these time points. The mesh of the dressing is small but the surface, holes and lower fibres were coated with bacteria. The silver may have begun its antimicrobial effect at this point, but some bacteria were seen to be growing in the lower layers of the tissue.

The PHMBD showed little change from the 24 hour results with thin layers still being present beneath the dressing. This once again showed a minimal gap between the dressing and the tissue due to its design, but it nonetheless demonstrated the presence of some bacteria remaining on the dressing when

removed. It did not appear to debride, which would be of concern if the bacteria were still viable when a dressing was removed from a wound.

The CID had made no improvement from 24 to 48 hours, confirming that the antimicrobial agent, molecular iodine, had been exhausted. Bacteria were wrapped around and encasing the cadexomer beads, indicative of biofilm formation, providing further evidence that the availability of molecular iodine had been exhausted.

### **3.8.5 72 hour models**

72 hour growth showed a reduction in biofilm growth with all dressings, even the control dressings, except for the CID. These results were best demonstrated using statistical analysis. Pooled standard deviations were used to calculate interval plots and the pattern of growth compared for 24, 48 and 72 hours. These plots demonstrated the performance and consistency of the dressings, which could be seen on the same axes. The difference between the dressings was noted when the data of the ANOVA interval plots performed at each of the 24, 48 and 72 hour groupings were transferred into Figure 3.134. This figure shows the best and worst performing of the dressings according to the analysis. The following is the analysis of these statistical results.

The gauze, CES-SD and the NC-SD-dressed models all had a similar pattern of growth. The amount of bacterial growth on the surface of the model dressed with gauze was found, surprisingly, to gradually decrease from  $0.1519 \pm 0.0687 \text{ mm}^2$  to  $0.0785 \pm 0.0391 \text{ mm}^2$ , between 24 and 72 hours (Figure 3.104). The difference

between the area of biofilm at 24 and 72 hours was statistically significant ( $p=0.022$ ), but not between 24 and 48 hours, or between 48 and 72 hours. Gauze has been shown to have slower healing times compared to other dressings (Singh et al., 2004) likely due to it causing loss of moisture within a wound (Wu et al., 1996). This drying out of a wound is contrary to the agreed principle of moist wound healing (Jones, 2005). The removal of gauze from a wound is often painful and can cause trauma, due to it sticking more to the wound than other dressings and creating a non-selective physical debridement (Daunton et al., 2012). This debridement effect could be the cause of the gradual decrease in biofilm area on these models, where the biofilm and bacteria had become wrapped around the lattice-type network of the dressing fibres, causing the drying gauze to pull off some of the biofilm.

The CES-SD-treated models had similar patterns of growth to the gauze (Figure 3.116), with a gradual decrease in the amount of biofilm area remaining on the surface from  $0.04372 \pm 0.02774 \text{ mm}^2$  to  $0.01253 \pm 0.00472 \text{ mm}^2$ , between 24 and 72 hours. As with gauze, CES-SD had 24 and 48 hour showing similar grouping, with Tukey pairwise comparison, as did the 48 and 72 hour models (not significantly different), but the 24 and 72 hour growth were found to be significantly different ( $p=0.003$ ). It would seem therefore that the models would have to be grown to 72 hours to show any significant reduction in biofilm growth using CES-SD. As expected from an interactive dressing (Byrne, 2014), the CES-SD was more effective than the gauze, as the overall quantity of the area of biofilm growth was smaller than that of the gauze in each instance. This CES-SD claims to form a



cohesive gel to keep the wound moist to aid healing and to release ionic silver as an antimicrobial (Bullough et al., 2015). The observation with this study, demonstrated the fibres of the CES-SD only showing some probable matting at 72 hours (Figure 3.115). In almost all the CES-SD models there were fibres remaining stuck to the sample surfaces and bacteria were present in clusters. The shedding and sticking of the CES-SD fibres might suggest that the tissue was not kept moist enough by the dressing. However, all the models beneath the CES-SD were supplied with plenty of nutrient fluid. This would suggest that the fibres did not swell as much as the other dressing types such as the Hydrofibers, that the CES-SD did not absorb as much exudate, and that the structure of the dressing was not as cohesive as expected. Fibres remaining on a patient's wound would have to be removed, which could cause discomfort and disturb granulation tissue formation (Seaman, 2002).

The NC-SD -treated models followed a similar biofilm growth trend to the gauze and CES-SD, by showing a gradual decrease in biofilm area over the 24 to 72 hour period (Figure 3.122). The NC-SD resulted in comparative biofilm area means for all three times ( $p=0.386$ ), and it also resulted in a lower quantity of growth compared to the gauze and CES-SD. The deeper tissue layers on the model were seen to contain dark areas of silver staining not seen in the other ionic silver dressing models. NC-SD claims to remain active for a minimum of 3 days ([www.smith-nephew.com](http://www.smith-nephew.com), 2016) and to have rapid and sustained bactericidal activity, due to the release of clusters of highly reactive silver cations from the nanocrystalline silver as it becomes moistened by exudate (Fong and Wood,

2006). This may help to reduce inflammation and promote healing. The amount of heavy silver staining present on the surfaces of the sections by LM and TEM was clearly visible. Although some clinical studies have stated that it is safe to use (Vlachou et al, 2007), and that no evidence has emerged of resistance or cytotoxicity to nanocrystalline silver (Dunn and Edwards-Jones, 2004), there are still reservations about the absorption of silver in the skin, and there have been reports of toxicity, recorded by checking the levels of silver in blood and urine (Trop et al., 2006).

An *in vitro* study on the effects of silver on keratinocytes and fibroblasts showed silver to be highly toxic, with a similar toxic dose range to that of bacteria (Poon and Burd, 2004). Silver toxicity was found to cause 10% inhibition of bacteria at the lowest concentrations ( $6.25 \times 10^{-4}$ ). Okkyoung et al., (2008) found inhibitions on growth by  $\text{Ag}^+$  ions, based on a prolonged microtiter assay, at about 0.5 mg/L  $\text{Ag}$ , t were 100%. A study on fibroblasts found their contraction rate in this NC-SD to be higher than SCHD and ACN-SD (Cochrane et al., 2006). This, therefore, may be of concern if wound healing cells are proliferating and trying to re-granulate and re-epithelialize the wound. The NC-SD notably had a better performance in reducing bacterial growth between the later times of 48 and 72 hours, compared to the 24 hour, which would be consistent with the slower release of the silver ions from the nanocrystalline silver compared to the ACN-SD, SCHD, and NGAD, ionic silver containing dressings. The disadvantage of this is that the bacteria appeared to have grown into the deeper layers of tissue by 48 hours and the dressing was

relying on the ability of the silver to penetrate these deeper layers to kill the bacteria (Lansdown, 2004).

The gradual decrease in growth of bacteria and biofilm beneath the CES-SD and NC-SD could be a result of the gradual increase in the presence of silver.

However, although the area of biofilm on the model from the gauze dressings was larger than any of the other dressing models, the fact that the gauze model had a decrease in growth area suggested that some of this decrease in the silver dressings, could have been due to debridement.

The NSHD control, SCHED, NGAD, ACN-SD and PHMBD all had a similar pattern of a small area of growth, which increased slightly from 24 to 48 hours, then was decreased in area at 72 hours (Figure 3.107; Figure 3.110; Figure 3.113; Figure 3.119; Figure 3.125). The NSHD control had the largest increase in growth area at 48 hrs (which was significantly greater than at 24 hours ( $p=0.007$ ), which was consistent with it not containing any form of antimicrobial, and the decrease at 72 hours would be consistent with the claims of the fibres continuing to swell, and it sequestering and removing biofilm from the surface of the tissue (Bowler et al., 1999; Jude et al., 2007). The decrease was such that the 72 hour growth was significantly less than the 48 hour growth by Tukey pairwise comparison ( $p=0.005$ ), but the mean grouping showed the 24 and 72 hours to be similar (Figure 3.108).

The prevention of bacterial biofilm growth with NSHD was greater than three of the antiseptic containing dressings at 48 hours (CES-SD, NC-SD, CID), and at 72 hours was more effective than four (CES-SD, ACN-SD, NC-SD, CID). This could

be due to the surface of this type of dressing conforming to the shape of the surface of the model more than the other dressings, due to its structure and composition. Lack of conformation and non-adherence can create fluid-filled pockets where bacteria can proliferate under a dressing surface and begin to form biofilm (Quinn et al., 1985). Prevention of these pockets by dressing conformation would help to prevent biofilm growth. By sequestering, Hydrofiber dressings can immobilise bacteria within its gel-like structure (Walker et al., 2003). The ability of a dressing to retain bacteria away from the wound is thought to help infection control (Tachi et al., 2004) and debriding a wound will lower the bacterial burden (Sibbald, 2005). This is especially important during dressing changes to prevent dispersal of bacteria (Bowler et al., 1999). The dressing is claimed to be easy to remove without causing pain or trauma (*AQUACEL datacard, www.dressings.org*). Results from clinical studies have indicated that patients managed with NSHD experienced significantly less pain and a rapid rate of epithelialization (Barnea et al., 2004). The dressing has been shown to remain in place for 7 days, which is a lower frequency of changes than most dressings, and hence is more cost-effective (Armstrong et al., 1997). This ability to form cohesive gels was observed in all the Hydrofiber dressings (NSHD, SCHED, NGAD) from 24 to 72 hours, showing the ability of this dressing to absorb fluid, and hence manage exudate (Williams, 1999).

The addition of silver ions as an antimicrobial to this dressing in the form of the SCHED, improved its ability to keep bacterial growth to the third lowest level of the dressings in this study at all time points (no significant difference between 24, 48 and 72 hours, as shown by Tukey plots (Figure 3.110)). The newer NGAD showed

the least bacterial growth of all the dressings tested at all time points (again, no significant difference between 24, 48 and 72 hours, as shown by Tukey plots, Figure 3.113).

Four dressings, SCHED and NGAD, ACN-SD and PHMBD, all had similar 24, 48 and 72 hour grouping patterns with Tukey pairwise comparison when viewed by interval plots which were not significantly different (SCHED  $p=0.057$ ; NGAD  $p=0.129$ ; ACN-SD  $p=0.263$ ; PHMBD  $p=0.068$ ). ACN-SD, comprising of an outer layer of ethylene methyl acrylate, claims to overcome the problems of adherence and fibre shed, maintaining its structural integrity (Galea, 2015). Although the CES-SD was found to shed the most fibres, there were a few fibres found on the surface of the ACN-SD meat models, visualised best by SEM. There also appeared to be pockets of bacteria forming in the holes of the outer dressing, which could conclude that the dressing did not conform completely to the surface of the tissue. Walker et al. (2003) studied the sequestration function of the NSHD compared to alginate dressings, with SEM. Using a technique of progressively lowering the temperature during processing for SEM, the study showed how the CMC fibres hydrated to form a cohesive gel, immobilising some of the bacteria within them, whereas alginate fibres were not fully hydrated and their rate of gel formation was slower. The alginates formed a patchwork of gelled areas and not a gelled matrix structure. TEM and CLSM demonstrated that these growths were of biofilm type with viable bacteria and EPS.

Parsons et al., (2005) tested dressings in wound fluid and measured the levels of antimicrobial effect, silver content and release. ACN-SD was found to have a higher content of silver but a much lower release than NC-SD, and a comparable kill rate of bacteria in wound fluid (planktonic bacteria). The ACN-SD overall performance in this present study, in prevention of biofilm growth, was better than the NC-SD. During the practical work it was also noted that the tissue under the ACN-SD 72 hour models appeared to be shrunken when compared with the other dressings. The thickness of the tissue was checked for consistency and all images at x2 with LM at 72 hours showed a thickness average of 1.907 mm. The ACN-SD showed a mean thickness of 0.946 mm, demonstrating a possible shrinkage of the tissue beneath the dressing, compared to all the other dressings. This would suggest that the model was not kept as moist beneath the dressing. Models of timed growth were performed for several dressings in the same instance for comparison.

The PHMBD performed marginally better than the SCHD at controlling biofilm formation, with no significant difference in the biofilm areas measured over the 24-72 hours (48 and 72 hour  $p=0.104$ ; 24 and 72 hour  $p=0.771$ ). As a low risk antiseptic, PHMB is used in a variety of products such as swimming pool cleaners, contact lens cleaning solutions and cosmetics (Jones, L., and Senchyna, M., 2007), and is considered safe and well tolerated (Gray et al., 2010), although a case of allergic reaction has been noted (Kautz et al., 2010). Its product guide does recommend removal of slough, and wound bed preparation before use, and

recommends treatment of the underlying condition to promote granulation and epithelialization in wound management.

Any bacteria seen on the PHMBD models were usually in the presence of a thin line, and not as clusters of bacteria. A clinical study by Wild et al., (2010) found this dressing to be particularly comfortable for patients. They compared it with the SCHD used in this study and found both dressings to demonstrate both cleansing and debridement properties. The surface of the PHMBD is smooth and cold to the touch, and moist and remained relatively flat throughout the models when viewed by SEM. This smooth surface could have contributed to the bacteria being present as a thin layer. However there was no great number of bacteria observable on the dressing surface by SEM viewing. The PHMBD may have assisted in the prevention of the biofilm formation and, with the antiseptic effect of PHMB and the limited contact of the dressing interface, prevented the bacteria from forming in pockets beneath it, as in some of the other dressings. This meat model had a relatively flat surface by nature, with occasional indents on the surface. A wound surface with all its imperfections might not be so forgiving for a flat surfaced dressing.

The CID had a different pattern of growth to any of the other dressings when examined by Tukey pairwise comparisons (Figure 3.128). The CID performed poorly in this study, with a continual increase in growth of biofilm, though there was no significant difference in biofilm formed between each time point ( $p=0.284$ ). At 72 hours the biofilm growth area for the CID was not dissimilar from the gauze dressing ( $0.07732 \pm 0.05567 \text{ mm}^2$  CID,  $0.07847 \pm 0.03908 \text{ m}^2$  gauze). It is claimed

to be antimicrobial and to remove slough and debris to clean the wound bed, and is recommended for use in wounds such as wet ulcers and diabetic foot ulcers (Smith & Nephew Professional products). The beads, which are said to absorb debris and remove it from the wound bed (Jones, 2000), were surrounded by a layer of biofilm at 24 hours which was visible by all microscopical methods, and stained mainly with the green-live stain when viewed by CLSM. The beads were not irrigated by the force of fluid added to the model, unlike the clinical setting where the data card suggests removal of the beads to 'cleanse' it (Iodoflex datacard, [www.dressings.org](http://www.dressings.org)). This would have been difficult to compare with the other dressings, as none of the other models were cleansed. This step was immaterial when the amount of biofilm growth was noted at 24 hours, as this amount of growth might have been present if this was a real wound.

It is also suggested on the data card that the secondary carrier layer can be left in place when the dressing is applied to a wound. The carrier layers are made of gauze. From the results of this chapter, it has been shown that gauze allows bacteria to grow within its mesh. The inclusion of gauze as part of the dressing could allow the bacterial biofilm to obtain an even better hold in the wound. A more sequestering dressing might be more appropriate, as long it did not sequester the molecular iodine from the beads. But as visible iodine was found to last only up to 12 hours in the CID, it might help to hold the iodine *in situ* a while longer. The dressing would have to be renewed regularly (e.g. every 12 hours), which is clinically unrealistic and would require a constant refreshed supply of molecular



iodine. Small amounts of iodine are relatively harmless, but iodine can be toxic to human cells and absorbed systemically from constant use (Grey, et al., 2002).

The consistency of the performance (whether good or poor) of the different dressings was evident when a test for equal variances was performed for each time slot (Figure 3.129; Figure 3.130; Figure 3.131). The NGAD and the PHMBD behaved more consistently than the other dressings throughout. The NC-SD was consistent from 48 hours but not at 24 hours. This was probably due to the slower release of silver ions from this type of dressing (Heggens et al., 2005) needing the oxidation process to take place before it could release the silver ions into the model (Kostenko et al., 2010). Other dressings with silver ions rather than nanocrystalline, appeared to have a more controlled release of the silver and hence were consistent more quickly, especially in the earlier stages of growth.

### **3.9 Conclusion**

In order for a dressing to be effective it should perform several functions. A dressing should help to control exudate levels whilst keeping a wound moist. The dressing should control the bacterial load (Sood et al., 2014), and perform some debridement by removing the bacteria, either physically by sequestering or antiseptically by silver, iodine, PHMB or some other chemical means that does not cause damage to the patient tissues and their overall health. .

The best performing dressing in this study was the NGAD which presented almost clean surfaces on SEM, and this was confirmed by the statistical analysis. This

dressing contained silver ions, as with the SCHED, but claims to have extra absorbency and strength, and anti-biofilm formulation. This may have helped in sequestering bacteria to prevent their growth and spread and in debriding the model. This was especially noted in the images of the 48 and 72 hour models (Figures 3.75; Figure 3.112), but overall statistical analysis showed it had the least bacterial growth beneath all the dressings used. The worst performing was the CID. By 24 hours there was a large amount of biofilm growth around the cadexomer beads in all the models, with very little evidence of the presence of iodine.

It was seen on physical removal of some dressings that there were differing degrees of debridement, and biofilm could be seen attached to the dressings removed, when viewed with SEM. Some dressings had absorbed some of the biofilm into their structure. This was particularly seen in the swelling of the Hydrofiber dressings. Unfortunately, it was not possible to perform TEM on the dressing alone to view the depth of absorption/sequestration, due to their structural nature not being conducive to TEM sectioning, as shown in the earlier chapter with bacterial growth on a gauze surface (Chapter 2.3.15). Some dressings left residual debris which in a wound may encourage colonisation and present an infection risk (Daunton et al., 2012). The CID relies on rinsing to remove the beads and debris from a wound. During the processing for SEM, despite gentle methods, one would expect the beads to be rinsed away by the washing steps in the processing, but they remained on the surface. The beads are 0.1-0.3 mm in diameter so may be difficult to remove by the naked eye. Lack of bead removal may therefore leave

biofilm bacteria on the surface of wound tissue in a clinical setting. In this study the CID was not an efficient dressing, and constant replacement would be neither cost-effective, clinically realistic, nor a safe alternative compared to other dressings in this study. A clinical study on this dressing found it to reduce the bacterial bioburden and decrease the wound size, although none of the wounds completely healed over the 6 week study (Schwartz et al. 2013). The dressing was changed in the study between 5 and 16 times per week, which this study shows would be necessary due to the constant exhaustion of the iodine.

The observations made, from the results of biofilm growth beneath the various dressings in this chapter, highlight the importance of dressing selection to deal with the increasing likelihood of bacterial and/or biofilm presence in wounds.

Considering the fact that the dressings were placed upon planktonic bacteria, the dressings should have eliminated all bacterial growth and prevented biofilm formation beneath. The nature of the spread of the bacteria on this model was designed to ensure that some bacteria remained on the edges, outside the area of the dressing, to grow unimpeded. If the dressing leached its antibacterial contents immediately and into the surrounding area, all bacteria on the model would have been killed. The speed with which bacteria grow (as shown in the graphs of chapter 2) is swift and their prevention depends on the ability of a dressing to release its antimicrobial and make it available at the dressing-wound interface. Even the smallest numbers of bacteria have the ability to multiply and form biofilm and possibly cause infection. Appropriate wound dressings should be selected following debridement and wound cleansing (Attinger et al., 2006). The cleansing

needs to be thorough, to remove as many bacteria as possible including planktonic and biofilm forms, before the selection of a dressing which should depend on the original status of the wound (Keast and Lindholm, 2012). The dressing should prevent biofilm formation. In this study the bacterial biofilm was seen to form at the edges of all the models where it was not protected from a dressing. This demonstrated that the original bacterial load had spread across the surface of the tissue as expected. This acted as a good control area for each dressing, and demonstrated that none of the dressings released its antiseptic properties into the surrounding tissue that was not in immediate contact with the dressing. This shows the importance of thorough cleansing, and that any dressings cover the whole area of a wound, including the peri-wound area, and ideally conform to a wound's shape.

Dressings such as ACN-SD, although resulting in a low biofilm formation, allowed small pockets of bacterial growth to take place on the tissue surface, possibly due to limited intimate contact of the tissue with the dressing (Jones et al., 2004). In these pockets biofilm may develop and thrive. Similar results on an agar plate model were shown by Bowler et al. (2010). The model in this study was designed with a flat slice of meat, but the surface had the natural shape of the muscle with small indents and crevices to which an ideal dressing should be able to conform. These studies, in conjunction with other published data (Bowler et al., 2010; Walker and Parsons, 2010, Walker et al., 2011), suggest that dressing technology and construction may be important factors in determining the antimicrobial activity of dressings. Dressings have varied responses due to their technological

differences, including the antimicrobial type, content and mode of release (Parsons et al., 2005).

Therefore from the above, it can be concluded that any dressings in this study which would appear to have absorbed biofilm away from the wound and deeper into the dressing would, in theory, be the better dressings of choice for a chronic wound. The best performing dressings, when comparing the bacteria and biofilm load, by measuring the area of these upon the surface of the model designed, were those of NGAD, PHMBD, ACN-SD, SCHED in this decreasing respective order as shown in the Figure 3.134. The most cost-effective dressings would be those demonstrating effectiveness against biofilm formation, removal of any biofilm and bacteria present, and consistency in performance.

# **Chapter 4**

## **General Discussion**

## 4.1 Discussion

Wound healing is a normal biological process in the human body, and is usually described in four phases: haemostasis, inflammation, proliferation, and re-epithelialization. Patient factors can affect this healing process such as oxygenation, infection, age, stress, diabetes, obesity, medications, alcoholism, smoking, and nutrition (Guo and DiPietro, 2010). A good wound clinic works to combine many aspects of a wound on a patient, taking the individual's health into consideration. Their vascular system, immune system and general health can all contribute to the chronicity of a wound and how quickly it might heal. Unless a wound is managed well from the start, an infection can take hold, and patients who go home with an apparently healing wound can return to clinic with it chronically infected. In a recent clinical study by Hurlow et al. (2016) it was found that 75% of wound beds contained microbial biofilms, despite the use of some currently available antiseptic wound dressings and an effort to provide biofilm-based wound care. In wound management, biofilm must now be considered as a major barrier to healing. Biofilm-based wound care is of great importance in the clinical setting, and it is important that strategies suppress, and ideally remove biofilm, and they should not damage host defences and healing mechanisms. An established principle of phase-adapted wound management is the acronym T.I.M.E. (Schultz et al, 2003). It takes four fundamental principles of wound treatment together: Tissue management (including debridement), Infection control, Moisture balance (i.e., exudate control) and the prevention of damage to the edge of a wound. If a wound becomes colonized or infected it can become chronic (i.e., non-healing) and

practitioners need to select an appropriate antimicrobial dressing (Schultz et al., 2003). Several factors influence the choice of a dressing. Some of these are: management of exudate, maintaining a moist environment, microbial sequestration, promoting debridement, conforming to maintain intimate contact with a wound surface, and using an antimicrobial to manage colonization or infection that does not harm the patient or irritate the wound.

Exudate management is relevant to the quality of life of a patient (Dowsett, 2008). The World Union of Wound Healing Societies positioning document (2016) states that from the patient's perspective, the key issues are that a wound dressing remains in place, prevents leakage, reduces odour and reduces pain (Chadwick and Rastogi, 2016). A lack of control of exudate can lead to problems of continuous dressing changes which leads to increased costs (White and Cutting, 2006). Exudate production is the natural result of inflammation in the early stages of a wound. It is when a wound becomes chronic that exudate increases to a level that can be detrimental to its healing, especially in the presence of colonisation or infection. The management of exudate by the use of advanced wound dressings can depend on the level of exudate and whether the wound is infected (White and Cutting, 2006). In cases of severe exudate production, compression therapy, negative pressure wound therapy, and some form of elevation and exercise may be recommended, especially for lower limb wounds (Kunimoto et al., 2001). However, there are limitations to these methods, especially in wounds with delicate peri-wound edges. Most commercial wound dressings are categorised as suitable for light, moderate or heavily exuding wounds and claim they work by absorption of



exudate, absorption then gelling, or absorption then retention away from the wound, and most can also be used to a degree with some form of applied compression. What matters is that as well as removing the exudate, the dressing should keep the wound moist (Winter, 1962; Bishop et al., 2003; McColl et al., 2007). Maintaining a moist wound facilitates the wound healing processes. It helps to increase the rate of breakdown of dead tissue (autolytic debridement), prevents cell death by dehydration, encourages the formation of blood vessels (Field and Kernstein, 1994), and increases the rate of epithelialisation (Jones et al., 2006). The principle of moist wound healing is that it mimics the interstitial fluid which would normally be maintained by the integrity of the skin (Bishop et al., 2003). Maintaining a moist wound environment, whilst controlling exudate, is a delicate balance. Too much moisture and maceration of the wound edge may occur; too little and the wound will not heal in a timely manner, with the possibility of scarring. The best way to create the best balance of moisture in a wound is to assess it regularly and ensure the dressing in use suits the wound, i.e., ensure that it is removing sufficient moisture without the wound drying out (Yarwood-Ross, 2013). Regular assessment is also useful in checking that the wound has not become infected. If this is suspected, an antimicrobial dressing should be employed. The addition of antimicrobial agents, such as silver, iodine or PHMB, to wound dressings continues to be used to reduce the risk of wound infection (Landis, 2008), yet the presence of protective mechanisms adopted by biofilm microorganisms means it is much more difficult for antimicrobial agents to penetrate through this defence (Serralta et al., 2001), and to manage wound

chronicity (Cowan, 2011). The decision of which antimicrobial dressing to employ can be based on verifiable observation or experience rather than theory, and is often focused on treating a critically colonized wound and infection (Landis, 2008) where the balance in a wound is tipped in favour of the bacteria and wound healing is compromised. Knowing what to look for is a skill, combining both clinical knowledge and wound healing expertise (Sibbald et al., 2006). The mere addition of silver to a non-antimicrobial dressing may not necessarily be sufficient to ensure antimicrobial activity (Walker et al., 2011). The use of ionic silver as an antimicrobial agent is generally accepted and it has been used in a variety of topical preparations including solutions (silver nitrate), creams (silver sulphadizine), and silver-containing dressings (as used in the present study). Topical preparations are still in use today in some clinics, as a cauterizing agent, or for the use in the removal of hypergranulation tissue (British Columbia Provincial Nursing Skin and Wound Committee, 2013). What is in question for clinicians is partly the type of antimicrobial used, but mainly the characteristic of the dressing and its delivery of the antimicrobial to the wound (Mooney et al., 2006). If a dressing cannot make the antimicrobial agent available effectively then its presence is pointless. Also, it should not release an antimicrobial too freely. Any substance that is freely soluble may present toxicity issues, or may be diluted in an exuding wound and thus the effective concentration will be reduced.

Ideally a wound dressing should facilitate autolytic debridement by the host's own proteolytic enzymes and phagocytic cells (Panuncialman and Falanga, 2009).

Some research has even suggested that low levels of bacteria may contribute to

wound healing by producing proteolytic enzymes that help wound debridement and stimulate the release of proteases from neutrophils (Ovington, 2003). The problem with not having a clean wound, however, is that it risks becoming colonized or chronically infected, especially in those patients that are immunocompromised, and the ultimate goal of treatment of a wound is that it does not become infected and heals (American Diabetes Association, 1999). Assisted debridement aids the host wound healing process (Schultz, et al., 2003), but the presence of biofilm in the wound bed can cause a chronic inflammatory reaction, resulting in more damage to the surrounding host tissues (Hurlow and Bowler. 2009). No method, as yet, completely debrides a wound, so biofilm would still be likely to exist (Young, 2011). Absorption would be a better process, as the biofilm would be sequestered out of the wound and into closer contact with any antimicrobial a dressing might contain, thus reducing microbial and biofilm burden, allowing the wound to attempt to heal.

Some of the ideal characteristics of a dressing are that it is strong, comfortable and conformable (Jones et al., 2006). The structure should be such that it can be removed easily and painlessly from a wound. Dressings that fail to do so can increase the risk of colonization or infection, especially if they leave residual debris in a wound (Daunton et al., 2012). Dressing structure can be a contributory factor in the effectiveness of a dressing making available its antimicrobial contents, but conformability is also essential as it helps reduce pockets where microbial proliferation can occur, or dead spaces where excess fluid can build up and cause tissue maceration (Walker and Parsons, 2010). To maximise antimicrobial potency,

a dressing should conform to each wounds' unique topography by so-called intimate contact, in order to maximise exposure.

The observations made, from the results of biofilm growth beneath the various dressings examined in this study, highlight the importance of dressing selection to deal with the increasing likelihood of microbial and/or biofilm presence in wounds. The preliminary work of fixation was necessary to examine the best fixation methods for bacteria, in order to obtain high quality images at the ultrastructural level. One of the best methods of preservation of bacteria for TEM studies is cryo-substitution, as shown in Hobot et al. (1985) with striking images of the detailed structure of the planktonic bacterium. However, this method uses expensive equipment that is not always accessible, and is limited to use by other microscopical techniques. The fixation and processing methods used in this study allowed the high quality images to be produced. The Agar Sandwich model developed in this study allows the researcher to view the whole biofilm without loss, at the LM and TEM level. The biofilm was encased and protected from the harsh processing methods in LM and TEM. The models were then available for LM histological staining techniques, as well as the possibility of the paraffin block being used for techniques such as immunocytochemistry and *in situ* hybridisation.

Studying the planktonic growth at the earlier stages by SEM demonstrated that bacteria begin to form a biofilm within a few hours. This has been suggested in other *in vitro* studies where, during the first few hours clusters or microcolonies of cells form as the consequence of individual cells twitching across the surface towards each other (O'Toole et al., 2000). This demonstrated that biofilm can form

early on a suitable surface, so clinically a wound must be kept clean from the start to reduce the risk of microbial attachment, contamination, colonization or infection. It has also been shown that biofilm can re-form daily, likely within hours, so regular debridement is important (O'Toole et al., 2000; Wolcott et al., 2009; Metcalf and Bowler, 2013). These early time-point studies guided selection of the time slots at which the growth on the models would be staged.

The examination of various surfaces allowed a choice of one which could provide a suitable surface to be used in all of the microscopy methods, without any noticeable artefactual processing damage. The model used for the growth of the biofilm was developed to mimic an exuding wound. The tissue and insert surface were continually supplied with nutrients to keep the surface moist, to examine whether the dressings could cope with a level of moisture typical of a chronic wound.

As an *in vitro* model, examining the activity of dressings upon bacterial and biofilm growth, it performed consistently well as supported by statistical analyses. Various *in vitro* models have been designed for examining the anti-biofilm effect of dressings, and some are designed to examine specific attributes of a dressing, but this novel model was designed to be used for the variety of microscopical methods of LM, TEM, SEM and CLSM. Unlike many models it allowed bacteria to develop from planktonic cells, rather than placing a dressing upon already cultured biofilm. This allowed for the demonstration of how bacteria, if not eradicated from a wound, can find a way of re-colonizing the area if the antimicrobial and retention capability of a dressing are not adequate. The continuous supply of exudate demonstrated

how an antimicrobial agent can be diluted and exhausted if not in continual supply.. The limitations to any *in vitro* model, including this one, are that with an *in vivo* wound model the host's biological processes are present. *In vitro* models allow biofilm to grow unimpeded by a host defence, and therefore dressings should in theory be less effective clinically. However, a recalcitrant wound is in a constantly repetitive inflammatory state and the host's defence is not as effective, but rather can actually be damaging to its own tissue. Biofilm releases antigens which stimulate the production of antibodies from the host, but these antibodies will only respond to the surface antigens and will often fail to penetrate into the matrix of the biofilm and will cause host tissue damage (Davis et al., 2006). The host's polymorphonucleocytes, in response to not being able to ingest biofilm, will release pro-inflammatory enzymes, proteases (e.g. matrix metalloproteinases and cytokines). This chronic inflammatory response unfortunately does not destroy the biofilm, but causes more damage to the surrounding host tissue (Hurlow and Bowler, 2009). Therefore, *in vitro* models have their use. By developing wound models, dressings can be examined without any biological variables which may present in a clinical environment and under controlled situations decisions can be made on which dressing is appropriate to different types of wound.

Wet-to-dry gauze was traditionally used to dress wounds but is now considered to be disruptive to wound healing because this dressing is likely to allow wound tissue and or biofilm to grow into the dressing resulting in a atraumatic removal for the patient (Daunton, et al., 2012). Hence it is no longer widely used in the UK (Jones et al., 2006). It does also not create an optimal moist environment, for which other

newer dressings have been designed. Gauze has still been used in some studies to compare with other dressings, and has always been shown to be less cost-effective and detrimental to healing, with wounds showing up to 72% more healing with more advanced dressings (Harding et al., 2000; Daniels et al., 2001; Singh et al., 2004). The amount of biofilm production in the gauze wound model in this study showed that it acted as a bacterial support and did not prevent biofilm growth.

The NSHD has been shown to be successful in the improving healing rates of wounds in *in vivo* studies (Hoekstra et al., 2002), and in clinical studies compared with gauze and alginates (Robinson, 2000; Foster, 2000). This agrees with the findings of the present study, where the NSHD performed better than the silver-containing ACN-SD at the 24 and 72 hour stages. Ionic silver, as opposed to silver compounds (e.g. silver nitrate), has lower toxicity, and the use of ionic silver in the Hydrofiber dressing (SCHD) showed improved bacterial and biofilm removal in the model, as it has in numerous studies (O'Neil et al., 2003; Ip et al., 2006; Saba et al., 2009; Barnea et al., 2010; Harding et al., 2012), including in burn wound care (Caruso et al., 2004; Muangman et al., 2010). The introduction of NGAD, a relative newcomer to wound management in comparison to the other dressings, has been quickly followed with recent studies which have suggested that clinically the NGAD can facilitate wound healing (Woo et al., 2014; Harding et al., 2015; Walker et al., 2015; Kammerlander et al., 2015; Metcalf et al., 2016a; Metcalf et al., 2016b). The 'Extra' element of the NGAD is in reference to its enhanced strength (two layers stitch-bonded in the Z-direction, and each layer stitch bonded in the XY-direction) compared to standard Hydrofiber dressings, as also found in AQUACEL Extra.

This extra strength has been studied clinically and found to have improved exudate control compared to the previous AQUACEL dressing (NSHD) and other dressings, with less strike-through (Tickle, 2012; Rafter et al, 2015). The modality of these dressings also reduces seepage and peri-wound maceration (Karlock, 2004). The + element of this dressing refers to three actions in the dressing. The first a metal chelator helps to sequester divalent metal ions thought to hold the biofilm polymer structure together. The second is a surfactant, used to reduce surface tensions within the dressing and to have a detergent-like effect on biofilm to loosen it. The third is a pH control of 5.5 to help the 1.2% ionic silver move more rapidly into the biofilm and hence increase the antimicrobial activity. All three are combined in this dressing in an optimum concentration (Metcalf et al., 2016). In a study by Halstead et al., (2016) a comparison was made of honey dressings with a selection of silver dressings, including the NGAD. The NGAD was found to result in a significantly reduced biofilm biomass compared to the other dressings. This is a similar finding to that observed in the present study. Previous clinical evaluations have demonstrated the clinical effectiveness of NGAD (Woo et al., 2014; Harding et al, 2015; Walker et al., 2015; Metcalf et al., 2016a; Metcalf et al., 2016b; Bowler, 2015), and these *in vitro* studies help to further elucidate its mode of action, by suggesting that it helps to reduce biofilm.

Independent evidence-based wound care is essential for clinical practices and is increasingly prominent in governmental health agendas (WUWHS, 2007).

Laboratory and clinical studies on the CES-SD used in this study have been limited and appear to have been performed by the manufacturer. Clinical studies



(Green, 2013; Forlee et al., 2014; Bullough et al., 2015) have used the CES-SD and found some success in management of wounds, but the studies were on a limited number of patients, and with no comparison to another dressing. Cellulose fibres have found a broad application in medical textile field owing to the adsorption, antistatic behaviour, and good mechanical properties. However, cellulose fibres provide an excellent surface for microorganisms' growth (Ristić et al., 2011). Despite the adsorption characteristics of the CES-SD, and it being designed for exudating wounds (Forlee et al., 2014), the CES-SD did not appear to absorb as much exudate as some of the dressings, such as the Hydrofibers, resulting in a lack of fibre swelling and in fibre shedding on to the tissue.

Reviews and studies on alginate dressings recommend it due to its haemostatic and gelling properties (Paul and Sharma, 2001). An *in vitro* study by Barnett and Varley (1987) showed that the ratio of alginate to wound fluid is critical, especially in later healing stages. Doyle et al. (1996) showed that alginate dressings may improve some cellular aspects of normal wound healing, but not others, with cellular reactions, such as an increase in fibroblasts proliferation but a decrease in proliferation in keratinocyte and microvascular cell, being provoked by calcium alginate. An *in vitro* comparison of the ACN-SD used in this study, with the SCHD, was performed by Bell and Hart (2007). They found that the ACN-SD kept its integrity better, but that this caused adherence to the wound tissue. A study by Lipp et al. (2010) concluded that only the silver-containing dressing (ACN-SD) contained fewer bacteria than the NSHD, but that neither eradicated bacteria completely. Walker et al. (2011) studied the effect of low adherent dressings on

microbial growth. They suggested that the results showed the outer, perforated surface created limited contact of the simulated wound surface with the antimicrobial dressing within the dressing. This was apparent in this study with areas of growth in the apparent holes of the dressing by SEM.

Comparisons of NC-SD and SCHED have shown that they have a similar ability to kill planktonic pathogens (O'Neil et al., 2003). Keratinocytes and fibroblasts are susceptible to concentrations of silver that are lethal to bacteria (Poon and Burd, 2004) and hence the visible deposition of nanocrystalline silver in the NC-SD model was of concern. This study showed that the silver was only starting to take effect by 72 hours and that there was a steady increase in the visual amount of silver. A clinical study by Vlachou et al. (2007) showed the silver levels in serum to increase to a maximum of 56.8 µg/l after nine days, with dressing changes every three days. A similar study found silver serum levels were positively associated with the size of burns (Wang et al., 2009b), but that they only reduced to an undetectable level after 6 weeks. Another study (Wang et al., 2009a) found that cutaneous tissue staining due to silver was a common finding of this NC-SD. Therefore cytotoxic effects of high-silver dressings may be of concern.

PHMB cytotoxicity and resistance is virtually non-existent (Kingsely et al., 2009) and the PHMBD has been shown to be well tolerated (Gilliver, 2009). A study on the action of PHMB on bacterial cells and mammalian cells found that PHMB could enter bacterial cells and effect the DNA, whereas mammalian cells trapped the PHMB nanoparticles within endosomes and the DNA was not affected (Chindera et al., 2016). A study comparing PHMBD with SCHED and NC-SD (Haemmerle et al.,

2012) found all the dressings to reduce the bacterial load and to be comparable, although it suggested that the PHMBD reduced it faster (by day 3, in 25% of wounds). The results of this present study also showed a greater reduction in bacterial biofilm by 72 hours in the PHMBD compared to all the dressings tested except the NGAD. The action of PHMB in dressings and the maximum level of toxicity need to be fully confirmed, but a recent review (Hurlow, 2017) concluded that PHMB dressings are an effective barrier to bacterial colonisation and infection.

Various studies have compared the CID to other dressings in a favourable light, such as Akiyama et al. (2004). The Akiyama study was upon bacterially inoculated, cut wounds of mice with various times of addition of the dressing. Although there would likely have been biofilm present, as in the present study, the molecular iodine may not have been diluted as the samples would not have been exposed to the exudative state of a chronic wound. However, this study compared the CID to a variety of antimicrobial and non-antimicrobial dressings, and was not considered effective with this exuding model. *In vivo* studies on this dressing include that of Hansonn (1998). The study compared a CID to two non-antimicrobial dressings - a hydrocolloid dressing and gauze- with similar results in exudation control, comparable dressing changes and more slough formation in the iodine and gauze dressings. This could be compared to the results in the present study of CID and gauze after 72 hours. There was no apparent microscopical work performed on the slough in the Hansonn study, which might have given more information as to whether there was any biofilm amongst the slough, the gauze or the cadexomer beads. Some clinicians and scientists use the terms “biofilm” (viable microbial

tissue) and “slough” (largely non-viable host-derived tissue) interchangeably, and some research proposes that programmed host cell death and autolysis are critical for the timing of microbial biofilm development and dispersion, suggesting that slough will contain biofilm as well as dead cells (Ma et al., 2009). Although this was visualised to some extent in this study, further studies need to be performed on the exact nature and relationship between biofilm and slough to help the development of more effective wound management protocols.

## 4.2 Conclusion

The following objectives have been achieved:

- demonstrating the exponential point, and the effect of the addition of an antimicrobial agent;
- obtaining the best methods of preservation and processing, for the visualisation of bacteria by various microscopy techniques, including:
  - finding a suitable processing protocol and observe planktonic bacteria by TEM;
  - observing the effect of silver nitrate on bacterial ultrastructure by TEM;
  - finding a suitable processing protocol and observe planktonic bacteria by SEM;
  - establishing an appropriate concentration of bacteria to provide a confluent biofilm.
- trialling surfaces for suitability to investigate initial biofilm growth;
- evaluating surfaces that would allow adequate biofilm growth;
- developing a novel, challenging meat model for culturing biofilm to view at 24, 48, and 72 hours by LM, TEM and SEM;
- using the model to test the efficacy of different dressings against biofilm formation, as determined by LM and SEM at 3, 6, 12, 24, 48 and 72 hours, and by TEM and CLSM at 24 and 48 hours.

Wound dressings need to reduce the impact of biofilm. This novel, challenging model has allowed the evaluation of a selection of dressings against an exuding colonized model wound, although it cannot fully reflect the reality of clinical practice. Current treatment strategies can only try to reduce the impact of biofilm and cannot completely rid a wound of it (Hurlow et al., 2016). The need for cleansing after debridement has been shown, by this model, to be important to remove as many bacteria as possible, as biofilm was shown to form within hours. Caution must be employed when using antimicrobial agents, and dressing choices must match the wound type, including exudate and microbial load. This model has shown how some dressings deposit excessive amounts of silver on a wound surface, without it having a more pronounced antimicrobial effect than those containing ionic silver. Excessive silver staining can make it difficult to examine a wound, especially in those patients with darker skin pigmentation (Karlock, 2004). The demonstration of the effect of cadexomer iodine in the model showed how this antimicrobial agent, when diluted by exudate as happens clinically, needs to be continually refreshed. The wound model in the agar sandwich method was designed for use in LM and TEM methods, and processing of the LM models was achieved using a routine histological processing schedule. This could be applied to clinical samples, if they were available, to demonstrate the thickness of a biofilm on the surface of a wound debridement sample (Oates et al., 2014) or tissue biopsy (Malone and Swanson, 2017).

All interactive dressing materials should have the ability to manipulate one or multiple aspects of a wounds environment. Deciding which to use will depend on

the wound, and the wound characteristics may change with time. Combining dressings or using dressings that are multifaceted may give the best solution to healing a wound (Sood et al., 2014). However, the decision of choice should be ultimately on an evidence-based approach, and on clinical experience in examining wounds. Therefore, research such as this, and education in wound care in clinics, is essential in more effectively managing patients with these often debilitating wounds.

### 4.3 Limitations to the study and future recommendations

- Only two bacterial species were examined in this study yet chronic wounds harbour numerous species of microorganism. This model could therefore be used to study other biofilm-forming microbes.
- Only silver, PHMB and iodine antimicrobial agents were studied. Some early work was performed on a Manuka honey-gauze type dressing but, due to the variety of honey dressings available, it was not considered a representative dressing for testing. The study could be repeated on a selection of honey dressings for comparison against the best performing dressings of this study.
- Charcoal dressings are claimed to help reduce wound toxicity and facilitate healing (Ovington, 2003). This model could be used to assess the ability of these dressing types, and others, to prevent biofilm formation.
- Only a routine haematoxylin and eosin stain was used in LM. A mixture of the bacteria was visualised with LM, TEM and SEM. Other histological stains and immunocytochemistry and molecular techniques could be performed on the histological models prepared, to differentiate the bacteria and visualise their location within the biofilm. This would also demonstrate if a particular dressing was more effective at eradicating one bacterial type over another.



- CLSM and TEM were only performed on the 24 and 48 hour models. These techniques could be performed at 12 and 72 hours to give a broader set of information as to the rate of the biofilm formation or reduction.
- X-ray micro-analysis could be used to find the extent of silver deposition in the tissue, as well as histological staining techniques for silver and iodine. Studies on the penetration of these antimicrobials could also be performed on models without a bacterial load, purely to demonstrate the depth of diffusion/penetration.
- Although the dressings were challenged with continuous simulated wound exudate, the absorption rate of the exudate was not measured. This could be performed using the model and measuring the amount of nutrient required to keep the dressings saturated over 72 hours.
- The meat was a relatively flat surface for biofilm development so this could be modified to be more curved, undulating or irregular, to assess the conformability of the dressings.
- The speed and cost of results of certain laboratory scientific studies has been criticised (Hurlow, 2012). The agar sandwich model could be applied to clinical samples. A fresh wound biopsy could be gently fixed then transferred into the agar for processing. This could then be examined in LM and TEM for biofilm growth, and could be compared to clinical work such as that of Hurlow et al. (2016). If used on punch biopsies, this model could be processed and examined for light microscopy within 24-48 hours.

# Appendices

## **Appendix I: Tryptone Soy Broth and Agar plates**

### TSB

Made up as 3% (6g plus 200mls double distilled water). Pour powder carefully into a flask containing the water ensuring it does not touch the sides, and stir well on magnetic stirrer. If using for growth cultures place cotton wool in the neck of the flask. Cover mouth of flask with aluminium foil. Autoclave.

### Agar Plates

Make up TSB and when mixed add 2% agar.

Each plate holds 20mls approx. Each universal holds 10mls approx

Do not make up too many at a time, max 20 plates. Autoclave in flask

Put plates with smallest diameter side as base. Lift lid slightly and pour in agar/TSB, taking care not to introduce possible contamination, and cover.

When set, invert and store in sealed plastic bag in fridge.

### Agar Plates

Make up 3% TSB as above and when mixed add 2% agar (4g).

Cover mouth of flask with aluminium foil. Autoclave.

Swirl flask gently to ensure agar has mixed thoroughly. Allow agar/TSB mix to cool slightly. Put Petri dish plates with smallest diameter side as base. Lift lid slightly and pour in agar/TSB, taking care not to introduce possible contamination, and cover. Each plate holds 20mls approx.

When set, invert and store in sealed plastic bag at 4°C

## Appendix 2: Autoclaving

Pour water over stumps in base. Put in pan and add items.

Put on lid and tighten screws alternately until on firmly. Switch on.

Ensure valve at front is shut and valve on top is open.

When hissing starts the temperature should be between 80-100°C.

Close top valve and wait for the temperature to reach 121°C with the pressure in the red. Time for 15mins then switch off and allow to cool before opening, about 30mins.

### Autoclaving (Dixons Express Autoclaver – Dixons Surgical Ltd)

Open and pour water over stumps in base. Put in pan and add items.

Put on lid and tighten screws alternately until on firmly. Switch on.

Ensure valve at front is shut and valve on top is open.

When hissing starts the temperature should be between 80-100°C.

Close top valve and wait for the temperature to reach 120°C with the pressure in the red.

Time for 15mins then switch off and allow to cool before opening, approximately 30mins.

## Appendix 3: RK buffer

		Total
A	0.59g NA Acetate 1.47g Na Barbitone 50ml distilled water	50ml
B	0.1N HCl	70ml
C	8.5%w/v NaCl                      1.7g in 20ml	20ml
D	1M CaCl <sub>2</sub> ·2H <sub>2</sub> O                      1.47g in 10ml	2.5ml
E	distilled water	110ml

Add totals together and check for pH 6- 6.1

### **Appendix 3: Preparation of agar pellets from cultures**

Agarose

Pipettes

Small diameter piece of plastic tubing

Preparations of cultures should be available, received fixed to filter and put in agar:

Prepare 10ml of 3% agarose solution. Warm up to dissolve thoroughly and keep warm in the heater. Put labelled 1.5 ml microcentrifuge tubestubes in heater ready and prepare labelled vials.

Put a filter in the vacuum mechanism that is smaller than the organism to be captured. Screw on the top and pour some of the culture in – enough to fill up to 5ml approx. Turn on tap and allow vacuum to work. When the culture has filtered through stop vacuum by turning off tap, and remove top.

Using a spatula, scrape off some of the culture and place in 1.5 ml microcentrifuge tubes tube.

Add a few drops of agar and mix well. Place in heater.

Remove filter and wash everything thoroughly.

To make pellets:

Insert metal rod into plastic tube and place into mix in microcentrifuge tubes. Pull up rod until agar mix is pulled up into the tube. Allow to cool. Using the rod, push the agar core out. Top and tail the core. Chop up carefully into small pellets and process.

**Appendix 4: TEM processing schedule using LR White  
(Newman and Hobot 1987; 2001)**

<b>LR White Resin Processing Schedule for Transmission Electron Microscopy</b>		
<b>STEP</b>	<b>REAGENT</b>	<b>TIME(min)</b>
1	Distilled Water	10
2	Distilled Water	10
3	50% ethanol	30
4	70% ethanol	30
5	70% ethanol	30
6	2:1 LR White:70% ethanol	30
7	LR White	30
8	LR White	30
9	LR White	30
10	LR White	Overnight
<p>0.64ml of LR White accelerator was added to 10ml of LR White and mixed thoroughly on ice, pipetted into gelatin capsules, then specimens dropped into base of capsules and cap added. Blocks left at 5°C overnight then placed in 50°C oven for 2 hours.</p>		

## Appendix 5: Histological processing schedule

Processing schedule for Thermo Scientific Excelsior Tissue Processors					
Program 1: "Routine Overnight"			Duration: 14:41hours		
Stage	Reagent	Temperature	Time	Drain	Vacuum
1	IDA	Ambient / 37°	1:00	30	On
2	IDA	Ambient / 37°	1:00	30	On
3	IDA	Ambient / 37°	1:00	30	On
4	IDA	Ambient / 37°	1:00	30	On
5	IDA	Ambient / 37°	1:30	30	On
6	IDA	Ambient / 37°	1:30	60	On
7	Xylene	Ambient / 37°	1:10	30	On
8	Xylene	Ambient / 45°	1:10	30	On
9	Xylene	Ambient / 45°	1:10	60	On
10	Wax	62°	1:20	60	On
11	Wax	62°	1:20	60	On
12	Wax	62°	1:20	60	On

## Appendix 6: Staining Procedure for Light Microscopy

Haematoxylin and Eosin Staining Programme		
STEP	REAGENT	TIME(min)
1	-	0:00
2	Xylene	1:30
3	Xylene	1:30
4	Xylene	1:30
5	Xylene	1:30
6	Alcohol	1:30
7	Alcohol	1:30
8	Water Wash	1:30
9	Haematoxylin	1:30
10	Haematoxylin	1:30
11	Water Wash	1:30
12	Acid alcohol	0:40
13	Water Wash	1:30
14	Scott's Tap Water Solution	0:30
15	Water Wash	1:30
16	Eosin	1:30
17	Water Wash	0:30
18	Alcohol	1:00
19	Alcohol	1:00
20	Xylene	1:30
21	Xylene	Coverslip slides



## Appendix 7: Processing Schedule for Scanning Electron Microscopy using Hexamethyldisilazane

Hexamethyldisilazane Processing Schedule		
STEP	REAGENT	TIME(min)
1	50% ethanol	5
2	70% ethanol	5
3	100% ethanol	5
4	100% ethanol	5
5	Hexamethyldisilazane	5
6	Hexamethyldisilazane	5
7	Hexamethyldisilazane	5
8	Air dry	overnight

## Appendix 8: Sputter coating samples with gold

Turn plug on at the wall. Close chamber vent (clockwise)

Open top and put stub in the centre (1 large per go)

Close the lid ensuring it fits on properly (must not touch top ring of lid)

Press lid down and switch on

Turn from 'standby' to 'pump'. Turn on argon cylinder

Allow chamber vacuum to get to 0.1 (approx 10mins)

Set the cycle time to 2 ½ minutes

Purge with argon

- Open purge – needle on chamber vacuum drops
- Allow 10-15 seconds
- Reclose and wait for needle to reach 0.1

Repeat these steps 5 times

After 5<sup>th</sup> purge allow needle to reach between 0.15 and 0.1

Immediately

- turn switch to sputter
- turn deposition control to get 15mA
- turn purge to keep it at a constant 15mA

Ensure the needle does not waver from 15mA

- if the needle goes right turn the purge dial right
- if the needle goes left turn the purge dial left

When timer finishes, it will switch off from coating. Turn the switch to standby

Turn the deposition control back to 12 o'clock and close purge valve

Open chamber vent. Switch off. Take out samples and close lid. Reclose chamber vent. Switch off at wall. Turn off argon cylinder

## **Appendix 9: Helber Chamber counter**

Ensure the slide is clean, wash with methylated spirit if necessary.

Drop 10  $\mu$ l of culture within the engraved circle on the slide.

Slide cover slip onto the slide, pressing firmly but gently on the edges.

If the cover slip has been correctly positioned, Newtons rings (colour diffraction) will be seen in the contact area between the cover slip and the slide.

Examine the slide under the microscope with lowered illumination. Extreme caution when coarsely adjusting the focus, as the cover slip is delicate.

Count the number of cells lying within 50 small squares.

Cells crossing the lower horizontal or left hand vertical borders are counted as being in that square while those crossing the upper or right hand boundaries are ignored.

## Appendix 10: Table of some wound dressings in use

Dressing name	Dressing materials	Antiseptic	Antiseptic form	Concentration of antiseptic	<i>In vitro</i> evidence for anti-biofilm effectiveness	Clinical evidence for dressing effectiveness
AQUACEL Ag+ Extra (ConvaTec)	CMC (Hydrofiber), Tencel strengthening fibres	Silver	Ionic	1.2% w/w	Parsons 2014; Bowler & Parsons 2016; Parsons et al 2017	Woo et al 2014; Harding et al 2015; Walker et al 2015; Metcalf et al 2016; Metcalf et al 2017
AQUACEL Ag (ConvaTec)	CMC (Hydrofiber), Tencel strengthening fibres	Silver	Ionic	1.2% w/w	Percival et al 2007; Thorn et al 2009; Bowler et al 2012	Hurlow & Bowler 2009; Thorn et al 2009; Hurlow & Bowler 2012; Oates et al 2014; Hurlow et al 2014; Walker et al 2015
Acticoat	Rayon/polyester core	Silver	Nanocrystalline	~10%	Ammonda et al 2011; Bourdillon et al 2017	Miller et al 2011; Tsang et al 2015; Tsang et al 2017
Mepilex Ag	Absorbent polyurethane foam dressing with Safetac™ Technology	silver	silver sulphate	1 - 2%	Halstead et al 2015	
Silver Sulphadiazine	Sulpha drug used as a cream	Silver	Silver sulphadiazine	1%	Bjarnsholt et al 2007	
UrgoClean Ag	non-adherent dressing of poly-absorbent fibres with lipido-colloid particles				Desroche et al 2016	

Dressing name	Dressing materials	Antiseptic	Antiseptic form	Concentration of antiseptic	<i>In vitro</i> evidence for anti-biofilm effectiveness	Clinical evidence for dressing effectiveness
Polyhexamethylene biguanide (PHMB) based dressings	Hydrophilic polyurethane foam dressing with polyhexamethylene biguanide or present in solution	PHMB	PHMB solution	0.1% - 0.5% Concentrations depending on product	Lipp et al 2010; Erberlein et al 2012; Shoukat et al 2015; Phillips et al 2015	Reitsma et al 2001; Seipp et al 2005; Kirker et al 2009
Iodoflex/Iodosorb	A 3D cross-linked polysaccharide starch matrix (Cadexomer), containing 0.9% iodine physically bound to the cadexomer matrix	Iodine	Cadexomer iodine (releases molecular iodine)	0.90%	Thorn et al 2009; Phillips et al 2015; Fitzgerald et al 2017	Miller et al 2011; Fitzgerald et al 2017
SilverCel	Hydro-alginate dressing with EasyLIFT™ Precision Film Technology				Lipp et al 2010	
Inanidine	Chemical complex of povidone, hydrogen iodide, and elemental iodine	Iodine	Solution/ointment	Usually at 10%	Hoekstra et al 2017	
Honey		Usually medical grade Manuka	Variety of components present in respective formulations		Camplin & Maddocks 2014; Phillips et al 2015; Shoukat et al 2015; Halstead et al 2016	Tsang et al 2015; Tsang et al 2017

# References

## REFERENCES

- ADAMS, C. J., MANLEY-HARRIS, M., MOLAN, P. C., (2009). The origin of methylglyoxal in New Zealand manuka (*Leptospermum scoparium*) honey. *Carbohydrate Research*, 344 (8): 1050-1053
- AGUILERA, A., (2008). Extraction of extracellular polymeric substances from extreme acidic microbial biofilm. *Applied Microbiology and Biotechnology*, 78:1079–1088
- AHAMED, M., KARNS, M., GOODSON, M., ROWE, J., HUSSAIN, S.M., SCHLAGER, J.J., HONG, Y., (2008). DNA damage response to different surface chemistry of silver nanoparticles in mammalian cells. *Toxicology and Applied Pharmacology*, 233 (3): 404-410
- AKIYAMA, H., OONO, T., SAITO, M. AND IWATSUKI, K., (2004). Assessment of cadexomer iodine against *Staphylococcus aureus* biofilm in vivo and in vitro using confocal laser scanning microscopy. *The Journal of Dermatology*, 31 (7): 529-534
- AKIYAMA, H., YAMASAKI, O., KANZAKI, H., TADA, J., ARATA, J., (1998). Effects of sucrose and silver on *Staphylococcus aureus* biofilm. *Journal of Antimicrobial Chemotherapy*, 46: 629-634
- ALANDEJANI, T., MARSAN, J., FERRIS, W., SLINGER, R., CHAN, F., (2009). Effectiveness of honey on *Staphylococcus aureus* and *Pseudomonas aeruginosa* biofilms. *Otolaryngology Head Neck Surgery*, 141 (1): 114-118
- AL-BAKRI, A.G., OTHMAN, G., BUSTANJI, Y., (2009). The assessment of the antibacterial and antifungal activities of aspirin, EDTA and aspirin–EDTA combination and their effectiveness as antibiofilm agents. *Journal of applied microbiology*, 107 (1): 280-286
- ALLISON D.G., MATTHEWS M.J., (1992). Effect of polysaccharide interactions on antibiotic susceptibility of *Pseudomonas aeruginosa*. *Journal of Applied Bacteriology* 73: 484–8
- AMERICAN DIABETES ASSOCIATION, (1999). Consensus Development Conference on Diabetic Foot Wound Care: 7-8 April 1999, Boston, MA. *Advances in Skin and Wound Care*, 12 (7): 353-361

AMMONS, M.C., WARD, L.S., JAMES, G.A. (2011) Anti-biofilm efficacy of a lactoferrin/xylitol wound hydrogel used in combination with silver wound dressings. *International Wound Journal*, 8 (3):268-73.

ANDERL, J. N., FRANKLIN, M. J., STEWART, P. S., (2000). Role of antibiotic penetration limitation in *Klebsiella pneumoniae* biofilm resistance to ampicillin and ciprofloxacin. *Antimicrobial Agents and Chemotherapy*, 44: 1818–1824

AQUACEL DATACARD [www.dressings.org/Dressings/aquacel](http://www.dressings.org/Dressings/aquacel), accessed 19/03/2017

ARAUJO, J., TERAN, F., OLIVIERA, R., (2003). Comparison of hexamethyldisilazane and critical point drying treatments for SEM analysis of anaerobic biofilms and granular sludge. *Journal of Electron Microscopy (Tokyo)*, 52 (4): 429-433

ARCHER, N.K., MAZAITIS, M.J., COSTERTON, J.W., LEID, J.G., (2011). Staphylococcus aureus biofilms: properties, regulation, and roles in human disease. *Virulence*, 2 (5): 445-459

ARMSTRONG, S.H., RUCKLEY, C.V., (1997). Use of a fibrous dressing in exuding leg ulcers. *Journal of Wound Care*, 6 (7): 322-324

ATIYEH, B.S., COSTAGLIOLA, M., HAYEK, S.N., DIBO, S.A., (2007). Effect of silver on burn wound infection control and healing: review of the literature. *Burns*, 33 (2): 139-148

ATIYEH, B.S., GUNN, S.W., HAYEK, S.N., (2005). State of the art in burn treatment. *World Journal of Surgery*, 29 (2): 131-148.

ATTINGER, C.E., JANIS, J.E., STEINBERG, J., SCHWARTZ, J., AL-ATTAR, A., COUCH, K., 2006. Clinical approach to wounds: debridement and wound bed preparation including the use of dressings and wound-healing adjuvants. *Plastic and Reconstructive Surgery*, 117 (7S): 72-109

AZEREDO, J., HENRIQUES, M., SILLANKOVA, S., OLIVEIRA, R., (2003). Extraction of exopolymers from biofilms: the protective effect of glutaraldehyde. *Water Science and Technology*, 47 (5):175-179

BAILLIE, G.S., DOUGLAS, J., (1998). Effect of growth rate on resistance of *Candida albicans* biofilms to antifungal agents. *Antimicrobial Agents and Chemotherapy*, 42: 1900–1905



- BARNEA, Y., WEISS, J. AND GUR, E., (2010). A review of the applications of the hydrofiber dressing with silver (Aquacel Ag) in wound care. *Therapeutics and Clinical Risk Management*, 6: 21-27
- BARNETT, S.E., VARLEY, S.J., (1987). The effects of calcium alginate on wound healing. *Annals of the Royal College of Surgeons of England*, 69 (4): 153
- BARRETT, S., (2012). Case series evaluation: the use of Durafiber on exuding wounds. *Wounds*, 6 (10): 469-73
- BASCHONG, W., BASCHONG-PRESCIANOTTO, C., WURTZ, M., CARLEMALM, E., KELLENBERGER, C., KELLENBERGER, E., (1984). Preservation of protein structures for electron microscopy by fixation with aldehydes and/or OsO<sub>4</sub>. *European Journal of Cell Biology*, 35: 21-26
- BELL, A., HART, J., (2007). Evaluation of two absorbent silver dressings in a porcine partial-thickness excisional wound model. *Journal of Wound Care*, 16 (10): 445-453
- BELL, D. C., ERDMAN, N. (Eds.) (2012). A historical Perspective. *Low voltage electron microscopy: principles and applications*, Chapter 1.2. Publishers: John Wiley & Sons
- BENJAMIN, T., MARSH, L.L., JONATHAN, N., WILLIAMS, D., (2016). A novel approach to antibiofilm susceptibility testing using a thermo-reversible matrix. *Journal of Wound Care*, 25 (2): 62-67
- BERGIN, S., WRAIGHT, P. (2006). Silver based wound dressings and topical agents for treating diabetic foot ulcers  
<http://onlinelibrary.wiley.com/doi/10.1002/14651858.CD005082.pub2>, accessed 19/03/2017
- BHUVANESWAR, C.G., EPSTEIN, L.A., STERN, T.A., (2007). Reactions to amputation: recognition and treatment. *Journal of Clinical Psychiatry*, 9 (4): 303-308
- BIANCHI, J., (2012). The effective management of exudate in chronic wounds. *Wounds International*, 3 (4): 1–38
- BIELECKI, P., PUCHAŁKA, J., WOS-OXLEY, M.L., LOESSNER, H., GLIK, J., KAWECKI, M., NOWAK, M., TUMMLER, B., WEISS, S., MARTINS DOS SANTOS, V.A.P., (2011). In-vivo expression profiling of *Pseudomonas Aeruginosa* infections

reveals niche-specific and strain-independent transcriptional programs.  
*www.plosone.org* , 6 (9): e24235, 1-11

BIRCH-ANDERSEN, A. (1960). The use of epoxy resins as embedding media for electron microscopy. *Fourth International Conference on Electron Microscopy*. Publishers: Springer Berlin Heidelberg

BISHOP, S.M., WALKER, M., ROGERS, A.A., CHEN, W.Y., (2003). Importance of moisture balance at the wound-dressing interface. *Journal of Wound Care*, 12 (4): 125

BISWAS, A., BHARARA, M., HURST, C., GRUESSNER, R., ARMSTRONG, D., RILO, H. (2010). Use of Sugar on the Healing of Diabetic Ulcers: A Review. *Journal of Diabetes Science and Technology*, 4 (5): 1139–1145

BJARNSHOLT, T., (2013). The role of bacterial biofilms in chronic infections. *Acta Pathologica, Microbiologica et Immunologica Scandinavica*, 121 (136): 1–51

BJARNSHOLT, T., KIRKETERP-MOLLER, K., JENSEN, P.O., MADSEN, K.G., PHIPPS, R., KROGFELT, K., HOIBY, N., GIVSKO, M., (2008). Why chronic wounds won't heal: A novel hypothesis. *Wound Repair and regeneration*, 16: 2-10

BJARNSHOLT, T., KIRKETERP-MOLLER, K., JENSEN, P.O., MADSEN, K.G., PHIPPS, R., KROGFELT, K., HOIBY, N., GIVSKO, M., (2007). Silver against *Pseudomonas aeruginosa* biofilms. *APMIS*. 115 (8):921-8

BJARNSHOLT, T., TOLKER-NEILSEN, T., GIVSKOV, M., (2011). Quorum Sensing Inhibitors Disable Bacterial Biofilms: Biofilms. *Emerging Trends in Antibacterial Discovery: Answering the Call to Arms*, Chapter 10: 214-215. Ed., Miller, A.A., Miller, P. F., Publishers: Caister Academic Press. Antibacterials Research Unit, Pharmatherapeutics Division, Pfizer Worldwide R&D, USA

BJORNSTI, M.A., HOBOT, J.A., KELUS, A.S., VILLIGER, W., KELLENBERGER, E., (1986). New electron microscopic data on the structure of the nucleoid and their functional consequences Introduction, *Bacterial chromatin*, 64-81. Publishers: Springer Berlin Heidelberg

BLASCHEK, H.P., WANG, H., AGLE, M.E., (2007). Intercellular communication within biofilm communities. *Biofilms in the Food Environment*, Chapter 5: 105-126. Eds., Blaschek, H. P., Wang, H. H., Agle, M. E. Publishers: Blackwell Ltd., Oxford

BLOKKER, E.J.M., VAN DE VEN, B.M., DE JONGH, C.M., SLAATS, P.G.G., (2013). Health Implications of PAH Release from Coated Cast Iron Drinking Water Distribution Systems in the Netherlands. *Environmental Health Perspectives*, 121 (5): 600-606

BLOME-EBERWEIN, S., JOHNSON, R.M., MILLER, S.F., CARUSO, C., JORDAN, M.H., MILNER, S., TREDGET, E.E., SITTIG, K.M., SMITH, L., (2009). Hydrofiber dressing with silver for the management of split-thickness donor sites: A randomized evaluation of two protocols of care. *Burns*, 36: 665-672

BOMBERGER, J.M., MACEACHRAN, D.P., COUTERMARSH, B.A., YE, S., O'TOOLE, G.A., STANTON, B.A., (2009). Long-distance delivery of bacterial virulence factors by *Pseudomonas aeruginosa* outer membrane vesicles. *PLoS pathogens*, 5 (4): p.e1000382.

BOURDILLON, K.A., DELURY, C.P., CULLEN, B.M. (2017). Biofilms and delayed healing - an in vitro evaluation of silver- and iodine-containing dressings and their effect on bacterial and human cells. *International Wound Journal*. doi: 10.1111/iwj.12761. Epub

BOWLER, P. (2015). A real-life clinical evaluation of a next-generation antimicrobial dressing on acute and chronic wounds. *Wounds*, 5 (6): 9

BOWLER, P., JONES, S., TOWERS, V., BOOTH, R., PARSONS, D., WALKER, M., (2010). Dressing conformability and silver-containing wound dressings. *Wounds UK*, 6 (2): 14-20

BOWLER, P., PARSONS, D., (2016). Combatting wound biofilm recalcitrance with a novel anti-biofilm Hydrofiber wound dressing. *Wound Medicine*, 14: 6-11

BOWLER, P.G., JONES, S.A., DAVIES, B.J., COYLE, E. (1999). Infection control properties of some wound dressings. *Journal of Wound Care*, 8 (10): 499-502

BOWLER, P.G., JONES, S.A., WALKER, M., PARSONS, D. (2004). Microbiocidal properties of a silver-containing hydrofiber dressing against a variety of burn wound pathogens. *Journal of Burn Care and Rehabilitation*, 25: 192-196

BOWLER, P.G., PARSONS, D., (2016). Combatting wound biofilm and anti-biofilm Hydrofiber® wound dressing. *Wound Medicine* 14:6-11.

BOWLER, P.G., WELSBY, S., TOWERS, V., BOOTH, V., HOGARTH, A., ROWLANDS, V., JOSEPH, A., JONES, S., (2012). Multidrug-resistant organisms,

wounds and topical antimicrobial protection. *International Wound Journal*,9: 387-396.

BRADLEY, D.F., WOLF, M.K., (1959). Aggregation of dyes bound to polyanions. *The Proceedings of the National Academy of Sciences USA*, 45: 944-952

BRAGA, P.C., CULICI, M., ALFIERI, M., SASSO, M.D., (2008). Thymol inhibits *Candida albicans* biofilm formation and mature biofilm. *International Journal of Antimicrobial Agents*, 31: 472–477

BRITISH COLUMBIA PROVINCIAL NURSING SKIN AND WOUND COMMITTEE IN COLLABORATION WITH WOUND CLINICIANS (2013)  
[www.clwk.ca/buddydrive/file/silver-nitrate-sticks-for-wound-care](http://www.clwk.ca/buddydrive/file/silver-nitrate-sticks-for-wound-care), Adapted from AMG product information sheet, accessed 20/03/2017

BROCKHURST, M.A., BUCKLING, A., RAINEY, P.B. (2005). The effect of a bacteriophage on diversification of the opportunistic bacterial pathogen, *Pseudomonas aeruginosa*. *Proceedings of the Royal Society of London B: Biological Sciences*, 272 (1570): 1385-1391

BROWN, A.F., LEECH, J.M., ROGERS, T.R., MCLOUGHLIN, R.M. (2013). Staphylococcus aureus Colonization: Modulation of Host Immune Response and Impact on Human Vaccine Design. *Frontiers in Immunology*, 4 (Article 507): 1-20

BRYAN, J., (2004). Moist wound healing: a concept that changed our practice, *Journal of Wound Care*, 13 (6): 227-228

BUGEDO, A., BOWLER, F., BISHOP, S.M., (2012). Assessment of the in vitro physical properties of AQUACEL™ Ag Extra™ and AQUACEL™ Ag dressings. *Technical Assessment. WHRI3602 TA235*. 2012, Data on File, ConvaTec Inc

BULLOUGH, L., FUMEROLA, S., FORSTER, E., IVINS, N., TIMMONS, J., (2015). A small multicentre evaluation of a new gelling fibrous silver dressing. *Journal of Community Nursing*, 29 (2): 34-40

BULLOUGH, L., WHITE, E., (2014). New approaches to combating antibiotic resistance. *Wounds UK*, 0 (4): 50-53

BYRNE, B., (2014). Wound Management and Bandaging. *ABC of Dermatology*, 241: 197

CAMPLIN, A.L., MADDOCKS, S.E. (2014). Manuka honey treatment of biofilms of *Pseudomonas aeruginosa* results in the emergence of isolates with increased honey resistance. *Annals of Clinical Microbiology Antimicrobials*, 12;13:19. doi: 10.1186/1476-0711-13-19.

CARDIFF UNIVERSITY WOUND HEALING RESEARCH UNIT (September 2014). <http://www.cardiff.ac.uk/news/view/47308-centre-launches-to-improve-wound-treatment>, accessed 13/03/16

CARUSO, D.M., FOSTER, K.M., HERMANS, M.H.E., RICKMANS, C. (2004). Aquacel® Ag in the management of partial thickness burns: Results of a clinical trial. *Journal of Burn Care and Rehabilitation*, 25 (1): 85-97

CAUSTON, B.E., (1984). The choice of resin for electron immunocytochemistry. *Immunolabelling for Electron Microscopy*, Chapter 3: 29-36 Eds., Polak, J.M., Varndell, I.M., Publishers: Elsevier, Amsterdam

CERCA, N., MARTINS, S., CERCA, F., JEFFERSON, K.K., PIER, G.B., OLIVEIRA, R., AZEREDO, J (2005). Comparative assessment of antibiotic susceptibility of coagulase-negative staphylococci in biofilm versus planktonic culture as assessed by bacterial enumeration or rapid XTT colorimetry. *Journal of Antimicrobiology and Chemotherapy*, 56 (2): 331–6

CHADWICK, P., RASTOGI, A., (2016). Local management of diabetic foot ulcers. *Wounds International*, World Union of Wound Healing Societies (WUWHS), Florence Congress, Position Document, Local Management of Diabetic Foot Ulcers, 12-16

CHANG, S., SIEVERT, D.M., HAGEMAN, J.C., BOULTON, M.L., TENOVER, F.C., DOWNES, F.P., SHAH, S., RUDRIK, J.T., PUPP, G.R., BROWN, W.J., CARDO, D., (2003). Infection with vancomycin-resistant *Staphylococcus aureus* containing the vanA resistance gene. *New England Journal of Medicine*, 348(14), pp.1342-1347.

CHINDERA, K., MAHATO, M., SHARMA, A.K., HORSLEY, H., KLOC-MUNIAK, K., KAMARUZZAMAN, N.F., KUMAR, S., MCFARLANE, A., STACH, J., BENTIN, T., GOOD, L., (2016). The antimicrobial polymer PHMB enters cells and selectively condenses bacterial chromosomes. *Scientific reports*, 6.

CLARKE, M. (2012) Technology update Rediscovering alginate dressings. *Wounds International*, 3 (2): 24-28

CLAXTON, N.S., FELLERS, T.J., DAVIDSON, M.W., (2005). Laser scanning confocal microscopy. Department of Optical Microscopy and Digital Imaging, Florida State University, Tallahassee, [http://www.olympusconfocal.com/theory/LSCMIntro. Pdf](http://www.olympusconfocal.com/theory/LSCMIntro.Pdf), accessed 30/10/2015

CLUTTERBUCK, A.L., COCHRANE, C.A., DOLMAN, J., PERCIVAL, S.L., (2007). Evaluating antibiotics for use in medicine using a poloxamer biofilm model. *Annals of Clinical Microbiology and Antimicrobials* 6:2, <http://www.ann-clinmicrob.com/content/6/1/2>, accessed 13/03/16

COCHRANE, C.A., WALKER, M., BOWLER, P., PARSONS, D., KNOTTENBELT, D. C. (2006). The effect of several silver-containing wound dressings on fibroblast function in vitro using the collagen lattice contraction model. *Wounds-A Compendium of Clinical Research and Practice*, 18 (2): 29-34

COCHRANE, C., RIPPON, M., ROGERS, A., WALMSLEY, A., KNOTTENBELT, D., BOWLER, P., (1999). Application of an in vitro model to evaluate bioadhesion of "fibroblasts and epithelial cells to two different dressings. *Biomaterials*, 20: 1237-1244

CONVATEC.COM, AQUACEL<sup>®</sup> Ag Extra<sup>™</sup> [www.convatec.com/products/pc-wound/aquacel-extra-hydrofiber-dressing](http://www.convatec.com/products/pc-wound/aquacel-extra-hydrofiber-dressing) accessed 12/01/2017

COOPER, R. (2010). Biofilms and wounds: much ado about nothing? *Wounds UK, Clinical Review*, 6 (4): 84-90

COOPER, R.A., MOLAN, P.C., HARDING, K.G., (1999). Antibacterial activity of honey against strains of *Staphylococcus aureus* from infected wounds. *Journal of the Royal Society of Medicine*, 92: 283-285

COSTERTON, J.W., (1984). The Aetiology and Persistence of Cryptic Bacterial Infections: A Hypothesis. *Reviews of Infectious Diseases*, 6 (3): 608-616

COSTERTON, J.W., GEESEY, G.G., CHENG, K.J., (1978). How bacteria stick. *Science America*, 238 (1): 86-95

COSTERTON, J.W., STEWART, P.S., GREENBERG, E.P., (1999). Bacterial biofilms: a common cause of persistent infections. *Science*, 284 (5418): 1318-1322

COSTERTON, W., VEEH, R., SHIRTLIFF, M., PASMORE, M., POST, C., EHRlich, G., (2003). The application of biofilm science to the study and control of chronic bacterial infections. *Journal of Clinical Investigation*, 112 (10): 1466–1477

- COSTERTON, W., WILSON, M., (2004). Introducing Biofilms. *Biofilms*, 1 (1): 1- 4
- COWAN, T., (2011). Biofilms and their management: implications for the future of wound care. *Journal of Wound Care*, 19 (3): 117-120
- COWAN, T., (2012). Visible biofilms — a controversial issue! *Journal of Wound Care*, 21 (3): 106
- CUTTING, K., WHITE, R., (2012). Wound biofilms - Are they visible? *Journal of Wound Care*, (Impact Factor: 1.07); 21 (3): 140-141
- DANAI, P.A., MOSS, M., MANNINO, D.M., MARTIN, G.S., (2006). The epidemiology of sepsis in patients with malignancy. *CHEST Journal*, 129 (6):1432-1440
- DANIELS, S., KERRIGAN, J., (2001). Modern wound dressings are more cost-effective than traditional gauze dressings in managing difficult to heal surgical wounds. *In 11th Conference of the European Wound Management Association*, Abstract 23: 17-19
- D'ARGENIO, D.A., WU, M., HOFFMAN, L.R., KULASEKARA, H.D., DÉZIEL, E., SMITH, E.E., NGUYEN, H., ERNST, R.K., LARSON FREEMAN, T.J., SPENCER, D.H. AND BRITTNACHER, M., (2007). Growth phenotypes of *Pseudomonas aeruginosa* lasR mutants adapted to the airways of cystic fibrosis patients. *Molecular Microbiology*, 64 (2): 512-533
- DAUNTON, C., KOTHARI, S., SMITH, L., STEELE, D. (2012). A history of materials and practices for wound management. *Wound Practice & Research: Journal of the Australian Wound Management Association*, 20 (4): 174
- DAVEY, M.E., O'TOOLE, G.A., (2000). Microbial Biofilms: from Ecology to Molecular Genetics. *Microbiology and Molecular Biology Reviews*, 64 (4): 847–867
- DAVIES, D.G., CHAKRABARTY, A.M., GEESEY, G.G., (1993). Exopolysaccharide production in biofilms: activation of alginate gene expression by *Pseudomonas aeruginosa*. *Applied Environmental Microbiology*, 59 (4): 1181-1186
- DAVIS, S., MARTINEZ, L., KIRSNER, R., (2006). The diabetic foot: the importance of biofilms and wound bed preparation. *Current Diabetic Reports*, 6: 439-445
- DELAQUIS, P.J., MAZZA, G. (1995). Antimicrobial properties of isothiocyanates in food preservation. *Food Technology*, 49 (11): 73-84

- DEMLING, R.H., DESANTI, L. (2001). Effects of silver on wound management. *Wounds*, 13 (1): 4-15
- DESROCHE, N., DROPET, C., JANOD, P., GUZZO, J., (2016). Antibacterial properties and reduction of MRSA biofilm with a dressing combining polyabsorbent fibres and a silver matrix. *Journal of Wound Care* 2;25(10):577-584.
- DONLAN, R.M., (2001). Biofilm formation a clinically relevant process. *Clinical Infectious Diseases*, 33: 1387–1392
- DONLAN, R.M., (2002). Biofilms Microbial Life on Surfaces. *Emerging Infectious Diseases*, 8 (9): 881-890
- DONLAN, R.M., COSTERTON, J.W., (2002). Biofilms: Survival mechanisms of clinically relevant microorganisms. *Clinical Microbiology Reviews*, 15: 167-193
- DOWSETT, C., (2008). Exudate management: a patient-centred approach. *Journal of Wound Care*, 17 (6): 249-252
- DOWSETT, C. AND NEWTON, H., (2005). Wound bed preparation: TIME in practice. *Wounds UK*, 1 (3): 58
- DOYLE, J.W., ROTH, T.P., SMITH, R.M., LI, Y.Q., DUNN, R.M., (1996). Effect of calcium alginate on cellular wound healing processes modelled in vitro. *Journal of Biomedical Materials Research Part A*, 32 (4): 561-568
- DRESSING DATACARD, <http://www.dressings.org/DressingsI>, accessed 21/07/15
- DUNMAN, P.Á., MURPHY, E., HANEY, S., PALACIOS, D., TUCKER-KELLOGG, G., WU, S., BROWN, E.L., ZAGURSKY, R.J., SHLAES, D., PROJAN, S.J., (2001). Transcription Profiling-Based Identification of *Staphylococcus aureus* Genes Regulated by the agr and/or sarA Loci. *Journal of Bacteriology*, 183 (24): 7341-7353
- DUNN, K., EDWARDS-JONES, V., (2004). The role of Acticoat with nanocrystalline silver in the management of burns. *Burns*, 30 (Supp 1):1–9
- DUNNE, W.M., Jr., (2002). Bacterial Adhesion: Seen Any Good Biofilms Lately? *Clinical Microbiology Reviews*, 15 (2): 155–166
- EBERLEIN, T., HAEMMERLE, G., SIGNER, M., GRUBER MOESENBACHER, U., TRABER, J., MITTLBOECK, M., ABEL, M., STROHAL, R.J., (2012). Comparison of PHMB-containing dressing and silver dressings in patients with



critically colonised or locally infected wounds. *Journal of Wound Care*, 21(1):12, 14-6, 18-20.

EDWARDS, J., STAPLEY, S. (2010). Debridement of diabetic foot ulcers. *The Cochrane Library*. Cochrane Database of Systematic Reviews 1. Art. No.: CD003556. DOI: 10.1002/14651858.CD003556.pub2., accessed 13/03/16

EGGER, M.D., PETRAN, M., (1967). New reflected light microscope for viewing unstained brain and ganglion cells. *Science*, 157: 305-30

ESPINAL, P., MARTI, S., VILA, J., (2012). Effect of biofilm formation on the survival of *Acinetobacter baumannii* on dry surfaces. *Journal of Hospital Infection*, 80: 56-60

EVANS, C.A., SMITH, W.M., JOHNSTON, E.A., GIBLETT, E.R., (October 1950). Bacterial Flora of the Normal Human Skin. *Journal of Investigative Dermatology*, 15 (4): 305–324

EWMA (2002-2008). European wound management association, Position documents <http://ewma.org/resources/for-professionals/ewma-documents/ewma-position-documents-2002-2008>, accessed 12/05/2008

FAZLI, M., BJARNSHOLT, T., KIRKETERP-MØLLER, K., JØRGENSEN, B., ANDERSEN, A.S., KROGFELT, K.A., GIVSKOV, M., TOLKER-NIELSEN, T., (2009). Non-random distribution of *Pseudomonas aeruginosa* and *Staphylococcus aureus* in chronic wounds. *Journal of clinical microbiology*, 47 (12): 4084-4089

#### FEI ELECTRON OPTICS

[web.pdx.edu/.../all%20you%20wanted%20to%20know%20about%20electron%20microscopy](http://web.pdx.edu/.../all%20you%20wanted%20to%20know%20about%20electron%20microscopy), accessed 12/05/2016

FELTS, A.D., GIRIDHAR, G., GRAINGER, D.W., SLUNT, J.B., (1999). Efficacy of locally delivered polyclonal immunoglobulin against *Pseudomonas aeruginosa* infection in a murine burn wound model. *Burns*, 25 :415–423

FENG, X., TAN, J., PAN, Y., WU, Q., RUAN, S., SHEN, R., CHEN, X., DU, Y. (2006). Control of hypertrophic scar from inception by using xenogenic (porcine) acellular dermal matrix (ADM) to cover deep second degree burn. *Burns*, 32 (3): 293-298

- FERNANDEZ, R., GRIFFITHS, R. (2012). Water for wound cleansing. *The Cochrane Library Cochrane Database of Systematic Reviews*, Issue 2. Art. No.: CD003861. DOI: 10.1002/14651858.CD003861.pub3, accessed 12/05/2016
- FERREIRA, C., PEREIRA, A.M., MELO, L.F., SIMÕES, M., (2010). Advances in industrial biofilm control with micro-nanotechnology. *Current Research, Technology and Education Topics in Applied Microbiology and Microbial Biotechnology*, 1: 845-854
- FIELD, C.K., KERSTEIN, M.D., (1994). Overview of wound healing in a moist environment. *The American Journal of Surgery*, 167 (1): S2-S6
- FINLEY, P.J., HUCKFELDT, R.E., WALKER, K.D., SHORNICK, L.P., (2013). Silver Dressings Improve Diabetic Wound Healing Without Reducing Bioburden. *Wounds*, 25 (10): 293-301
- FISCHER, E.R., HANSEN, B.T., NAIR, V., HOYT, F.H., DORWARD, D.W., (2013). Scanning Electron Microscopy. *Current protocols in Microbiology*, 25,2B.2: 1–47
- FITZGERALD, D.J., RENICK, P.J., FORREST, E.C., TETENS, S.P., EARNEST, D.N., MCMILLAN, J., KIEDAISCH, B.M., SHI, L., ROCHE, E.D., (2017). Cadexomer iodine provides superior efficacy against bacterial wound biofilms in vitro and in vivo. *Wound Repair and Regeneration*, (1):13-24.
- FLEMMING, H., WINGENDER, J., (2010). The Biofilm Matrix. *Nature Reviews Microbiology*, 8: 623-633
- FONG, J., WOOD, F., (2006). Nanocrystalline silver dressings in wound management: a review. *International Journal of Nanomedicine*, 1 (4): 441–449
- FORLEE, M., ROSSINGON, A., SEARLE, R., (2014), A prospective, open, multicentre study to evaluate a new gelling fibre dressing containing silver in the management of venous leg ulcers. *International Wound Journal*, 11: 438-445
- FOSTER, L., MOORE, P., CLARK, S., (2000). A comparison of hydrofibre and alginate dressings on open acute surgical wounds. *Journal of Wound Care*, 9 (9): 442-445
- FOSTER, T. J. (2004). The Staphylococcus aureus “superbug”. *The Journal of Clinical Investigation*, 114 (12): 1693-1696

- FUJITANI, S., SUN, H.Y., VICTOR, L.Y., WEINGARTEN, J.A., (2011). Pneumonia due to *Pseudomonas aeruginosa*: part I: epidemiology, clinical diagnosis, and source. *CHEST Journal*, 139 (4): 909-919
- FURR, J.R., RUSSELL, A.D., TURNER, T.D., ANDREWS, A. (1994). Antibacterial activity of Actisorb Plus, Actisorb and silver nitrate. *Journal of Hospital Infection*, 27: 201–208
- FUX, C.A., COSTERTON, J.W., STEWART, P.S., STOODLEY, P., (2005). Survival strategies of infectious biofilms. *Trends in Microbiology*, 13 (1): 34-40
- GALEA, E., 2015. Using SILVERCEL® Non-Adherent antimicrobial dressings. *Wounds*, 2 (1): 30-33
- GALILEO, <http://galileotelescope.org/> accessed 23/12/1313
- GARRETT, T.R., BHAKOO, M., ZHANG, Z., (2008). Bacterial adhesion and biofilms on surfaces. *Progress in Natural Science*, 18: 1049–105
- GILBERT, P., JONES, M.V., ALLISON, D.G., HEYS, S., MAIRA, T., WOOD, P., (1998). The use of poloxamer hydrogels for the assessment of biofilm susceptibility towards biocide treatments. *Journal of Applied Microbiology*, 85: 985-990
- GILBERT, P., PEMBERTON, D., WILKINSON, D.E., (1990). Synergism within polyhexamethylene biguanide biocide formulations. *Journal of Applied Bacteriology*, 69 (4): 593-8
- GILLIVER, S., (2009). PHMB: a well-tolerated antiseptic with no reported toxic effects. *Journal of Wound Care*, November supplement: 9-14
- GLAUERT, A.M., GLAUERT, R.H., (1958). Araldite as an embedding medium for electron microscopy. *Journal of Biophysics Biochemistry and Cytology*, 4: 191-194
- GLAUERT, A.M., THORNLEY, M.J., (1966). Glutaraldehyde fixation of gram negative bacteria. *Journal of the Royal Microscopical Society*, 85 (4): 449-453
- GLOVER, D., WICKS, G., (2009). Suprasorb X+ PHMB: the clinical evidence. *Journal of Wound Care*. November supplement: 15-21
- GOMES, A.M., MALCATA, F.X., (1999). *Bifidobacterium* spp. and *Lactobacillus acidophilus*: biological, biochemical, technological and therapeutical properties relevant for use as probiotics. *Trends in Food Science & Technology*, 10 (4): 139-157

- GÓMEZ, M.I., PRINCE, A. (2007). Opportunistic infections in lung disease: Pseudomonas infections in cystic fibrosis. *Current Opinion in Pharmacology*, 7 (3): 244-251
- GRAY, D., (2009). Silvercel™ Non-Adherent dressing: taking the pain out of antimicrobial use. *Wounds UK*, 5 (4): 118-20
- GRAY, D., BARRETT, S., BATTACHARYYA, M., BUTCHER, M., ENOCH, S., FUMEROLA, S., STEPHEN-HAYNES, J., EDWARDS-JONES, V., LEAPER, D., STROHAL, R., WHITE, R., (2010). PHMB and its potential contribution to wound management. *Wounds UK*, 6 (2): 40-46
- GREEN, B., (2013). Making an informed decision: how to choose the correct wound dressing: wound care. *Wound Healing Southern Africa*, 6 (1): 12-20
- GREGORY, K.E. (2011). Microbiome aspects of perinatal and neonatal health. *The Journal of perinatal & neonatal nursing*, 25 (2): 158
- GREY, V., JONES, K.E., HARDING, K.G., (2002). Treatment of the chronic wound. *The Diabetic Foot: Medical and Surgical Management*. Edited by Veves, A., Giurini, J. M., LoGerfo, F. Pub: Springer Science Business Media
- GRICE, E.A., SEGRE, J.A. (2011). The skin microbiome. *Nature Reviews Microbiology*, 9 (4): 244-253
- GUO, S.A., DIPIETRO, L.A., (2010). Factors affecting wound healing. *Journal of Dental Research*, 89 (3): 219-229
- GUPTA, S., BATES-JENSEN, B., GABRIEL, A., HOLLOWAY, A., NIEZGODA, J., WIER, D., (2007). Differentiating negative pressure wound therapy devices: An illustrative case series. *Wounds*, 19 (1 supplement): 1-9
- GURJALA, A.N., GERINGER, M.R., SETH, A.K., HONG, S.J., SMELTZER, M.S., GALIANO, R.D. (2011) Development of a novel, highly quantitative in vivo model for the study of biofilm-impaired cutaneous wound healing. *Wound Repair and Regeneration*, 19: 400-410
- HAEMMERLE, G., DUELLI, H., ABEL, M., STROHAL, R. (2011). The wound debrider: a new monofilament fibre technology. *British Journal of Nursing*, 20 (6): 35

HAEMMERLE, G., SIGNER, M., MITTLBOECK, M., (2012.) Comparison of PHMB-containing dressing and silver dressings in patients with critically colonised or locally infected wounds. *Journal of Wound Care*, 21: 12

HALCÓN, L., MILKUS, K., (2004). Staphylococcus aureus and wounds: a review of tea tree oil as a promising antimicrobial. *American Journal of Infection Control*, 32 (7): 402-408

HALSTEAD, F.D., WEBBER, M.A., RAUF, M., BURT, R., DRYDEN, M., OPPENHEIM, B.A., (2016). In vitro activity of an engineered honey, medical-grade honeys, and antimicrobial wound dressings against biofilm-producing clinical bacterial isolates. *Journal of Wound Care*, 25 (2): 93-102

HANNA, R., RAAD, I.I., (2005). Diagnosis of catheter-related bloodstream infection. *Current Infectious Disease Reports*, 7 (6): 413-419

HÄNSCH, G. M., (2012). Host defence against biofilms-Mission Impossible. *International Scholarly Research Network, Immunology 2012*, Article ID 853123: 1-17, accessed 26/03/16

HANSSON, M.D., (1998). The effects of cadexomer iodine paste in the treatment of venous leg ulcers compared with hydrocolloid dressing and paraffin gauze dressing. *International Journal of Dermatology*, 37 (5): 390-396

HARDING, K.G., JONES, V., PRICE, P., (2000). Topical treatment: Which dressing to choose. *Diabetes/Metabolism Research and Reviews*, 16 (Supplement 1): 47-50

HARDING, K.G., PRICE, P., ROBINSON, B., THOMAS, S., HOFMAN, D., (2001). Cost and dressing evaluation of Hydrofiber and Algnate dressings in the management of community-based patients with leg ulceration. *Wounds*, 13 (6): 229-236

HARDING, K., CUTTING, K., PRICE, P., (2000). The cost-effectiveness of wound management protocols of care. *British Journal of Nursing*, 9 (Suppl 3): S6-S24

HARDING, K.G., SZCZEPKOWSKI, M., MIKOSIŃSKI, J., TWARDOWSKA-SAUCHA, K., BLAIR, S., IVINS, N.M., SAUCHA, W., CAINS, J., PETERS, K., PARSONS, D., BOWLER, P., (2015). Safety and performance evaluation of a next-generation antimicrobial dressing in patients with chronic venous leg ulcers. *International Wound Journal ISSN 1742-4801:1-7*

HEGGERS, J., GOODHEART, R.E., WASHINGTON, J., MCCOY, L., CARINO, E., DANG, T., EDGAR, P., MANESS, C., CHINKES, D., (2005). Therapeutic efficacy

of three silver dressings in an infected animal model. *Journal of Burn Care and Research*, 26 (1): 53-56

HEIMSTAEDT, O., (1911). Das Fluoreszenzmikroskop. *Zeitschrift fur Zellforschung und Mikroskopische Anatomie*, 28: 330–337

HENRICKSON, K.J., AXTELL, R.A., HOOVER, S.M., KUHN, S.M., PRITCHETT, J., KEHL, S.C., KLEIN, J.P., (2000). Prevention of central venous catheter–related infections and thrombotic events in immunocompromised children by the use of vancomycin/ciprofloxacin/heparin flush solution: a randomized, multicenter, double-blind trial. *Journal of Clinical Oncology*, 18 (6): 1269-1278

HOBBIE, J.E., DALEY, R.J., JASPER, S., (1977). Use of Nuclepore filters for counting bacteria by fluorescence microscopy. *Applied Environmental Microbiology*, 33: 1225-1228

HOBOT, J.A., (1990). New aspects of bacterial ultrastructure as revealed by modern acrylics for electron microscopy. *Journal of Structural Biology*, 104: 169-177

HOBOT, J.A., (2015). Bacterial Ultrastructure. *Molecular Medical Microbiology Part 1*, Chapter 2: 7-32. 2nd Edition. Ed., Sussman, M. Publishers: Academic Press, London

HOBOT, J.A., BJÖRNSTI, M.A., KELLENBERGER E., (1987). Use of on-section immunolabeling and cryosubstitution for studies of bacterial DNA distribution. *Journal of Bacteriology*, 169: 2055-2062

HOBOT, J.A., CARLEMALM, E., VILLIGER, W., KELLENBERGER, E., (1984). Periplasmic gel: new concept resulting from the reinvestigation of bacterial cell envelope ultrastructure by new methods. *Journal of Bacteriology*, 160: 143-152

HOBOT, J.A., VILLIGER, W., ESCAIG, J., MAEDER, M., RYTER, A., KELLENBERGER, E., (1985). Shape and fine structure of nucleoids observed on sections of ultra-rapidly frozen and cryosubstituted bacteria. *Journal of Bacteriology*, 162: 960-971

HOBOT, J., WALKER, M., NEWMAN, G., BOWLER, P., (2008). Effect of Hydrofiber® wound dressings on bacterial ultrastructure. *Journal of Electron Microscopy*, 57: 67-75

HOEKSTRA, M.J., HERMANS, M.H.E., RICHTERS, C.D., DUTRIEUX, R.P., (2002). A histological comparison of acute inflammatory responses with a hydrofibre or tulle gauze dressing. *Journal of Wound Care*, 11 (3): 113-117

HOEKSTRA, M.J., WESTGATE, S.J., MUELLER, S., (2017). Povidone-iodine ointment demonstrates in vitro efficacy against biofilm formation. *International Wound Journal*, 14(1):172-179.

HOLLANDER, D., Aquacel Ag Surgical/Trauma Wound Study Group (2007). Randomised clinical trial of Hydrofiber dressing with silver versus povidone–iodine gauze in the management of open surgical and traumatic wounds. *International Wound Journal*, 4 (1): 66-76

HÜBNER, N.O., KRAMER, A., (2010). Review on the efficacy, safety and clinical applications of polihexanide, a modern wound antiseptic. *Skin Pharmacology and Physiology*, Supplement, 23: 17-27

HUNT, T.K., HOPF, H., HUSSAIN, Z. (2000). Physiology of wound healing. *Advances in Skin and Wound Care*, 13 (Supplement 2) :6-11

HURLOW, J., (2012). Response to White and Cutting Critique. *Journal of Wound Care*, Letters, 21 (4): 198

HURLOW, J., BLANZ, E., GADDY, J.A., (2016), Clinical Investigation of Biofilm on Non-Healing Wounds by High Resolution Microscopy Techniques. *Journal of Wound Care* Wuwhs Supplement, 25 (9): S11-22

HURLOW, J., BOWLER, P.G., (2009). Clinical experience with wound biofilm and management: a case series. *Ostomy/Wound Management*, 55 (4): 38-49

HURLOW, J., BOWLER, P.G., (2012). Potential implications of biofilm in chronic wounds: a case series. *Journal of Wound Care* 21: 109-119.

HUTCHINSON, J.J., MCGUCKIN, M., (1990). Occlusive dressings: a microbiologic and clinical review. *American Journal of Infection Control*, 18 (4): 257-268

IFIC, The International Federation of Infection (2011). *Control Basic Concepts of Infection Control, 2nd Edition*, Editors Candace Friedman William Newsom Published by the International Federation of Infection Control, N Ireland, UK [theific.org/wp-content/uploads/2014/08/IFIC-Book.pdf](http://theific.org/wp-content/uploads/2014/08/IFIC-Book.pdf) IFIC

IKUMA, K., DECHO, A.W., LAU, B.L., (2013). The Extracellular Bastions of Bacteria — A Biofilm Way of Life. *Nature Education Knowledge*, 4 (2): 2

INNES, M.E., UMRAW, N., FISH, J.S., GOMEZ, M., CARTOTTO, R.C., (2001). The use of silver coated dressings on donor site wounds: a prospective, controlled matched pair study. *Burns*, 27 (6): 621-627

INTERNATIONAL CASE SERIES: Using PROMOGRAN®/PROMOGRAN PRISMA® on wounds with elevated protease activity: case studies. London: Wounds International, 2013.

IP, M., LUI, S.L., POON, V.K., LUNG, I., BURD, A., (2006). Antimicrobial activities of silver dressings: an in vitro comparison. *Journal of Medical Microbiology*, 55 (1): 59-63

IZANO, E.A., SADOVSKAYA, I., VINOGRADOV, E., MULKS, M.H., VELLIYAGOUNDER K., RAGUNATH, C., KHER, W.B., RAMASUBBU, N., JABBOURI, S., PERRY, M.B., KAPLAN, J.B., (2007). Poly-N-acetylglucosamine mediates biofilm formation and antibiotic resistance in *Actinobacillus pleuropneumoniae*. *Microbial Pathogenesis*, 43: 1

JAHN, A., NIELSEN, P.H. (1998). Cell biomass and exopolymer composition in sewer biofilms. *Water Science and Technology*, 37 (1): 17-24

JAHN, A., GRIEBE, T., NIELSEN, P.H. (1999). Composition of *Pseudomonas putida* biofilms: accumulation of protein in the biofilm matrix. *Biofouling*, 14 (1): 49-57

JAMES, G.A., SWOGER, E., WOLCOTT, R., SECOR, P., SESTRICH, J., COSTERTON, J.W., STEWART, P.S., (2008). Biofilms in chronic wounds. *Wound Repair and Regeneration*, 16: 37-44

JARRAUD, S., MOUGEL, C., THIOULOUSE, J., LINA, G., MEUGNIER, H., FOREY, F., NESME, X., ETIENNE, J., VANDENESCH, F., (2002). Relationships between *Staphylococcus aureus* genetic background, virulence factors, agr groups (alleles), and human disease. *Infection and immunity*, 70 (2): 631-641.

JENKINS, R., BURTON, N., COOPER, R., (2011). Manuka honey inhibits cell division in methicillin-resistant *Staphylococcus aureus*. *Journal of Antimicrobial Chemotherapy*, 66: 2536–2542

JONES, J., (2005). Winter's concept of moist wound healing: a review of the evidence and impact on clinical practice. *Journal of Wound Care*, 14 (6): 273–276



JONES, L., SENCHYNA, M. (2007). Soft contact lens solutions review part 1: Components of modern care regimens. *Optometry in Practice*, 8 (2): 45

JONES, S., BOWLER, P.G., WALKER, M., (2005). Antimicrobial activity of silver-containing dressings is influenced by dressing conformability with a wound surface. *Wounds-A Compendium of Clinical Research and Practice*, 17 (9): 263-270

JONES, S.A., BOWLER, P.G., WALKER, M., PARSONS, D. (2004). Controlling wound bioburden with a novel silver-containing Hydrofiber® dressing. *Wound Repair and Regeneration*, 12: 288-294

JONES, V., (2000). When and how to use iodine dressings. *Nursing Times Wound Care*, 96 (45): 2

JONES, V., GREY, J.E., HARDING, K.G., (2006). Wound dressings. *British Medical Journal*, 332 (7544): 777

JUNG, W.K., KOO, H.C., KIM, K.W., SHIN, S., KIM, S.H., PARK, Y.H., (2008). Antibacterial Activity and Mechanism of Action of the Silver Ion in Staphylococcus aureus and Escherichia coli. *Applied Environmental Microbiology*, 74 (7): 2171-2178

KAUTZ, O., SCHUMANN, H., DEGERBECK, F., VENEMALM, L., JAKOB, T., (2010). Severe anaphylaxis to the antiseptic polyhexanide. *Allergy*, 65 (8): 1068-1070

KEAST, D., LINDHOLM, C., (2012). Ensuring that the correct antimicrobial dressing is selected. *Wounds International*, 3 (3): 21-28

KEAST, D., SWANSON, T., CARVILLE, K., FLETCHER, J., SCHULTZ, G., BLACK, J., (2014). Clinical Update, ten top tips: Understanding and managing wound biofilm. *Wounds International*, 5 (2): 20-24

KELLENBERGER, E., CARLEMALM, E., VILLIGER, W., ROTH, J., GARAVITO, R.M., (1980). Low Denaturation Embedding for Electron Microscopy of Thin Sections. *Journal of Cell Biology*, 17: 208-212

KELLENBERGER, E., CARLMAN, E., STAUFFER, E., KELLENBERGER, C., (1981). In vitro studies of the fixation of DNA, nucleoprotamine, nucleohistone and proteins. *European Journal of Cell Biology*, 25: 1-4

KELLENBERGER, E., RYTER, A., (1964). In Bacteriology. *Modern Developments in Electron Microscopy*, 335-393. Ed., Siegel, B. M. Publishers: Academic Press, London

KELLENBERGER, E., RYTER, A., SECHAUD, J., (1958). Electron Microscope study of DNA-containing plasms. *Journal of Biophysical and Biochemical cytology*, 4: 671-688

KELLENBERGER, E., SECHAUD, J., BLONDEL, B., (1972). A micromethod for the embedding of small amounts of cells from liquid suspension. *Journal of Ultrastructure Research*, 39: 606-607

KERR, M., (2012). Foot care for people with diabetes: the economic Case for Change. NHS Diabetes and Kidney Care, London.  
[http://webarchive.nationalarchives.gov.uk/\\*/http://www.diabetes.nhs.uk](http://webarchive.nationalarchives.gov.uk/*/http://www.diabetes.nhs.uk), accessed 20/12/2013

KHAN, S., ALAM, F., AZAM, A., KHAN, A.U., (2012). Gold nanoparticles enhance methylene blue–induced photodynamic therapy: a novel therapeutic approach to inhibit *Candida albicans* biofilm. *International Journal of Nanomedicine*, 7: 3245–32

KINGSLEY, A., TADEJ, M., COLBOURN, A., KERR, A., BREE-ASLAN, C., (2009). Suprasorb® X+PHMB: antimicrobial and hydrobalance action in a new wound dressing. *Wounds UK*, 5 (1): 72-77

KIRKER, K., FISHER, S., GARTH, J., MCGHEE, D., SHAH, C., (2009) Efficacy of Polyhexamethylene Biguanide-containing Antimicrobial Foam Dressing Against MRSA Relative to Standard Foam Dressing. *Wounds*. 21(9):229-333

KIRKER, K.R., SECOR, P.R., JAMES, G.A., FLECKMAN, P., OLERUD, J.E., STEWART, P.S., (2009). Loss of viability and induction of apoptosis in human keratinocytes exposed to *Staphylococcus aureus* biofilms in vitro. *Wound Repair and Regeneration*, 17 (5): 690–699

KIRKETERP-MØLLER, K., JENSON, P.O., FAZLI, M., MADSEN, K.G., PEDERSEN, J., MOSER, C., TOLKER-NIELSEN, T., GIVSVOV, M., HOIBY, N., (2008). Distribution, organisation, and ecology of bacteria in wounds. *Journal of Clinical Microbiology*, 46: 2712-22

KLAUSEN, M., HEYDORN, A., RAGAS, P., LAMBERTSEN, L., AES-JORGENSEN, A., MOLIN, S., TOLKER-NIELSEN, T., (2003). Biofilm formation by *Pseudomonas aeruginosa* wild type, flagella and type IV pili mutants. *Molecular Microbiology*, 48: 1511–1524

KLUYTMANS, J.A.J.W., MOUTON, J.W., IJZERMAN, E.P.F., VANDENBROUCKE-GRAULS, C.M.J.E., MAAT, A.W.P.M., WAGENVOORT, J.H.T., VERBRUGH, H.A., (1995). Nasal carriage of *Staphylococcus aureus* as a major risk factor for wound infections after cardiac surgery. *Journal of Infectious Diseases*, 171 (1): 216-219

KNOLL, A. H. (2008). Cyanobacteria and earth history. The Cyanobacteria: Molecular Biology, *Genomics, and Evolution*, Chapter 1: 1-20. Ed., Herrero, A. Publisher: Horizon scientific Press

KORBER, D.R., LAWRENCE, J.R., (2004) Biofilm Formation, *Encyclopedia of Meat Sciences*. Edited by Carrick Devine, M. Dikeman. Elsevier Ltd Editor-in-Chief: Werner Klinth Jensen, ISBN: 978-0-12-464970-5: 59-68

KOSEKI, H., (2014). Early Staphylococcal biofilm formation on solid orthopaedic implant materials: an in vitro study. *Public Library of Science*, 9 (10) ref no: e107588

KOSTENKO, V., LYCZAK, J., TURNER, K., MARTINUZZI, R.J., (2010). Impact of silver-containing wound dressings on bacterial biofilm viability and susceptibility to antibiotics during prolonged treatment. *Antimicrobial Agents and Chemotherapy*, 54 (12): 5120-5131

KOZIEL, J., POTEMPA, J., (2013). Protease-armed bacteria in the skin. *Cell and Tissue Research*, 351(2): 325-337

KURODA, M., OHTA, T., UCHIYAMA, I., BABA, T., YUZAWA, H., KOBAYASHI, I., CUI, L., OGUCHI, A., AOKI, K.I., NAGAI, Y., LIAN, J., (2001). Whole genome sequencing of methicillin-resistant *Staphylococcus aureus*. *The Lancet*, 357 (9264): 1225-1240

KUNIMOTO, B., COOLING, M., GULLIVER, W., HOUGHTON, P., ORSTED, H., SIBBALD, R.G., (2001). Best practices for the prevention and treatment of venous leg ulcers. *Ostomy Wound Management*, 47 (2): 34-51

LANDIS, S. J., (2008). Chronic wound infection and antimicrobial use. *Advances in Skin and Wound Care*, 21 (11): 531-540

LANSDOWN, A.B.G., (2002). Silver I: its antibacterial properties and mechanism of action. *Journal of Wound Care*, 11 (4): 125-30

- LANSDOWN, A. B. (2004). A review of the use of silver in wound care: facts and fallacies. *British Journal of Nursing Supplement*, 13 (6): 6-19
- LANTIS, J., SCHULTZ, G., EDMONDSON-JONES, M., (2016). Effects of Cadexomer Iodine on biofilm in diabetic foot ulcers: A pilot study. *In World Union of Wound Healing Societies Congress Meeting*
- LASA, I., DEL POZO, J.L., PENADÉS, J.R., LEIVA, J., (2005). Bacterial biofilms and infection. *Anales del Sistema Sanitario del Navarra*, 28 (2): 163-175
- LAWRENCE K., (2004). What You Should Know About Using Silver Products. *Wound Care podiatry today*, 17 (11) <http://www.podiatrytoday.com/article/3156>, accessed 07/07/16
- LAWRENCE, J.R., KORBER, D.R., HOYLE, B.D., COSTERTON, J.W., CALDWELL, D.E., (1991). Optical sectioning of microbial biofilms. *Journal of Bacteriology*, 173 (20): 6558
- LEHMANN, H., (1913). Das Lumineszenz-Mikroskop, seine Grundlagen und seine Anwendungen. *Zeitschrift fur Zellforschung und Mikroskopische Anatomie*, 30: 418–470
- LEMBKE, C., PODBIELSKI, A., HIDALGO-GRASS, C., JONAS, L., HANSKI, E., KREIKEMEYER, B., (2006). Characterization of Biofilm Formation by Clinically Relevant Serotypes of Group A Streptococci. *Applied Environmental Microbiology*, 72 (4): 2864-2875
- LEWANDOWSKI, Z., (2005). Biofilms: recent advances in their study and control. *Structure and function of biofilms*, Chapter 1: 1-18. ED., Evans, L. V. Publishers: Harwood Academic, Amsterdam
- LEWIS, K., (2001). Riddle of Biofilm Resistance. *Antimicrobial agents and chemotherapy*, 45 (4): 999–1007
- LIMA, K.C., FAVA, L.R., SIQUEIRA, J.F.JR. (2001). Susceptibilities of *Enterococcus faecalis* biofilms to some antimicrobial medications. *Journal of Endodontics*, 10: 616-9
- LIPP, C., KIRKER, K., AGOSTINHO, A., JAMES, G., STEWART, P., (2010). Testing wound dressings using an in vitro wound model. *Journal of Wound Care*, 19 (6): 220–226

LOH, J.V., PERCIVAL, S.L., WOODS, E.J., WILLIAMS, N.J., COCHRANE, C.A., (2009). Silver resistance in MRSA isolated from wound and nasal sources in humans and animals. *International Wound Journal*, 6 (1): 32-38

LUPPENS, S.B., TEN CATE, J.M., (2005). Effect of biofilm model, mode of growth, and strain on streptococcus mutans protein expression as determined by two-dimensional difference gel electrophoresis. *Journal of Proteome Research*, 4 (2): 232-237

MA, L., CONOVER, M., LU, H., PARSEK, M.R., BAYLES, K., WOZNIAK, D.J., (2009). Assembly and Development of the *Pseudomonas aeruginosa* Biofilm Matrix. *Public Library of Science Pathogens*, 5 (3): 1-11

MAALØE, O., BIRCH-ANDERSEN, A., (1956). On the organization of the 'nuclear material' in *Salmonella typhimurium*. Bacterial Anatomy, *Symposium for the Society of General Microbiology*, 6: 261-278. Publishers: Cambridge University Press

MAJTAN, J., BOHOVA, J., HORNIACKOVA, M., KLAUDINY, J., MAJTAN, V. (2013). Anti-biofilm Effects of Honey Against Wound Pathogens *Proteus mirabilis* and *Enterobacter cloacae*. *Phytotherapy Research*, 28 (1): 69-75

MALIK, A., MOHAMMAD, Z., AHMAD, J., (2013). The diabetic foot infections: Biofilms and antimicrobial resistance. *Diabetes and Metabolic Syndrome: Clinical Research and Reviews*, 7: 101–10

MALONE, M., BJARNSHOLT, T., MCBAIN, A.J., JAMES, G.A., STOODLEY, P., LEAPER, D., TACHI, M., SCHULTZ, G., SWANSON, T., WOLCOTT, R.D., (2017). The prevalence of biofilms in chronic wounds: a systematic review and meta-analysis of published data. *Journal of Wound Care*, 26 (1): 20-25

MANDAL, M.D., MANDAL, S. (2011). Honey: Its medicinal property and antibacterial activity. *Asian Pacific Journal of Tropical Biomedicine*, 1 (2): 154-160

MARSH, P.D., BRADSHAW, D.J., (1995). Dental Plaque as a Biofilm. *Journal of Industrial Microbiology*, 15: 169-175

MARTINEAU, L., DOSCH, H.M. (2007). Biofilm reduction by a new burn gel that targets nociception. *Journal of Applied Microbiology*, 103 (2): 297-304

MASON, D.J., POWELSON, D.M., (1956). Nuclear division as observed in live bacteria by a new technique. *Journal of Bacteriology*, 71: 474-479

MATH INSIGHT Harvest of natural populations

[mathinsight.org/harvest\\_natural\\_populations](http://mathinsight.org/harvest_natural_populations), accessed 26/06/2016

MCBAIN A.J. (2009). In Vitro Biofilm Models: An Overview. *Advances in Applied Microbiology*, 69: 99-132

MCNAMARA, K.J., AWRAMIK, S.M. (1992). Stromatolites: a key to understanding the early evolution of life. *Science Progress (1933-2010)*: 345-364

MCCOLL, D., CARTLIDGE, B., CONNOLLY, P., (2007). Real-time monitoring of moisture levels in wound dressings in vitro: An experimental study. *International Journal of Surgery*, 5 (5): 316-322

MEADS, C., LOVATO, E., LONGWORTH, L. (2015). The Debrisoft® monofilament debridement pad for use in acute or chronic wounds: A NICE medical technology guidance. *Applied health economics and health policy*, 13 (6): 583-594

MERCKOLL, P., JONASSEN, T.O., VAD, M.E., JEANSSON, S.L., MELBY, K.K. (2009) Bacteria, biofilm and honey: A study of the effects of the honey on 'planktonic' and biofilm-embedded wound bacteria. *Scandinavian Journal of Infectious Diseases*, 41(5): 341–7

METCALF, D.G., BOWLER, P.G. (2013). Biofilm delays wound healing: A review of the evidence. *Burns and Trauma*, 1 (1): 5

METCALF, D.G., BOWLER, P.G., HURLLOW, J., (2014). A clinical algorithm for wound biofilm identification. *Journal of Wound Care*, 23 (3): 137-142

METCALF, D., PARSONS, D., BOWLER, P., (2016). A next-generation antimicrobial wound dressing: a real-life clinical evaluation in the UK and Ireland. *Journal of wound care*, 25 (3): 132-134

METCALF, D., PARSONS, D., BOWLER, P., (2017). Clinical safety and effectiveness evaluation of a new antimicrobial wound dressing designed to manage exudate, infection and biofilm *International Wound Journal*, 14:203-213.

METCALF, D., PARSONS, D., BOWLER, P., (2016b). Development of a next-generation antimicrobial wound dressing. *Acta medica Croatica: časopis Hrvatske akademije medicinskih znanosti*, 70 (1): 49-56

MIKKELSEN, H., DUCK, S., LILLEY, K.S., WELCH, M., (2007). Interrelationships between Colonies, Biofilms, and Planktonic Cells of *Pseudomonas aeruginosa*. *Bacteriology*, 189 (6): 2411–2416

MILLER, C.N., CARVILLE, K., NEWALL, N., KAPP, S., LEWIN, G., KARIMI, L., SANTAMARIA, N., (2011) Assessing bacterial burden in wounds: comparing clinical observation and wound swabs. *International Wound Journal*, 8(1):45-55.

MILLER-KEANE (2003). *Encyclopedia and Dictionary of Medicine, Nursing, and Allied Health*, 7th Edition. Eds., Miller, B. F., O'Toole, M. T. Publishers: Saunders

MINSKY, M., (1988). Memoirs on Inventing the Confocal Scanning Microscope. *Scanning*, 10: 128-138

MITCHELL, P.D., BOSTON, C., CHAMBERLAIN, A.T., CHAPLIN, S., CHAUHAN, V., EVANS, J., WITKIN, A. (2011). The study of anatomy in England from 1700 to the early 20th century. *Journal of anatomy*, 219 (2): 91-99

MONCANY, M.L. J., KELLENBERGER, E., (1981). High magnesium content of *Escherichia coli* B. *Experientia*, 37: 846-847

MOONEY, E.K., LIPPITT, C., FRIEDMAN, J. and Plastic Surgery Educational Foundation DATA Committee, (2006). Silver dressings. *Plastic and Reconstructive Surgery*, 117 (2): 666-669

MOORE, K., GRAY, D. (2007). Using PHMB antimicrobial to prevent wound infection. *Wounds UK*, 3 (2): 96–102

MORGAN, T. (2014). Wound care in the community: infection, exudate and conformability. *Journal of Community Nursing*, 28 (5): 43-48

MOTTA, G.J., MILNE, C.T., CORBETT, L.Q., (2004). Impact of antimicrobial gauze on bacterial colonies in wounds that require packing. *Ostomy Wound Management*, 50 (8): 48-62

MUANGMAN, P., PUNDEE, C., OPASANON, S., MUANGMAN, S., (2010). A prospective, randomized trial of silver containing hydrofiber dressing versus 1% silver sulfadiazine for the treatment of partial thickness burns. *International Wound Journal*, 7 (4): 271-276

MUDGE, E., PRICE, P., NEAL, W., HARDING, K.G., (2014). A randomized controlled trial of larval therapy for the debridement of leg ulcers: Results of a multicenter, randomized, controlled, open, observer blind, parallel group study. *Wound Repair and Regeneration*, 22: 43–51

MUSUMECI, G. (2014). Past, present and future: overview on histology and histopathology. *Journal of Histology and Histopathology* 1: 5.  
<http://dx.doi.org/10.7243/2055-091X-1-5>, accessed 12/12/20

NADELL, C.D., XAVIER, J.B., FOSTER, K.R., (2009). The socio-biology of biofilms. *FEMS Microbiology Review*, 33: 206-244

NEU, T.R., LAWRENCE, J.R., (2014). Advanced techniques for in situ analysis of the biofilm matrix (structure, composition, dynamics) by means of laser scanning microscopy. *Microbial biofilms: methods and protocols*, 1147: 43-64

NEW SCIENTIST, <https://www.newscientist.com/.../dn27563-leeuwenhoeks-animalcules>, accessed 17/07/2016

NEWMAN, G.R., HOBOT, J.A., (1987). Modern acrylics for post-embedding immunostaining techniques. *Journal of Histochemistry and Cytochemistry*, 35: 971-981

NEWMAN, G.R., HOBOT, J.A., (1999). Resins for combined light and electron microscopy: a half century of development. *Histochemical Journal*, 31: 495-505

NEWMAN, G.R., HOBOT, J.A., (2001). Resin Microscopy and On-Section *Immunocytochemistry*. (2nd edition) Springer-Verlag, Heidelberg

NEWMAN, G.R., WALKER, M., HOBOT, J.A., BOWLER, P.G., (2006). Visualisation of bacterial sequestration and bacterial activity within hydrating Hydrofiber® wound dressings. *Biomaterials*, 27: 1129-1139

NICHOLSON, D., DEPARTMENT OF HEALTH (2012) Governments Quality, Innovation, *Productivity and Prevention agenda* [www.gov.uk/doh](http://www.gov.uk/doh), accessed 20/01/2016

NIVENS, D.E, OHMAN, D.E, WILLIAMS, J., FRANKLIN, M.J., (2001). Role of alginate and its O acetylation in formation of *Pseudomonas aeruginosa* microcolonies and biofilms. *Journal of Bacteriology* 183: 1047–57

NNIS, National Nosocomial Infections Surveillance System Report (2004), Data summary from January 1992 through June 2004, issued October 2004. *American Journal of Infection Control*, 32 (8): 470–85

NOMARSKI, G., WEILL, A.R., (1955). Application a la metallographie des methodes interferentielles a deux ondes pclarisees. *Revue Metallurgie*, 52: 121-134



- NUSBAUM, A.G., KIRSNER, R.S., CHARLES, C.A. (2012). Biofilms in dermatology. *Skin Therapy Letters*, 17 (7): 1-5
- O'NEILL, M.A.A., VINE, G.J., BEEZER, A.E., BISHOP, A.H., HADGRAFT, J., LABETOULLE, C., WALKER, M., BOWLER, P.G., (2003). Antimicrobial properties of silver-containing Wound dressings: a micro-calorimetric study: *International Journal of Pharmacy*, 263: 61-68
- O'TOOLE, G., KAPLAN, H.B., KOLTER, R., (2000). Biofilm Formation as Microbial Development. *Annual Review of Microbiology*, 54: 49–79
- OATES, A., BOWLING, F.L., BOULTON, A.J.M., BOWLER, P.G., METCALF, D.G., MCBAIN, A.J., (2014). The Visualization of Biofilms in Chronic Diabetic Foot Wounds Using Routine Diagnostic Microscopy Methods. *Journal of Diabetes Research*, Article ID:153586, accessed 26/06/2016
- OATLEY, C.W., The early history of the electron microscope. *Advances in Imaging and Electron Physics*, 133: 7-32. Ed., Hawkes, P. W. Publishers: Academic Press
- CHOI, O., YU, C.P., FERNÁNDEZ, G.E., HU, Z., (2010). Interactions of nanosilver with Escherichia coli cells in planktonic and biofilm cultures. *Water research*, 44 (20): 6095-6103.
- OLSON, J.M., PIERSON, B.K., (1986) Photosynthesis 3.5 thousand million years ago. *Photosynthesis Research*, 9 (1): 251–259
- OMI, S., (2007). People-centred health care: a policy framework. Geneva: WHO (Regional Committee for the Western Pacific) policy document :1-7
- ORIEL, J.D., (1991). Eminent Venereologists 5: Carl Crede. *Genitourinary Medicine*, 67: 67-69
- OVINGTON, L. (2003). Bacterial toxins and wound healing. *Ostomy/wound Management*, 49, Supplement 7A: 8-12
- OVINGTON, L.G., (2004). The truth about silver. *Ostomy/wound management*, 50 (9A Suppl): 1S-10S
- PALUCKA, T., (2002). Overview of Electron Microscopy, 1931-2000. History of Recent Science and Technology. *The Dibner Institute for the History of Science and Technology*,

[http://authors.library.caltech.edu/ElectronMicroscope/EM\\_HistOverview](http://authors.library.caltech.edu/ElectronMicroscope/EM_HistOverview), accessed 20/01/2016

PAMP, S.J., GJERMANSEN, M., TOLKER-NIELSEN, T. (2007). The biofilm matrix: a sticky framework. *The biofilm mode of life: mechanisms and adaptations*, 37-69

PANUNCIALMAN, J., FALANGA, V. (2009). The science of wound bed preparation. *Surgical Clinics of North America*, 89 (3): 611-626

PARSEK, M.R., SINGH, P.K., (2003). Bacterial Biofilms: An Emerging Link to Disease Pathogenesis. *Annual Review of Microbiology*, 57: 677–701

PARSONS, D., (2014). Designing a dressing to address local barriers to wound healing. Next-generation antimicrobial dressings: AQUACEL™ Ag+ Extra™ and Ribbon. London: Wounds International, (Supplement): 6-9

PARSONS, D., BOWLER, P.G., MYLES, V., JONES, S., (2005). Silver antimicrobial dressings in wound management: a comparison of antibacterial, physical, and chemical characteristics. *Wounds - A Compendium of Clinical Research and Practice*, 17 (8): 222-232

PARSONS, D., MEREDITH, K., ROLANDS, V.J., SHORT, D., METCALF, D.G., BOLWER, P.G. (2016). Enhanced performance and mode of action of a novel antibiofilm Hydrofiber® wound dressing. *Biomedical Research International*. 14 pages. Art. ID 7616471. <http://dx.doi.org/10.1155/2016/7616471>, accessed 13/03/16

PARSONS, D., METCALF, D., (2014). Understanding local barriers to wound healing. Next-generation antimicrobial dressings: AQUACEL™ Ag+ Extra™ and Ribbon. *Wounds International* Supplement:1-5 [www.woundsinternational.com](http://www.woundsinternational.com). accessed 17/07/2016

PASTAR, I., NUSBAUM, A.G., GIL, J., PATEL, S.B., CHEN, J., VALDES, J., STOJADINOVIC, O., PLANO, L.R., TOMIC-CANIC, M., DAVIS, S.C., (2013). Interactions of Methicillin Resistant Staphylococcus aureus USA300 and Pseudomonas aeruginosa in Polymicrobial Wound Infection. *Public Library of Science*, 8 (2): 1-11

PAUL, W., SHARMA, C.P., (2004). Chitosan and alginate wound dressings: a short review. *Trends in Biomaterials and Artificial Organs*, 18 (1): 18-23

PERCIVAL, S.L., BOWLER, P.G., (2004). Biofilms and their potential role in wound healing. *Wounds*, 16 (7): 234-240

PERCIVAL, S.L., BOWLER, P., DOLMAN, J., (2007). Antimicrobial activity of silver-containing dressings on wound microorganisms using an in vitro biofilm model. *International Wound Journal*, 4 (2): 186-191

PERCIVAL, S.L., BOWLER, P., WOODS, E.J., (2008). Assessing the effect of an antimicrobial wound dressing on biofilms. *Wound Repair and Regeneration*, 16 (1): 52-57

PERCIVAL, S.L., HILL, K.E., WILLIAMS, D.W., HOOPER, S.J., THOMAS, D.W. AND COSTERTON, J.W., (2012). A review of the scientific evidence for biofilms in wounds. *Wound repair and regeneration*, 20 (5): 647-657

PERCIVAL, S.L., KITE, P., EASTWOOD, K., MURGA, R., CARR, J., ARDUINO, M.J., DONLAN, R.M. (2005) Tetrasodium EDTA as a novel central venous catheter lock solution against biofilm. *Infection Control and Hospital Epidemiology*, 26: 511–514

PERCIVAL, S.L., MALIC, S., CRUZ, H., WILLIAMS, D.W. (2011). Introduction to biofilms. *Biofilms and veterinary medicine*, 41-68. Publishers: Springer Berlin Heidelberg

PERCIVAL, S.L., SULEMAN, L., (2015). Slough and biofilm: removal of barriers to wound healing by desloughing. *Journal of Wound Care*, 24 (11): 498-510

PHILLIPS, P.L., WOLCOTT, R.D., FLETCHER, J., SCHULTZ, G S., (2010). Biofilms Made Easy. *Wounds International*, 1 (3): 1-6

PHILLIPS, P.L., YANG, Q., DAVIS, S., SAMPSON, E.D., AZEKE, J.I., HAMADM A., SCHULTZ, G.S. (2013). Antimicrobial dressing efficacy against mature *pseudomonas aeruginosa* biofilm on porcine skin explants. *International Wound Journal* 12 (4): 469-483

PHILLIPS, P.L., YANG, Q., SAMPSON, E., SCHULTZ, G., (2010). Effects of Antimicrobial Agents on an In Vitro Biofilm Model of Skin Wounds, *Advances in Wound Care*, 1: 299 – 304

PINNEGAR, M.D., PINNEGAR, F.C. (1986). History of burn care: A survey of important changes in the topical treatment of thermal injuries. *Burns*, 12 (7): 508-517

POON, V.K., BURD, A. (2004). In vitro cytotoxicity of silver: implication for clinical wound care. *Burns*, 30 (2): 140-147

PORTER, J.R. (1976). Antony van Leeuwenhoek: tercentenary of his discovery of bacteria. *Bacteriological reviews*, 40 (2): 260

POSNETT, J., FRANKS, P.J., (2007). The costs of skin breakdown and ulceration in the UK. *Skin Breakdown: The Silent Epidemic*: 6-12. Ed., Pownall, M. Publishers: Hull, Smith & Nephew Foundation

POSNETT, J., FRANKS, P.J., (2008). The burden of chronic wounds. *UK.Nursing Times*, 104 (3): 44–45

PRAKASH, B., VEEREGOWDA, B.M., KRISHNAPPA, G., (2003). Biofilms: A Survival Strategy of Bacteria. *Current Science*, 85 (9): 1299-1307

PROAL, A. (2008). Understanding biofilms. *Bacteriality—Exploring Chronic Disease 26*. <http://bacteriality.com/2008/05/26/biofilm>, accessed 17/07/2015

QUEEN, D. (2010). Technology Update; Understanding Hydrofiber Technology, *Wounds International*, 1 (5): 1-6

QUINN, K.J., COURTNEY, J.M., EVANS, J.H., GAYLOR, J.D.S., REID, W.H., (1985). Principles of burn dressings. *Biomaterials*, 6 (6): 369-377

RAFTER, L., ANTHONY, D., COLLIER, M., RAFTER, M., 2015. Stopping the strikethrough: An audit of patient outcomes on four superabsorbent dressings. *Wounds UK*, 11 (4): 60-67

RAMUNDO, J., GRAY, M. (2008). Enzymatic wound debridement. *Journal of Wound Ostomy and Continence Nursing*, 35 (3): 273-280

REINKE, J.M., SORG, H., (2012). Wound Repair and Regeneration. *European Surgical Research*, 49: 35–43

REITSMA, A.M., RODEHEAVER, G.T., (2001). Effectiveness of a new antimicrobial gauze dressing as a bacterial barrier. Mansfield, Mass: Tyco Healthcare Group LP:14

RHOADS, D.D., WOLCOTT, R.D., PERCIVAL, S.L. (2008). Biofilms in wounds: management strategies. *Journal of Wound Care*, 17: 502-508

RICHARD, P., FLOCH, R.L., CHAMOIX, C., PANNIER, M., ESPAZE, E. AND RICHT, H., (1994). *Pseudomonas aeruginosa* outbreak in a burn unit: role of

antimicrobials in the emergence of multiply resistant strains. *The Journal of Infectious Diseases*, 170 (2): 377-383

RICE, S.A., KOH, K.S., QUECK, S.Y., LABBATE, M., LAM, K.W., KJELLEBERG, S., (2005). Biofilm Formation and Sloughing in *Serratia marcescens* are Controlled by Quorum Sensing and Nutrient Cues. *Journal of Bacteriology*, 187 (10): 3477–3485

RISTIĆ, T., ZEMLJIČ, L.F., NOVAK, M., KUNČIČ, M.K., SONJAK, S., CIMERMAN, N.G., STRNAD, S., (2011). Antimicrobial efficiency of functionalized cellulose fibres as potential medical textiles. *Science Against Microbial Pathogens: Communicating Current Research and Technological Advances*, 6: 36-51

ROBINOW, C.F., (1956). The chromatin bodies of bacteria. *Bacteriology Reviews*, 20: 207-242

ROBINOW, C., KELLENBERGER, E., (1994). The bacterial nucleoid revisited. *Microbiology and Molecular Biology Reviews*, 58 (2): 211-232

ROBINSON, B.J., (2000). The use of a hydrofibre dressing in wound management. *Journal of Wound Care*, 9 (1): 32-34

ROCHE, E.D., RENICK, P.J., TETENS, S.P., RAMSEY, S.J., DANIELS, E.Q., CARSON, D. (2012). Increasing the presence of biofilm and healing delay in a porcine model of MRSA-infected wounds. *Wound Repair and Regeneration* 20 (4): 537-543

RÖMLING, U., BALSALOBRE, C., (2012). Biofilm infections, their resilience to therapy and innovative treatment strategies. *Journal of Internal Medicine*, 272 : (6) 541–561

ROSENTHAL, M., GOLDBERG, D., AIELLO, A., LARSON, E., FOXMAN B., (2011). Skin microbiota: microbial community structure and its potential association with health and disease. *Infection Genetics and Evolution*, 11 (5): 839-848

ROVEE, D.T., MAIBACH, H.I., (2003). Management of infected wounds. CRC Press, *The Epidermis in Wound Healing, Dermatology: Clinical and Basic Science*, Series 12 (5): 228-231

ROWLANDS, V., JONES, S., PARSONS, D., (2013). A new anti-biofilm Hydrofiber® dressing: demonstration of enhanced silver penetration and biofilm removal in vitro. *Wounds International poster*

RUSTOGI, R., MILL, J., FRASER, J.F., KIMBLE, R.M., (2005). The use of Acticoat™ in neonatal burns. *Burns*, 31 (7): 878-882

RUTALA, R.W., WEBER, D.J., (2008) and the Healthcare Infection Control Practices Advisory Committee. Guideline for Disinfection and Sterilization in Healthcare Facilities. Centers for Disease Control and Prevention, <https://www.cdc.gov/infectioncontrol/guidelines/disinfection>, accessed 12/04/17

RYTER, A., (1995). French contribution of electron microscopy to bacteriology. *Biology of the Cell*, 80: 139-141

RYTER, A., KELLENBERGER, E., (1958). L'inclusion au polyester pour l'ultramicrotomie. *Journal of Ultrastructure Research*, 2: 200-214

RYTER, A., KELLENBERGER, E., BIRCH-ANDERSON, A., MAALØE, O., (1958). Étude au microscope électronique de plasmas contenant de l'acide désoxyribonucléique. *Zeitschrift für Naturforschung*, 13b: 597-605

SABA, S.C., TSAI, R., GLAT, P., (2009). Clinical Evaluation Comparing the Efficacy of Aquacel® Ag Hydrofiber® Dressing Versus Petrolatum Gauze With Antibiotic Ointment in Partial-Thickness Burns in a Pediatric Burn Center. *Journal of Burn Care and Research*, 30 (3): 380-385

SAID, J., WALKER, M., PARSONS, D., STAPLETON, P., BEEZER, A.E., GAISFORD, S., (2014). An in vitro test of the efficacy of an anti-biofilm wound dressing. *International Journal of Pharmaceutics*, 474 (1): 177-181

SAINSBURY, D.C.G., (2009). Evaluation of the quality and cost-effectiveness of Versajet\_hydrosurgery. *International Wound Journal*, 6 (1): 24-29

SANDERS, M.E., GUARNER, F., GUERRANT, R., HOLT, P.R., QUIGLEY, E.M., SARTOR, R.B., SHERMAN, P.M., MAYER, E.A., (2013). An update on the use and investigation of probiotics in health and disease. *Gut*, 62 (5): 787-796

SCHOOLING, S.R., BEVERIDGE, T.J., (2006). Membrane vesicles: an overlooked component of matrices of biofilms. *Journal of Bacteriology*, 188: 5945-5957

SCHREIL W.H., (1964). Studies on the fixation of artificial and bacterial DNA plasms fir the electron microscopy of thin sections. *Journal of Cell Biology*, 22: 1-20

SCHULTZ, G.S., BARILLO, D.J., MOZINGO, D.W., CHIN, G.A., (2004). Wound bed preparation and a brief history of TIME. *International Wound Journal*, 1 (1): 19-32

SCHULTZ, G.S., GIBSON, D.J., LANTIS, J., NAKAGAMI, G., (2016). Biofilm update. *Wound Practice & Research: Journal of the Australian Wound Management Association*, 24 (4): 228

SCHULTZ, G.S., SIBBALD, R.G., FALANGA, V., AYELLO, E.A., DOWSETT, C., HARDING, K., ROMANELLI, M., STACEY, M.C., TEOT, L., VANSCHIEDT, W., (2003). Wound bed preparation: a systematic approach to wound management. *Wound Repair and Regeneration*, 11 (S1): 1-28

SCHWARTZ, J.A., LANTIS, J.C., GENDICS, C., FULLER, A.M., PAYNE, W., OCHS, D., (2013). A prospective, non comparative, multicenter study to investigate the effect of cadexomer iodine on bioburden load and other wound characteristics in diabetic foot ulcers. *International Wound Journal*, 10 (2): 193-199

SEAMAN, S. (2002). Dressing selection in chronic wound management. *Journal of the American Podiatric Medical Association*, 92 (1): 24-33

SECHAUD, J., KELLENBERGER, E., (1972). Electron Microscopy of DNA containing plasms: IV. Glutaraldehyde – uranyl acetate fixation of virus infected bacteria for thin sectioning. *Journal of Ultrastructure Research*, 39: 598-607

SEIPP, H.M., HOFMANN, S., HACK, A., SKOWRONSKY, A., HAURI, A., (2005) Efficacy of various wound irrigation solutions against biofilms. *Journal of Wound Care* 4:160–164.

SETH, A.K., GERINGER, M.R., GALIANO, R.D., LEUNG, K.P., MUSTOE, T.A., HONG, S.J., (2012). Quantitative comparison and analysis of species-specific wound biofilm virulence using an in vivo, rabbit-ear model. *Journal of the American College of Surgeons*, 215 (3): 388-399.

SERRALTA, V.W., HARRISON-BELESTRA, C., CAZZANIGA, A.L., DAVIS, S.C., MERTZ, P.M., (2001). Lifestyles of bacteria in wounds: presence of biofilms? *Wounds*, 13 (1): 29–34

SHERMAN, R.A., HALL, M.J.R., THOMAS, S., (2000). Medicinal Maggots: An Ancient Remedy for Some Contemporary Afflictions. *Annual Review of Entomology*, 45: 55-81

SHOUKAT, K., PILLING, S., ROUT, S., BRADBURY, J., HUMPHREYS, P.N., (2015). A systematic comparison of antimicrobial wound dressings using a planktonic cell and an immobilized cell model. *Journal of Applied Microbiology*, 119(6):1552-60.

- SIBBALD, R.G., WOO, K., AYELLO, E.A., (2006). Increased bacterial burden and infection: the story of NERDS and STONES. *Advances in Skin and Wound Care*, 19 (8): 447-461
- SILVA, M.T., SANTOS MOTA, J.M., MELO, J.V.C., CARVALHO GUERRA, F., (1971). Uranyl salts as fixatives for electron microscopy and phospholipid loss in bacilli. *Boichimica et Biophysica Acta*, 233: 513-520
- SIMPSON J.A., SMITH S.E., DEAN R.T., (1989) Scavenging by alginate of free radicals released by macrophages. *Free Radical Biology and Medicine* 6: 347–53
- SINDE, E., CARBALLO, J., (2000). Attachment of Salmonella spp. and Listeria monocytogenes to stainless steel, rubber and polytetrafluorethylene: the influence of free energy and the effect of commercial sanitizers. *Food Microbiology*, 17: 439–447
- SINGH, A., HALDER, S., CHUMBER, S., MISRA, M. C., SHARMA, L.K., SRIVASTAVA, A., MENON, G.R., (2004). Meta-analysis of randomized controlled trials on hydrocolloid occlusive dressing versus conventional gauze dressing in the healing of chronic wounds. *Asian Journal of Surgery*, 27 (4): 326-332
- SINGH, R., RAY, P., DAS, A., SHARMA, M., (2010). Penetration of antibiotics through Staphylococcus aureus and Staphylococcus epidermidis biofilms. *Journal of Antimicrobial Chemotherapy*, 65 (9): 1955-1958
- SLADEK, R.E., FILOCHE, S.K., SISSONS, C.H., STOFFELS, E., (2007). Treatment of Streptococcus mutans biofilms with a nonthermal atmospheric plasma. *Letters of Applied Microbiology*, 45 (3): 318-323
- SMITH & NEPHEW U.K. product website, [www.smith-nephew.com/uk/products/wound\\_management/product](http://www.smith-nephew.com/uk/products/wound_management/product), accessed 12/11/2016
- SMITH & NEPHEW UK Professional products, [www.smith-nephew.com/professional/products/advanced-wound-management/iodosorb--iodoflex/iodoflex-pads](http://www.smith-nephew.com/professional/products/advanced-wound-management/iodosorb--iodoflex/iodoflex-pads), accessed 12/11/ 2016
- SMITH, A.G., POWIS, R.J., PRITCHARD, D.I., BRITLAND, S.T., (2006). Greenbottle (*Lucilia sericata*) Larval Secretions Delivered from a Prototype Hydrogel Wound Dressing Accelerate the Closure of Model. *Wounds*, 22 (6): 1690–1696



- SNYDER, K.N., COMPLIMENT, J.M., BUCHINSKY, F.J., HALL-STOODLEY, L., STOODLEY, P., POST, J.C., (2009). Biofilms: A new enemy. *The Nurse Practitioner*, 34 (9): 35-39
- SOOD, A., GRANICK, M.S., TOMASELLI, N.L., (2014). Wound dressings and comparative effectiveness data. *Advances in wound care*, 3 (8): 511-529
- SOUSA, C., (2011). Staphylococcus epidermidis: Adhesion and Biofilm Formation on to Biomaterials. LAP LAMBERT Academic Publishing  
[https://www.researchgate.net/publication/277114132\\_Staphylococcus\\_epidermidis\\_adhesion\\_and\\_biofilm\\_formation\\_onto\\_biomaterials](https://www.researchgate.net/publication/277114132_Staphylococcus_epidermidis_adhesion_and_biofilm_formation_onto_biomaterials), accessed 13/03/16
- STEWART, P.S., COSTERTON, J.W., (2001). Antibiotic resistance of bacteria in BIOFILMS. *LANCET*, 358: 135–138
- STOODLEY, P., LEWANDOWSKI, Z., (1994). Liquid flow in biofilm systems. *Applied and Environmental Microbiology*, 60 (8): 2711-2716
- STOODLEY, P., DODDS, I., BOYLE, J.D., LAPPIN-SCOTT, H.M., (1999). Influence of hydrodynamics and nutrients on biofilm structure. *Journal of Applied Microbiology Symposium Supplement*, 85: 19-28
- STORM-VERSLOOT, M.N., VOS, C.G., UBBINK, D.T., VERMEULEN, H., (2010). Topical silver for preventing wound infection (Review). Published by John Wiley & Sons, Ltd. <http://onlinelibrary.wiley.com/cochranelibrary>, accessed 04/11/16
- STOVER, C.K., PHAM, X.Q., ERWIN, A.L., MIZOGUCHI, S.D., WARRENER, P., HICKEY, M.J., BRINKMAN, F.S.L., HUFNAGLE, W.O., KOWALIK, D.J., LAGROU, M. AND GARBER, R.L., (2000). Complete genome sequence of Pseudomonas aeruginosa PAO1, an opportunistic pathogen. *Nature*, 406 (6799): 959-964
- STRUTT, J. W., (1879). Resolving or separating power of optical instruments. *Philosophical Magazine*, Series 5, 8 (49): 261-274
- STUBBS, S., HOBOT, J.A., WADDINGTON, R.J., EMBERY, G., LEWIS, M.A.O., (1999). Effect of environmental Haemin upon the physiology and biochemistry of *Prevotella intermedia* R78. *Letters of Applied Microbiology*, 29: 31-36
- SULLIVAN, T.P., EAGLSTEIN, W.H., DAVIS, S.C., MERTZ, P., (2001). The pig as a model for human wound healing. *Wound Repair and Regeneration*, 9 (2): 66–76

SUN, Y., DOWD, S.E., SMITH, E., ROADS, D.D., WOLCOTT, R.D., (2008). In vitro multispecies Lubbock chronic wound biofilm model. *Wound Repair and Regeneration*, 16: 805–813

SUTHERLAND, I.W., (2001a). The biofilm matrix – an immobilized but dynamic microbial environment. *Trends in Microbiology*, 9 (5): 222-227

SUTHERLAND, I.W., (2001b). Biofilm exopolysaccharides: a strong and sticky framework. *Microbiology*, 147: 3–9

TACHI, M., HIRABAYASHI, S., YONEHARA, Y., SUZUKI, S. BOWLER, P., (2004). Development of an experimental model of infected skin ulcer. *International Wound Journal*, 1: 49–55

THE SCIENTIST,

<http://www.thescientist.com/?articles.view/articleNo/25576/title/The-Hooke-Microscope/> - accessed 23/12/13

THORN, R.M.S., AUSTIN, A.J., GREENMAN, J., WILKINS, J.P.G., DAVIS, P.J., (2009). *In Vitro* comparison of antimicrobial activity of iodine and silver dressings against biofilms. *Journal of Wound Care* 18(8): 343-346.

THORN, R.M.S., GREENMAN, J., (2009). A novel in vitro flat-bed perfusion biofilm model for determining the potential antimicrobial efficacy of topical wound treatments. *Journal of Applied Microbiology*, ISSN: 1364-5072

TICKLE, J., (2012). Effective management of exudate with AQUACEL extra. *British Journal of Community Nursing, Wound Care Supplement*: 38-46

TODAR, K., (2012). The Growth of Bacterial Populations [textbookofbacteriology.net/growth\\_3.html](http://textbookofbacteriology.net/growth_3.html), accessed 13/03/16

TOKUDA, H., (1969). Excretion of carbohydrate by a marine pennate diatom, *Nitzschia closterium*. *Recreation Oceanography Works Japan*, 10: 109-122

TOY, L.W., MACERA, L., (2011). Evidence-based review of silver dressing use on chronic wounds. *Journal of the American Academy of Nurse Practitioners*, 23 (4):183-92

TREDGET, E.E., SHANKOWSKY, H.A., GROENEVELD, A., BURRELL, R., (2002). A matched pair, randomized study evaluating the efficacy and safety of

Acticoat\* Silver-Coated Dressing for the Treatment of Burn Wounds. *Journal of Burn Care and Research*, 19 (6): 531-537

TROP, M., NOVAK, M., RODL, S., HELLBOM, B., KROELL, W., GOESSLER, W., (2006). Silver-coated dressing acticoat caused raised liver enzymes and argyria-like symptoms in burn patient. *Journal of Trauma and Acute Care Surgery*, 60 (3): 648-652

TSANG, K.K., KWONG, E.W., WOO, K.Y., TO, T.S., CHUNG, J.W., WONG, T.K. (2015). The Anti-Inflammatory and Antibacterial Action of Nanocrystalline Silver and Manuka Honey on the Molecular Alternation of Diabetic Foot Ulcer: A Comprehensive Literature Review. Evidence Based Complement Alternative Medicine .2015:218283. doi: 10.1155/2015/218283. Epub 2015 Jul 28.

TSANG, K.K., KWONG, E.W., TO, T.S., CHUNG, J.W., WONG, T.K. (2017). A Pilot Randomized, Controlled Study of Nanocrystalline Silver, Manuka Honey, and Conventional Dressing in Healing Diabetic Foot Ulcer. Evid Based Complement Alternat Med. 2017;2017:5294890. doi: 10.1155/2017/5294890. Epub 2017 Jan 25

TSUNEDA, S., AIKAWA, H., HAYASHI, H., YUASA, A., HIRATA, A., (2003). Extracellular polymeric substances responsible for bacterial adhesion on to solid surface. *Federation of European Microbiological Societies, Microbiology Letters* 223:287-292

ULUÇ, K., KUJOTH, G.C., & BASKAYA, M.K., (2009). Operating microscopes: past, present, and future. *Neurosurgical focus*, 27 (3): E4

VALKENBURG, J.A.C., WOLDRINGH, C.L., BRAKENHOFF, G.J., VOORT VAN DER, H.T.M., NANNINGA, N., (1985). Confocal scanning light microscopy of the Escherichia coli nucleoid: comparison with phase-contrast and electron microscopic images. *Journal of Bacteriology*, 161: 478-483

VAN DELDEN, C., IGLEWSKI, B.H., (1998). Cell-to-cell signaling and Pseudomonas aeruginosa infections. *Emerging Infectious Diseases*, 4 (4): 551

VAN ITERSON, W., (1984). *Inner structures of bacteria*. Publisher: Van Nostrand Reinhold Co., Inc., NewYork

VILAIN, S., PRETORIUS, J.M., THERON, J., BROEZEL, V.S., (2009). DNA as an adhesion: Bacillus cereus requires extracellular DNA to form biofilms. *Applied Environmental Microbiology*, 75: 2861–2868

VLACHOU, E., CHIPPI, E., SHALE, E., WILSON, Y.T., PAPINI, R., MOIEMEN, N.S., (2007) The safety of nanocrystalline silver dressings on burns: a study of systemic silver absorption. *Burns*, 33 (8): 979-985

VON REGE, H., SAND, W., (1998). Evaluation of biocides by microcalorimetry in biofilms. *Journal of Microbiological Methods*, 33: 227–235

VU, B., CHEN, M., CRAWFORD, R.J., IVANOVA, E.P., (2009). Bacterial Extracellular Polysaccharides Involved in Biofilm Formation. *Molecules*, 14: 2535-2554

WALKER J.T., MACKERNESS C.W., ROGERS J., KEEVIL C.W., (1995). Heterogeneous mosaic—a haven for waterborne pathogens. *Microbial Biofilms*, Chapter 11: 196–204. Eds. Lappin-Scott H. M., Costerton J. W., Publisher: Cambridge University Press, UK

WALKER, M., HOBOT, J.A., NEWMAN, G.R., BOWLER, P.G., (2004). Scanning electron microscopic examination of bacterial immobilisation of a carboxymethyl cellulose (AQUACEL) and alginate dressings. *Biomaterials*, 24: 883-890

WALKER, M., JONES, S., PARSONS, D., BOOTH, R., COCHRANE, C., BOWLER, P., (2011). Evaluation of low-adherent antimicrobial dressings. *Wounds UK*, 7 (2): 32-45

WALKER, M., METCALF, D., PARSONS, D., BOWLER, P., (2015). A real-life clinical evaluation of a next-generation antimicrobial dressing on acute and chronic wounds. *Journal of wound care*, 24 (1): 11-22

WANG, X.Q., CHANG, H.E., FRANCIS, R., OLSZOWY, H., LIU, P.Y., KEMPF, M., CUTTLE, L., KRAVCHUK, O., PHILLIPS, G.E., KIMBLE, R.M., (2009a). Silver deposits in cutaneous burn scar tissue is a common phenomenon following application of a silver dressing. *Journal of Cutaneous Pathology*, 36 (7): 788-792.

WANG, X.Q., KEMPF, M., MOTT, J., CHANG, H.E., FRANCIS, R., LIU, P.Y., CUTTLE, L., OLSZOWY, H., KRAVCHUK, O., MILL, J., KIMBLE, R.M., (2009b). Silver Absorption on Burns After the Application of Acticoat™: Data From Pediatric Patients and a Porcine Burn Model. *Journal of burn care & research*, 30 (2): 341-348.

WEBSTER, P., WU, S., GOMEZ, G., APICELLA, M., PLAUT, A.G., ST GEME III. J.W., (2006). Distribution of Bacterial Proteins in Biofilms Formed by Non-typeable

Haemophilus influenza. *Journal of Histochemistry and Cytochemistry*, 54 (7): 829–842

WERTHEIM, H.F., VOS, M.C., OTT, A., VAN BELKUM, A., VOSS, A., KLUYTMANS, J.A., VAN KEULEN, P.H., VANDENBROUCKE-GRAULS, C.M., MEESTER, M.H. AND VERBRUGH, H.A., (2004). Risk and outcome of nosocomial Staphylococcus aureus bacteraemia in nasal carriers versus non-carriers. *The Lancet*, 364 (9435): 703-705

WHITE, R., CUTTING, K.F., (2006). Modern exudate management: a review of wound treatments. *WorldWideWounds.com*, Revision 1, accessed 12/03/17

WHITE, W., (2011). Sharp wound debridement in the management of recalcitrant, locally infected chronic venous leg ulcers: A narrative review. *Wound Practice and Research*, 19 (4): 222-228

WHITEHEAD, N.A., BARNARD, A.M.L., SLATER, H., SIMPSON, N.J.L., SALMOND, G.P.C., (2001). Quorum-sensing in Gram-negative bacteria. *FEMS Microbiology Reviews*, 25: 365-404

WILD, T., EBERLEIN, T., ANDRIESEN, A., (2010). Wound cleansing efficacy of two cellulose-based dressings. *Wounds UK*, 6 (3): 14-21

WILKING, J.N., ZABURDAEV, V., DE VOLDER, M., LOSICK, R., BRENNER, M. P., WEITZ, D.A., (2013). Liquid transport facilitated by channels in Bacillus subtilis biofilms. *Proceedings of the National Academy of Science of the United States of America*, 110 (3): 848–852

WILKS, S., PRIETO, J., FADER, M., KEEVIL, C.W., (2008). Unravelling catheter biofilms: A new approach. *Institute of Life Sciences (University of Southampton)* [www.southampton.ac.uk/ifls](http://www.southampton.ac.uk/ifls), accessed 20/07/2015

WILLIAMS, C., (1999). An investigation of the benefits of Aquacel Hydrofibre wound dressing. *British Journal of Nursing*, 8 (10): 676-680

WILSON, M., (1999). Use of constant depth film fermentor in studies of biofilms of oral bacteria. *Methods in Enzymology*, 310 (21):264-279

WIMENNY, J.W.T., COLASANTI, R., (1997). A unifying hypothesis for the structure of microbial biofilms based on cellular automaton models. *FEMS Microbiology Ecology*, 22: 1-16

WINTER, G.D., (1962). Formation of the scab and the rate of epithelialisation of superficial wounds in the skin of young domestic pigs. *Nature*, 192: 293-294

WINZER, K., HARDIE, K.R., WILLIAMS, P., (2002). Bacterial cell-to-cell communication: sorry, can't talk now —gone to lunch! *Current Opinion in Microbiology*, 5: 216–222

WIRRAL COMMUNITY NHS TRUST 2013 Wound Management Formulary and Guidelines Wound Management 2015: 1-15. *Medicinewatch.org*  
[www.wirralct.nhs.uk/.../WoundManagementFormularyGuidelines](http://www.wirralct.nhs.uk/.../WoundManagementFormularyGuidelines), accessed 20/07/2015

WOLCOTT, R.D., FLETCHER, J., (2014). Technology update: role of wound cleansing in the management of wounds. *Wounds UK*, 10 (2): 58-63

WOLCOTT, R.D., KENNEDY, J.P., DOWD, S.E., (2009). Regular debridement is the main tool for maintaining a healthy wound bed in most chronic. *Journal of Wound Care*, 18 (2): 54-56

WOLCOTT, R.D., RHOADS, D.D., DOWD, S. E., (2008). Biofilms and chronic wound inflammation. *Journal of Wound Care*, 17 (8): 333-341

WOLDRINGH, C.L., (1973). Effect of cations on the organisation of the nucleoplasm in *Escherichia coli* prefixed with osmium tetroxide or glutaraldehyde. *Cytobiologie*, 8: 97-111

WONG, V.W., MARTINDALE, R.G., LONGAKER, M.T., GURTNER, G.C., (2013). From Germ Theory to Germ Therapy: Skin Microbiota, Chronic Wounds, and Probiotics. *Skin Microbiota, Wounds, and Probiotics*, 132 (5): 854-861

WOO, K.Y., (2014). AQUACEL™ Ag+ Dressings: In practice. Next-generation antimicrobial dressings: AQUACEL™ Ag+Extra™ and Ribbon. *London: Wounds International (Supplement):10-11*

WORLD UNION OF WOUND HEALING SOCIETIES' EXPERT WORKING GROUP (2004). Minimising pain at wound dressing-related procedures. *A consensus document*, 10 pages. *WUWHS Principles of best practice: A working group review*. Publisher: Medical Education Partnership Ltd, London

WORLD UNION OF WOUND HEALING SOCIETIES' EXPERT WORKING GROUP (2007), Principles of Best Practice: Wound Exudate and the Role of Dressings: A Consensus Document. *WUWHS Medical Education Partnership Ltd, London. [woundsinternational.com/pdf/content\\_42.pdf](http://woundsinternational.com/pdf/content_42.pdf)*, accessed 29/04/2017

WORLD UNION OF WOUND HEALING SOCIETIES' EXPERT WORKING GROUP (2008). Principles of best practice: Wound infection in clinical practice. An international consensus. *WUWHS* London: MEP Ltd. [www.mepltd.co.uk](http://www.mepltd.co.uk), accessed 20/07/2015

WOUND SOURCE. Skin care: moisture barriers, Overview (2016) <http://www.woundsource.com/product-category/skin-care/moisture-barriers>, accessed 20/07/2015

WOUNDS INTERNATIONAL EXPERT WORKING GROUP (2012). Optimising wellbeing in people living with a chronic wound. A working group review: International Consensus, <http://www.woundsinternational.com>. Publisher: Wounds International, London

WOUNDS INTERNATIONAL, (2012). International case series: Using SILVERCEL Non-Adherent: Case Studies. London. <http://www.woundsinternational.com>, accessed 03/04/2017

WU, P., NELSON, E.A., REID, W.H., RUCKLEY, C.V., GAYLOR, J.D.S., (1996). Water vapour transmission rates in burns and chronic leg ulcers: influence of wound dressings and comparison with in vitro evaluation. *Biomaterials*, 17 (14): 1373-1377

WUERTZ, S., BISHOP, P.L., WILDERER, P.A., (2003). *Biofilms in Wastewater Treatment: An Interdisciplinary Approach*, Publisher: IWA Publishing, London, 400: 211-231

YARWOOD-ROSS, L., (2013). Theory of moist wound healing. [independentnurse.co.uk/clinical-article/theory-of-moist-wound-healing/63534](http://independentnurse.co.uk/clinical-article/theory-of-moist-wound-healing/63534), accessed 19/04/2017

YOUNG, T., (2011). Debridement – Is it time to revisit clinical practice? *British Journal of Nursing* (Tissue viability supplement), 20 (11): S24-S28

ZERAIK, A.E., NITSCHKE, M, (2012). Influence of growth media and temperature on bacterial adhesion to polystyrene surfaces. *Brazilian Archives of Biology and Technology*, 55 (4): 569-576

ZHANG, X.Q., BISHOP, P.L., KUPFERLE M.J., (1998). Measurement of polysaccharides and proteins in biofilm extracellular polymers. *Water Science and Technology*, 37: 345-348

ZHAO, G., USUI, M.L., UNDERWOOD, R.A., SINGH, P.K., JAMES, G.A., STEWART, P.S., FLECKMAN, P., OLERUD, J.E., (2012). Time course study of delayed wound healing in a biofilm-challenged diabetic mouse model. *Wound Repair and Regeneration*, 20: 342–352

ZWORYKIN, V.K., MORTON, G.A., RAMBERG, E.G., HILLIER, J., VANCE, A.W., (1945). *Electron Optics and the Electron Microscope*. Publisher: John Wiley & Sons, Inc., New York